CHANGES IN THE TESTICULAR CAPSULE AND PERITUBULAR BOUNDARY TISSUE IN PRE-PUBERTAL, PUBERTAL AND ADULT JAPANESE QUAILS (*COTURNIX COTURNIX JAPONICA*)

By

Lindokuhle Innocent Khumalo

A dissertation submitted in partial fulfilment of the requirements for Master's degree

Student number: 17402108

In the Department of Anatomy and Physiology

Faculty of Veterinary Science

University of Pretoria

Supervisor: Professor M.N. Madekurozwa

2020

Acknowledgments

I wish to express my most profound gratitude to the following people who have ensured that the months of hard work finally culminated into a tangible piece of work:

My supervisor, Professor Mary-Cathrine N. Madekurozwa, for believing in me and granting me the opportunity to be a part of her team, for her continual support, guidance, constructive criticism and encouragement throughout this project.

Dr Mahdy Mohammed, for his guidance and assistance in the laboratory and during data collection.

Dr. Lizette Du Plessis and Ms. Antoinette Lensink (EM Unit) for their assistance with using the image analyzer.

My colleagues, for their assistance with data collection and for being there whenever I needed to bounce off ideas.

Last, but certainly not least, I would like to express deepest love and gratitude to my amazing parents, Enock Khumalo and Thembi Khanyile, and my whole family. Thank you for your love and unceasing support.

Table of Contents

Acknowledgments i
Table of Contents ii
List of figures v
List of tables xiii
Summary xiv
Chapter one: 1
1.0 General introduction 1
1.1 Background on the Japanese quail (*Coturnix coturnix japonica*) 3
1.2. Cells and fibres of connective tissue 5
1.2.1 Fibroblasts 5
1.2.2 Fibrocytes 5
1.2.3 Smooth muscle cells 6
1.3 Connective tissue fibres 7
1.3.1 Collagen fibres 7
1.3.2. Reticular fibres 7
1.3.3 Elastic fibres 8
1.4 Avian testicular anatomy 9
1.5 Aim and specific objectives 11
1.5.1 Aim 11
1.5.2 Specific objectives 11
1.6 Study methodology 11
1.6.1 Animals and management 11
1.6.2 Necropsy 12
1.6.3 Tissue processing for light microscopy and morphometry 13
1.6.5 Immunohistochemistry 14
1.6.5 Transmission electron microscopy 16
Chapter two: 17
The testicular capsule of pre-pubertal, pubertal and adult male Japanese quails (*Coturnix coturnix japonica*): a histological, morphometric, immunohistochemical and ultrastructural study. 17
2.1 Introduction 17
2.2 Literature review 17
2.2.1 Composition of the testicular capsule in mammals 17

2.2.2 Composition of the testicular capsule in birds 19
2.2.3 Cytoskeletal proteins in the testicular capsule 21
2.2.4 Functionality of the testicular capsule in mammals and birds 23
2.3 Materials and methods 24
2.3.1 Light microscopy and morphometry 24
2.3.2 Immunohistochemistry 24
2.3.3 Transmission electron microscopy 25
2.3.4 Statistical analysis 25
2.4 Results 26
2.4.1 Gross morphology 26
2.4.2 Gross parameters: statistical analysis 29
2.4.2.1 Biometric parameters 30
2.4.2.2 Testicular capsule thickness 34
2.4.3. Testicular architecture of the Japanese quail (*Coturnix coturnix japonica*). 36
2.4.4 Light microscopy 36
2.4.5 Cytoskeletal protein immunohistochemistry 47
2.4.5.1 Desmin 48
2.4.5.2 Smooth muscle actin 52
2.4.5.3 Tubulin 56
2.4.5.4 Vimentin 58
2.4.6 Basement membrane immunohistochemistry 64
2.4.6.1 Collagen type IV 64
2.4.6.2 Fibronectin 69
2.4.6.3 Laminin 72
2.4.7 Transmission electron microscopy 76
2.5 Discussion 111
2.5.1 Gross morphology 111
2.5.2 Biometric parameters 112
2.5.3 Testicular capsule thickness 114
2.5.4 Light microscopy 115
2.5.5 Cytoskeletal protein immunohistochemistry 117
2.5.6 Basement membrane immunohistochemistry 121
2.5.7 Transmission electron microscopy 122

Chapter three: 125
The peritubular boundary tissue of pre-pubertal, pubertal, and adult male Japanese quails (*Coturnix coturnix japonica*): a histological, morphometric, immunohistochemical and ultrastructural study. 125
3.1 Introduction 125
3.1.1 The peritubular boundary tissue in mammals. 127
3.1.2 The peritubular boundary tissue in birds 129
3.1.3 Functions of the peritubular boundary tissue in mammals and birds 130
3.2 Materials and methods 132
3.2.1 Light microscopy 132
3.2.2 Immunohistochemistry 132
3.2.3 Transmission electron microscopy 133
3.2.4 Statistical analysis 134
3.3 Results 134
3.3.1. Light microscopy 134
3.3.2. Cytoskeletal protein immunohistochemistry 147
3.3.2.1 Desmin 148
3.3.2.2 Smooth muscle actin 150
3.3.2.3 Tubulin 154
3.3.2.4 Vimentin 158
3.3.3. Basement membrane immunohistochemistry 162
3.3.3.1 Collagen type IV 162
3.3.3.2 Fibronectin 165
3.3.3.3 Laminin 167
3.3.4. Transmission electron microscopy 173
3.4 Discussion 198
Chapter four: 204
Conclusion 204
References 205

List of figures

Figure 1. 1: Photographs of pre-pubertal (A), pubertal (B) and adult (C) Japanese quails used in the present study. 12

Figure 2. 1: Photograph of the *in situ* position of the testes in a pre-pubertal Japanese quail……..27

Figure 2. 2: Photograph of the *in situ* position of the testes in a pubertal Japanese quail..... 28

Figure 2. 3: Photograph of the *in situ* position of the testes in an adult Japanese quail..... 29

Figure 2. 4: The mean bodyweights of pre-pubertal, pubertal, and adult male Japanese quails.. 32

Figure 2. 5: The mean absolute testicular weights of pre-pubertal, pubertal, and adult male Japanese quails. 33

Figure 2. 6: The mean relative testicular weights of pre-pubertal, pubertal, and adult male Japanese quails. 33

Figure 2. 7: The gonadosomatic index (GSI) of pre-pubertal, pubertal, and adult male Japanese quails.. 34

Figure 2. 8: The mean testicular capsule thickness of pre-pubertal, pubertal, and adult male Japanese quails.. 35

Figure 2. 9: Light photomicrograph of the testicular capsule of a pre-pubertal Japanese quail.. 37

Figure 2. 10: Light photomicrograph of the testicular capsule of a pre-pubertal Japanese quail.. 38

Figure 2. 11: Light photomicrograph of the testicular capsule of a pre-pubertal Japanese quail. 39

Figure 2. 12: Light photomicrograph of the testicular capsule of a pre-pubertal Japanese quail. 39
Figure 2. 13: Light photomicrographs (A, B) of testicular capsules from pubertal Japanese quails. Thin arrows: oval and elongated nuclei of mesothelial cells in the *tunica serosa*.. 41
Figure 2. 14: Light photomicrograph of a testicular capsule from a pubertal Japanese quail..... 42
Figure 2. 15: Light photomicrograph of a testicular capsule from a pubertal Japanese quail..... 43
Figure 2. 16: Light photomicrographs (A, B) of testicular capsules from adult Japanese quails. 45
Figure 2. 17: Light photomicrograph of a testicular capsule from an adult Japanese quail..... 46
Figure 2. 18: Light photomicrograph of a testicular capsule from an adult Japanese quail..... 47
Figure 2. 19: Light photomicrograph of a testicular capsule from an adult Japanese quail..... 47
Figure 2. 20: Light photomicrographs showing desmin immunoexpression in the testicular capsule of pre-pubertal (A, B), pubertal (C, D), and adult (E, F) quails..... 51
Figure 2. 21: Light photomicrographs showing smooth muscle actin immunoexpression in the testicular capsule of pre-pubertal (A, B), pubertal (C, D), and adult (E, F) quails. 55
Figure 2. 22: Light photomicrographs showing tubulin immunoexpression in the testicular capsule of pre-pubertal (A), pubertal (B, C), and adult (D, E) quails. 58

Figure 2. 23: Light photomicrographs showing vimentin immunoexpression in the testicular capsule of pre-pubertal (A, B), pubertal (C, D), and adult (E, F) quails. 61
Figure 2. 24: Light photomicrographs showing collagen type IV immunoexpression in the testicular capsules of pre-pubertal (A, B), pubertal (C, D), and adult (E, F) quails. 68
Figure 2. 25: Light photomicrographs showing fibronectin immunoexpression in the testicular capsule of pre-pubertal (A, B), pubertal (C, D), and adult (E) quails. 72
Figure 2. 26: Light photomicrographs showing laminin immunoexpression in the testicular capsule of pre-pubertal (A, B), pubertal (C, D), and adult (E) quails. 75
Figure 2. 27: Transmission electron photomicrograph of mesothelial cells lining the testicular capsule of a pre-pubertal bird. 79
Figure 2. 28: Transmission electron micrograph of the *tunica serosa* of a pre-pubertal bird.. 80
Figure 2. 29: Transmission electron photomicrograph of mesothelial cells lining the testicular capsule of a pre-pubertal bird. 81
Figure 2. 30: Transmission electron photomicrograph of mesothelial cells in the *tunica serosa* of a pre-pubertal bird.. 82
Figure 2. 31: Survey transmission electron photomicrograph of the testicular capsule of a pre-pubertal bird. 83
Figure 2. 32: Transmission electron micrograph showing the superficial region of the *tunica albuginea* of a pre-pubertal bird. 84
Figure 2. 33: Transmission electron photomicrograph showing a smooth muscle cell in the superficial region of the *tunica albuginea* of a pre-pubertal bird.. 85
Figure 2. 34: Transmission electron photomicrograph showing a fibroblast in the superficial region of the *tunica albuginea* of a pre-pubertal bird. 86

Figure 2. 35: Transmission electron micrograph showing part of a vein located in the *tunica albuginea* of a pre-pubertal bird.. 87
Figure 2. 36: Transmission electron micrograph showing part of a vein located in the *tunica albuginea* of a pre-pubertal bird.. 88
Figure 2. 37: Transmission electron micrograph showing smooth muscle cells in the deeper regions of the *tunica albuginea* of a pre-pubertal bird.. 89
Figure 2. 38: Transmission electron micrograph showing a smooth muscle cell in the deep region of the *tunica albuginea* of a pre-pubertal bird.. 90
Figure 2. 39: Transmission electron micrograph showing part of a smooth muscle cell located in the deep region of the *tunica albuginea* of a pre-pubertal bird. N. 91
Figure 2. 40: Transmission electron micrograph showing fibroblasts in the deep region of the *tunica albuginea* of a pre-pubertal bird.. 92
Figure 2. 41: Transmission electron micrograph of a fibroblast in the deep region of the *tunica albuginea* of a pre-pubertal bird. 93
Figure 2. 42: Transmission electron micrograph of a mesothelial cell in the *tunica serosa* of a pubertal bird..... 95
Figure 2. 43: Transmission electron micrograph of a mesothelial cell in the *tunica serosa* of a pubertal bird..... 96
Figure 2. 44: Transmission electron micrograph of the *tunica albuginea* (superficial region) of a pubertal bird. 97
Figure 2. 45: Transmission electron micrograph of smooth muscle cells in the *tunica albuginea* of a pubertal quail. 98
Figure 2. 46: Transmission electron micrograph of a vein dividing the *tunica albuginea* in a pubertal bird into superficial and deep regions..... 99

Figure 2. 47: Transmission electron micrograph of the testicular capsule and parenchyma of a pubertal bird..... 100
Figure 2. 48: Transmission electron micrograph of a fibroblast in the *tunica albuginea* of a pubertal bird. 101
Figure 2. 49: Transmission electron micrograph of the testicular capsule of an adult bird.. 103
Figure 2. 50: Transmission electron micrograph showing the superficial region of the *tunica albuginea* in an adult bird..... 104
Figure 2. 51: Transmission electron micrograph showing the superficial region of the *tunica albuginea* in an adult bird..... 105
Figure 2. 52: Transmission electron micrograph showing a smooth muscle cell in the superficial region of the *tunica albuginea* in an adult bird.. 106
Figure 2. 53: Transmission electron micrograph of a blood vessel contributing to the venous network in the *tunica albuginea*.. 107
Figure 2. 54: Transmission electron micrograph of smooth muscle cells (Sm) in the *tunica albuginea* (deep region) of an adult bird.. 108
Figure 2. 55: Transmission electron micrograph of a smooth muscle cell in the *tunica albuginea* (deep region) of an adult bird..... 109
Figure 2. 56: Transmission electron micrograph of cells in the deep region of the *tunica albuginea* in an adult bird..... 110
Figure 2. 57: Transmission electron micrograph of the *tunica albuginea* (black bracket) and *tunica vasculosa* (red bracket) of an adult bird. 111
Figure 3. 1. Light photomicrograph of the testicular parenchyma in a pre-pubertal bird. SC:……136

Figure 3. 2. Light photomicrograph of the testicular parenchyma in a pre-pubertal bird. 137
Figure 3. 3. Light photomicrograph of the testicular parenchyma in a pre-pubertal bird.. 138
Figure 3. 4. Light photomicrograph of the testicular parenchyma in a pre-pubertal bird. 139
Figure 3. 5: A light photomicrograph of the testicular parenchyma in a pubertal bird. 140
Figure 3. 6: A light photomicrograph of the testicular parenchyma in a pubertal bird. ST:..... 141
Figure 3. 7: A light photomicrograph of the testicular parenchyma in a pubertal bird.. 142
Figure 3. 8: A light photomicrograph of the testicular parenchyma in a pubertal bird.. 143
Figure 3. 9: A light photomicrograph of the testicular parenchyma in an adult bird. ST:..... 144
Figure 3. 10: A light photomicrograph of the testicular parenchyma in an adult bird. 145
Figure 3. 11: A light photomicrograph of the testicular parenchyma in an adult bird.. 146
Figure 3. 12: A light photomicrograph of the testicular parenchyma in an adult bird. 147
Figure 3. 13: Light photomicrographs showing desmin immunoexpression in the peritubular boundary tissue of pre-pubertal (A), pubertal (B, C), and adult (D, E) quails. A light photomicrograph (F) of the negative control section is included. 150

Figure 3. 14: Light photomicrographs showing the immunolocalization of smooth muscle actin in the peritubular boundary tissue and interstitium of pre-pubertal (A, B), pubertal (C, D), and adult (E, F) quails. A light photomicrograph (G) of the negative control section is included. 153

Figure 3. 15: Light photomicrographs showing tubulin immunostaining in the peritubular boundary tissue of pre-pubertal (A), pubertal (B, C), and adult (D, E) quails. 157

Figure 3. 16: Light photomicrographs showing vimentin immunoexpression in the peritubular boundary tissue and interstitium of pre-pubertal (A), pubertal (B, C), and adult (D, E) quails 160

Figure 3. 17: Light photomicrographs showing collagen type IV immunostaining in the peritubular boundary tissue of pre-pubertal (A, B), pubertal (C, D), and adult (E, F) birds. 164

Figure 3. 18: Light photomicrographs showing fibronectin immunostaining in the peritubular boundary tissue of pre-pubertal (A), pubertal (B, C) and adult (D, E) birds. 167

Figure 3. 19: Light photomicrographs showing laminin immunostaining in the peritubular boundary tissue of pre-pubertal (A, B), pubertal (C, D) and adult (E, F) birds. 170

Figure 3. 20: Transmission electron photomicrograph of the peritubular boundary tissue of a pre-pubertal bird. 174

Figure 3. 21: Transmission electron photomicrograph of the peritubular boundary tissue of a pre-pubertal bird. 175

Figure 3. 22: Transmission electron photomicrograph of the peritubular boundary tissue of a pre-pubertal bird. 176

Figure 3. 23: Transmission electron photomicrograph of the peritubular boundary tissue of a pre-pubertal bird..... 177
Figure 3. 24: Transmission electron photomicrograph of the peritubular boundary tissue of a pre-pubertal bird..... 178
Figure 3. 25: Transmission electron photomicrograph of the peritubular boundary tissue of a pre-pubertal bird..... 179
Figure 3. 26: Transmission electron photomicrograph of the interstitial tissue of a pre-pubertal bird.. 180
Figure 3. 27: Transmission electron photomicrograph of the peritubular boundary tissue of a pubertal bird. 182
Figure 3. 28: Transmission electron photomicrograph of the peritubular boundary tissue of a pubertal bird. 183
Figure 3. 29: Transmission electron photomicrograph of the peritubular boundary tissue of a pubertal bird.. 184
Figure 3. 30: Transmission electron photomicrograph of the peritubular boundary tissue of a pubertal bird.. 185
Figure 3. 31: Transmission electron photomicrograph of an intertubular blood vessel in the interstitial tissue of a pubertal bird. 186
Figure 3. 32: Transmission electron photomicrograph of an intertubular blood vessel in the interstitial tissue of a pubertal bird. 187
Figure 3. 33: Transmission electron photomicrograph of the peritubular boundary tissue of an adult bird 189
Figure 3. 34: Transmission electron photomicrograph of the peritubular boundary tissue of an adult bird.. 190

Figure 3. 35: Transmission electron photomicrograph of the peritubular boundary tissue in an adult bird.. 191
Figure 3. 36: Transmission electron photomicrograph of the peritubular boundary tissue in an adult bird.. 192
Figure 3. 37: Transmission electron photomicrograph of an intertubular blood vessel in an adult bird..... 193
Figure 3. 38: Transmission electron photomicrograph of the peritubular boundary tissue in an adult bird. 194
Figure 3. 39: Transmission electron photomicrograph of the peritubular boundary tissue in an adult bird.. 195
Figure 3. 40: Transmission electron photomicrograph of peritubular boundary tissue in an adult birds..... 196
Figure 3. 41: Transmission electron photomicrograph of an intertubular blood vessel in the peritubular boundary tissue of an adult bird..... 197

List of tables

Table 1. 1: Antibodies used for immunohistochemistry in this study. 15

Table 2. 1: Summary of intensities of cytoskeletal proteins (desmin, smooth muscle actin, tubulin and vimentin,) in the layers of the testicular capsule of pre-pubertal, pubertal, and adult Japanese quails (*coturnix coturnix japonica*).……63

Table 2. 2: Summary of intensities of basement membrane proteins (collagen type IV, fibronectin and laminin) in the layers of the testicular capsule of pre-pubertal, pubertal, and adult Japanese quails (*coturnix coturnix japonica*). 76

Table 3. 1: Antibodies used for immunohistochemistry in this study……..133

Table 3. 2**:** Summary of intensities of cytoskeletal proteins (desmin, smooth muscle actin, tubulin and vimentin) in the cells of the peritubular boundary tissue in pre-pubertal, pubertal, and adult Japanese quails (*coturnix coturnix japonica*). 161

Table 3. 3**:** Summary of intensities of extracellular matrix proteins (collagen type IV, fibronectin and laminin) in the basement membranes of components of the testicular parenchyma in pre-pubertal, pubertal, and adult Japanese quails (*coturnix coturnix japonica*)..... 172

Summary

CHANGES IN THE TESTICULAR CAPSULE AND PERITUBULAR BOUNDARY TISSUE IN PRE-PUBERTAL, PUBERTAL AND ADULT JAPANESE QUAILS (*COTURNIX COTURNIX JAPONICA*)

By

Lindokuhle Innocent Khumalo

Supervisor: Professor Mary-Cathrine N. Madekurozwa (BVSc, BSc (Hons), PhD (UK))

Department: Anatomy and Physiology

Faculty: Veterinary Science

Degree: MSc

The aim of this study was to investigate age-related changes in the morphology of the peritubular boundary tissue and the testicular capsule of pre-pubertal, pubertal, and adult Japanese quails. The peritubular boundary tissue and testicular capsule are involved in the propulsion of spermatozoa from the seminiferous tubules into the excurrent duct system. In addition, the peritubular boundary tissue is thought to contribute to the formation of the blood-testis barrier. The use of transmission electron microscopy, as well as the immunolocalization of key cytoskeletal proteins revealed that the testicular capsule in the Japanese quail was composed predominantly of smooth muscle cells with relatively few fibroblasts. Furthermore, the use of histochemistry demonstrated the presence of collagen and reticular fibres in the testicular capsule, with a few elastic fibres present only in adult quails.

In the current study, the morphology of the peritubular boundary tissue varied with testicular maturation. The results showed a reduction in the number of peritubular cell layers surrounding the seminiferous tubules as the birds matured. In addition, immunohistochemistry revealed age-related changes in the localization of cytoskeletal and basement membrane proteins.

Chapter one:

1.0 General introduction

The testicular capsule and peritubular boundary tissue are important in spermatozoal transport due to their contractile abilities (Rothwell and Tingari, 1973; Rothwell, 1975). The movement of spermatozoa from the seminiferous tubules to the *rete testis* and epididymis is due to the contraction of smooth muscle cells of the *tunica albuginea* (Banks *et al.*, 2006) and peritubular boundary tissue (Hargrove *et al.*, 1977). The contractility can be studied *in vivo*, following the removal of the *tunica albuginea*, or *in vitro* using sections of the seminiferous tubules (Davis and Horowitz, 1978; Ellis *et al.*, 1981). Due to their expression of androgen receptors, peritubular myoid cells or smooth muscle cells of the peritubular boundary tissue also play a role in androgen signaling (Maekawa *et al.*, 1996; Zhou *et al.*, 2002). In addition, they also serve as a barrier to the passage of substances into the germinal epithelium (Dym and Fawcett, 1970).

The testicular capsule is the dense, irregular fibro-elastic connective tissue that covers the testes of mammals (Leeson and Cookson, 1974; Banks *et al.*, 2006) and birds (Aire and Ozegbe, 2007; Hassanzadeh *et al.*, 2014; Dharani *et al.*, 2017). The testicular capsule is generally composed of collagen fibres, a few elastic fibres, fibroblasts, and an abundance of contractile cells (Middendorff *et al.*, 2002; Kannan *et al.*, 2015). Three distinct layers form the testicular capsule: an outer *tunica serosa*, a middle *tunica albuginea,* and an inner *tunica vasculosa* (Middendorff *et al., 2002;* Kannan *et al.,* 2015).

The peritubular boundary tissue is a loose connective tissue that invests the seminiferous tubules of vertebrates (Maekawa *et al*., 1996; Aire, 1997). The peritubular boundary tissue consists of fibrous and cellular layers (Rothwell and Tingari, 1973; Dharani *et al*., 2017). The contractile cell population of the peritubular boundary tissue is composed of peritubular myoid cells, which are also termed "myofibroblasts".

The structure of the testicular capsule and peritubular boundary tissue in adult birds of various species has been studied in detail (Aire and Ozegbe, 2007; Ozegbe *et al*., 2008). In addition, developmental studies, using histochemical (Kannan *et al*., 2015) and immunohistochemical techniques (Madekurozwa, 2013) have been conducted on the testicular capsule and peritubular boundary tissue of the Japanese quail.

Currently a significant amount of research on avian reproductive biology, as well as on the effect of environmental toxins on birds is conducted using the Japanese quail as an avian model (Artoni *et al*., 1999; Halldin, 2005; Aire and Ozegbe, 2007; Ball and Balthazart, 2010; Madekurozwa, 2013; Nunome *et al*., 2017). The Japanese quail (*Coturnix coturnix japonica*) offers several advantages over other avian species due to its ease of breeding, as well as its unique attributes, such as small body size, early maturation, and short generation intervals (Halldin, 2005; Nunome *et al*., 2017). Furthermore, the Japanese quail is an excellent model for data extrapolation and has, to a large extent, replaced the domestic fowl as an avian model in research (Satterlee *et al*., 2002; Kannan *et al*., 2015). However, despite the intensive use of the Japanese quail in research, there is currently a paucity of information on the morphological changes occurring in the testicular capsule and peritubular boundary tissue of this species during sexual maturation. Such information is important as

these two components of the testes are crucial for sperm transportation and may be disrupted by testicular toxins and infectious agents. Therefore, the purpose of the present study was to provide baseline information on changes in the testicular capsule and peritubular boundary tissue of the Japanese quail, during sexual maturation, using histological, immunohistochemical, and ultrastructural techniques. The information gained from this study will provide a morphological baseline for further studies on the effects of environmental toxins on the elements forming the testicular capsule and peritubular boundary tissue of birds.

1.1 Background on the Japanese quail (*Coturnix coturnix japonica*)

The Japanese quail (*Coturnix coturnix japonica*) is a small bird that belongs to the order *Galliformes* and the family *Phasianidae* (Minvielle, 2004). According to Ball and Balthazart (2010) the Japanese quail is morphologically similar to the common quail (*Coturnix coturnix*). Intensive production of Japanese quails began in the 1920's in Japan (Mills *et al.*, 1997). The species was later developed for meat and egg production (Nunome *et al.,* 2017). Quail production subsequently extended across Europe, America, and the Middle East between the 1930's and the 1950's (Minvielle, 2004; Ball and Balthazart, 2010; Nunome *et al.*, 2017).

Japanese quail production has gained popularity in recent years due to the following traits of the birds: fast growth rate; early sexual maturity; short generation interval (3-4 generations/ annum); high egg production rate (300 eggs per year); short egg incubation period, and low vulnerability to common poultry diseases. In addition, the Japanese quail requires a limited floor space (200-250 cm^2 in litter and 150-200 cm^2 in a cage system), and a relatively small amount of feed (20-25 g/adult bird/day).

The reproductive system of the Japanese quail develops rapidly. By day 12 post-hatch, the testes of the Japanese quail contain distinct seminiferous tubules with prominent lumina (Mather and Wilson, 1964). Puberty occurs at approximately 6 weeks of age, while the birds are sexually mature at 10 weeks of age (Marin and Satterlee, 2004; Huss *et al*., 2008). Male Japanese quails are considered to have reached puberty when foam is produced from the cloacal gland (Sezer *et al.*, 2006), and are sexually mature when spermatozoa are present in the epididymis (Nixon *et al.*, 2014). Lighting regimes used in poultry production, as well as natural daylight, have an influence on the growth, sexual maturity attainment, and breeding of the Japanese quail (Artoni *et al*., 1997; Mills *et al.*, 1997). When maintained under long daylength photoperiods Japanese quails reach puberty and sexual maturity earlier than quails raised under short daylength photoperiods (Coban *et al.*, 2009). Long daylengths trigger the rapid production and release of gonadotropins which results in the stimulation of gonadal growth (Mills *et al*., 1997).

In addition to its commercial uses, the Japanese quail is also used as a laboratory animal (Nunome *et al.*, 2017). The Japanese quail is generally regarded as a suitable representative of terrestrial birds and is consequently used as an avian model in toxicological studies (Kendall *et al.*, 1996), neurobiology (Derégnaucourt *et al.*, 2009; Ball and Balthazart, 2010), and genetics (Nunome *et al*., 2017).

1.2. Cells and fibres of connective tissue

1.2.1 Fibroblasts

Fibroblasts are mesenchymal cells that synthesize and remodel extracellular matrices in tissues (Flavell *et al.*, 2008). Fibroblasts primarily produce extracellular matrix proteins, such as collagen types I and III, fibronectin, as well as proteoglycans (Smith, 1993; Martin, 1997; Ebihara *et al.*, 2006). Fibroblasts are interspersed between collagen bundles and form the outermost cellular layer of the peritubular boundary tissue (Davidoff *et al.*, 1990). Morphologically, fibroblasts are generally stellate in shape with attenuated cytoplasmic extensions (Rothwell, 1975). Due to their mesenchymal origin, fibroblasts are vimentin immunopositive (Bucala *et al.*, 1994; Middendorff *et al*., 2002; Madekurozwa, 2013).

Ultrastructural features of fibroblasts in the testicular capsule and peritubular boundary tissue of the turkey, domestic fowl (Rothwell and Tingari, 1973; Rothwell, 1975), Japanese quail (Aire and Ozegbe, 2007) and duck (Aire and Ozegbe, 2007) have been described. Ultrastructurally fibroblasts are characterized by the presence of ovoid nuclei, which contain condensed chromatin (Gorgas and Böck, 1974; Ebihara *et al*., 2006). The cytoplasm of fibroblasts contains abundant rough endoplasmic reticulum, free ribosomes, polyribosomes, lysosomes and Golgi complexes (Gorgas and Böck, 1974).

1.2.2 Fibrocytes

Fibrocytes occur in the peritubular boundary tissue, as well as in the intertubular area (Wrobel *et al*., 1988) of the testis. Histologically, fibrocytes in the peritubular boundary tissue are flat cells with dense nuclei (Wrobel *et al.,* 1988). Ultrastructurally

these cells contain heterochromatic, spindle-shaped nuclei and attenuated cytoplasm with prominent rough endoplasmic reticulum and distinct Golgi complexes (Leeson and Cookson, 1974). Free ribosomes, mitochondria, small pinocytotic vesicles and occasional coated vesicles may also be apparent (Leeson and Cookson, 1974).

1.2.3 Smooth muscle cells

Smooth muscle cells are elongated, fusiform cells with finely tapered ends which occur as bundles or sheets (Michael *et al.*, 1995). Adjacent smooth muscle cells are connected via gap junctions (Michael *et al*., 1995). Smooth muscle cells are characterized by cytoplasm which contains abundant myofilaments and a centrally-positioned nucleus (Sweeney *et al.*, 2006).

When smooth muscle cells are viewed under the light microscope, they show no cross-striations because their myofilaments do not have the same degree of order in their arrangement as skeletal muscle cells (Michael *et al.*, 1995). Smooth muscle cells usually range in length from 20nm (in the walls of small blood vessels) to 200nm (in the walls of the intestine) and contain eosin-stained cytoplasm (Michael *et al.,* 1995). Each smooth muscle cell is encircled by a basement membrane (Sweeney *et al.*, 2006). When smooth muscle cells are viewed under the electron microscope, they show caveolae, which are flask-shaped invaginations (50 to 100nm in diameter) of the plasma membrane (Polyák *et al.*, 2009). Smooth muscle cells have a contractile apparatus of thin and thick filaments and a cytoskeleton of actin and desmin intermediate filaments, which enables them to play a role in contraction (Michael *et al*., 1995).

1.3 Connective tissue fibres

Connective tissue fibre type and content is dependent on the functional and structural needs of the tissue (Michael *et al*., 1995). Connective tissue contains collagen, reticular and elastic fibres in varying proportions (Ushiki, 2002).

1.3.1 Collagen fibres

Collagen is the major structural protein of the extracellular matrix (Ghazanfari *et al.*, 2016). The mechanical properties of a tissue are determined by its collagenous content (Ghazanfari *et al.*, 2016). Collagen fibres are macromolecular in form, flexible and possess great tensile strength (Michael *et al*., 1995). Collagen fibres play an important role in conferring mechanical strength to tissues, such as tendons (Kew *et al.*, 2011). Collagen fibres are classified into five types: type I occurs in skin, tendon, bone, and ligaments; type II is present in cartilage; type III has been identified in skin and embryonic connective tissues; type IV is a component of *basal laminae*, and type V occurs during embryonic development (Smith, 1993).

In general, collagen fibres are tape- or cord-shaped, with wavy, thick strands, which stain pink with the haematoxylin and eosin stain (Ushiki, 2002). Ultrastructurally, collagen fibres are composed of bundles of fine, thread–like subunits known as collagen fibrils (Michael *et al*., 1995; Ushiki, 2002).

1.3.2. Reticular fibres

Using silver impregnation staining techniques, reticular fibres are demonstrated as thin, darkly-stained fibres (Ushiki, 2002). These fibres occur in loose connective tissue, as well as in haemopoietic tissue (Fakoya, 2002). Reticular fibres consist of type III collagen (Michael *et al.*, 1995; Fakoya, 2002). These fibres provide a

supportive framework for the cellular constituents of several tissues and organs (Michael *et al.*, 1995; Fakoya, 2002). Reticular fibres are arranged in a mesh-like pattern and are formed by fibroblasts (Michael *et al*., 1995). The individual collagen fibrils forming reticular fibres are visible ultrastructurally, while thread-like units are observed under the light microscope (Michael *et al*., 1995)

1.3.3 Elastic fibres

Elastic fibres are composed of elastin and microfibrillar glycoproteins (Lannoy *et al.*, 2014). These fibres provide resilience, as well as elasticity to tissues (Lannoy *et al.*, 2014). Elastic fibres impart elasticity to many organs allowing a wide range of deformability and passive recoil without energy inputs (Kielty *et al.*, 2002; Hernández-Morera *et al.*, 2017). Elastic fibres form cords or sheets, which stain purple with recorsin-fuchin stains (Michael *et al.,* 1995; Ushiki, 2002). Elastic fibres are approximately 0.2-1.5 μm in diameter. These fibres occur in either twisted or straight strands that occasionally branch to form a coarse network (Ushiki, 2002). The spatial organization of elastic fibres is vastly variable in the extracellular matrices of different tissues (Lannoy *et al*., 2014).

Elastin assembly occurs extracellularly by elastin-producing cells (Morrione, 1952). The elastin is secreted as a soluble monomer (tropoelastin) which is then cross-linked into a functional polymer (Morrione, 1952). Formation of elastic fibres in early development involves deposition of tropoelastin polymers onto a pre-formed template of microfibrils (Kielty *et al*., 2002).

1.4 Avian testicular anatomy

In contrast to mammals, the testes of birds are retained within the abdominal cavity and are only visible after the thoraco-abdominal cavity has been opened and the gastrointestinal tract reflected (Deviche *et al.*, 2011; Kannan *et al.*, 2015). The testes of most avian species show testicular dimensional asymmetry in adulthood with the left testis being typically larger than the right (Calhim and Montgomerie, 2015). However, the testes of the tree swallow (*Tachycineta bicolor*) and domestic fowl are symmetrical in terms of dimensions (Kempenaers *et al.*, 2002a; Deviche *et al*., 2011). Age-dependent changes in the size, shape, and colour of the testes have been reported in the Japanese quail (Kannan *et al.*, 2015). In immature quails, the testes are small, pointed in shape, and yellow-white in colour, while in mature quails the testes are large, round in shape, and white in colour (Vatsalya and Arora, 2012; Kannan *et al*., 2015).

A histological examination of the testis in the Japanese quail reveals that this organ is a compound tubular gland, enclosed by a dense irregular connective tissue capsule (Deviche *et al*., 2011). The testicular capsule consists of three layers: *tunica vasculosa, tunica albuginea,* and *tunica serosa*. In mammals, connective tissue septa from the *tunica albuginea* divide the parenchyma of the testis into lobules (Abd-Elhafeez *et al.*, 2017). However, in the Muscovy duck (Gerzilov *et al.*, 2016), ostrich (Wang *et al.*, 2009), emu (Rajendranath *et al*., 2016), and greater rhea (Freneau *et al.*, 2016), the testis is not clearly divided into lobules due to the limited interstitial connective tissue septa within the parenchyma .

The testicular parenchyma is composed of two main components, which are the seminiferous tubules and the interstitial tissue (Deviche *et al*., 2011; Campion *et al.*,

2012). The seminiferous tubules, which are the sites of spermatogenesis, form most of the testicular mass in the mature testis (Deviche *et al.*, 2011). Each seminiferous tubule is lined by a seminiferous epithelium, which consists of the male germ cells and Sertoli cells (Jones and Lopez, 2014). The interstitial tissue is sub-divided into the interstitium, which contains Leydig cells (Deviche *et al.*, 2011; Kannan *et al*., 2015), and the peritubular boundary tissue, which is comparable to the *lamina propria* of mammals (Davidoff *et al.*, 1990).

The peritubular boundary tissue surrounds the seminiferous tubules in birds (Rothwell, 1975; Skinner and Fritz, 1985), reptiles (Unsicker and Burnstock, 1975), and mammals (Gröschel-Stewart and Unsicker, 1977; Virtanen *et al.*, 1986; Santamaria *et al.*, 1992; Maekawa *et al.*, 1996). The peritubular boundary tissue is generally composed of inner fibrous and outer cellular layers (Madekurozwa, 2013). The latter layer is characterized by the presence of peritubular myoid cells and fibroblasts. These two cell types are located between collagen bundles (Rothwell and Tingari, 1973; Davidoff *et al.*, 1990; Ozegbe *et al.*, 2008).

1.5 Aim and specific objectives

1.5.1 Aim

The present study aims to compare the morphology of the testicular capsule and peritubular boundary tissue in pre-pubertal, pubertal and adult male Japanese quails (*Coturnix coturnix japonica*).

1.5.2 Specific objectives

1. To study the histology and ultrastructure of the testicular capsule and peritubular boundary tissue in pre-pubertal, pubertal, and adult Japanese quails.
2. To compare the morphometry of the testicular capsule in pre-pubertal, pubertal and adult Japanese quails.
3. To investigate age-related differences in the distribution and staining intensities of cytoskeletal proteins (desmin, smooth muscle actin, tubulin and vimentin) in the cells of the testicular capsule and peritubular boundary tissue using immunohistochemistry.
4. To use immunohistochemistry to determine age-related differences in components (collagen type IV, fibronectin, and laminin) of the basement membranes associated with various structures in the testis.

1.6 Study methodology

1.6.1 Animals and management

A total of 7 pre-pubertal (4 weeks old), 7 pubertal (6-7 weeks old) and 7 adult (12 weeks old) male Japanese quails were used in the present study (Figure 1.1). The birds were maintained in individual cages. The attainment of puberty was determined

as the first day of release of cloacal foam. The bodyweights of the quails were measured prior to decapitation.

Figure 1. 1: Photographs of pre-pubertal (A), pubertal (B) and adult (C) Japanese quails used in the present study.

1.6.2 Necropsy

The thoraco-abdominal cavity of each bird was opened, and the intestinal tract reflected to expose the testes. The testes were then freed from the adherent fat and adjacent connective tissue. Both testes were then individually weighed using a

weighing balance. The mean testicular weights (left and right) for each animal were calculated. The relationship between the left and right testicular weights was also determined, and the gonadosomatic index (GSI) was expressed as the percentage of the total body weight in relation to the testis weight (GSI = [testis weight/ total body weight] × 100). Testicular samples were then collected for light microscopy.

1.6.3 Tissue processing for light microscopy and morphometry

Testicular samples were fixed in 10% buffered neutral formalin for 5 days. Samples were processed for histology using an automated tissue processor (Shandon Excelsior Thermo Scientific, city, Germany). Tissue processing included dehydration in ascending series of alcohol concentrations (50%, 60%, 80%, 95% and 100%), clearance in xylene (two changes), infiltration, as well as embedding using molten paraffin wax. Tissue sections (5 µm thick) were cut, mounted on glass slides, and stained with haematoxylin and eosin. In addition, sections were stained for collagen (Masson trichrome stain. Trichrome stain, ab150686, Abcam), elastic (Verhoeff-Van Gieson stain. Elastic stain kit, ab150667, Abcam), and reticular fibres (Gomori's silver impregnation stain. Reticulum stain kit, ab150684, Abcam). Stained sections were viewed and photographed using an Olympus BX-63 microscope attached to a computer.

The thickness of the testicular capsule and peritubular boundary tissue in 10 random regions of one section per bird was measured using an image analyzer (CellSens dimension software) connected to an Olympus BX-63 microscope.

1.6.5 Immunohistochemistry

The immunostaining technique was performed on 5 µm thick paraffin sections using a Biogenex super sensitive one-step polymer-HRP detection system kit (Emergo Europe, The Hague, The Netherlands). The sections were deparaffinized and endogenous peroxidase activity was blocked, using a 3% (v/v) hydrogen peroxide solution in water for 5 minutes. The slides were then rinsed in a 0.01 M phosphate buffered saline solution (PBS, pH 7.4) for 5 minutes. For antigen retrieval, the sections for desmin, smooth muscle actin, tubulin and vimentin were microwaved for three cycles of 7 minutes each in citrate buffer (pH 6.0), whereas the sections for fibronectin and type IV collagen were microwaved in tris-EDTA buffer (pH 9.0). Thereafter, the sections were allowed to cool for 20 minutes and then rinsed in PBS. Sections for laminin immunohistochemistry were treated with proteinase K (ab64220, Abcam) for 7 minutes at room temperature.

The sections were incubated for 1 hour at room temperature with the primary antibodies against desmin, smooth muscle actin, tubulin, vimentin, laminin, collagen type IV and fibronectin at dilutions detailed in Table 1.0. The slides were then rinsed in PBS and then incubated for 15 minutes with the one-step polymer-HRP reagent (Biogenex, Emergo Europe, The Hague, The Netherlands). Slides were then rinsed in PBS and bound antibody was visualized using a 3,3'-diaminobenzidine tetrachloride solution (Biogenex, Emergo Europe, The Hague, The Netherlands). The sections were counter-stained with Mayer's haematoxylin.

In the negative controls the monoclonal antibodies were replaced with mouse IgG1 (Dakocytomation, Glostrup, Denmark), while the polyclonal antibodies were substituted with rabbit immunoglobulin fraction (Dakocytomation, Glostrup,

Denmark). The negative control reagents were diluted to the same concentration as the primary antibodies. Appropriate positive control sections were used. Variations in the immunostaining of sections used in this study were minor. No background staining was detected in the negative control sections.

On the basis of visual examination, the relative immunointensities were designated as absent (-), weak (+), moderate (++) and strong (+++) as described previously (Madekurozwa and Kimaro, 2006).

Table 1. 1: Antibodies used for immunohistochemistry in this study.

Antibody	Clone	Manufacturer	Antigen retrieval	Dilution PBS
Anti-collagen type IV	Polyclonal rabbit ab6586	Abcam	Tris-EDTA (pH 9.0)	1:100
Anti- desmin	Monoclonal mouse ab6322	Abcam	Citrate buffer (pH 6.0)	1:300
Anti-fibronectin	Polyclonal rabbit ab2413	Abcam	Tris-EDTA (pH 9.0)	1:250
Anti-laminin	Polyclonal rabbit	DakoCytomation, Glostrup, Denmark	Proteinase K (ab64220)	1:50
Anti-smooth muscle actin	Monoclonal mouse 1A4	DakoCytomation, Glostrup, Denmark	Citrate buffer (pH 6.0	1:50
Anti-tubulin	Monoclonal mouse ab44928	Abcam	Tris-EDTA (pH 9.0)	1:500

Anti -vimentin	Monoclonal mouse Vim 3B4	DakoCytomation, Glostrup, Denmark	Citrate buffer (pH 6.0)	1:25

1.6.5 Transmission electron microscopy

The testicular capsule and parenchyma were processed separately for transmission electron microscopy. Tissue samples were placed in 2.5% glutaraldehyde in 0.075M phosphate buffer (pH 7.4) for 24 hours. Thereafter, the tissue samples were post-fixed in 0.5% osmium tetroxide for 2 hours. The tissue samples were then rinsed in phosphate buffer (pH 7.4), dehydrated in a series of ethanol concentrations and embedded in epoxy:resin at a ratio of 1:2 for 1 hour, 1:1 for 2 hours and 100% resin overnight. Semi-thin sections were cut using a diamond knife and stained with toluidine blue. Ultra-thin sections were cut using a diamond knife, stained with lead acetate and counter-stained with uranyl citrate. The samples were viewed with a Philips CM10 transmission electron microscope (FEI, The Netherlands), fitted with an Olympus Mega View III imaging system.

Chapter two:

The testicular capsule of pre-pubertal, pubertal and adult male Japanese quails (*Coturnix coturnix japonica*): a histological, morphometric, immunohistochemical and ultrastructural study.

2.1 Introduction

The testes of mammals (Leeson and Cookson, 1974; Chacon-Arellano and Woolley, 1980) and birds (Aire and Ozegbe, 2007; Madekurozwa, 2013; Kannan *et al*., 2015) are surrounded by a testicular capsule composed of dense irregular connective tissue. The thickness of the testicular capsule is inter- and intra-species dependent, being very thin in birds (Aire and Ozegbe, 2007) and relatively thicker in mammals. The testicular capsule of ratites, such as the ostrich and emu, is thicker than that of *Galloanserae* species, which include the Japanese quail, domestic fowl, duck, and turkey (Aire and Ozegbe, 2007; Ozegbe *et al.*, 2008). The thickness of the testicular capsule tissue increases with age due to a proportional increase in collagen bundles (Kannan *et al.,* 2015).

2.2 Literature review

2.2.1 Composition of the testicular capsule in mammals

Several histological and ultrastructural studies have provided information on the composition and organization of the testicular capsule in mammals, including the human (Leeson and Cookson, 1974; Banks *et al*., 2006), sheep (Chacon-Arellano and Woolley, 1980), pig (Chacon-Arellano and Woolley, 1980), dog (Leeson and

Cookson, 1974), rabbit (Leeson and Forman, 1981), cat (Leeson and Cookson, 1974), rat (Leeson and Cookson, 1974; Banks *et al*., 2006), and mouse (Banks *et al*., 2006). The mammalian testicular capsule is composed of three layers, which are from the exterior to the interior: the *tunica serosa* or *vaginalis*; *tunica albuginea* and *tunica vasculosa* (Leeson and Cookson, 1974; Chacon-Arellano and Woolley, 1980).

The *tunica serosa* is composed of ovoid mesothelial cells (Leeson and Cookson, 1974; Leeson and Forman, 1981). The organelles of the mesothelial cells include numerous mitochondria and short profiles of rough endoplasmic reticulum (Leeson and Forman, 1981). In the testicular capsule of the human, the *tunica serosa* is a visceral peritoneum (epi-orchium), supported by a sub-mesothelial connective tissue layer (Middendorff *et al.*, 2002). The epi-orchium is a single layer of cells, while the sub-mesothelial layer contains fibroblasts and collagen fibres (Middendorff *et al.*, 2002).

Immediately beneath the *tunica serosa* is the *tunica albuginea* which is formed by fibroblasts, contractile cells and dense connective tissue containing collagen and elastic fibres (Leeson and Cookson, 1974). In addition, capillaries, venules, and arterioles are present in the *tunica albuginea* (Leeson and Cookson, 1974). The contractile cells within the *tunica albuginea* have been identified as smooth muscle cells and myofibroblasts (Middendorff *et al*., 2002). These cells are distributed between the fibroblasts and collagen fibres of the *tunica albuginea* (Middendorff *et al*., 2002). The density of smooth muscle cells is species-specific (Leeson and Cookson, 1974). Smooth muscle cells are abundant in the testicular capsules of the dog and cat and less prominent in those of the human and rat (Leeson and Cookson, 1974). Furthermore, the *tunica albuginea* of the pig is less muscular than that of the

horse (Chacon-Arellano and Woolley, 1980). Smooth muscle cells have centrally-located cylindrical nuclei (Banks *et al*., 2006). The cytoplasm of these cells contains numerous dense bodies, myofilaments, dense cell membrane-adherent plaques, and micropinocytotic vesicles (Banks *et al*., 2006).

The innermost layer of the testicular capsule, the *tunica vasculosa*, is composed of sparse collagen fibrils, fibroblasts, as well as numerous capillaries, arterioles, and lymph vessels (Leeson and Cookson, 1974; Ohanian *et al*., 1979).

2.2.2 Composition of the testicular capsule in birds

As in mammals the testicular capsule of birds consists of three layers: the *tunica serosa, tunica albuginea,* and *tunica vasculosa* (Leeson and Cookson, 1974; Chacon-Arellano and Woolley, 1980; Aire and Ozegbe, 2007; Ozegbe *et al*., 2008; Ozegbe *et al*., 2012; Madekurozwa, 2013). The *tunica serosa* is composed of a single layer of squamous or occasionally cuboidal cells, known as the mesothelium (Aire and Ozegbe, 2007; Ozegbe *et al*., 2008; Dharani *et al.,* 2017). The *tunica serosa* resembles the mesothelial cell layer of the peritoneum (Aire and Ozegbe, 2007). The mesothelial cell layer lies on a basement membrane supported by an amorphous tissue layer (Ozegbe *et al*., 2008). The mesothelial cells have heterochromatic irregular-shaped nuclei, which dominate the cytoplasm (Ozegbe *et al.,* 2008; Dharani *et al*., 2017). In the Japanese quail, the nuclei of the mesothelial cells vary in shape according to age from ovoid-shaped (up to 13 days post-hatch), to elongated in 15 to 60-day old quails (Madekurozwa, 2013). Extending from the surfaces of the mesothelial cells are a few short microvilli (Aire and Ozegbe, 2007).

The *tunica albuginea*, which is the middle and thickest layer of the testicular capsule, is situated immediately below the *tunica serosa* (Dharani *et al.,* 2017). Extending from the *tunica albuginea* are septa which in mammals divide the testicular parenchyma into lobules (Kühnel, 2003). Testicular lobules are not observed in the Japanese quail due to the fact that the *tunica albuginea* does not extend septa into the parenchyma (Artoni *et al*., 1999).

In the Japanese quail (Aire and Ozegbe, 2007) and greater rhea (Freneau *et al.*, 2016), the *tunica albuginea* contains a few elastic fibres and numerous collagen fibres, which alternate with smooth muscle cells. In the masked weaver (*Ploceus velatus*), the *tunica albuginea* is a compact layer of collagen with a few fibroblasts and smooth muscle cells (Ozegbe *et al.*, 2012). In the domestic fowl, the *tunica albuginea* is composed of fibroelastic connective tissue in immature birds (6 weeks-old) and dense connective tissue in mature (28 weeks-old) fowls (González-Morán and Soria-Castro, 2010). In Japanese quails, the number of cell layers of the *tunica albuginea* changes with age, being 4-5 cell layers in the 1-to 5-day old quails, 11–13 cell layers in the 7- to 24-day-old quails, and 5–8 cell layers in 31- to 60-day-old quails (Madekurozwa, 2013).

The *tunica vasculosa*, the innermost layer of the testicular capsule, is located adjacent to the testicular parenchyma (Aire and Ozegbe, 2007; Madekurozwa, 2013; Freneau *et al*., 2016; Dharani *et al*., 2017). The demarcation between the *tunica vasculosa* and *tunica albuginea* is ill-defined (Dharani *et al*., 2017). The *tunica vasculosa* consists of blood vessels, fibroblasts, and loose connective tissue (Aire and Ozegbe, 2007; Dharani *et al.,* 2017). The blood vessels of the *tunica vasculosa* are present from day 7 post-hatch in quails and increase as the bird matures (Madekurozwa, 2013; Kannan *et al.,* 2015).

2.2.3 Cytoskeletal proteins in the testicular capsule

According to Devkota and co-workers (2006a, b) the cytoskeleton is a framework of active cytosolic proteins composed of microfilaments (smooth muscle actin), intermediate filaments (cytokeratin, desmin and vimentin), and microtubules (tubulin). These cytoskeletal proteins are present in several testicular cell types, including Sertoli cells (Steinert *et al.*, 1984; Wang, 1985), peritubular myoid cells (Virtanen *et al*., 1986), and Leydig cells (Ortega *et al.*, 2004). Cytoskeletal proteins play important roles in cell structure and function. These functions include: maintenance of cell polarity and shape; arrangement of intracellular organelles; formation of cytoplasmic extensions, and adhesion of organelles to the plasma membrane (Hess and França, 2005).

Specific antibodies against cytoskeletal proteins have been used to visualize their distribution in different cells at the light microscopic level (Steger *et al.*, 1994; Devkota *et al.*, 2006a, b; Aire and Ozegbe, 2007; Ozegbe *et al*., 2008; Madekurozwa, 2013). The immunohistochemical localizations of the cytoskeletal proteins, smooth muscle actin, desmin and vimentin, have been demonstrated in the smooth muscle cells of the testicular capsule in birds (Aire and Ozegbe, 2007; Ozegbe *et al*., 2008; Ozegbe *et al.,* 2012; Madekurozwa, 2013), rats (Maekawa *et al*., 1996), sheep (Steger and Wrobel, 1994), and cattle (Devkota *et al*., 2006a, b).

Smooth muscle actin is present in all smooth muscle and myoepithelial cells (Skalli *et al.*, 1989). Smooth muscle actin is used to differentiate between smooth muscle cells and fibroblasts in normal and pathological tissues (Skalli *et al.*, 1986). The occurrence of smooth muscle actin expression has been correlated with testicular maturation in the mammalian testis (Steger and Wrobel, 1994). Holt *et al*. (2004)

opined that smooth muscle actin expression was a crucial marker of sexual development that could be used as a grouping parameter for the identification of individuals at different stages of testicular development. In addition, the emergence of smooth muscle actin expression in peritubular myoid cells has been correlated with the increase in testis weight and seminiferous tubule diameter (Skalli *et al.,* 1986; Holt *et al.*, 2004).

Desmin is a muscle-specific cytoskeletal protein and is known to be a principal subunit of intermediate filaments in smooth, cardiac, and skeletal muscle (Anthony and Skinner, 1989; Paulin and Li, 2004). This cytoskeletal protein forms a supportive latticework, from the sarcolemma to nuclear envelope, which stabilizes myofibrils and the nucleus (McLendon and Robbins, 2011). Desmin immunoreactivity has been demonstrated in the *tunica albuginea* of the testicular capsule, as well as in the peritubular boundary tissue of the turkey, duck, fowl (Aire and Ozegbe, 2007), Japanese quail (Aire and Ozegbe, 2007; Madekurozwa, 2013), and masked weaver (Ozegbe *et al*., 2012). Furthermore, desmin is used as a marker for peritubular cell differentiation (Anthony and Skinner, 1989).

Vimentin is expressed by cells of mesenchymal origin which include peritubular myoid cells, fibroblasts, and Sertoli cells (Steger *et al.,* 1994). The intensity of vimentin is highest towards the apical region of the cell and around the nucleus (Steger *et al.*, 1994; Lydka *et al.*, 2011).

Microtubules are essential for cell division (Charles, 1996). The microtubule α-tubulin is prominent in the cytoplasm of spermatogonia, spermatids (Holt *et al*., 2004), and Sertoli cells (Steger *et al*., 1994). α-tubulin is used as a marker in investigations on changes in Sertoli cell size and shape (Steger *et al*., 1994).

2.2.4 Functionality of the testicular capsule in mammals and birds

The testicular capsule provides protection and structural support to the testicular parenchymal tissue (Leeson and Forman, 1981). In addition, the testicular capsule is associated with the establishment of the appropriate intra-testicular pressure to maintain fluid homeostatis within the testis (Leeson and Forman, 1981). Furthermore, the capsule is involved in a spermatozoal propelling mechanism, which is vital in the transportation of semen into the excurrent duct system (Davis *et al*., 1970ab; Davis and Horowitz, 1978; Ellis *et al.,* 1981). The *tunica albuginea* is central to the functionality of the spermatozoal propelling mechanism in mammals. Smooth muscle cells are abundant in the *tunica albuginea* of the testicular capsule in various mammals, such as, the pig, horse, and sheep (Chacon-Arellano and Woolley, 1980), as well as in birds including the Japanese quail (Aire and Ozegbe, 2007; Ozegbe *et al*., 2008; Madekurozwa, 2013), guinea fowl (Dharani *et al*., 2017), duck (Gerzilov *et al*., 2016), and greater rhea (Freneau *et al*., 2016). The contractility of smooth muscle cells has been investigated *in vitro* using strips of *tunica albuginea* isolated from various regions of the testis (Ohanian *et al*., 1979). Maximum contractility was recorded in the posterior border region of the testis, which contained numerous smooth muscle cells (Ohanian *et al*., 1979).

Although the role of smooth muscle cells in the spermatozoal propelling mechanism of mammals has been well-defined, little is known about the possible components of this apparatus in birds. In addition, there is a lack of information regarding the differentiation of smooth muscle cells in the testicular capsule during sexual maturation in birds. Therefore, the purpose of the present study was to investigate morphological changes of the components of the testicular capsule in the Japanese

quail during sexual maturation. It is envisaged that the results of this study will provide baseline information on the possible cellular components involved in the spermatozoal propelling mechanism in birds.

2.3 Materials and methods

2.3.1 Light microscopy and morphometry

Testicular tissue was fixed in 10% buffered neutral formalin for 5 days. After fixation, the samples were routinely processed for histology and embedded in paraffin wax. Tissue sections (5 µm thick) were cut, mounted on glass slides, and stained with haematoxylin and eosin. Further sections were stained for collagen (Masson trichrome stain. Trichrome stain, ab150686, Abcam), elastin (Verhoeff-Van Gieson stain. Elastic stain kit, ab150667, Abcam), and reticular fibres (Gomori's silver impregnation stain. Reticulum stain kit, ab150684, Abcam). Stained sections were then viewed and photographed using an Olympus BX-63 microscope attached to a computer. The thickness of the testicular capsule in 10 random regions of one section per bird was measured using an image analyzer (CellSens dimension software) connected to an Olympus BX-63 microscope.

2.3.2 Immunohistochemistry

The immunostaining technique was performed on 5 µm thick paraffin sections using a Biogenex super sensitive one-step polymer-HRP detection system kit (Emergo Europe, The Hague, The Netherlands). Antibodies against cytoskeletal proteins (desmin, smooth muscle actin, tubulin and vimentin) and basement membrane

components (collagen type IV, fibronectin and laminin) were used. The immunostaining procedure is detailed in chapter one.

2.3.3 Transmission electron microscopy

Small pieces of testicular capsule were fixed for 24 hours in 2.5% glutaraldehyde in 0.075M phosphate buffer (pH 7.4). Thereafter, the tissue samples were post-fixed in 0.5% osmium tetroxide for 2 hours. After post-fixation, tissue samples were routinely processed for transmission electron microscopy. The sections were examined using a Phillips CM10 transmission electron microscope (Phillips Electron Optical Division, Eindhoven, The Netherlands), operated at 80kV. A megaview III side-mounted digital camera (Olympus Soft Imaging Solutions GmbH, Munster, Germany) was used to capture the images and iTEM software (Olympus Soft Imaging Solutions GmbH, Munster, Germany) was used to adjust the brightness and contrast.

2.3.4 Statistical analysis

Statistical analysis was performed using the statistical software package IBM SPSS (version 25.0, SPSS Inc., Chicago, USA). One-way ANOVA was used to assess significant differences between all age groups after testing for variance homogeneity and normality. Statistical differences between different age groups were achieved using the Tukey's Multiple Comparison Test. The level of statistical significance was set at $p < 0.05$.

2.4 Results

2.4.1 Gross morphology

In pre-pubertal birds, the testes were small, elongated to ovoid in shape and cream in colour (Figure 2.1). The testes at this stage of development were in contact with the apical extremities of the cranial divisions of the kidneys (Figure 2.1).

The testes of pubertal (Figure 2.2) and adult (Figure 2.3) birds were large, round in shape and yellow in colour. Branches of testicular blood vessels ramified over the surfaces of the testes. In pubertal and adult quails, the testes occupied approximately a third of the thoraco-abdominal cavity and covered the cranial, middle and part of the caudal divisions of the kidneys.

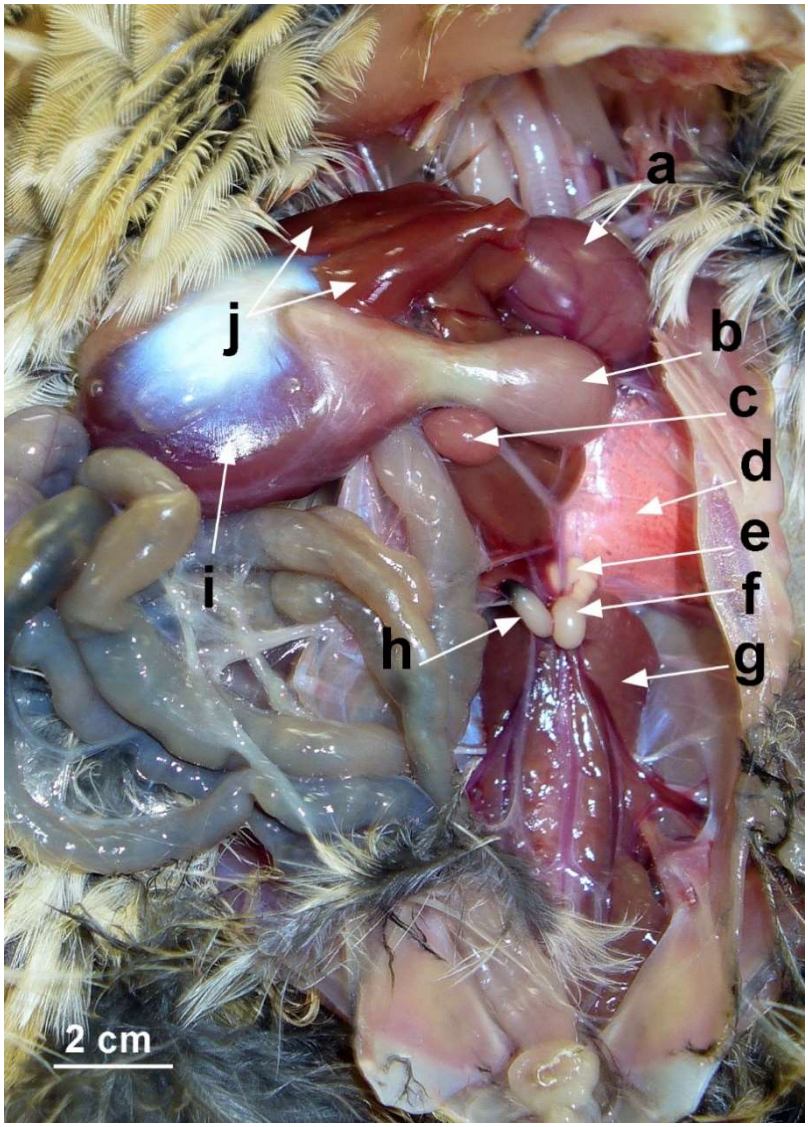

Figure 2. 1: Photograph of the *in situ* position of the testes in a pre-pubertal Japanese quail. a: heart. b: proventriculus. c: spleen. d: lung. e: adrenal gland. f: left testis. g: kidney. h: right testis. i: gizzard. j: liver.

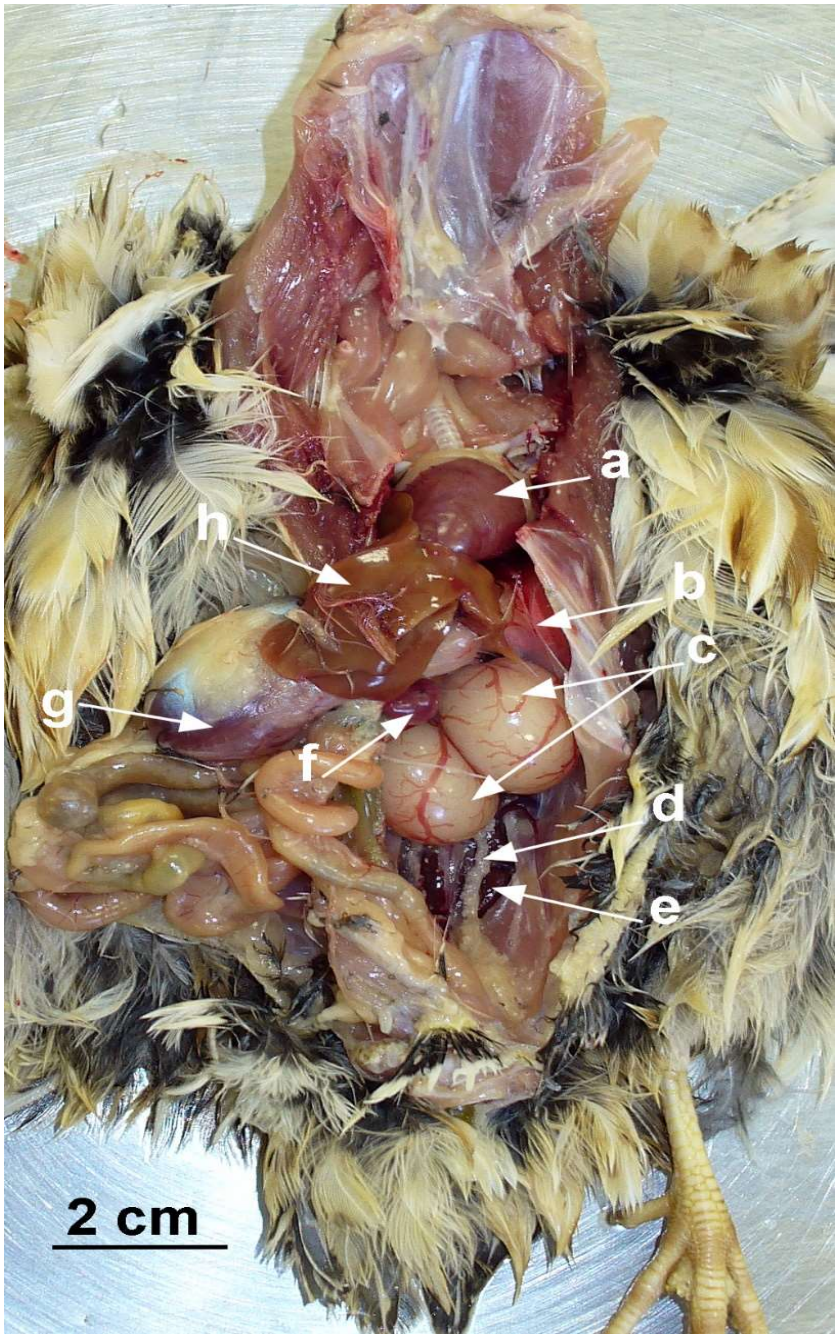

Figure 2. 2: Photograph of the *in situ* position of the testes in a pubertal Japanese quail. a: heart. b: lung. c: testes. d: *ductus deferens*. e: kidney. f: spleen. g: gizzard. h: liver.

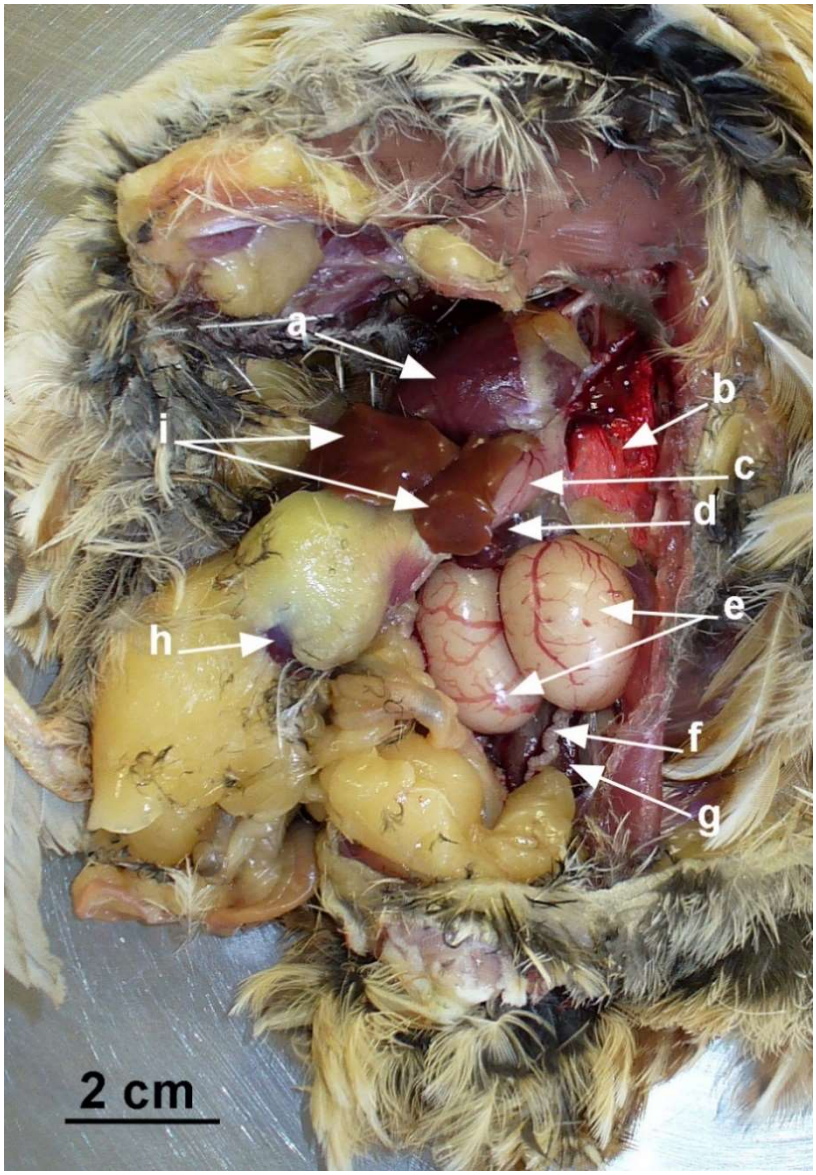

Figure 2. 3: Photograph of the *in situ* position of the testes in an adult Japanese quail. a: heart. b: lung. c: proventriculus. d: spleen. e: testes. f: *ductus deferens*. g: kidney. h: gizzard. i: liver.

2.4.2 Gross parameters: statistical analysis

In order to test the relationship between age and biometric parameters (i.e. body weight and testicular weights), as well as between age and testicular capsule thickness, one-way analysis of variance (ANOVA) and Kruskal-Wallis tests were

performed accordingly. Prior to ANOVA and Kruskal-Wallis analysis, a test for normality was performed. The homogeneity of variance was also determined. Pearson's correlation (*r*) was used to determine whether there was a correlation between age and testicular weight, as well as between body weight and testicular weight.

2.4.2.1 Biometric parameters

The biometric parameters (bodyweight, testicular weight, and gonadosomatic indices) of pre-pubertal, pubertal and adult Japanese quails are shown in Figures 2.4, 2.5, and 2.7. The normality test indicated that the data for bodyweight, absolute left testicular weight, relative left testicular weight, and the gonadosomatic index was normally distributed ($p>0.05$), whereas the data for absolute right testicular weight and relative right testicular weight was not normally distributed ($p<0.05$). Consequently, the data for bodyweight, absolute left testicular weight, relative left testicular weight, and the gonadosomatic index was analysed using one-way ANOVA, while the data for absolute right testicular weight and relative right testicular weight was analysed using the Kruskal-Wallis test. The variances of the relative left testicular weight and the gonadosomatic index were homogenous ($p>0.05$), while the variances of bodyweight and absolute left testicular weight were non-homogenous ($p<0.05$).

One-way ANOVA indicated that the differences in mean bodyweights, gonadosomatic indices, and absolute left testicular weights were statistically significant ($p<0.05$) between pre-pubertal, pubertal and adult birds. There was a

statistically significant (p<0.05) difference in mean relative left testicular weight between pre-pubertal and adult birds. The Kruskal-Wallis test showed a statistical significance difference (p<0.05) in mean absolute right testicular weight and relative right testicular weight between pre-pubertal and adult birds. The mean absolute right testicular weight between pre-pubertal and pubertal birds was not statistically significant (p<0.05). The mean relative testicular weight between pre-pubertal and pubertal birds was statistically significant (p<0.05). The statistically significant differences between the age groups are shown in Figures 2.4, 2.5, 2.6 & 2.7. The bodyweight, absolute testicular weights (left and right) and gonadosomatic index significantly (p<0.05) increased from pre-pubertal to pubertal and adult birds. With the exception of pubertal birds, the left testis was significantly larger (p<0.05) than the right one. However, the right testis was significantly (p<0.001) more positively correlated (r = 0.904) to bodyweight than the left testis (r = 0.884). Similarly, the right testis was significantly (p<0.001) more positively (r = 0.915) correlated to age than the left testis (r = 0.831).

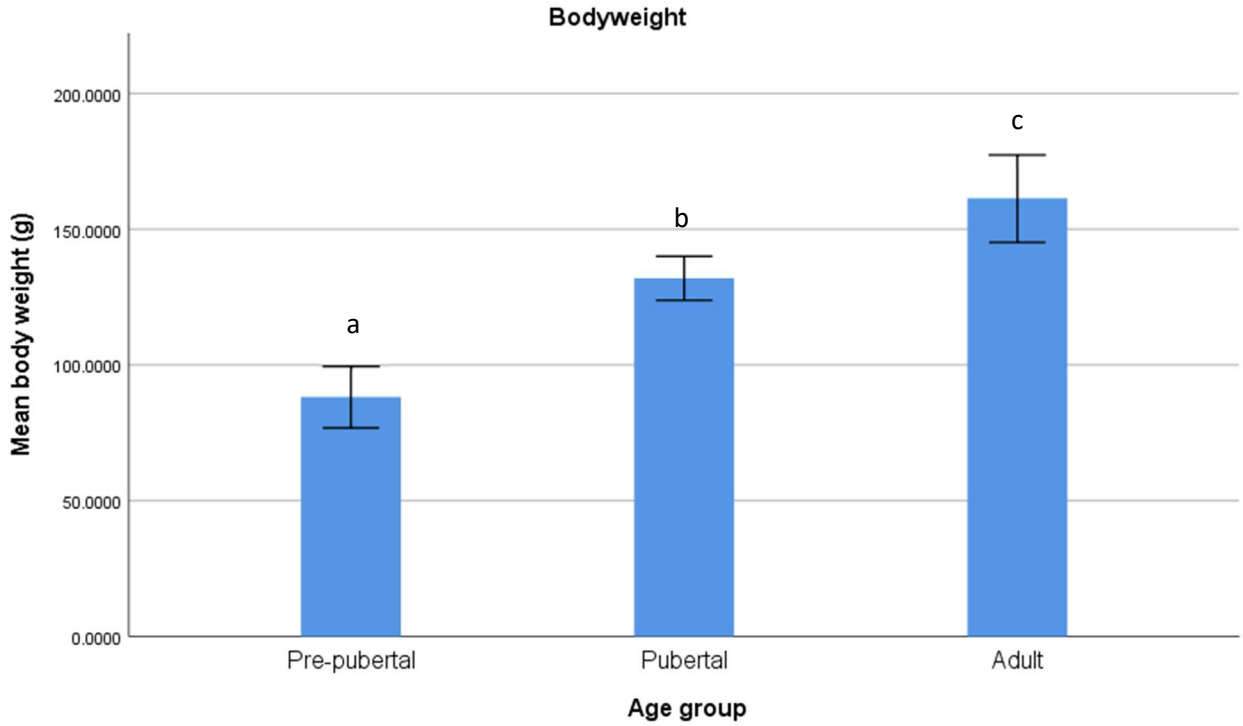

Figure 2. 4: The mean bodyweights of pre-pubertal, pubertal, and adult male Japanese quails. [abc]Bars with different letters are significantly (p<0.05) different from each other.

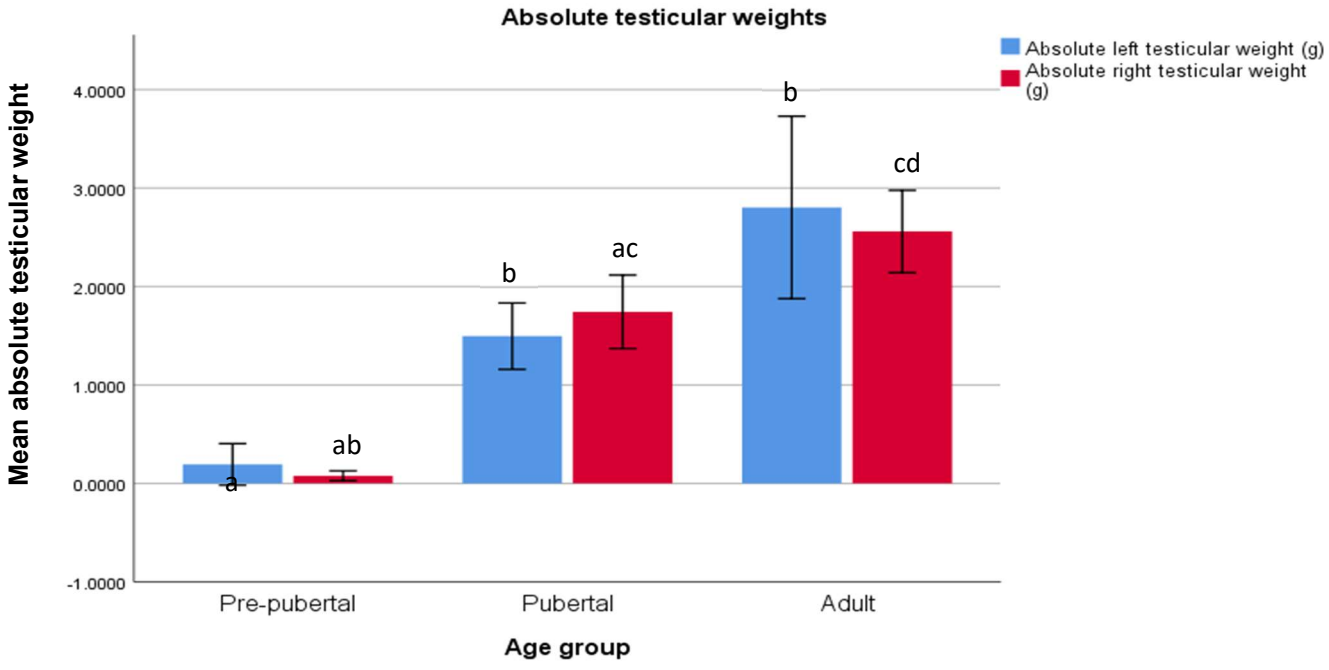

Figure 2. 5: The mean absolute testicular weights of pre-pubertal, pubertal, and adult male Japanese quails. [abcd]Bars with different letters are significantly (p<0.05) different from each other.

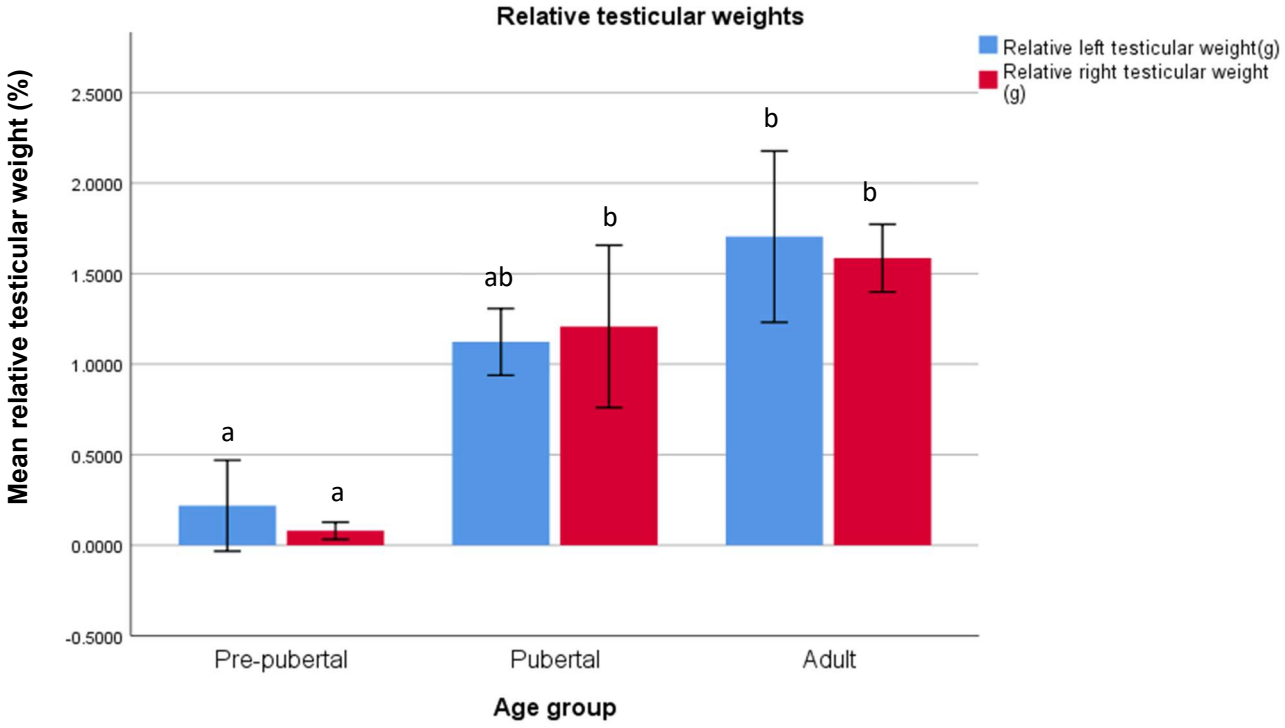

Figure 2. 6: The mean relative testicular weights of pre-pubertal, pubertal, and adult male Japanese quails. [abc]Bars with different letters are significantly (p<0.05) different from each other.

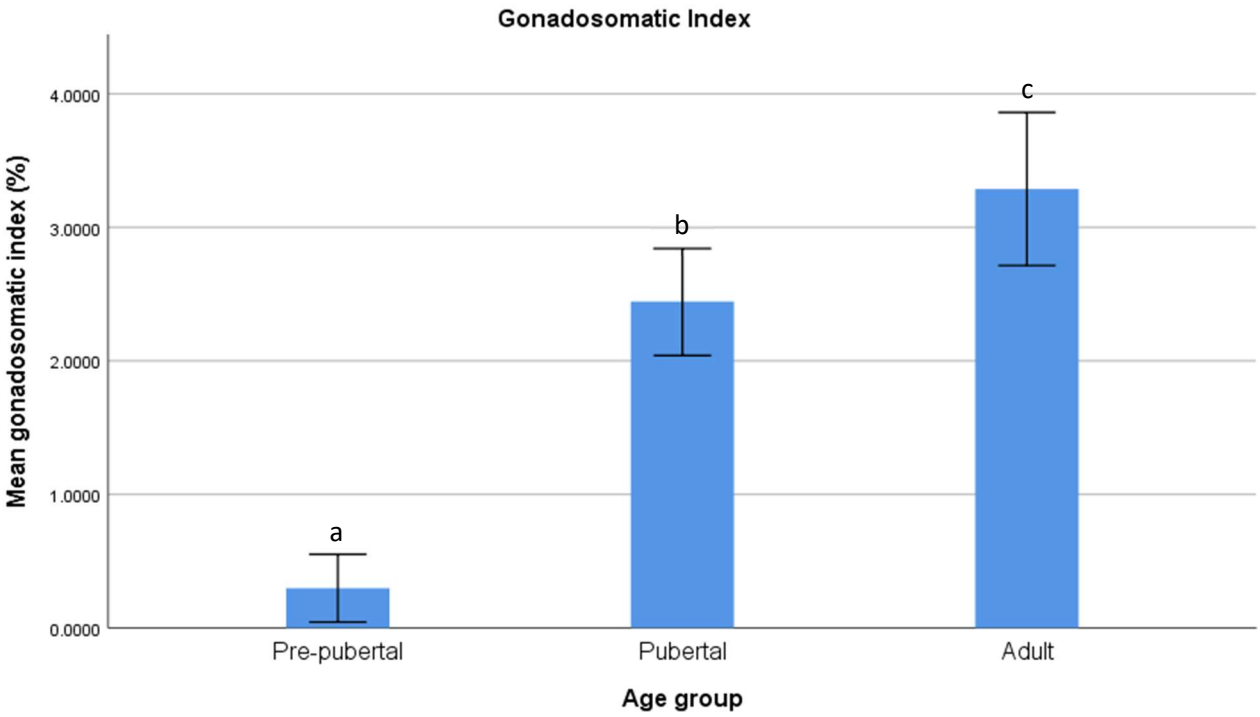

Figure 2. 7: The gonadosomatic index (GSI) of pre-pubertal, pubertal, and adult male Japanese quails. [abc]Bars with different letters are significantly (p<0.05) different from each other.

2.4.2.2 Testicular capsule thickness

In the current study, the testicular capsule thickness was measured with a computer-assisted image analyzer. The thicknesses of the testicular capsules in pre-pubertal, pubertal and adult Japanese quails are shown in Figure 2.8. All the data were recorded as mean ± standard error. The normality test showed that the data for testicular capsule thickness was not normally distributed (p<0.05). Therefore, the Kruskal-Wallis test for non-parametric data was used to analyse the data.

The Kruskal-Wallis test showed a statistically significance difference (p<0.05) in mean testicular capsule thickness between pre-pubertal and pubertal, as well as between pre-pubertal and adult birds. The decrease in the thickness of the testicular capsule from pre-pubertal to pubertal and adult age groups was significant (p<0.05) as shown in Figure 2.8. The testicular capsule in pre-pubertal birds was approximately double the thickness of that in pubertal and adult quails.

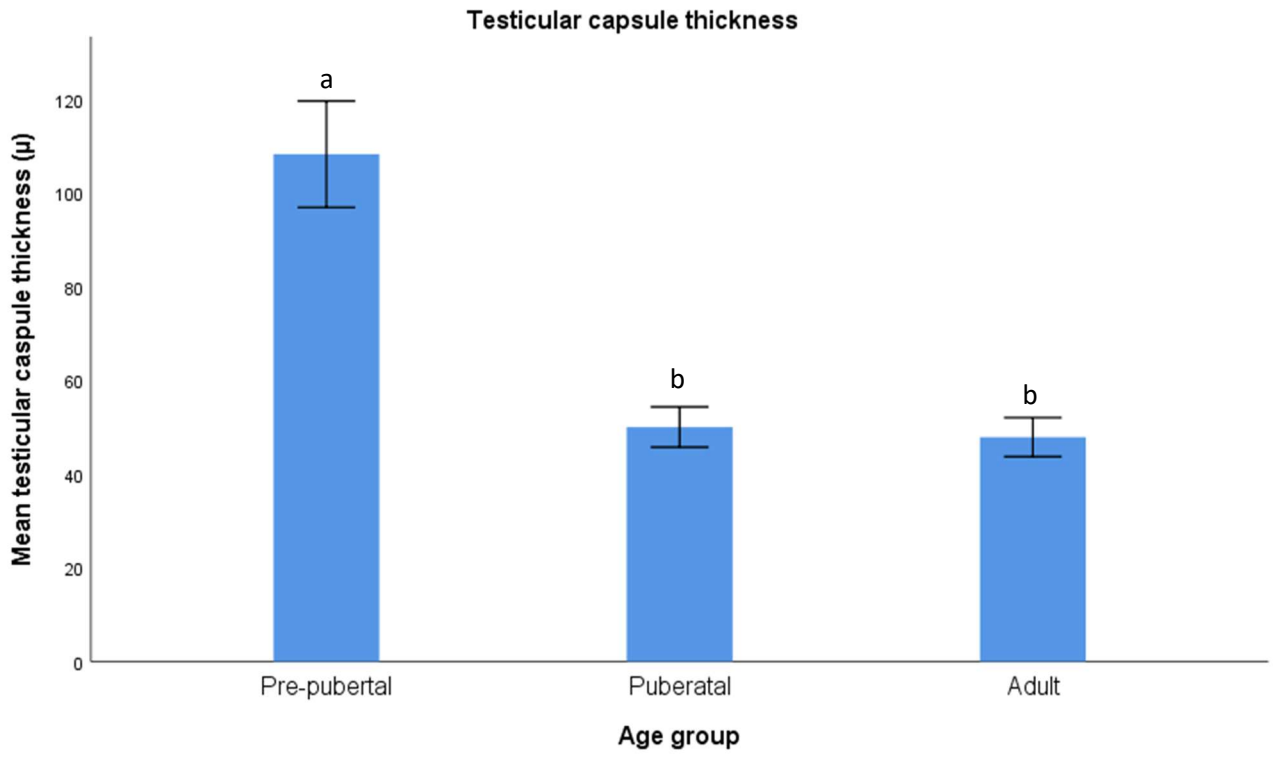

Figure 2. 8: The mean testicular capsule thickness of pre-pubertal, pubertal, and adult male Japanese quails. [abc]Bars with different letters are significantly (p<0.05) different from each other.

2.4.3. Testicular architecture of the Japanese quail (*Coturnix coturnix japonica*).

In all birds studied, the testes comprised of testicular parenchyma enclosed in a capsule (Figures 2.9, 2.10 & 2.11). The testicular capsule was composed of three layers: an outermost *tunica serosa*, a middle *tunica albuginea*, and an innermost *tunica vasculosa.* The testicular parenchyma was composed of a tubular compartment, peritubular boundary tissue, and an interstitium. The tubular compartment contained seminiferous tubules which were surrounded by peritubular boundary tissue composed of connective tissue and peritubular cells (detailed in chapter 3). In pre-pubertal birds, the seminiferous tubules were small and round, whereas in pubertal and adult birds they were large and had a hexagonal conformation. The interstitium contained connective tissue, Leydig cells, and blood vessels.

2.4.4 Light microscopy

In all age groups, the testicular capsule was formed by an outer *tunica serosa,* a middle *tunica albuginea* and an inner *tunica vasculosa* (Figures 2.9, 2.13 & 2.16)

Pre-pubertal birds

The *tunica serosa* was composed of a single layer of mesothelial cells with an underlying layer of connective tissue (Figures 2.9 & 2.10). The nuclei of the mesothelial cells were oblong- or oval-shaped (Figure 2.9). A well-defined layer of reticular fibres was associated with the basement membrane of the mesothelial cell layer (Figure 2.11). Situated below the *tunica serosa* was the *tunica albuginea* which was composed of a few collagen, and reticular fibres in addition to numerous

fibroblasts and smooth muscle cells (Figures 2.9, 2.10 & 2.11). This layer did not appear to contain elastic fibres (Figure 2.12). The *tunica albuginea* formed the largest portion of the testicular capsule. Immediately below the *tunica albuginea* was a poorly defined *tunica vasculosa* which was formed by a few blood vessels (Figure 2.9).

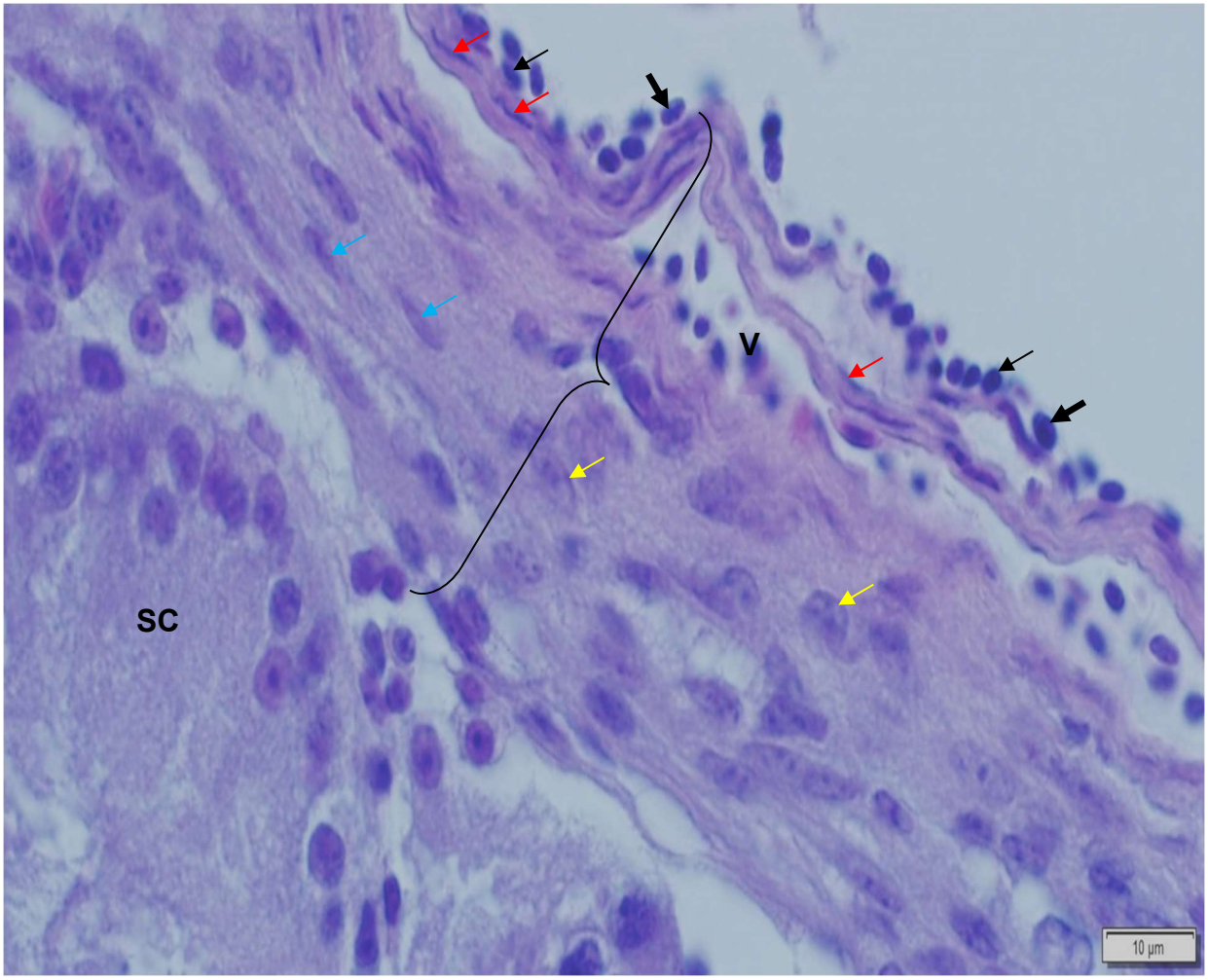

Figure 2. 9: Light photomicrograph of the testicular capsule of a pre-pubertal Japanese quail. Thick black arrows: oblong-shaped nuclei of mesothelial cells. Thin black arrows: oval-shaped nuclei of mesothelial cells. Red arrows: elongated nuclei of vascular smooth muscle cells forming the *tunica media* of a vein (V) in the superficial region of the *tunica albuginea* (bracket). Blue arrows: smooth muscle cells

in the deep region of the *tunica albuginea*. Yellow arrows: fibroblasts. SC: seminiferous cord. Haematoxylin and eosin stain.

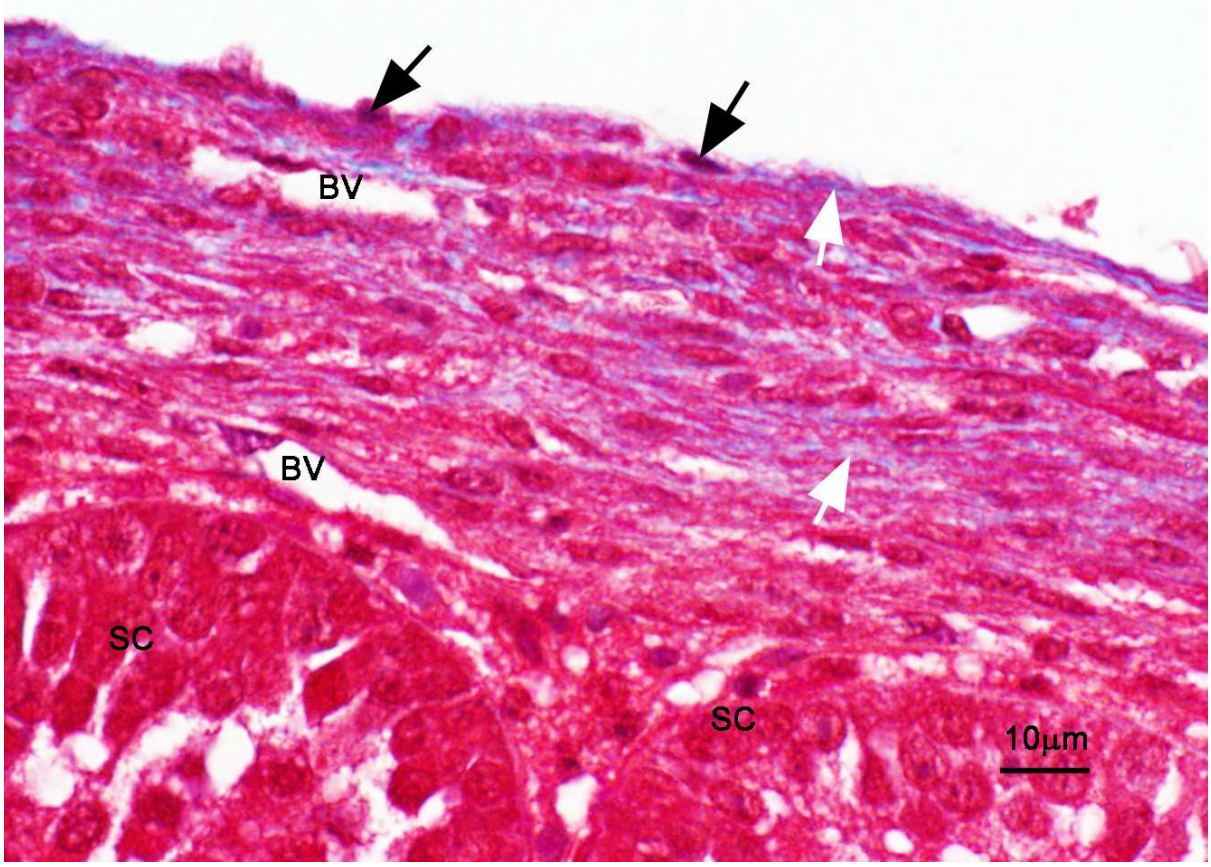

Figure 2. 10: Light photomicrograph of the testicular capsule of a pre-pubertal Japanese quail. Black arrows: mesothelial cells. White arrows: collagen fibres. SC: seminiferous cords. BV: blood vessels. Masson trichrome stain.

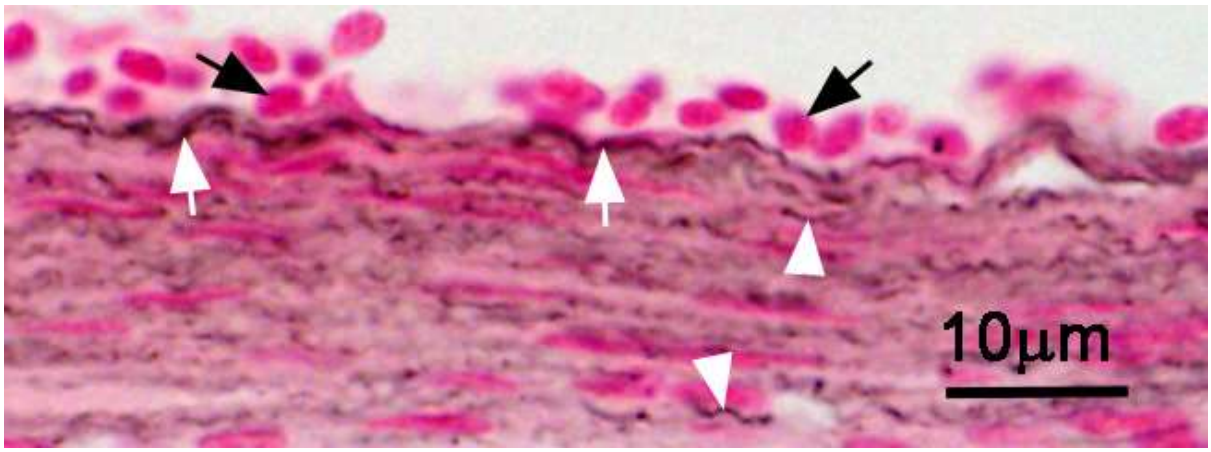

Figure 2. 11: Light photomicrograph of the testicular capsule of a pre-pubertal Japanese quail. Black arrows: mesothelial cells. White arrows: reticular fibres associated with the basement membrane of the mesothelial cells. Arrowheads: reticular fibres in the tunica albuginea. Gomori's silver impregnation stain.

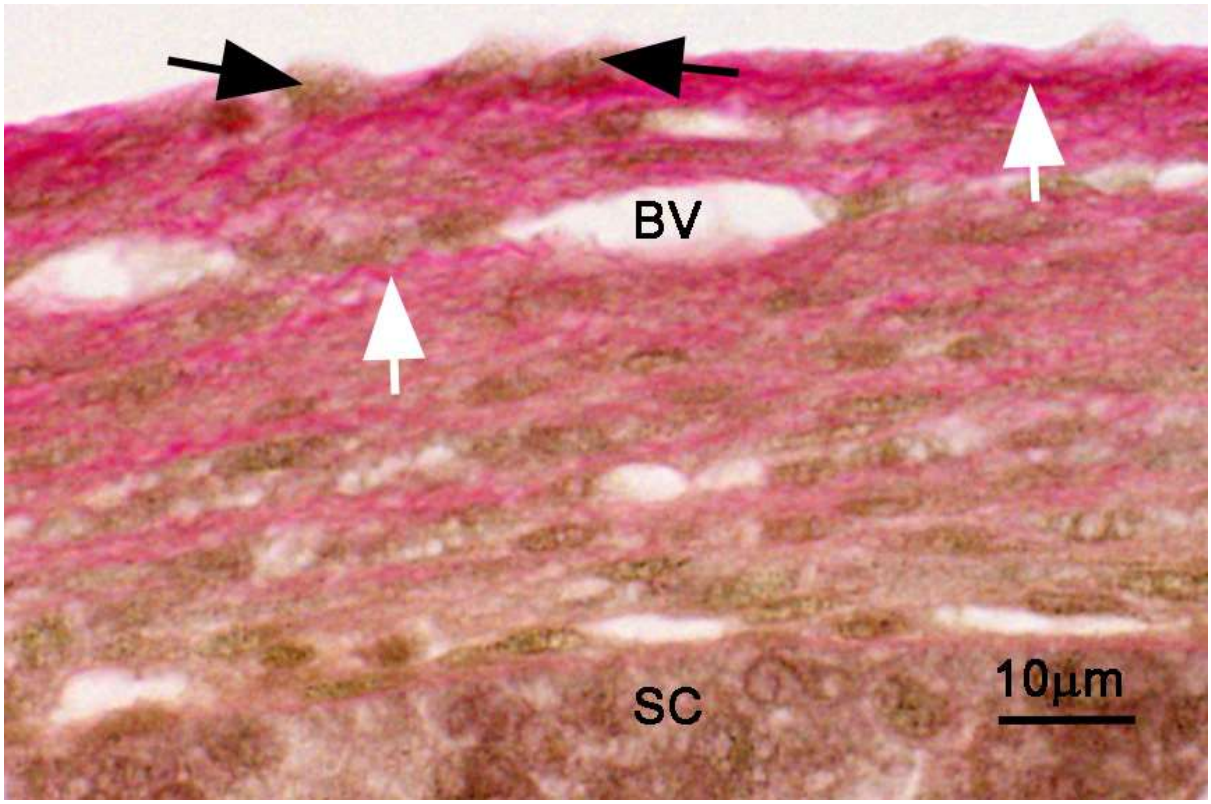

Figure 2. 12: Light photomicrograph of the testicular capsule of a pre-pubertal Japanese quail. Black arrows: mesothelial cells. White arrows: collagen fibres. BV: blood vessel. SC: seminiferous cord. Verhoeff-Van Gieson stain.

Pubertal birds

The *tunica serosa* was formed by mesothelial cells displaying a combination of oval-shaped (Figure 2.13 A) and elongated nuclei (Figure 2.13 B). Below the *tunica serosa* was the *tunica albuginea* which contained collagen fibre bundles (Figure

2.14), reticular fibres (Figure 2.15), but no distinct elastic fibres. Interspersed between the collagen and reticular fibres were a few smooth muscle cells (Figures 2.13 A & B) and occasional fibroblasts. The *tunica albuginea* was divided by a venous network into superficial and deep regions. The *tunica vasculosa* was located between the *tunica albuginea* and testicular parenchyma. Blood vessels and scant loose connective tissue formed the *tunica vasculosa*.

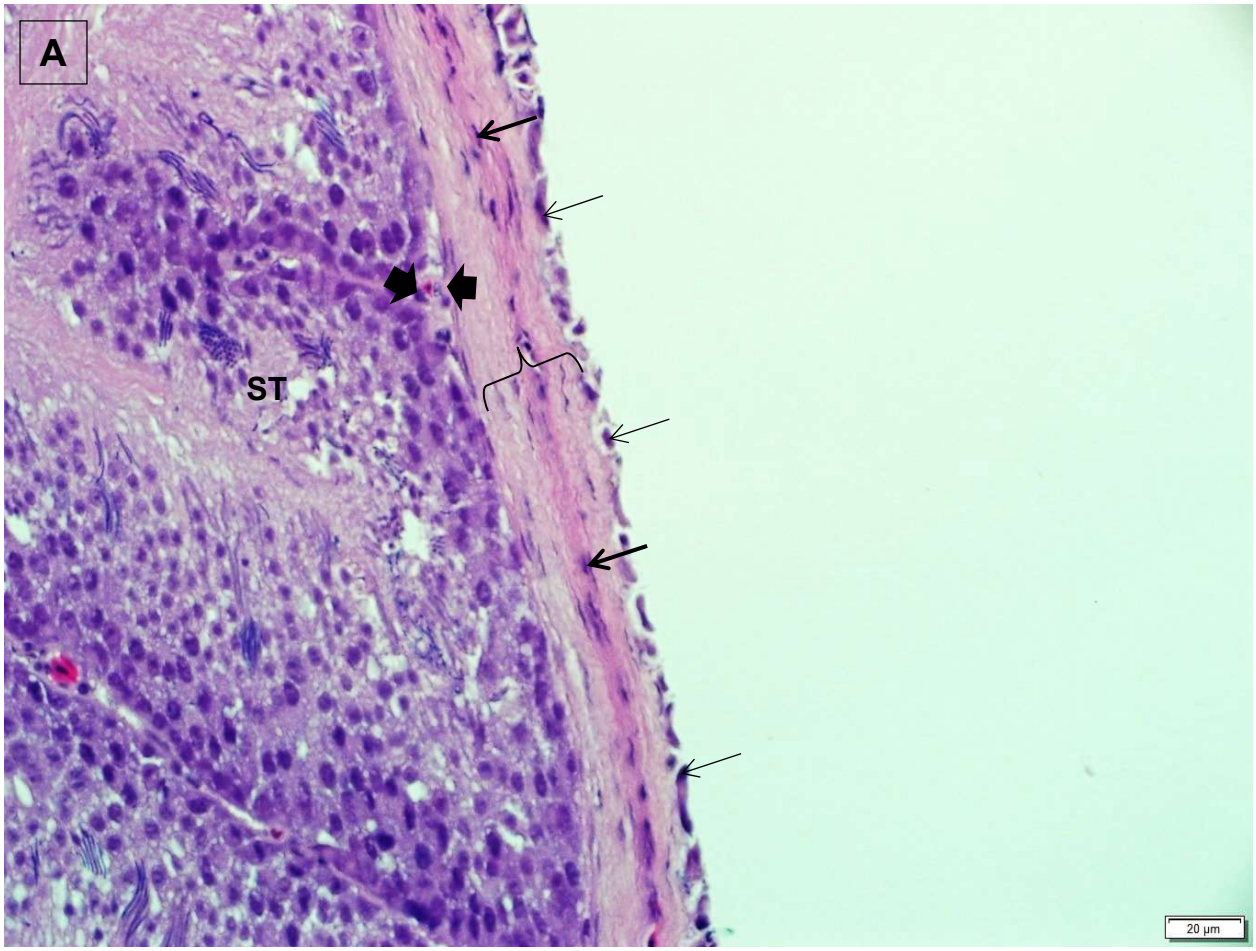

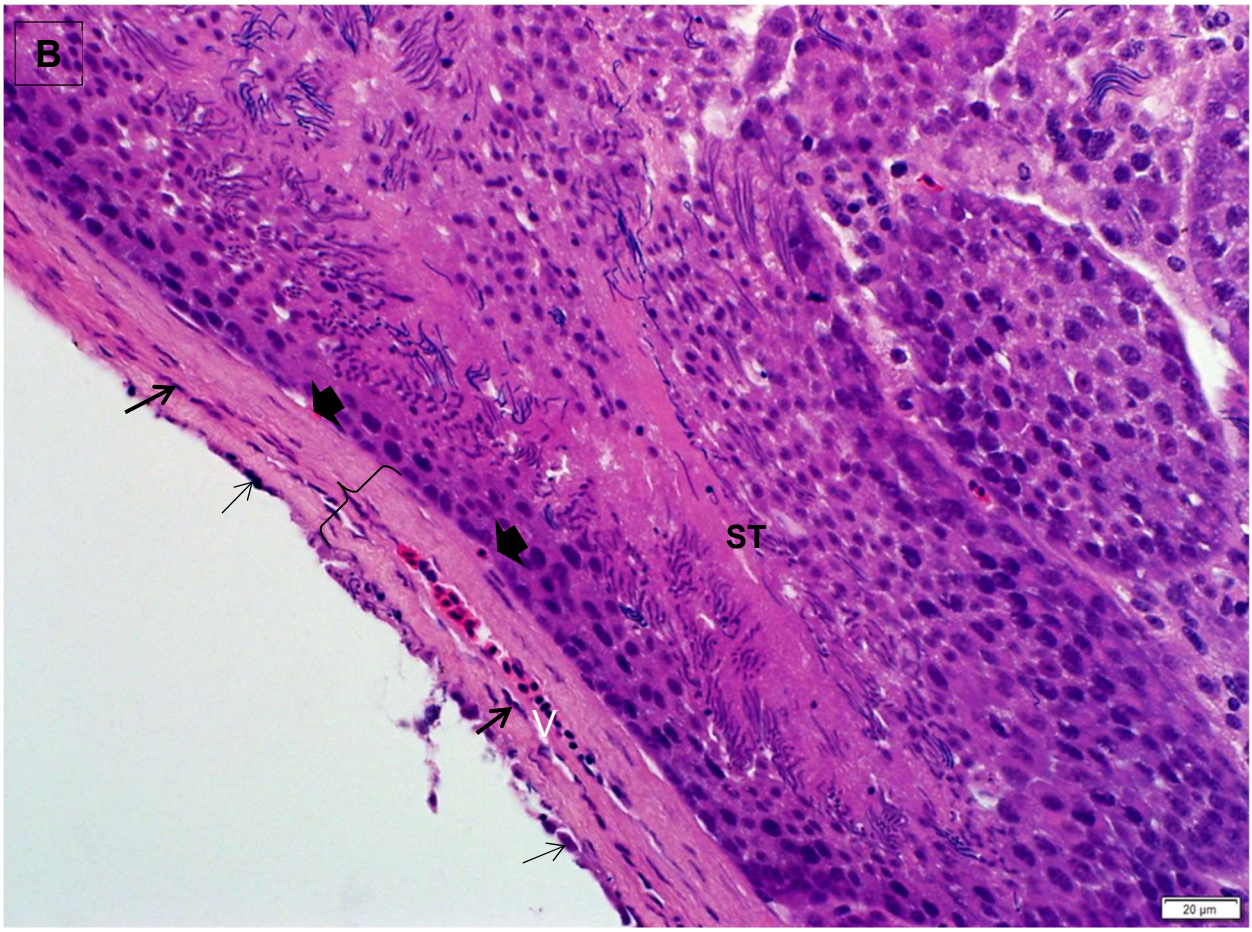

Figure 2. 13: Light photomicrographs (A, B) of testicular capsules from pubertal Japanese quails. Thin arrows: oval and elongated nuclei of mesothelial cells in the *tunica serosa*. Thick arrows: smooth muscle cells forming the wall of a vein (V) in the *tunica albuginea* (brackets). Arrowheads: poorly differentiated *tunica vasculosa*. Note the vein (V) in B which subdivides the *tunica albuginea* into superficial and deep regions. ST: seminiferous tubules. Haematoxylin and eosin stain.

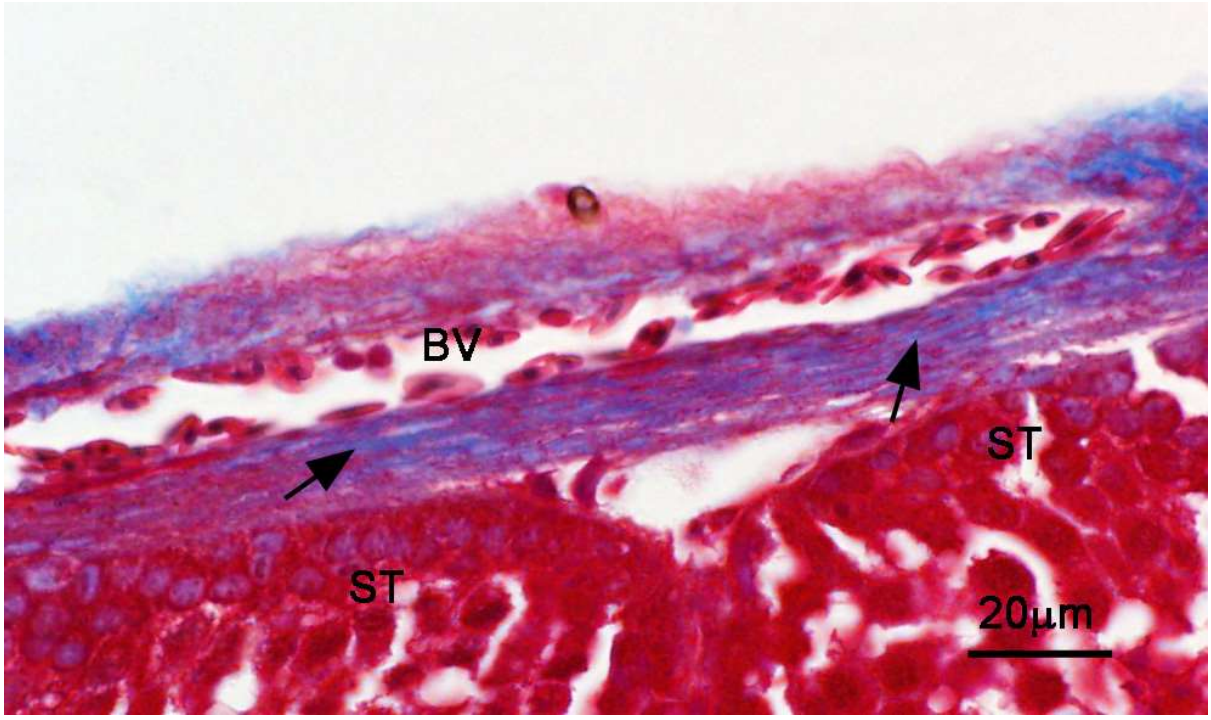

Figure 2. 14: Light photomicrograph of a testicular capsule from a pubertal Japanese quail. Arrows: collagen bundles. BV: blood vessel. ST: seminiferous tubules. Masson trichrome stain.

Figure 2. 15: Light photomicrograph of a testicular capsule from a pubertal Japanese quail. Black arrows: mesothelial cells. Arrowheads: reticular layer associated with the basement membrane of the mesothelial cells. White arrows: reticular fibres in the *tunica albuginea*. Gomori's silver impregnation stain.

Adult birds

In adult birds, the *tunica serosa* was formed by mesothelial cells with elongated nuclei (Figure 2.16 A & B). As in pubertal birds, the underlying *tunica albuginea* in adult quails was formed by collagen bundles (Figure 2.17) and reticular fibres (Figure 2.18) interspersed with a few predominantly smooth muscle cells. In addition, the *tunica albuginea* in adult birds contained occasional elastic fibres (Figure 2.19). A network of veins divided the *tunica albuginea* into superficial and deep regions (Figure 2.16 B). The innermost layer of the testicular capsule, the *tunica vasculosa*, was located adjacent to the testicular parenchyma. Blood vessels and loose connective tissue formed the *tunica vasculosa*.

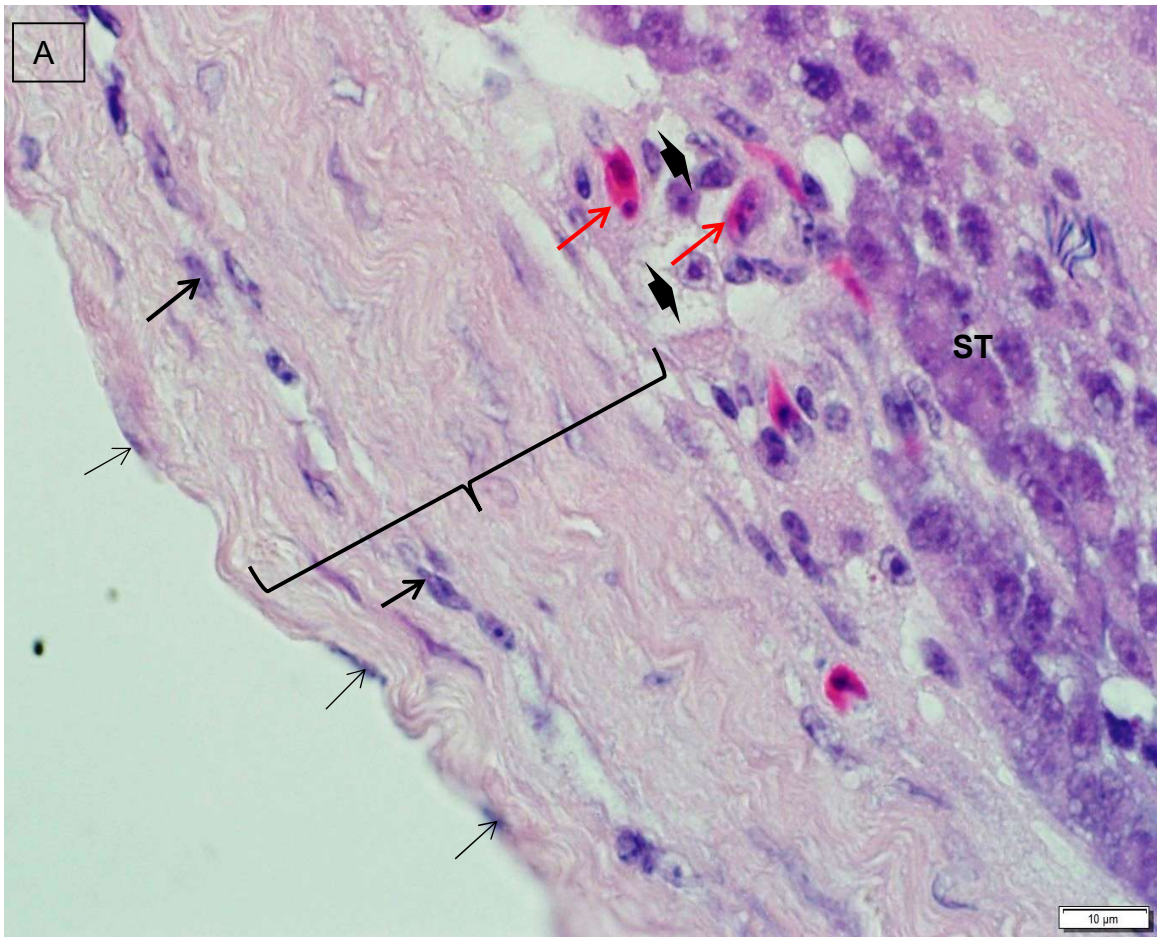

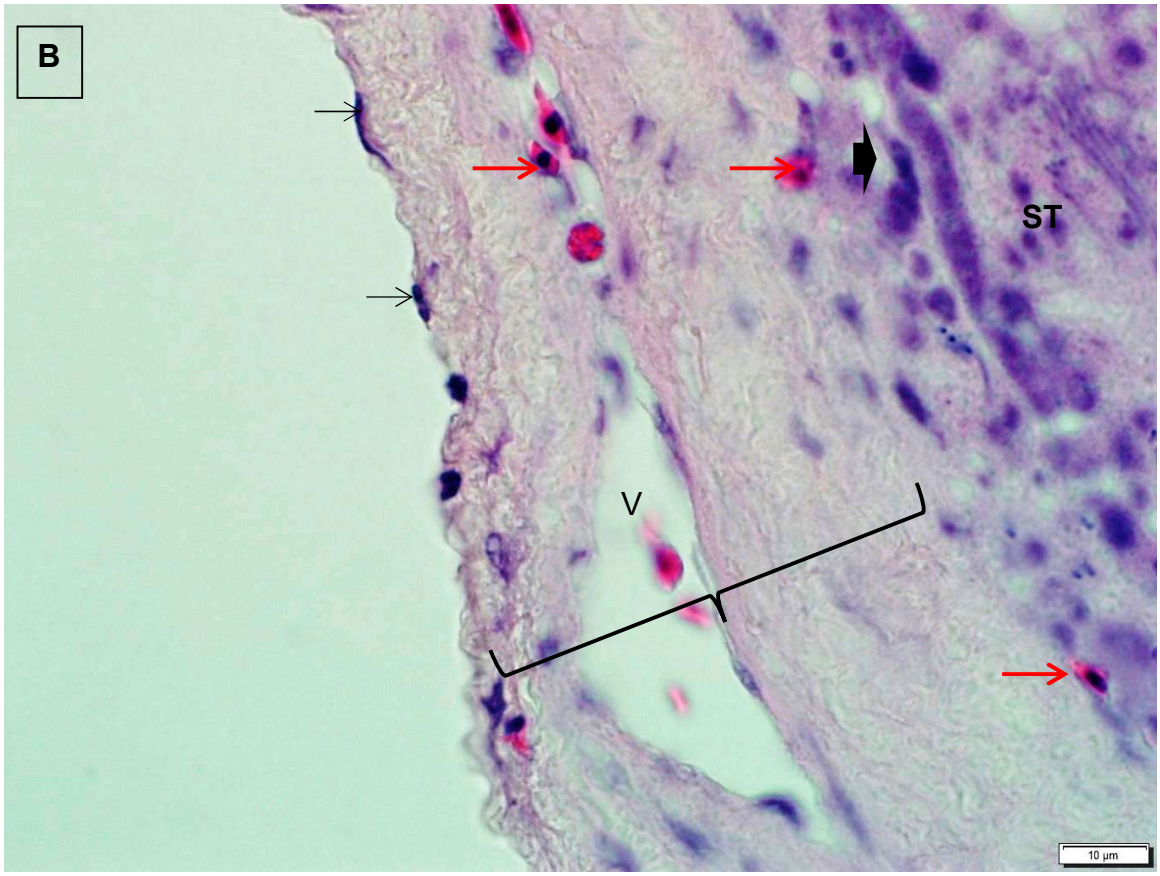

Figure 2. 16: Light photomicrographs (A, B) of testicular capsules from adult Japanese quails. Thin arrows: mesothelial cells of the *tunica serosa*. Thick arrows: smooth muscle cells forming the *tunica media* of a vein in the *tunica albuginea* (brackets). Arrowheads: *tunica vasculosa*. Note the nucleated red blood cells (red arrows) in veins (V) located in the *tunica albuginea* and *tunica vasculosa.* ST: seminiferous tubules. Haematoxylin and eosin stain.

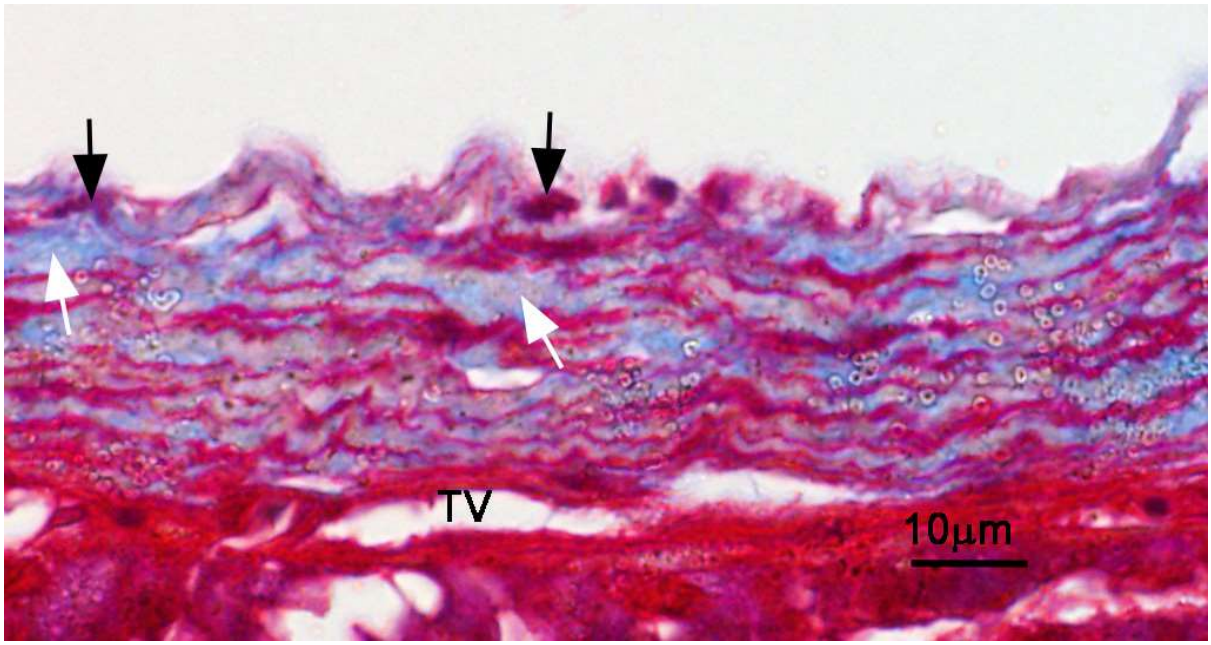

Figure 2. 17: Light photomicrograph of a testicular capsule from an adult Japanese quail. Black arrows: mesothelial cells. White arrows: collagen bundles in the *tunica albuginea*. TV: *tunica vasculosa*. Masson trichrome stain.

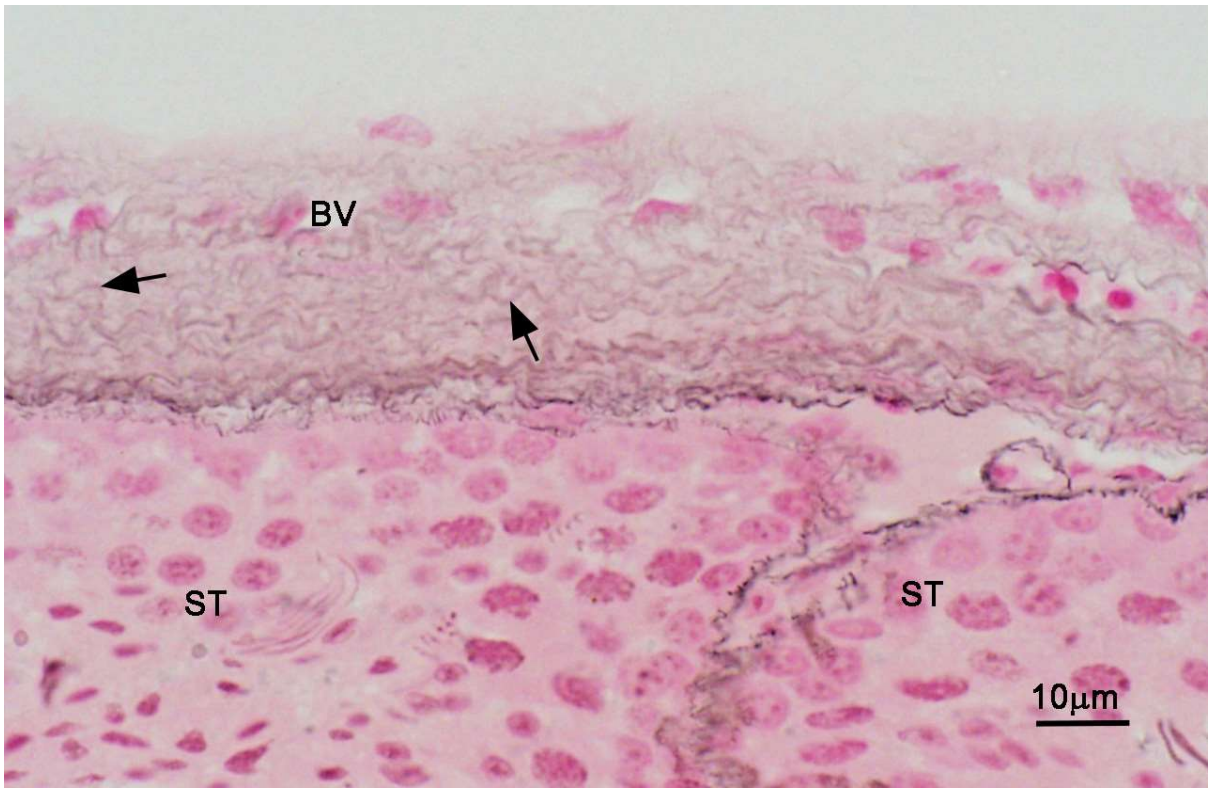

Figure 2. 18: Light photomicrograph of a testicular capsule from an adult Japanese quail. Black arrows: reticular fibres. BV: blood vessel. ST: seminiferous tubules. Gomori's silver impregnation stain.

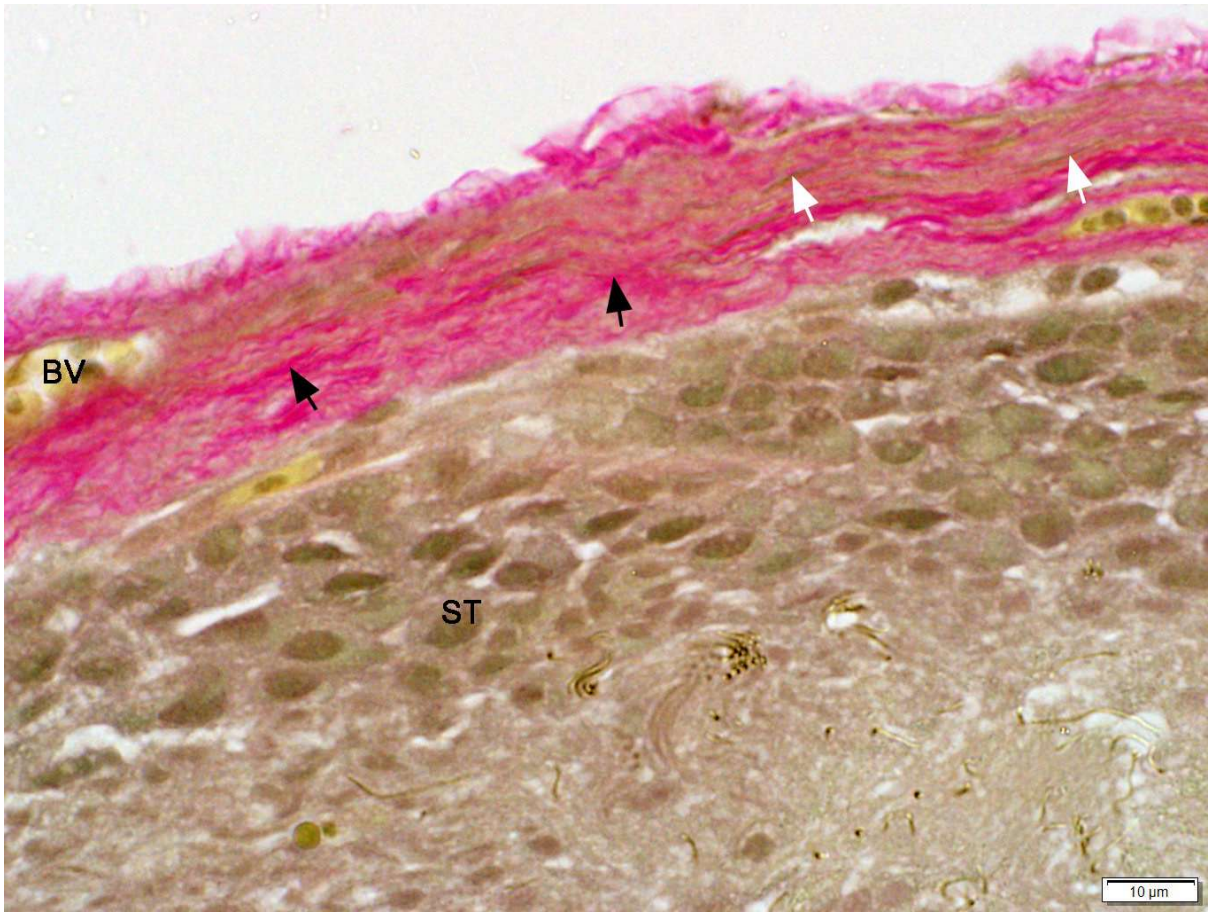

Figure 2. 19: Light photomicrograph of a testicular capsule from an adult Japanese quail. White arrows: elastic fibres. Black arrows: collagen fibres. BV: blood vessel. ST: seminiferous tubule. Verhoeff-Van Gieson stain.

2.4.5 Cytoskeletal protein immunohistochemistry

Cytoskeletal proteins (desmin, smooth muscle actin, tubulin, and vimentin) were immunolocalized in the testicular capsule of pre-pubertal, pubertal and adult

Japanese quails (Figures 2.20, 2.21, 2.22 & 2.23). Variations in the staining intensities of the cytoskeletal proteins are shown in Table 2.3.

2.4.5.1 Desmin

Pre-pubertal birds

The *tunica serosa* in pre-pubertal birds was desmin-immunonegative (Figure 2.20 A, B). Similarly, fibroblasts in the *tunica albuginea* did not display desmin immunostaining (Figure 2.20 A). Strong desmin immunostaining was observed in smooth muscle cells of the *tunica albuginea*. Similarly, vascular smooth muscle cells forming the *tunica mediae* of the venous network in the *tunica albuginea* displayed strong desmin immunostaining (Figure 2.20 B). Vascular smooth muscle cells forming the walls of blood vessels in the *tunica vasculosa* also showed strong desmin immunostaining.

Pubertal birds

In pubertal birds, mesothelial cells forming the *tunica serosa* were desmin-immunonegative (Figure 2.20 C, D). Likewise, fibroblasts of the *tunica albuginea* did not display desmin immunostaining. Smooth muscle cells in the upper region of the *tunica albuginea* displayed faint or no desmin immunostaining. Strong desmin immunostaining was observed in smooth muscle cells forming the deeper region of the *tunica albuginea* (Figure 2.20 C, D). Similarly, vascular smooth muscle cells forming the walls of blood vessels in the *tunica vasculosa* exhibited strong desmin immunostaining.

Adult birds

The mesothelial layer of the *tunica serosa* in adult birds did not display desmin immunostaining (Figure 2.20 E). Similarly, fibroblasts in the *tunica albuginea* were desmin-immunonegative. Weak to moderate desmin immunostaining was observed in smooth muscle cells forming the upper region of the *tunica albuginea*. Vascular smooth muscle cells forming the walls of the venous network in the *tunica albuginea* showed strong desmin immunostaining (Figure 2.20 F). Similarly, strong desmin immunostaining was observed in smooth muscle cells situated in the deeper regions of the *tunica albuginea* (Figure. 2.20 E, F). Vascular smooth muscle cells of the *tunica vasculosa* also exhibited strong desmin immunostaining (Figure 2.20 E).

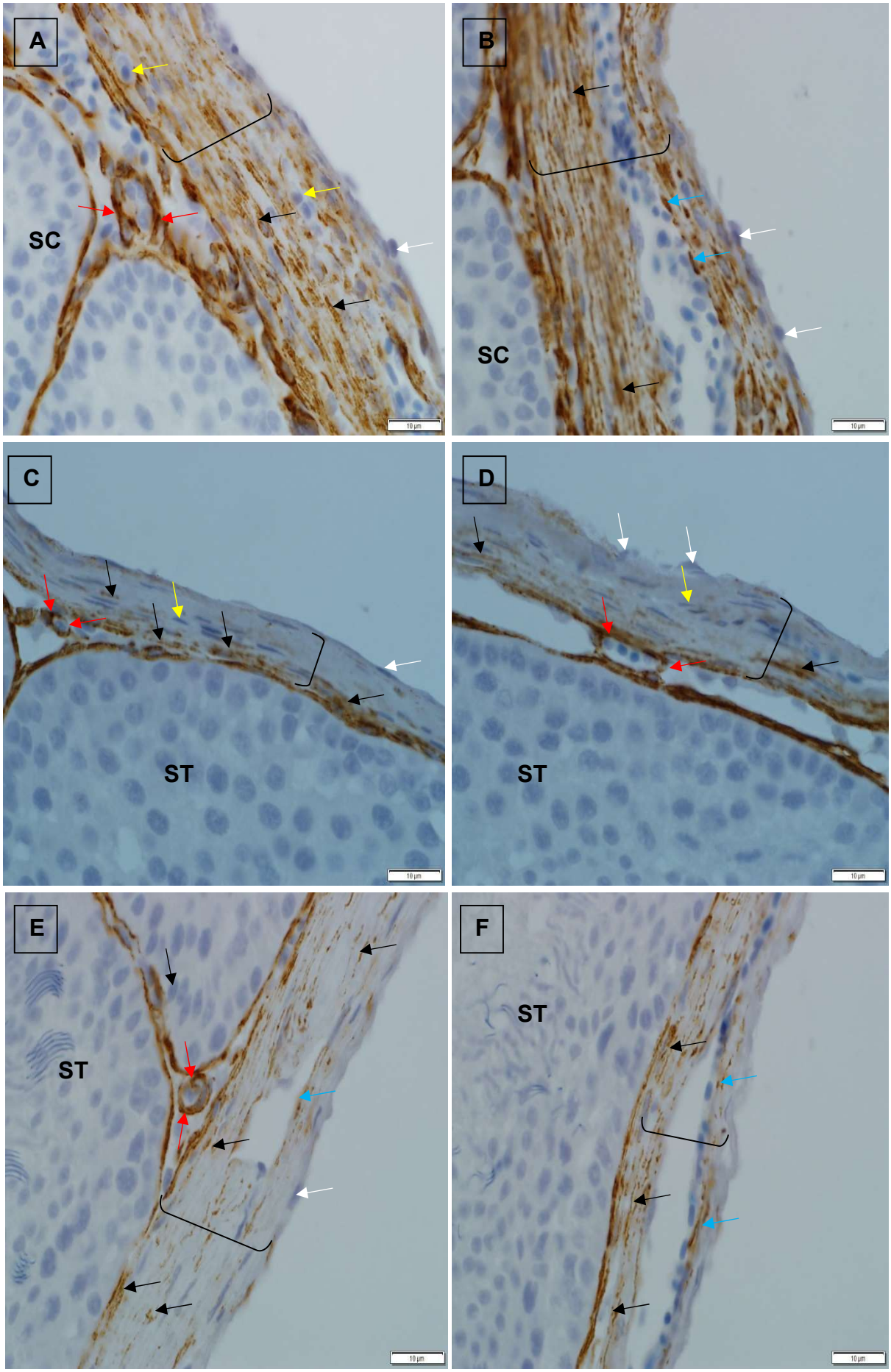
A
SC
B
SC
C
ST
D
ST
E
ST
F
ST

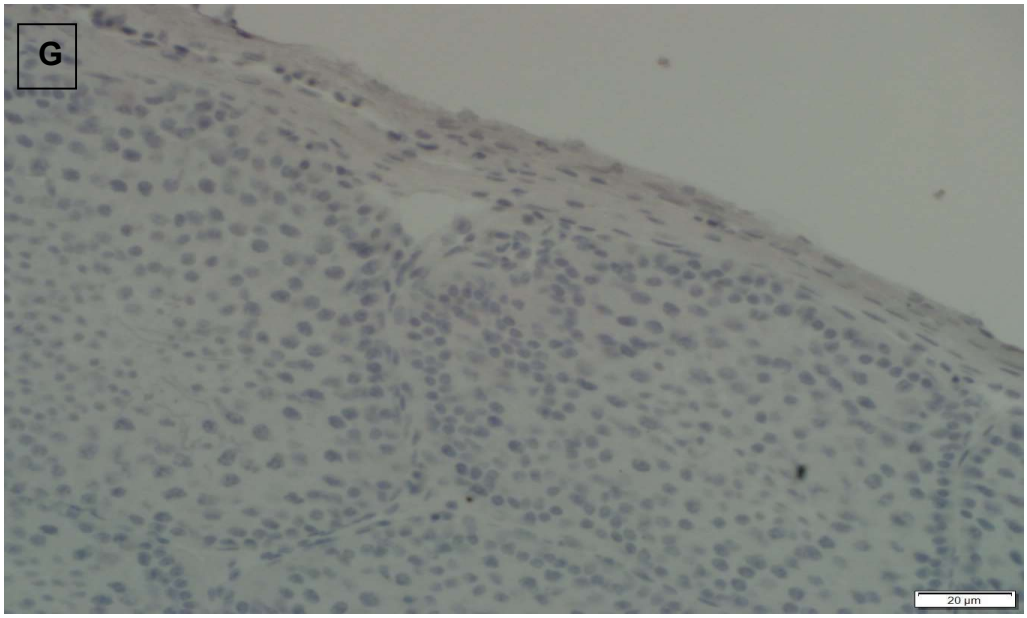

Figure 2. 20: Light photomicrographs showing desmin immunoexpression in the testicular capsule of pre-pubertal (A, B), pubertal (C, D), and adult (E, F) quails.

A, B. Testicular capsules of pre-pubertal quails. White arrows: Desmin-immunonegative mesothelial cells of the *tunica serosa*. Yellow arrows: desmin-immunonegative fibroblasts. Black arrows: strong desmin immunostaining in smooth muscle cells of the *tunica albuginea* (bracket). Blue arrows: strong desmin immunostaining in vascular smooth muscle cells of a blood vessel within the *tunica albuginea*. Red arrows: strong desmin immunostaining in vascular smooth muscle cells of the *tunica vasculosa*. SC: seminiferous cord. Scale bars = 10 μm.

C, D. Testicular capsules of pubertal quails. White arrows: desmin-immunonegative mesothelial cells. Yellow arrows: desmin-immunonegative fibroblasts. Black arrows: strong desmin immunostaining in smooth muscle cells located in the deeper regions of the *tunica albuginea* (bracket). Red arrows: strong desmin immunostaining in vascular smooth muscle cells of the *tunica vasculosa*. ST: seminiferous tubules. Scale bars = 10μm.

E, F. Testicular capsules of adult quails. White arrow: desmin immunonegative mesothelial cells of the *tunica serosa*. Black arrows: strong desmin immunostaining in smooth muscle cells located in the *tunica albuginea* (bracket). Blue arrows: strong desmin immunostaining in vascular smooth muscle cells forming the wall of a blood vessel in the *tunica albuginea.* Red arrows: strong desmin immunostaining in vascular smooth muscle cells of the *tunica vasculosa*. ST: seminiferous tubules. Scale bars = 10μm.

G. Negative control section. Scale bar = 20μm.

2.4.5.2 Smooth muscle actin

Pre-pubertal birds

The *tunica serosa* in pre-pubertal birds was smooth muscle actin immunonegative (Figure 2.21 A). Similarly, fibroblasts in the *tunica albuginea* were smooth muscle actin-immunonegative. Strong smooth muscle actin immunostaining was observed in smooth muscle and vascular smooth muscle cells of the *tunica albuginea* (Figure 2.21 A, B). Similarly, vascular smooth muscle cells of the *tunica vasculosa* displayed strong smooth muscle actin immunostaining (Figure 2.21 A, B).

Pubertal birds

The *tunica serosa* in pubertal birds was smooth muscle actin-immunonegative (Figure 2.21 C, D). Similarly, fibroblasts in the *tunica albuginea* did not demonstrate smooth muscle actin immunostaining. Strong smooth muscle actin immunostaining was seen in smooth muscle cells of the *tunica albuginea*. In addition, vascular smooth muscle cells forming the venous system of the *tunica albuginea* showed

strong smooth muscle actin immunostaining (Figure 2.21 D). In addition, strong smooth muscle actin immunostaining was also observed in vascular smooth muscle cells of the *tunica vasculosa* (Figure 2.21 C).

Adult birds

The *tunica serosa* was smooth muscle actin-immunonegative (Figure 2.21 E). Similarly, fibroblasts within the *tunica albuginea* were smooth muscle actin-immunonegative. Strong smooth muscle actin immunostaining was observed in smooth muscle cells of the *tunica albuginea.* Additionally, vascular smooth muscle cells of the venous network in the *tunica albuginea* displayed strong smooth muscle actin immunostaining (Figure 2.21 F). Strong smooth muscle actin was also demonstrated in vascular smooth muscle cells forming the *tunica mediae* of blood vessels in the *tunica vasculosa* (Figure 2.21 E, F).

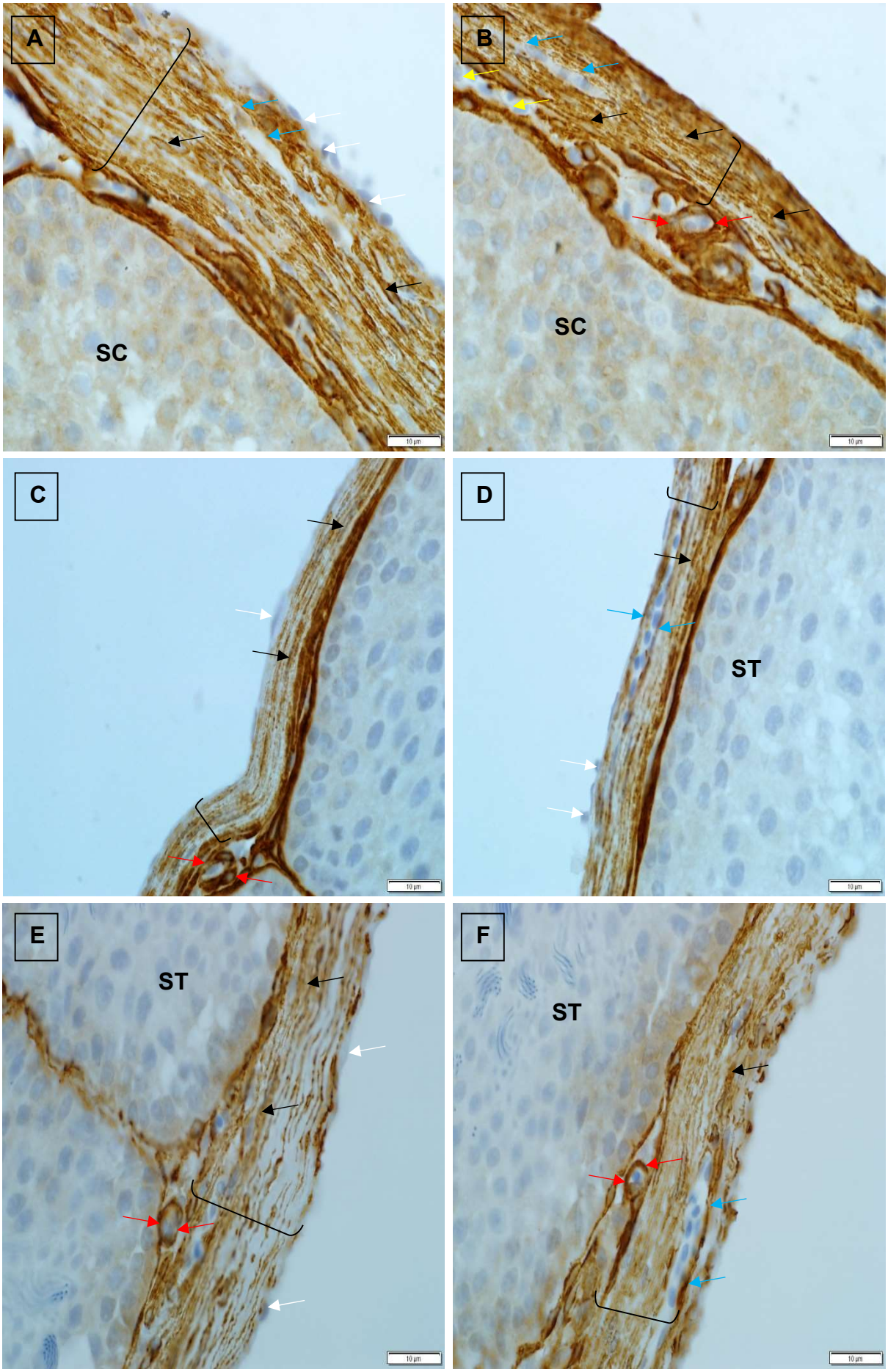
A
SC
B
SC
C
D
ST
E
ST
F
ST

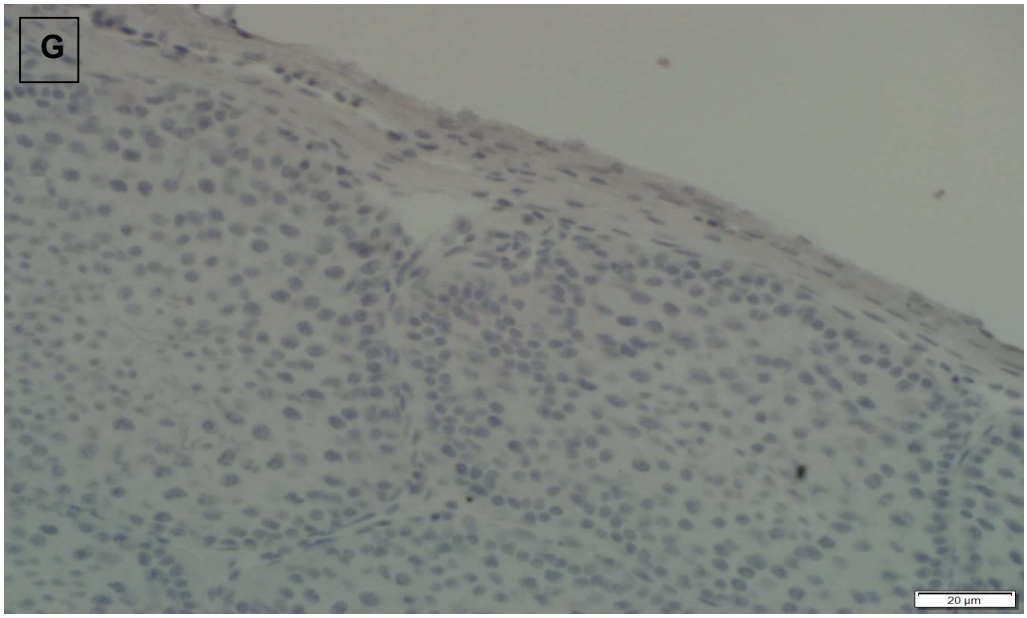

Figure 2. 21: Light photomicrographs showing smooth muscle actin immunoexpression in the testicular capsule of pre-pubertal (A, B), pubertal (C, D), and adult (E, F) quails.

A-F. Testicular capsules of pre-pubertal, pubertal and adult quails. White arrows: smooth muscle actin immunonegative *tunica serosa* in A. Black arrows: strong smooth muscle actin immunostaining in smooth muscle cells of the *tunica albuginea* (bracket). Blue arrows: strong smooth muscle actin immunostaining in vascular smooth muscle cells of the *tunica albuginea*. Red arrows: strong smooth muscle actin immunostaining in vascular smooth muscle cells of the *tunica vasculosa*. SC: seminiferous cord, ST: seminiferous tubules. Scale bars = 10 μm.

G. Negative control section. Scale bar = 20μm.

2.4.5.3 Tubulin

Pre-pubertal birds

The mesothelial cells of the *tunica serosa* in pre-pubertal birds were tubulin-immunonegative (Figure 2.22 A). Strong tubulin immunostaining was observed in vascular smooth muscle cells forming the walls of venous networks in the *tunica albuginea* and *vasculosa*. Similarly, smooth muscle cells of the *tunica albuginea* exhibited strong tubulin immunostaining.

Pubertal birds

No tubulin immunostaining was seen in mesothelial cells of the *tunica albuginea* (Figure 2.22 B). Strong tubulin immunostaining was observed in smooth muscle cells of the *tunica albuginea* (Figure 2.22 B, C). Similarly, vascular smooth muscle cells of the *tunica albuginea* displayed strong tubulin immunostaining (Figure 2.22 C). Vascular smooth muscle of the *tunica vasculosa* also exhibited strong tubulin immunoreactivity (Figures 2.22 B).

Adult birds

The mesothelial cell layer of the *tunica serosa* was tubulin-immunonegative (Figure 2.22 D). Weak to moderate tubulin immunostaining was observed in a few smooth muscle cells of the *tunica albuginea* (Figure 2.22 D, E). Strong tubulin immunostaining was demonstrated in smooth muscle cells in the *tunica mediae* of veins in the *tunica albuginea* (Figure 2.22 E). Similarly, strong tubulin immunostaining was seen in vascular smooth muscle cells of the *tunica vasculosa* (Figure 2.22 E).

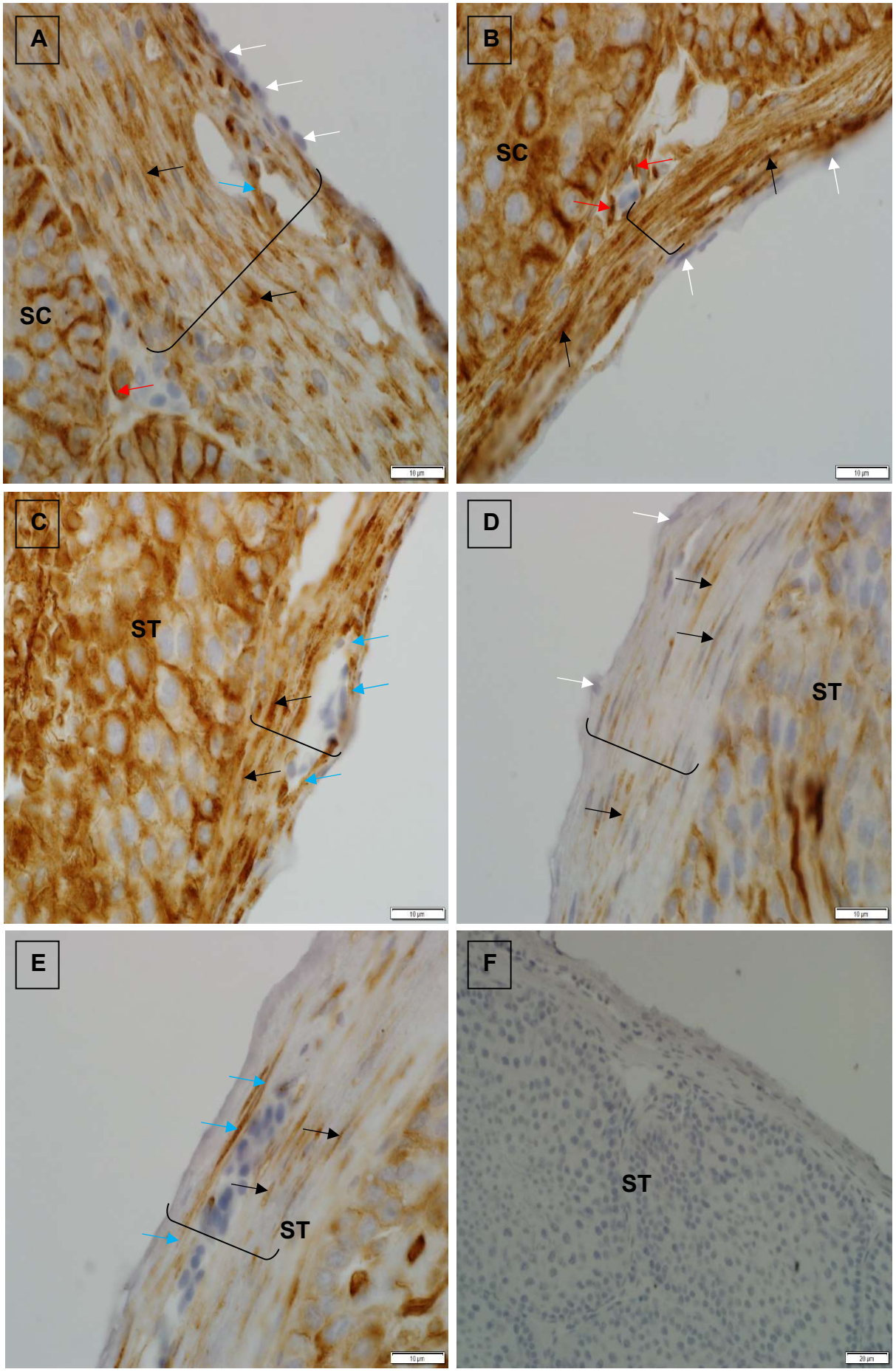
A
SC
B
SC
C
ST
D
ST
E
ST
F
ST

Figure 2. 22: Light photomicrographs showing tubulin immunoexpression in the testicular capsule of pre-pubertal (A), pubertal (B, C), and adult (D, E) quails.

A-C. Testicular capsules of pre-pubertal and pubertal quails. White arrows: immunonegative mesothelial cells of the *tunica serosa*. Blue arrows: strong tubulin immunostaining in smooth muscle cells of venous networks in the *tunica albuginea* (bracket). Black arrows: strong tubulin immunostaining in smooth muscle cells of the *tunica albuginea*. Red arrows: strong tubulin immunostaining in vascular smooth muscle cells of the *tunica vasculosa*. SC: seminiferous cord. ST: seminiferous tubules. Scale bars = 10μm.

D, E. Testicular capsules of adult birds. White arrows: tubulin immunonegative mesothelial cells in the *tunica serosa*. Blue arrows: strong tubulin immunostaining in vascular smooth muscle cells of the *tunica albuginea* (bracket). Black arrows: moderate to strong tubulin immunostaining in smooth muscle cells of the *tunica albuginea*. ST: seminiferous tubules. Scale bars = 10μm.

F. Negative control section. Scale bar = 20μm.

2.4.5.4 Vimentin

Pre-pubertal birds

In pre-pubertal birds, moderate vimentin immunostaining was observed in the mesothelial layer of the *tunica serosa* (Figure 2.23 A). Smooth muscle cells of the *tunica albuginea* were vimentin immunonegative (Figure 2.23 A, B). Strong vimentin immunostaining was observed in numerous fibroblasts distributed throughout the *tunica albuginea* (Figure 2.23 A, B). Similarly, endothelial cells lining the veins of the

tunicae albuginea and *vasculosa* displayed strong vimentin immunostaining (Figure 2.23 B).

Pubertal birds

Vimentin immunostaining was strong in the mesothelial cells of the *tunica serosa* (Figure 2.23 C). Apart from strong vimentin immunostaining in vascular endothelial cells, the superficial region of the *tunica albuginea* was vimentin immunonegative (Figure 2.23 D). However, strong vimentin immunostaining was demonstrated in the few fibroblasts located in the deeper region of the *tunica albuginea* (Figure 2.23 C). Vascular endothelial cells of the *tunica vasculosa* displayed strong vimentin immunostaining (Figure 2.23 C, D).

Adult birds

The mesothelial lining of the *tunica serosa* in adult birds exhibited strong vimentin immunostaining (Figure 2.23 E). Similarly, endothelial cells forming the venous network of the *tunica albuginea* displayed strong vimentin immunostaining (Figure 2.23 F). No vimentin immunostaining was observed in smooth muscle cells of the *tunica albuginea*. Vimentin immunostaining in the few fibroblasts located in the *tunica albuginea* was weak or absent (Figure 2.23 E). Strong vimentin immunostaining was observed in vascular endothelial cells of the *tunica vasculosa* (Figure 2.23 E, F).

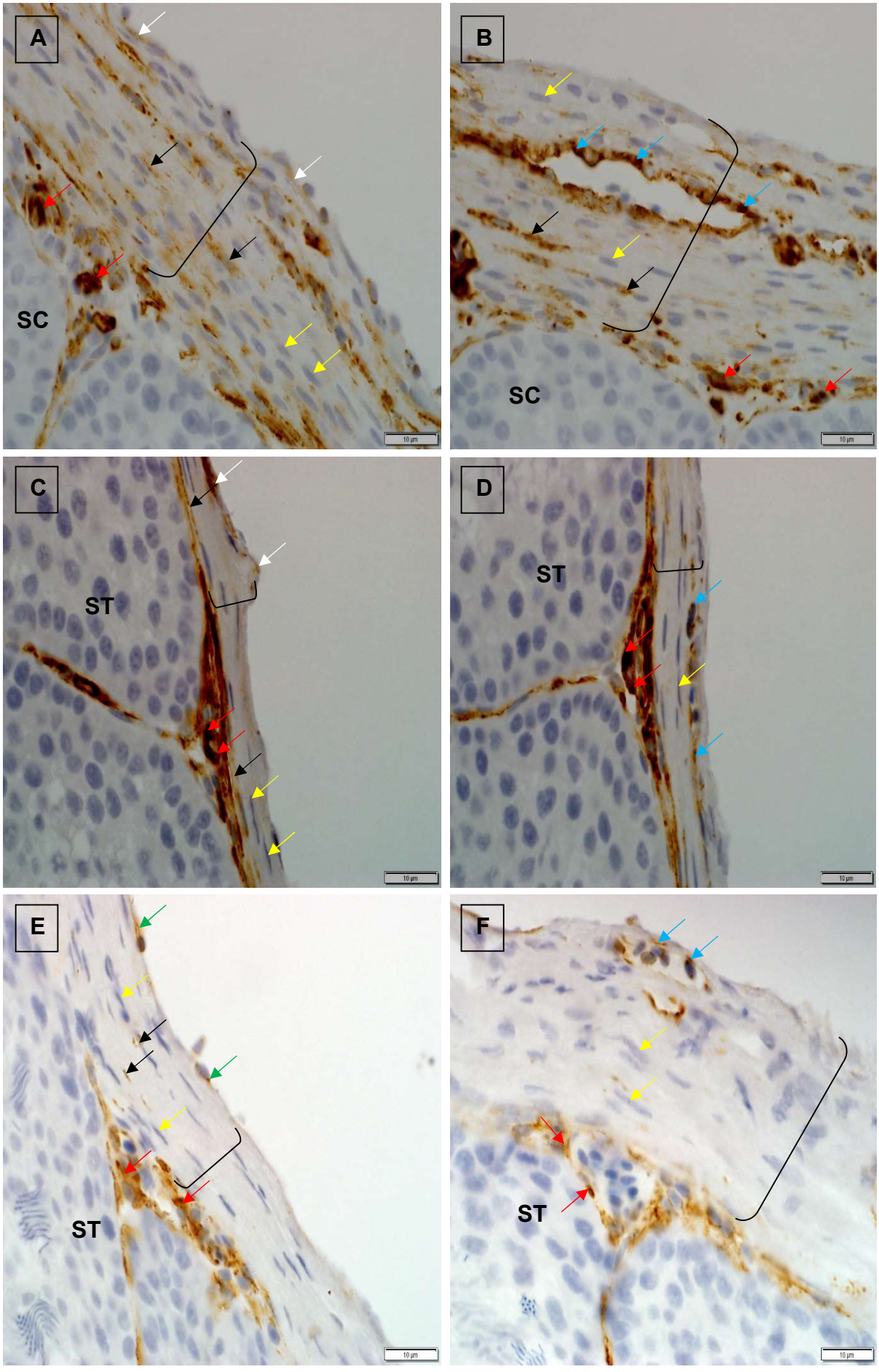
A
SC
B
SC
C
ST
D
ST
E
ST
F
ST

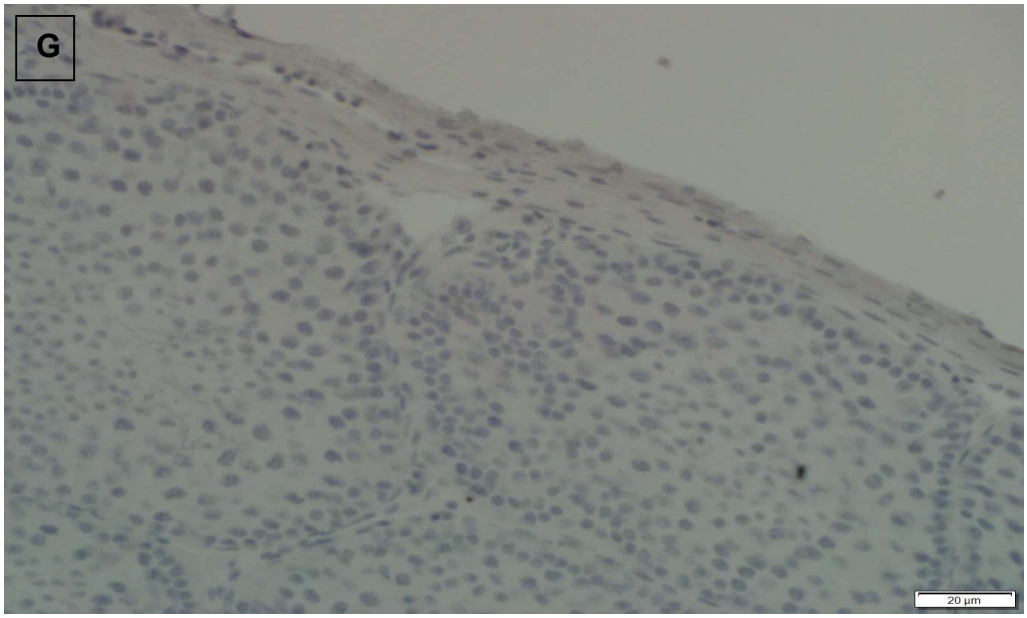

Figure 2. 23: Light photomicrographs showing vimentin immunoexpression in the testicular capsule of pre-pubertal (A, B), pubertal (C, D), and adult (E, F) quails.

A, B. Testicular capsules of pre-pubertal birds. White arrows: moderate vimentin immunostaining in mesothelial cells of the *tunica serosa*. Yellow arrows: vimentin immunonegative smooth muscle cells. Black arrows: strong vimentin immunostaining in fibroblasts of the *tunica albuginea* (bracket). Blue arrows: strong vimentin immunostaining in vascular endothelial cells of the *tunica albuginea*. Red arrows: strong vimentin immunostaining in endothelial cells of the blood vessels of the *tunica vasculosa*. SC: seminiferous cord. Scale bars = 10 μm.

C, D. Testicular capsules of pubertal birds. White arrows: strong vimentin immunostaining in mesothelial cells of the *tunica serosa*. Blue arrows: strong vimentin immunostaining in vascular endothelial cells of the *tunica albuginea*. Black arrows: strong immunostaining in fibroblasts of the *tunica albuginea* (bracket). Red arrows: strong vimentin immunostaining in vascular endothelial cells of the *tunica*

vasculosa. Yellow arrows: vimentin immunonegative smooth muscle cells. ST: seminiferous tubules. Scale bars = 10μm.

D, E. Testicular capsules of adult birds. Green arrows: strong vimentin immunostaining in mesothelial cells of the *tunica serosa*. Blue arrows: strong vimentin immunostaining in vascular endothelial cells of the *tunica albuginea* (bracket). Yellow arrows: vimentin immunonegative smooth muscle cells. Black arrows: weak or no vimentin immunostaining in fibroblasts of the *tunica albuginea.* Red arrows: strong vimentin immunostaining in vascular endothelial cells of the *tunica vasculosa*. ST: seminiferous tubules. Scale bars = 10μm.

G. Negative control section. Scale bar = 20μm.

Table 2. 1: Summary of intensities of cytoskeletal proteins (desmin, smooth muscle actin, tubulin and vimentin,) in the layers of the testicular capsule of pre-pubertal, pubertal, and adult Japanese quails (*Coturnix coturnix japonica*).

Age	Antibody	*Tunica serosa*	*Tunica albuginea*	*Tunica vasculosa*
Pre-pubertal	Desmin	-	+++[a,c]	+++[c]
	Smooth muscle actin	-	+++[a,c]	+++[c]
	Tubulin	-	+++[a,c]	+++[c]
	Vimentin	++[e]	+++[b,d]	+++[d]
Pubertal	Desmin	-	+[a]/+++[a,c]	+++[c]
	Smooth muscle actin	-	+++[a,c]	+++[c]
	Tubulin	-	+++[a,c]	+++[c]
	Vimentin	+++[e]	+++[b,d]	+++[d]
Adult	Desmin	-	+[a]/++[a]/+++[c]	+++[c]
	Smooth muscle actin	-	+++[a,c]	+++[c]
	Tubulin	-	+[a]/++[a]/+++[c]	+++[c]
	Vimentin	+++[e]	+[b]/+++[d]	+++[d]

Intensities of immunostaining: - absent, + weak, ++ moderate, +++ strong.

Types of cells: [a]smooth muscle cells, [b]fibroblasts, [c]vascular smooth muscle cells, [d]vascular endothelial cells, [e]mesothelial cells.

2.4.6 Basement membrane immunohistochemistry

Basement membrane proteins (collagen type IV, fibronectin and laminin) were immunolocalized in the testicular capsule of pre-pubertal, pubertal and adult Japanese quails (Figures 2.24, 2.25, & 2.26). Variations in the staining intensities of the basement membrane proteins are shown in Table 2.4.

2.4.6.1 Collagen type IV

Pre-pubertal birds

The mesothelial layer of the *tunica serosa* did not display collagen type IV immunostaining (Figure 2.24 A). However, weak to moderate collagen type IV immunostaining was demonstrated in the basement membranes and collagen fibres underlying the mesothelial cells. Fibroblasts were collagen type IV immunonegative. Moderate collagen type IV immunostaining was observed in basement membranes of smooth muscle cells in the *tunica albuginea* (Figure 2.24 A, B). In addition, basement membranes of vascular endothelial and smooth muscle cells forming the veins of the *tunica albuginea* exhibited moderate to strong collagen type IV immunostaining (Figure 2.24 B). Collagen type IV immunostaining was also demonstrated in the basement membranes of vascular endothelial and smooth muscle cells of the *tunica vasculosa* (Figure 2.24 A).

Pubertal birds

Mesothelial cells of the *tunica serosa* were collagen type IV-immunonegative (Figure 2.24 C). In addition, no collagen type IV immunostaining was demonstrated in fibroblasts of the testicular capsule (Figure 2.24 C, D). Collagen type IV immunostaining was weak or absent in the basement membranes of the mesothelial

cells, as well as the basement membranes associated with smooth muscle cells in the *tunica albuginea* (Figure 2.24 C, D). However, basement membranes of endothelial and smooth muscle cells of venous networks in the *tunica albuginea* displayed moderate to strong collagen type IV immunostaining (Figure 2.24 C). Likewise, moderate to strong collagen type IV immunostaining was observed in the basement membranes of vascular endothelial and smooth muscle cells of the *tunica vasculosa* (Figure 2.24 D).

Adult birds

Mesothelial cells forming the cellular component of the *tunica serosa* did not display collagen type IV immunostaining (Figure 2.24 E). Fibroblasts throughout the testicular capsule were collagen type IV-immunonegative (Figure 2.24 E, F). Weak or negative collagen type IV immunostaining was observed in the basement membranes of mesothelial cells and smooth muscle cells in the *tunica albuginea* (Figure 2.24 E, F). The basement membranes of vascular endothelial and smooth muscle cells of veins in the *tunica albuginea* and *vasculosa* exhibited weak to

moderate collagen type IV immunostaining (Figure 2.24 E).

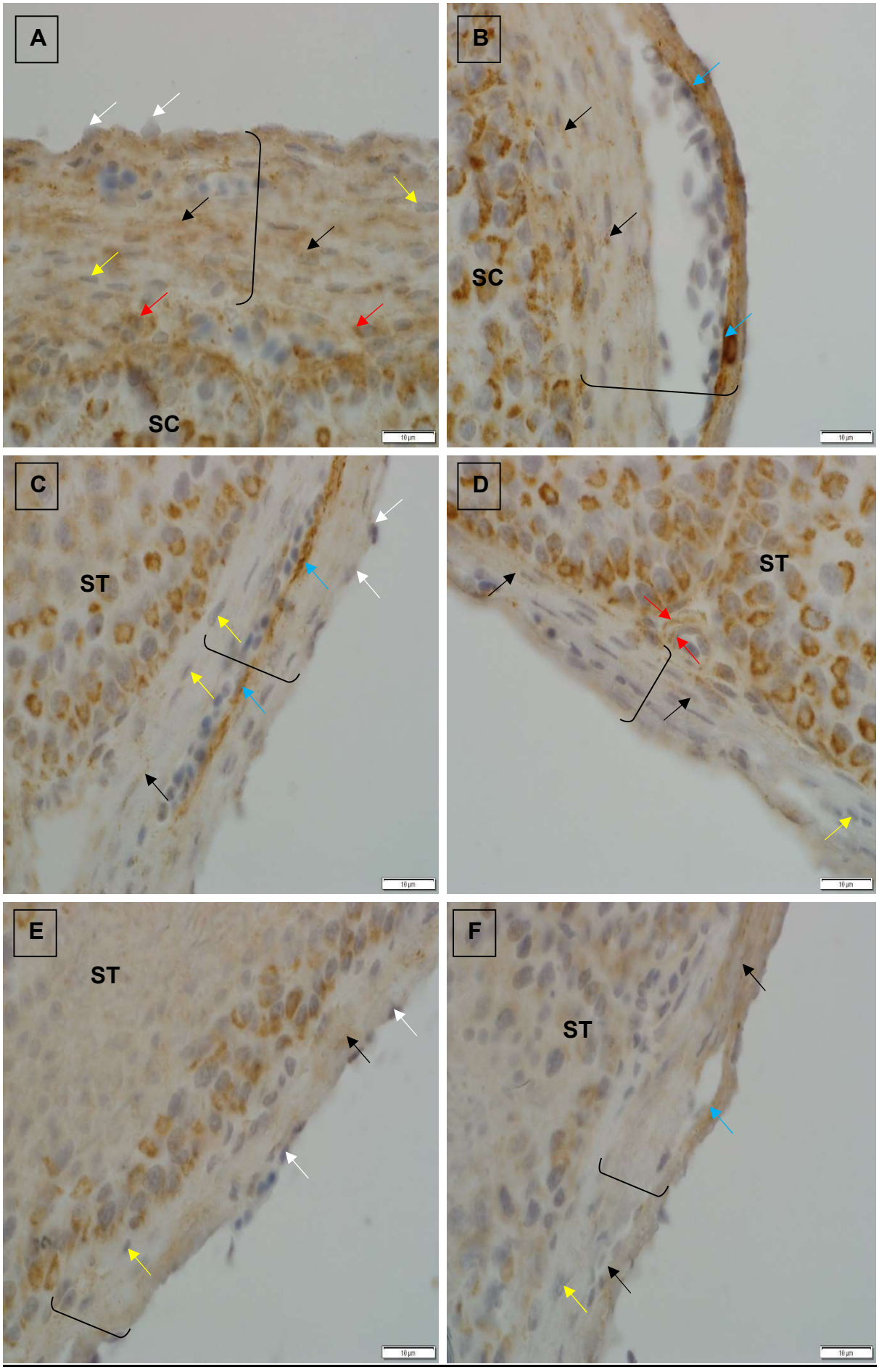
A
SC
B
SC
C
ST
D
ST
E
ST
F
ST

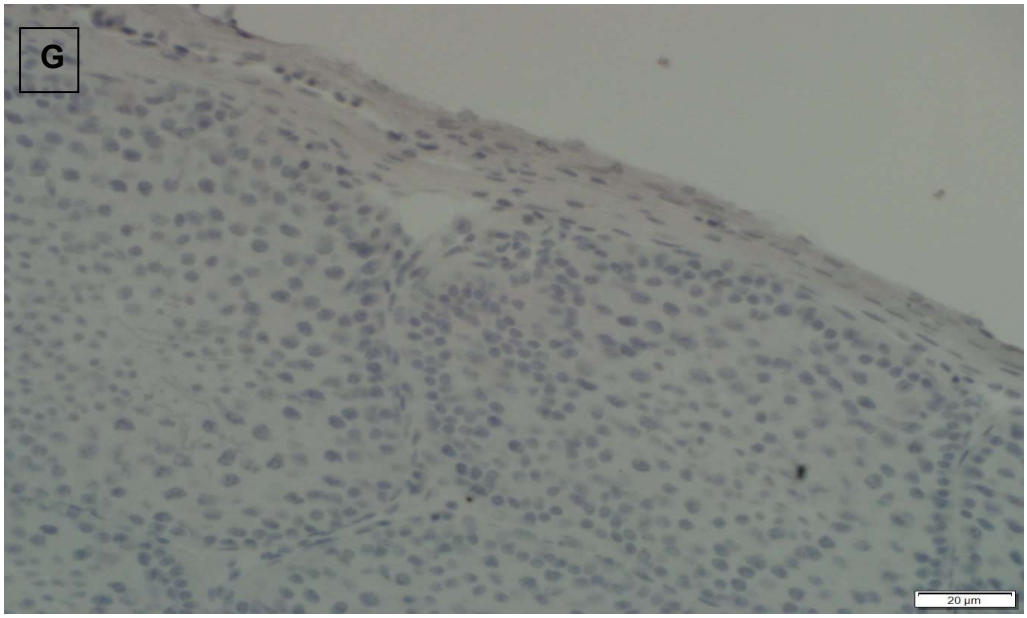

Figure 2. 24: Light photomicrographs showing collagen type IV immunoexpression in the testicular capsules of pre-pubertal (A, B), pubertal (C, D), and adult (E, F) quails.

A, B. Testicular capsules of pre-pubertal birds. White arrows: collagen type IV immunonegative mesothelial cells of the *tunica serosa*. Yellow arrows: collagen type IV-immunonegative fibroblasts. Black arrows: moderate collagen type IV immunostaining in smooth muscle cells of the *tunica albuginea*. Blue arrows: strong collagen type IV immunostaining in vascular endothelial cells of the *tunica albuginea* (bracket). Red arrows: moderate to strong collagen type IV immunostaining in vascular endothelial cells of the *tunica vasculosa*. SC: seminiferous cord. Scale bars = 10 µm.

C, D. Testicular capsules of pubertal birds. White arrows: collagen type IV immunonegative mesothelial cells of the *tunica serosa*. Yellow arrows: collagen type IV-immunonegative fibroblasts. Black arrows: weak collagen type IV immunostaining in smooth muscle cells of the *tunica albuginea*. Blue arrows: strong collagen type IV immunostaining in vascular endothelial cells of the *tunica albuginea* (bracket). Red

arrows: moderate collagen type IV immunostaining in vascular smooth muscle cells of the *tunica vasculosa*. ST: seminiferous tubules. Scale bars = 10 μm.

E, F. Testicular capsules of adult birds. White arrows: collagen type IV immunonegative mesothelial cells of the *tunica serosa*. Yellow arrows: collagen type IV-immunonegative fibroblasts. Black arrows: weak collagen type IV immunostaining in smooth muscle cells of the *tunica albuginea* (bracket). Blue arrow: weak collagen type IV immunostaining in vascular endothelial cells of the *tunica albuginea.* ST: seminiferous tubules. Scale bars = 10 μm.

G. Negative control section. Scale bar = 20μm.

2.4.6.2 Fibronectin

Pre-pubertal birds

Moderate to strong fibronectin immunostaining was demonstrated in the basement membranes of mesothelial cells in the *tunica serosa* (Figure 2.25 A, B). In addition, moderate to strong fibronectin immunostaining was observed in the basement membranes of smooth muscle cells in the *tunica albuginea* (Figure 2.25 A, B). Basement membranes of the endothelial component of veins in the *tunicae albuginea* and *vasculosa* displayed strong fibronectin immunostaining, while immunostaining in the basement membranes associated with smooth muscle cells in these blood vessels was moderate to strong (Figure 2.25 B).

Pubertal birds

Fibronectin immunostaining in the basement membranes of the *tunica serosa* were moderate to strong (Figure 2.25 C). Strong fibronectin immunostaining was observed in basement membranes of smooth muscle cells in the *tunica albuginea* (Figure 2.25

C, D). Vascular endothelial and smooth muscle cells of the *tunica vasculosa* also displayed strong fibronectin immunostaining (Figure 2.25 D).

Adult birds

Basement membranes of the mesothelial layer in the *tunica serosa* were fibronectin-immunopositive (Figure 2.25 E). Basement membranes of smooth muscle cells in the *tunica albuginea* exhibited strong fibronectin immunostaining. Similarly, basement membranes enclosing vascular endothelial and smooth muscle cells of the *tunica vasculosa* also displayed strong fibronectin immunostaining.

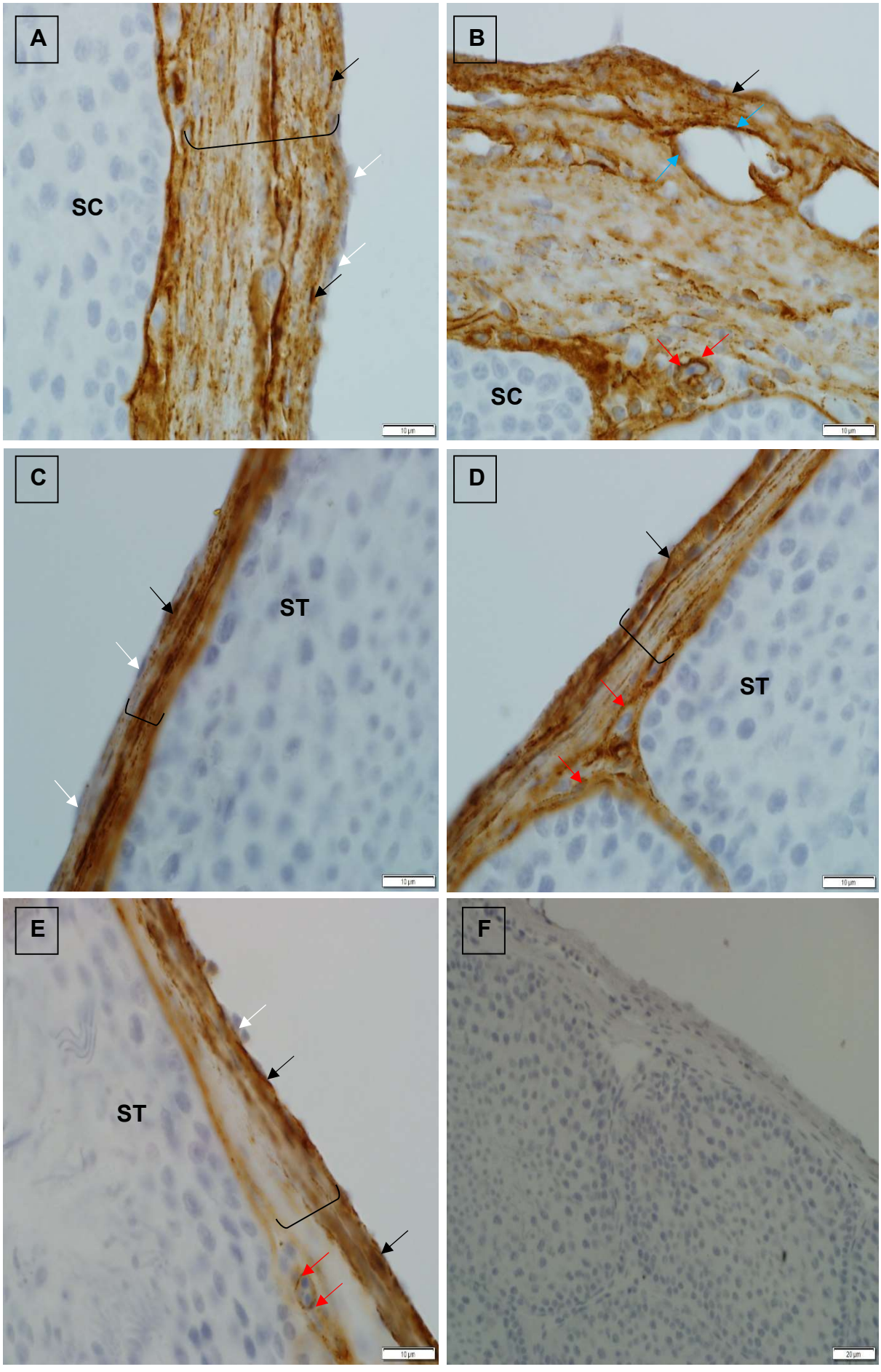
A
SC
B
SC
C
ST
D
ST
E
ST
F

Figure 2. 25: Light photomicrographs showing fibronectin immunoexpression in the testicular capsule of pre-pubertal (A, B), pubertal (C, D), and adult (E) quails.

A, B. Testicular capsules of pre-pubertal birds. White arrows: fibronectin immunonegative mesothelial cells of the *tunica serosa*. Moderate to strong fibronectin immunostaining is demonstrated in the basement membranes of mesothelial cells (black arrows) and smooth muscle cells in the *tunica albuginea* (bracket). Blue arrows: strong fibronectin immunostaining in basement membranes of endothelial cells of the venous network in the *tunica albuginea.* Red arrows: strong fibronectin immunostaining in basement membranes of endothelial cells of the *tunica vasculosa*. SC: seminiferous cord. Scale bars = 10 μm.

C-E. Testicular capsules of pubertal birds. White arrows: fibronectin immunonegative mesothelial cells of the *tunica serosa*. Black arrows: strong fibronectin immunostaining in basement membranes of smooth muscle cells in the *tunica albuginea.* Red arrows: strong fibronectin immunostaining in basement membranes of vascular endothelial and smooth muscle cells in the *tunica vasculosa*. ST: seminiferous tubules. Scale bars = 10 μm.

F. Negative control section. Scale bar = 20μm.

2.4.6.3 Laminin

Pre-pubertal birds

Weak to moderate laminin immunostaining was demonstrated in the basement membranes of the mesothelial cell layer (Figure 2.26 A). Moderate to strong laminin immunostaining was observed in basement membranes associated with smooth

muscle cells in the *tunica albuginea* (Figure 2.26 A, B). Laminin immunostaining in basement membranes of endothelial cells lining blood vessels in the *tunica albuginea* and *vasculosa* was generally strong (Figure 2.26 A). Moderate to strong laminin immunostaining was demonstrated in the vascular smooth muscle cells of the *tunica albuginea* and *vasculosa* (Figure 2.26 B). Fibroblasts in the *tunica albuginea* were laminin immunonegative.

Pubertal birds

Basement membranes of mesothelial cells in the *tunica serosa* were laminin-immunopositive (Figure 2.26 C). The basement membranes of smooth muscle cells in the *tunica albuginea* displayed moderate to strong laminin immunostaining (Figure 2.26 C, D). Similarly, moderate to strong immunostaining was exhibited in the basement membranes of smooth muscle cells forming the walls of blood vessels in the *tunica albuginea* and *vasculosa* (Figure 2.26 C, D). Basement membranes associated with the endothelial cells of blood vessels in the *tunica albuginea* and *vasculosa* exhibited moderate laminin immunostaining.

Adult birds

Weak to moderate laminin immunostaining was observed in the basement membranes of mesothelial cells in the *tunica serosa.* Moderate to strong laminin immunoreactivity was demonstrated in the basement membranes of smooth muscle cells in the *tunica albuginea* (Figure 2.26 E). Likewise, the basement membranes of smooth muscle cells in veins coursing through the *tunica albuginea* exhibited moderate to strong laminin immunostaining. A similar intensity of laminin immunoreactivity was observed in basement membranes associated with smooth muscle cells in the blood vessels of the *tunica vasculosa*.

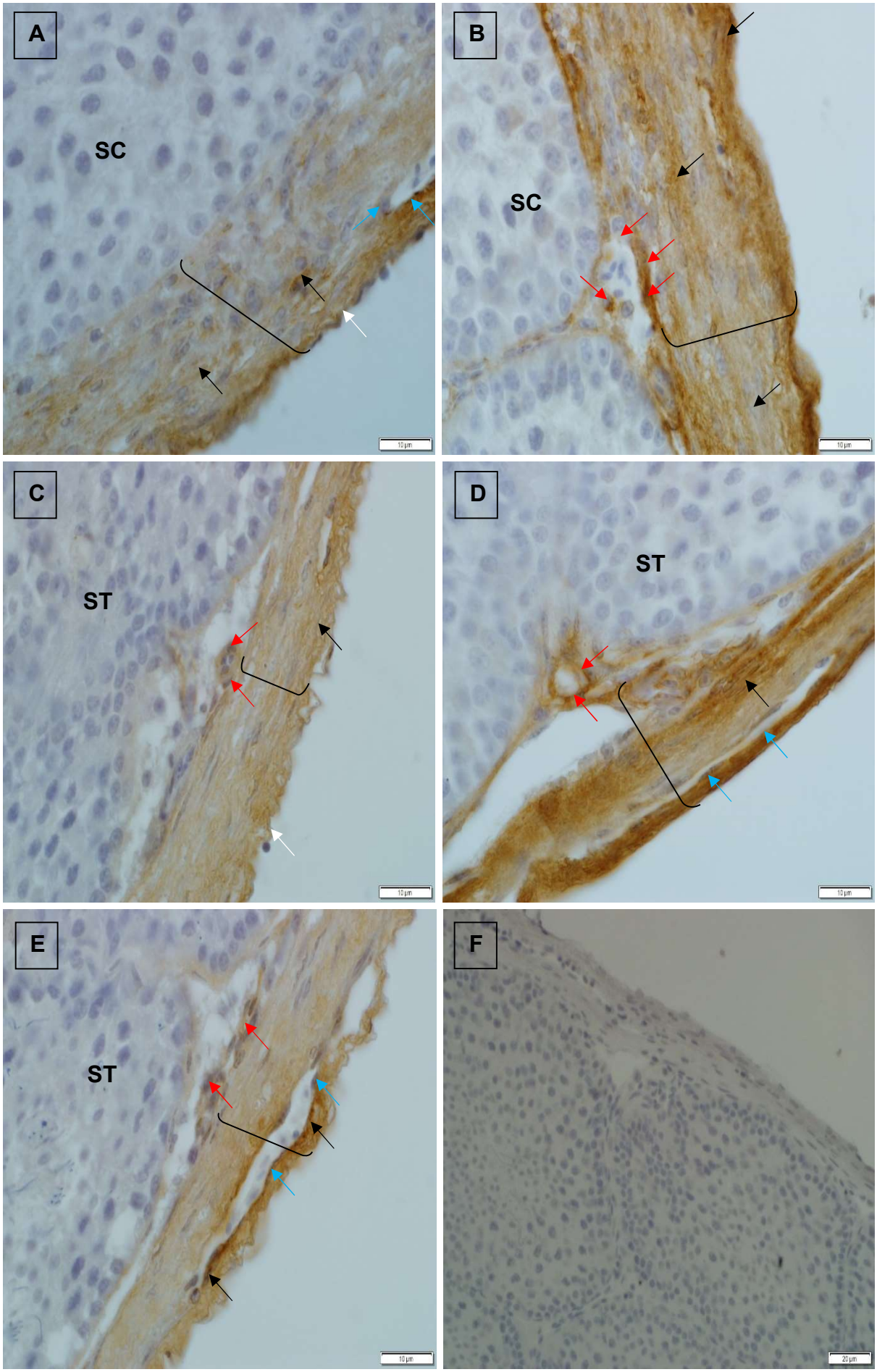
A
SC
B
SC
C
ST
D
ST
E
ST
F

Figure 2. 26: Light photomicrographs showing laminin immunoexpression in the testicular capsule of pre-pubertal (A, B), pubertal (C, D), and adult (E) quails.

A-D. White arrows: laminin immunopositive basement membranes of mesothelial cells in the *tunica serosa*. Black arrows: moderate to strong laminin immunostaining in basement membranes of smooth muscle cells in the *tunica albuginea* (bracket). Blue arrows: moderate to strong laminin immunostaining in basement membranes of vascular endothelial and smooth muscle cells of venous networks in the *tunica albuginea.* Red arrows: moderate to strong laminin immunostaining in basement membranes of vascular endothelial and smooth muscle cells of the *tunica vasculosa*. SC: seminiferous cord. Scale bars = 10 μm.

E. Black arrow: moderate to strong laminin immunostaining in basement membranes of smooth muscle cells of the *tunica albuginea* (bracket). Blue arrows: moderate to strong laminin immunostaining in basement membranes of vascular endothelial and smooth muscle cells of the *tunica albuginea.* Red arrows: moderate to strong laminin immunostaining in basement membranes of vascular endothelial and smooth muscle cells of the *tunica vasculosa.* ST: seminiferous tubules. Scale bars = 10 μm.

F. Negative control section. Scale bar = 20μm.

Table 2. 2: Summary of intensities of basement membrane proteins (collagen type IV, fibronectin and laminin) in the layers of the testicular capsule of pre-pubertal, pubertal, and adult Japanese quails (*coturnix coturnix japonica*).

Age	Antibody	*Tunica serosa*	*Tunica albuginea*	*Tunica vasculosa*
Pre-pubertal	Collagen type IV	+/++	++[a]/+++[c,d]	++/[c,d]+++[c,d]
	Fibronectin	++/+++	++[a,c]/+++[a,c,d]	++[c]/+++[c,d]
	Laminin	+/++	++/[a,c]+++[a,c,d]	++[c]/+++[c,d]
Pubertal	Collagen type IV	-/+	+[a]/+++[c,d]	++[c,d]/+++[c,d]
	Fibronectin	++/+++	+++[a,c,d]	+++[a,c,d]
	Laminin	+/++	++[a,c,d]/+++[a,c]	++[c,d]/+++[c]
Adult	Collagen type IV	-/+	+[a,c,d]/++[c,d]	+[c,d]/++[c,d]
	Fibronectin	++/+++	+++[a,c,d]	+++[a,c,d]
	Laminin	+/++	++[a,c,d]/+++[ac]	++[c,d]/+++[c]

Intensities of immunostaining: - absent, + weak, ++ moderate, +++ strong.

Types of cells: [a]smooth muscle cells, [b]fibroblasts, [c]vascular smooth muscle cells, [d]vascular endothelial cells.

2.4.7 Transmission electron microscopy

Pre-pubertal birds

The *tunica serosa* was formed by a single layer of predominantly cuboidal mesothelial cells and an underlying layer of connective tissue, which contained collagen bundles (Figures 2.27, 2.28, 2.29 & 2.30). The mesothelial cells contained oval- or oblong- shaped heterochromatic nuclei (Figures 2.27 – 2.29). The cytoplasm

of the mesothelial cells was electron-lucent and contained several mitochondria (Figures 2.27 & 2.29), rough endoplasmic reticulum (RER) cisternae (Figure 2.27), as well as pinocytotic vesicles (Figure 2.29). A series of gap junctions (Figure 2.29) and tight junctions (Figure 2.30) linked the plasma membranes of adjacent mesothelial cells.

Below the *tunica serosa* was the *tunica albuginea* which formed the largest portion of the testicular capsule (Figure 2.31). The *tunica albuginea* comprised of superficial and deep regions (Figure 2.31). The superficial region of the *tunica albuginea* was formed by smooth muscle cells and fibroblasts with intervening collagen fibre bundles (Figure 2.32). The smooth muscle cells displayed elongated heterochromatic nuclei, with dense clumps of peripherally-located chromatin (Figure 2.32). The cytoplasmic organelles contained within the smooth muscle cells included mitochondria and pinocytotic vesicles (Figure 2.33). Tight junctions linked the smooth muscle cells to adjacent cells (Figure 2.33).

Fibroblasts in the superficial regions of the tunica albuginea were characterized by the presence of oblong-shaped euchromatic nuclei, as well as cytoplasm which contained dilated RER cisternae and developing collagen fibres (Figures 2.32 & 2.34).

A venous network separated the superficial and deep regions of the *tunica albuginea*. The veins forming the network were lined by endothelial cells with euchromatic elongated nuclei. Cytoplasmic organelles contained within endothelial cells included RER cisternae and clumps of round mitochondria (Figure 2.35). Underlying the endothelial cells was a discontinuous basal lamina (Figure 2.35). The

tunica media of the veins was formed by a single layer of smooth muscle cells (Figure 2.36).

The deeper region of the *tunica albuginea* was adjacent to the testicular parenchyma. This region contained longitudinally-orientated smooth muscle cells and collagen bundles (Figures 2.31 & 2.37). The cytoplasmic organelles contained within smooth muscle cells included numerous mitochondria, pinocytotic vesicles, coated pits and microfilaments (Figures 2.38 & 2.39). Fibroblasts were observed in the *tunica albuginea* adjacent to the testicular parenchyma (Figures 2.40 & 2.41). The fibroblasts were characterized by the presence of irregular-shaped, euchromatic nuclei, as well as numerous elongated mitochondria (Figure 2.41).

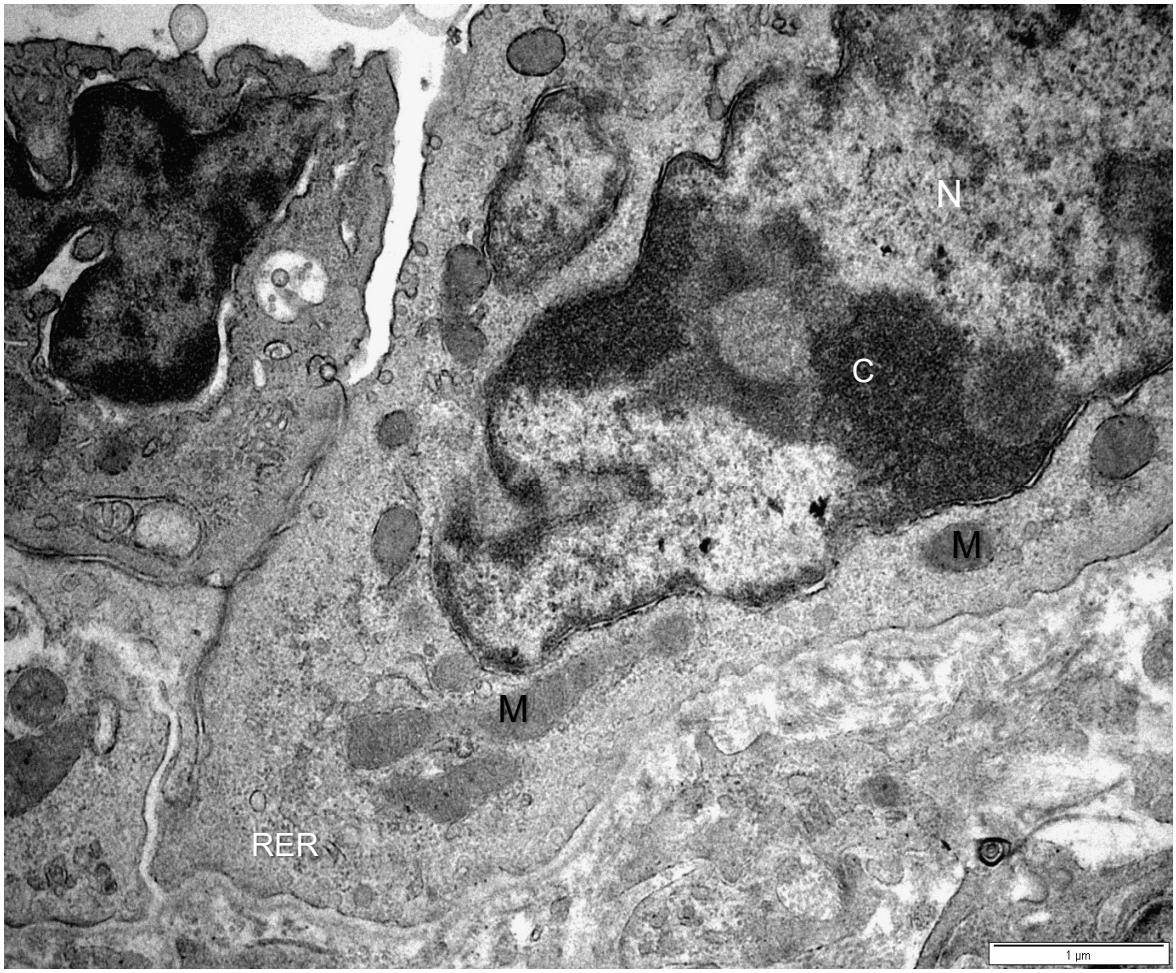

Figure 2. 27: Transmission electron photomicrograph of mesothelial cells lining the testicular capsule of a pre-pubertal bird. Dense clumps of chromatin (C) are observed in the nucleus of a mesothelial cell. M: mitochondria. RER: rough endoplasmic reticulum.

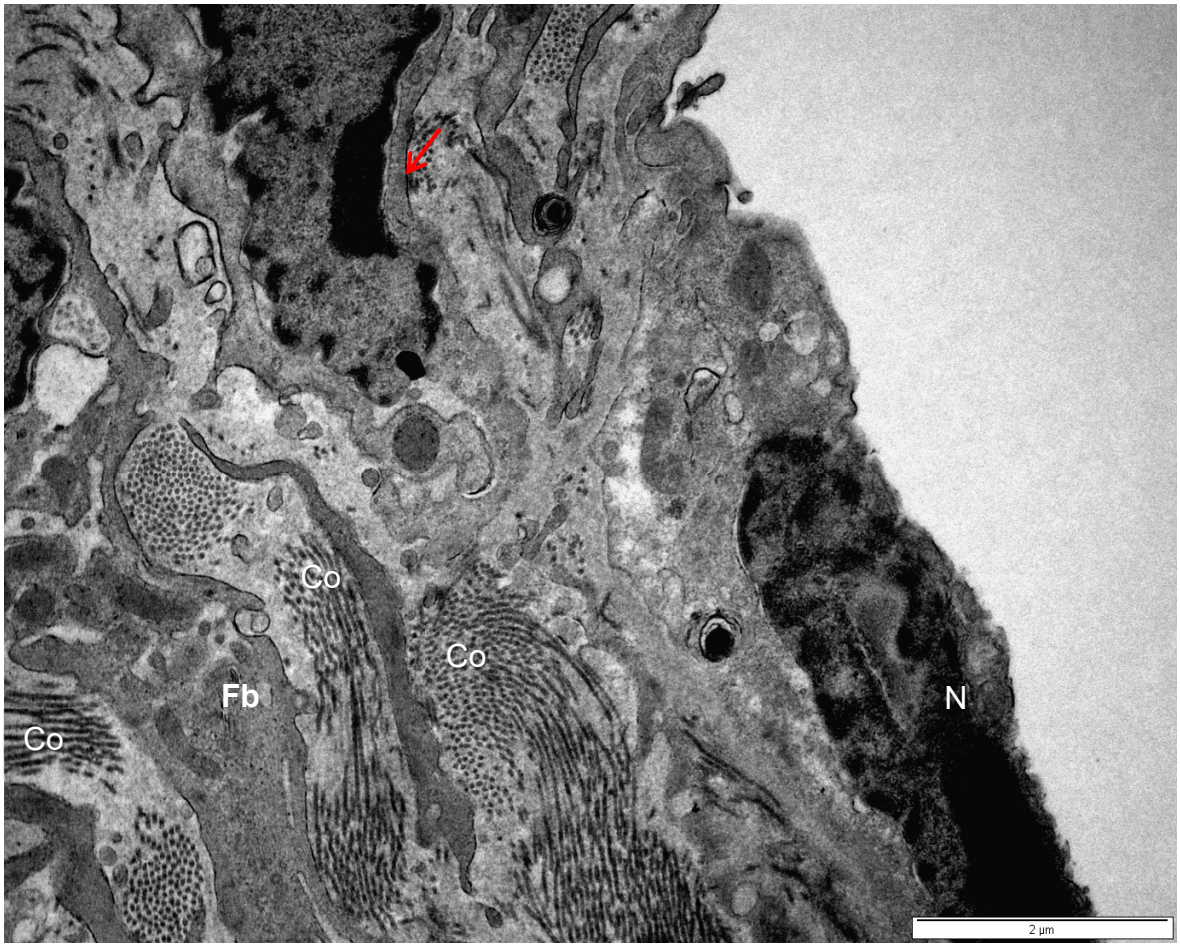

Figure 2. 28: Transmission electron micrograph of the *tunica serosa* of a pre-pubertal bird. N: nucleus of a mesothelial cell. Fb: fibroblast. Red arrow: nucleus of a fibroblast in the superificial region of the *tunica albuginea*. Co: collagen bundles.

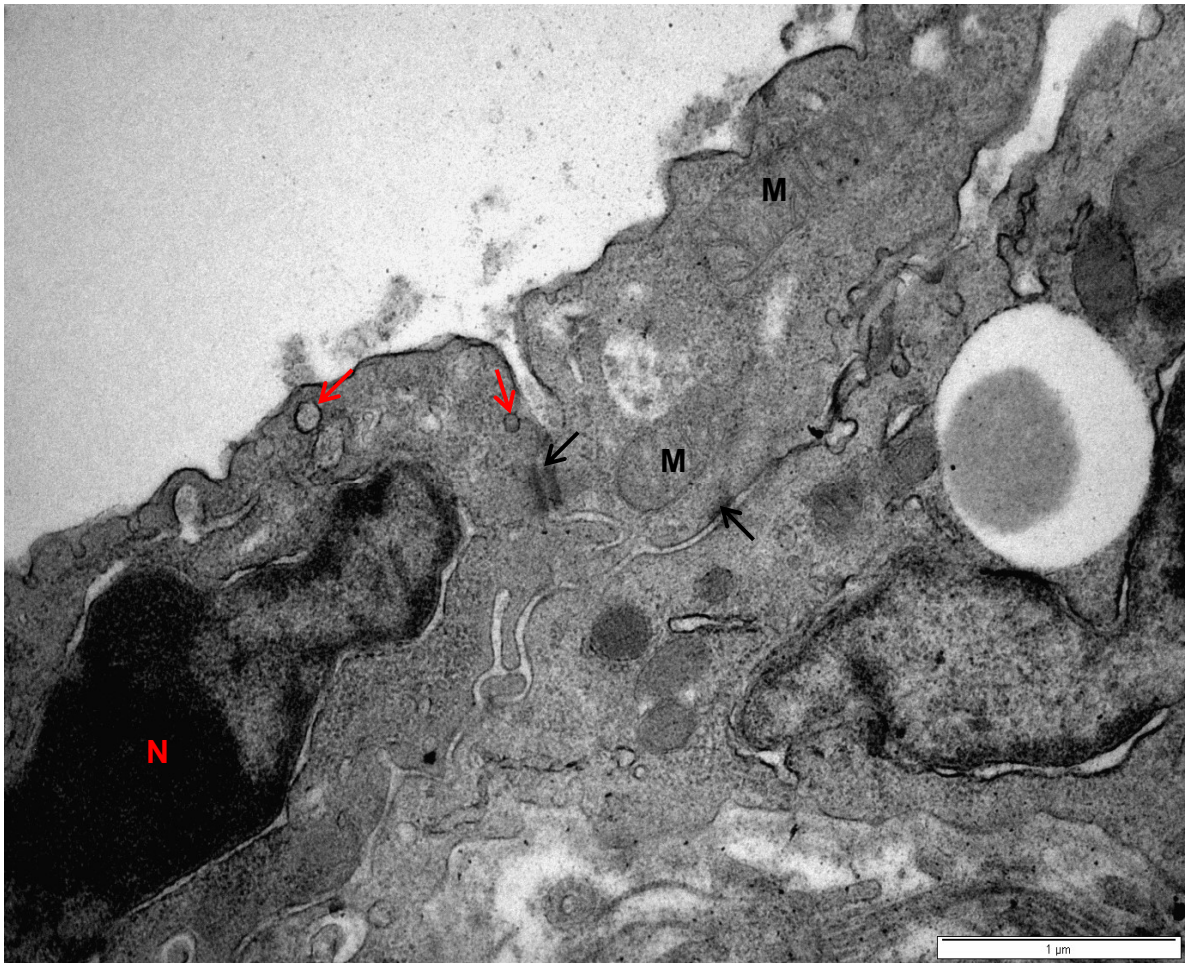

Figure 2. 29: Transmission electron photomicrograph of mesothelial cells lining the testicular capsule of a pre-pubertal bird. Black arrows: gap junctions connecting the plasma membranes of adjacent mesothelial cells. Red arrows: pinocytotic vesicles. M: mitochondria with prominent cristae. N: nucleus of a mesothelial cell.

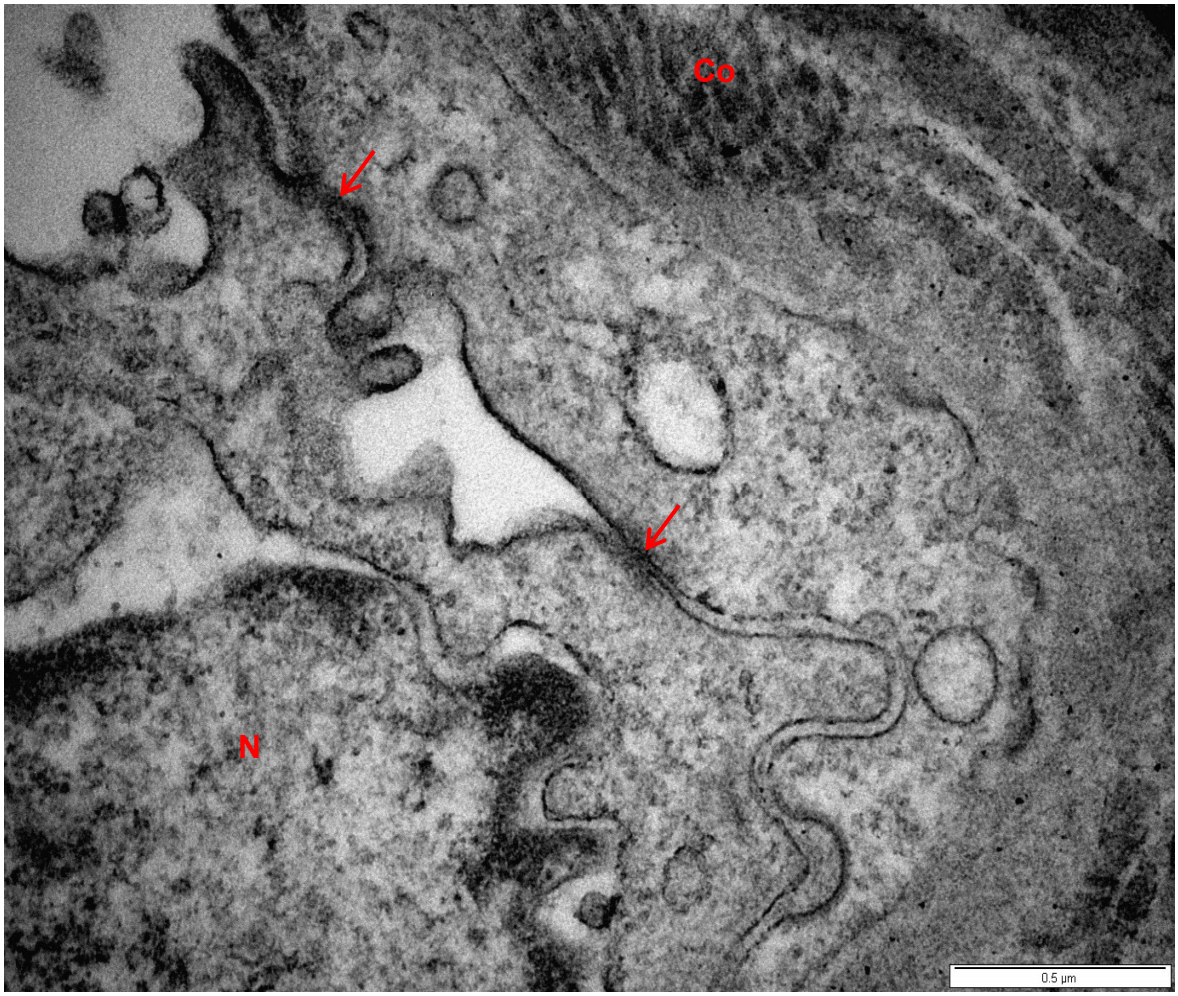

Figure 2. 30: Transmission electron photomicrograph of mesothelial cells in the *tunica serosa* of a pre-pubertal bird. Red arrows: tight junctions linking the plasma membranes of adjacent mesothelial cells. N: nucleus of a mesothelial cell. Co: collagen bundles.

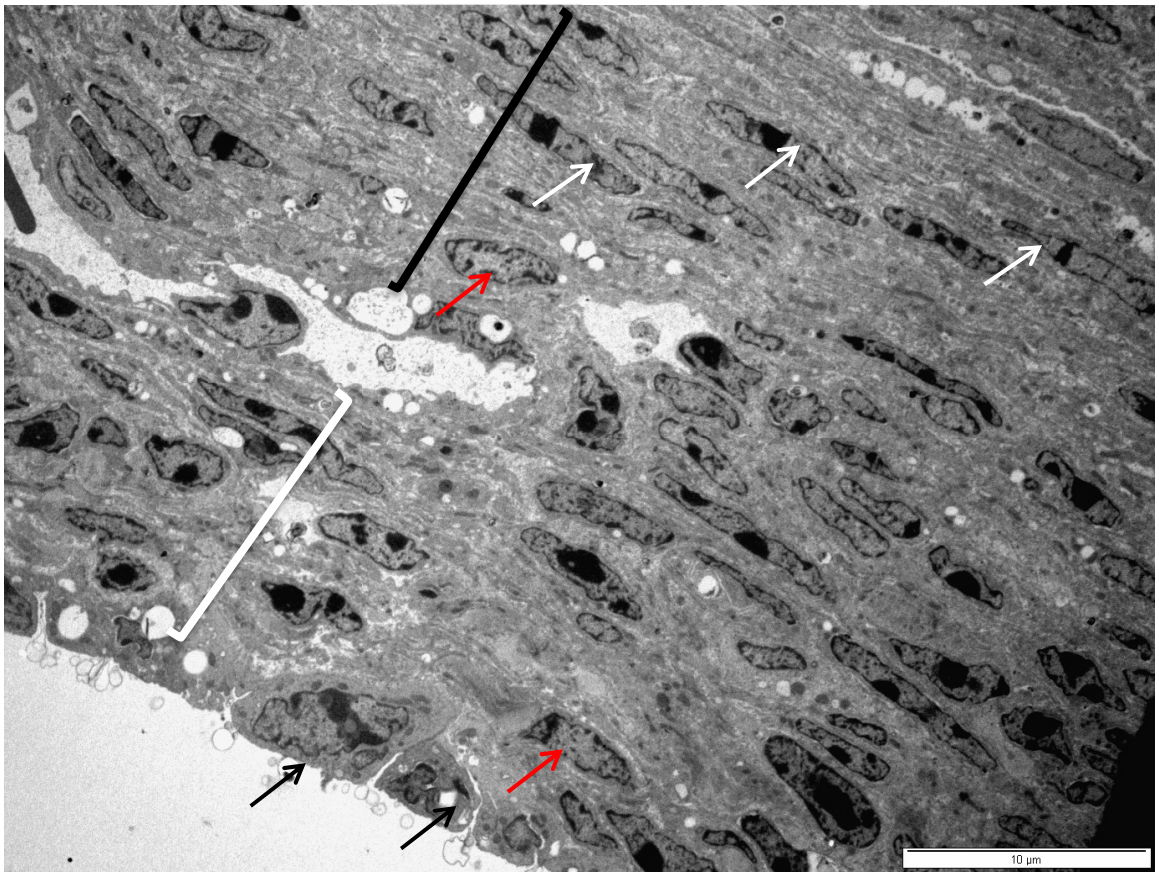

Figure 2. 31: Survey transmission electron photomicrograph of the testicular capsule of a pre-pubertal bird. The *tunica albugine*a is divided into superficial (white bracket) and deep (black bracket) parts. Red arrows: fibroblasts. White arrows: smooth muscle cells.

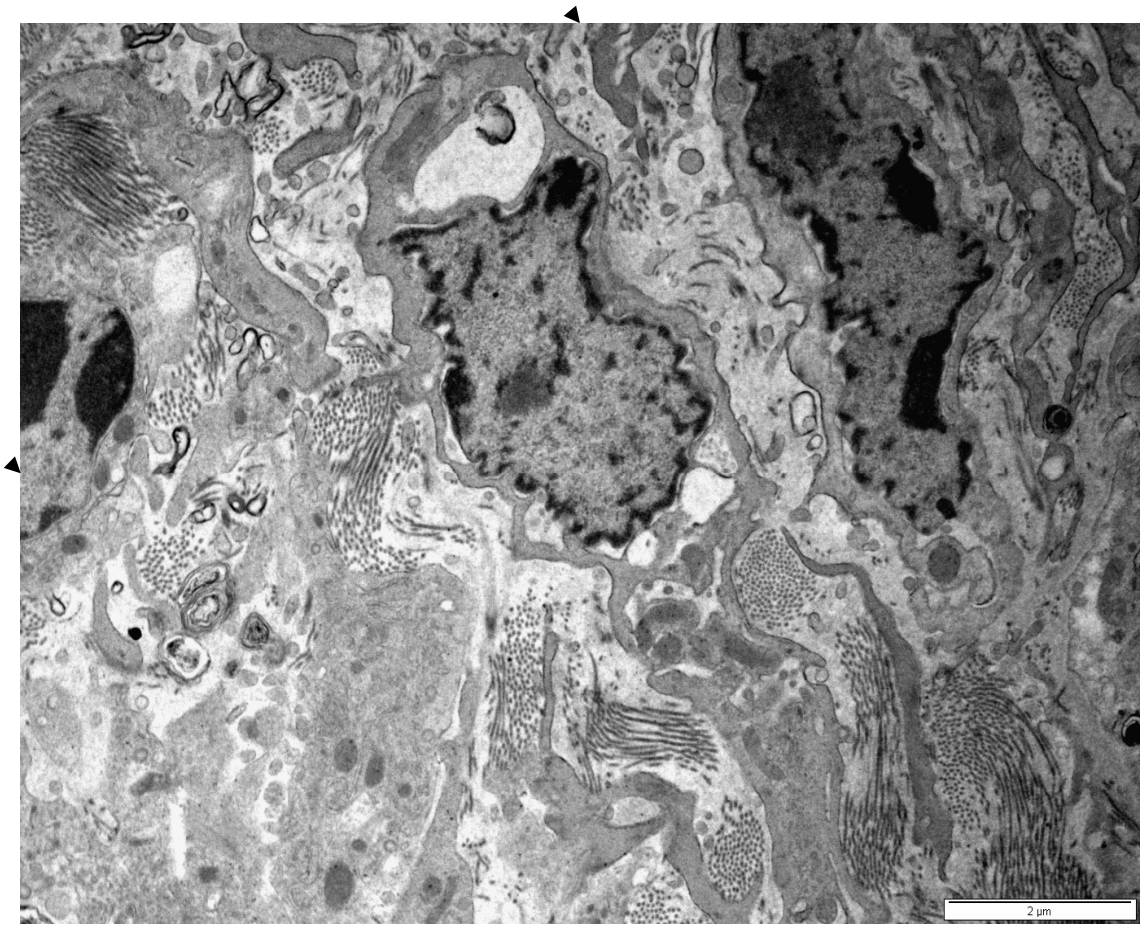

Figure 2. 32: Transmission electron micrograph showing the superficial region of the *tunica albuginea* of a pre-pubertal bird. Sm: smooth muscle cell. Fb: fibroblast. Co: collagen fibres.

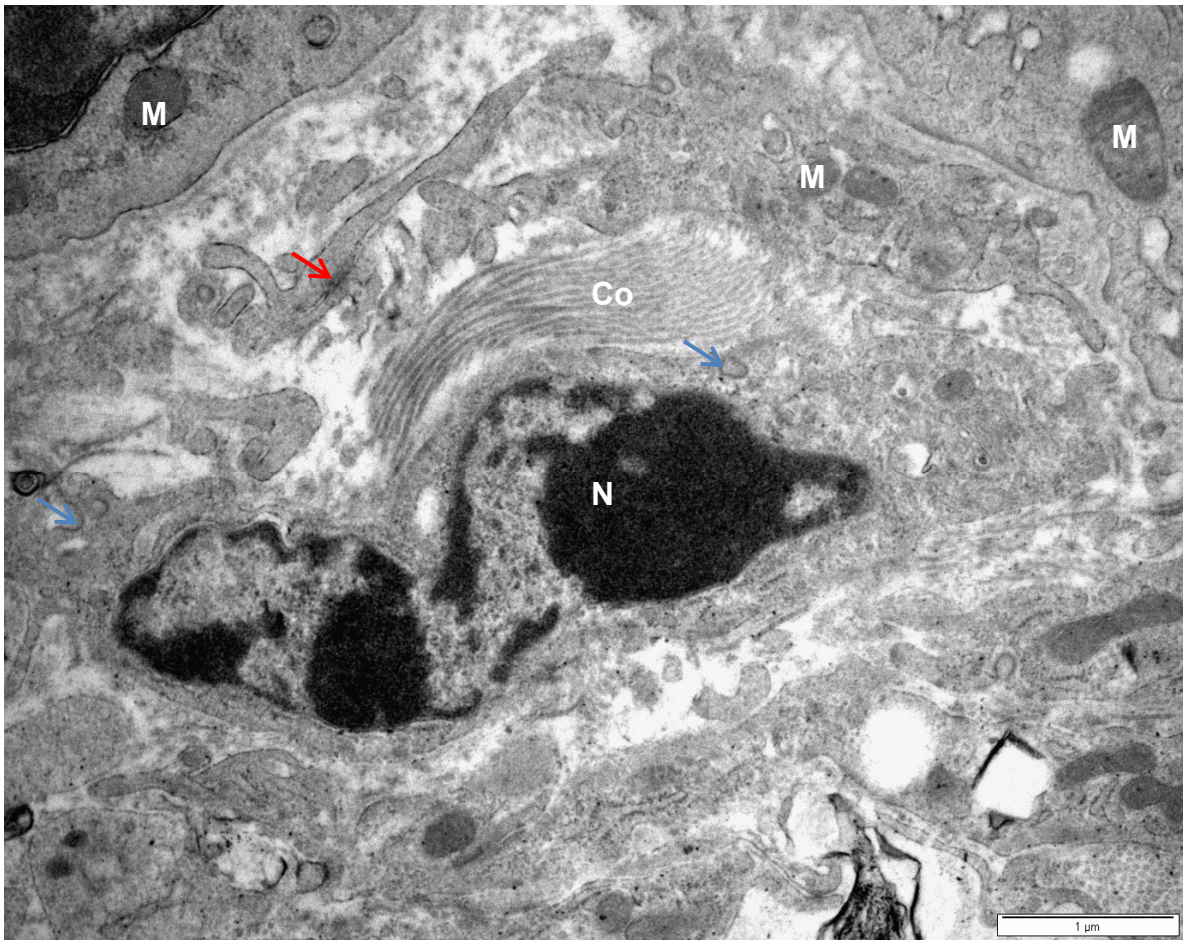

Figure 2. 33: Transmission electron photomicrograph showing a smooth muscle cell in the superficial region of the *tunica albuginea* of a pre-pubertal bird. N: nucleus of the smooth muscle cell. Blue arrows: pinocytotic vesicles. Red arrow: tight junction linking the cytoplasmic processes of neighbouring. M: mitochondria. Co: collagen bundle.

Figure 2. 34: Transmission electron photomicrograph showing a fibroblast in the superficial region of the *tunica albuginea* of a pre-pubertal bird. N: nucleus of the fibroblast. M: mitochondrion. Co: forming collagen fibre. Red arrow: gap junction linking the fibroblast with an adjacent cell.

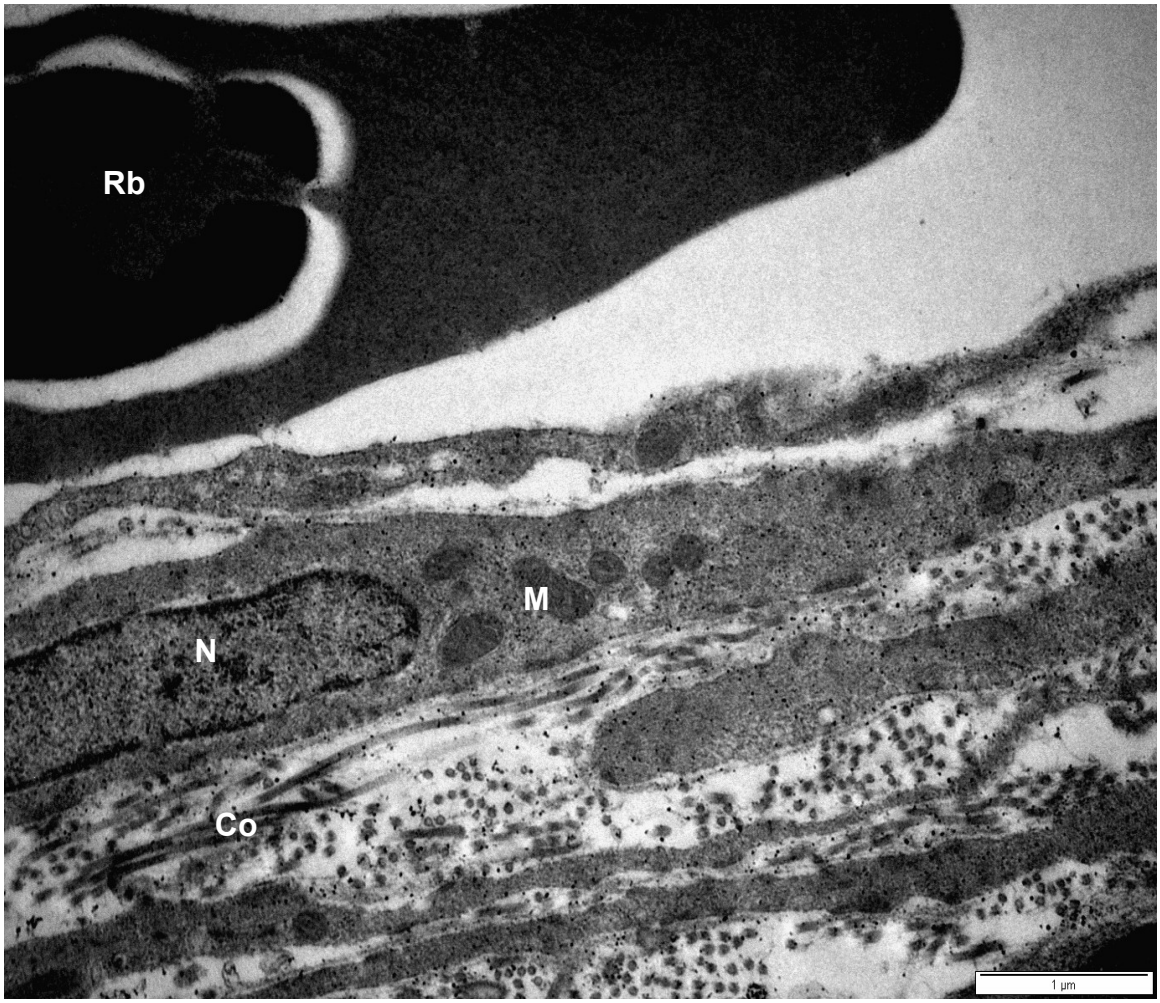

Figure 2. 35: Transmission electron micrograph showing part of a vein located in the *tunica albuginea* of a pre-pubertal bird. N: nucleus of an endothelial cell. M: mitochondrion. Co: collagen fibres. Rb: nucleated red blood cell.

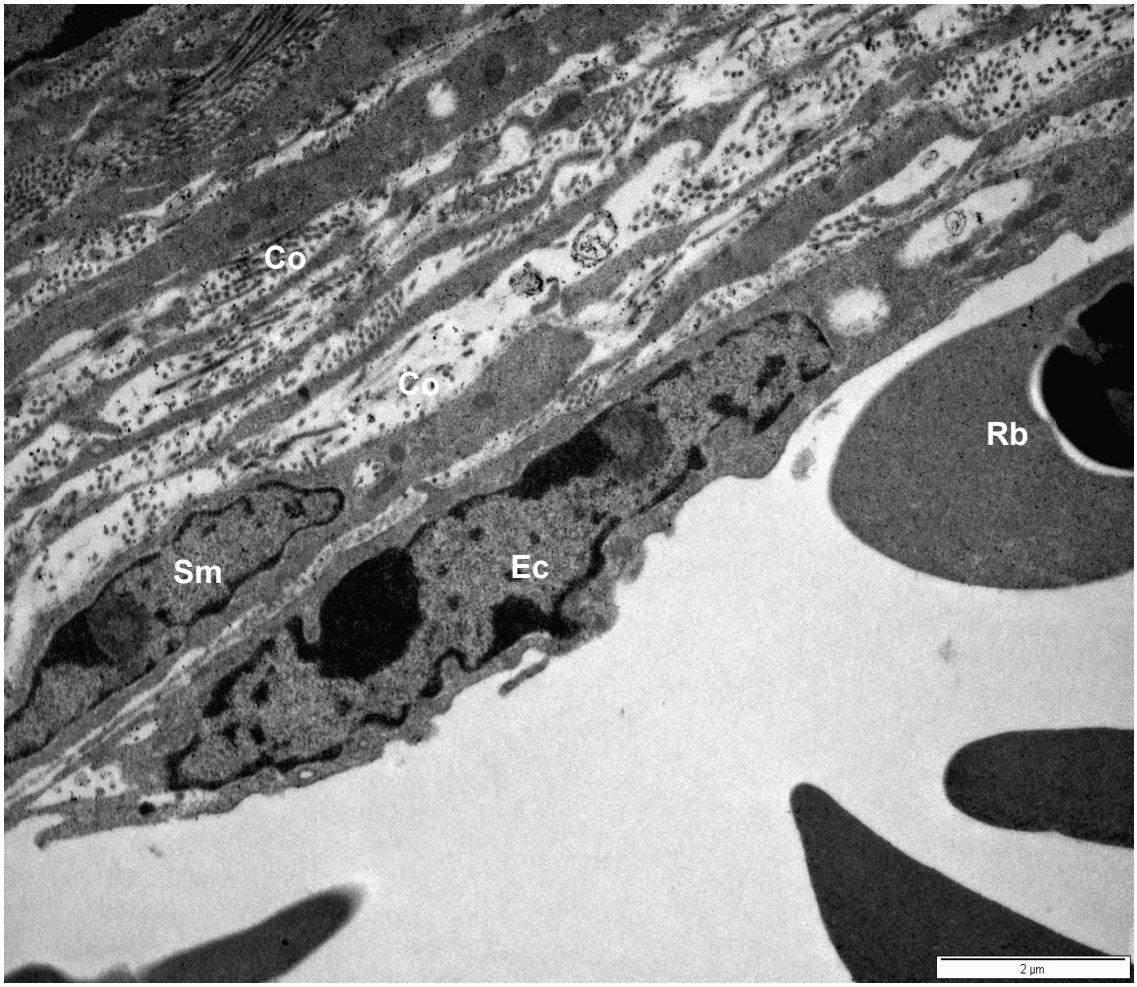

Figure 2. 36: Transmission electron micrograph showing part of a vein located in the *tunica albuginea* of a pre-pubertal bird. Sm: vascular smooth muscle cell. Ec: vascular endothelial cell. Rb: nucleated red blood cell. Co: collagen bundles.

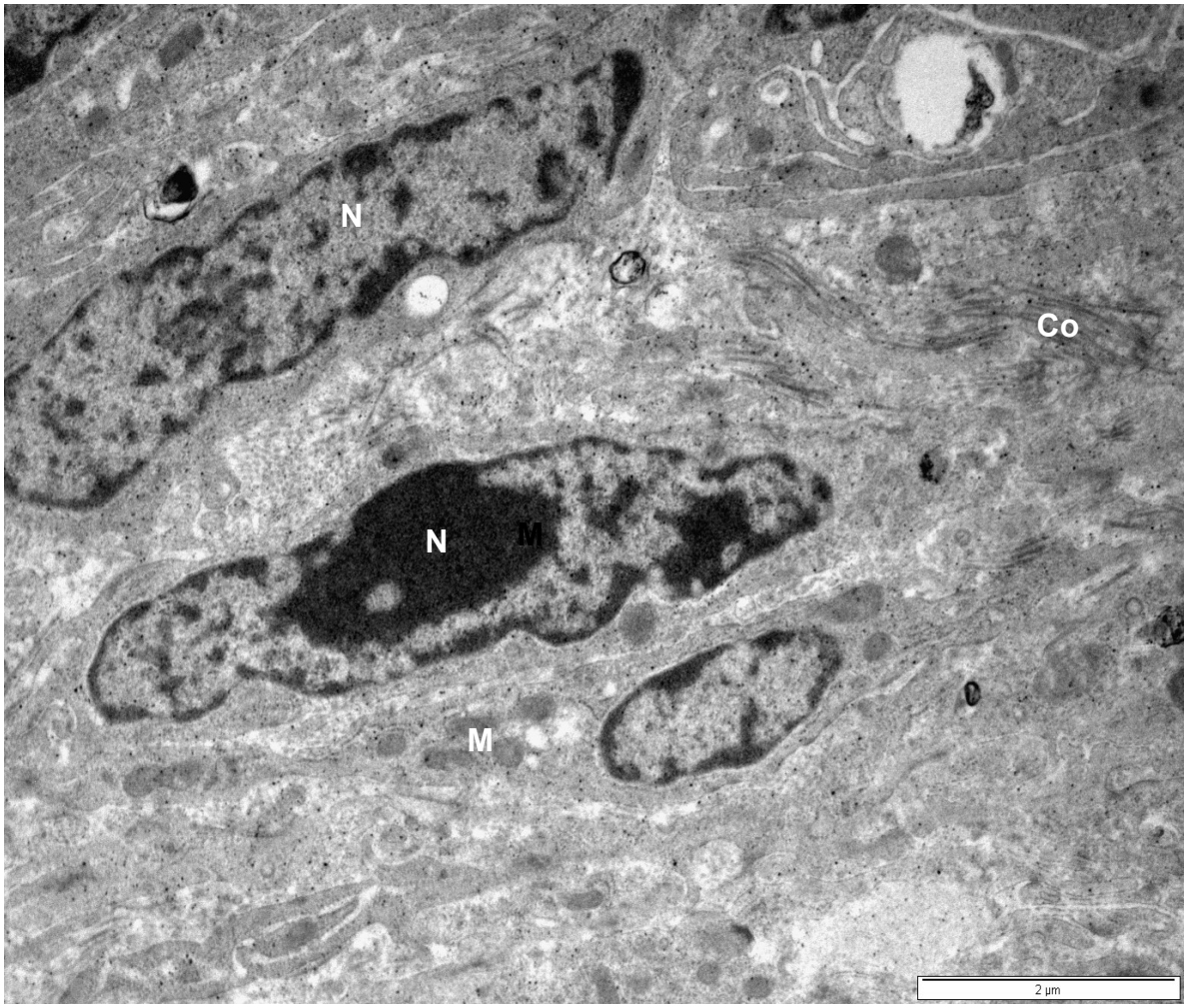

Figure 2. 37: Transmission electron micrograph showing smooth muscle cells in the deeper regions of the *tunica albuginea* of a pre-pubertal bird. N: nuclei of smooth muscle cells. Co: collagen fibre bundles. M: mitochondrion.

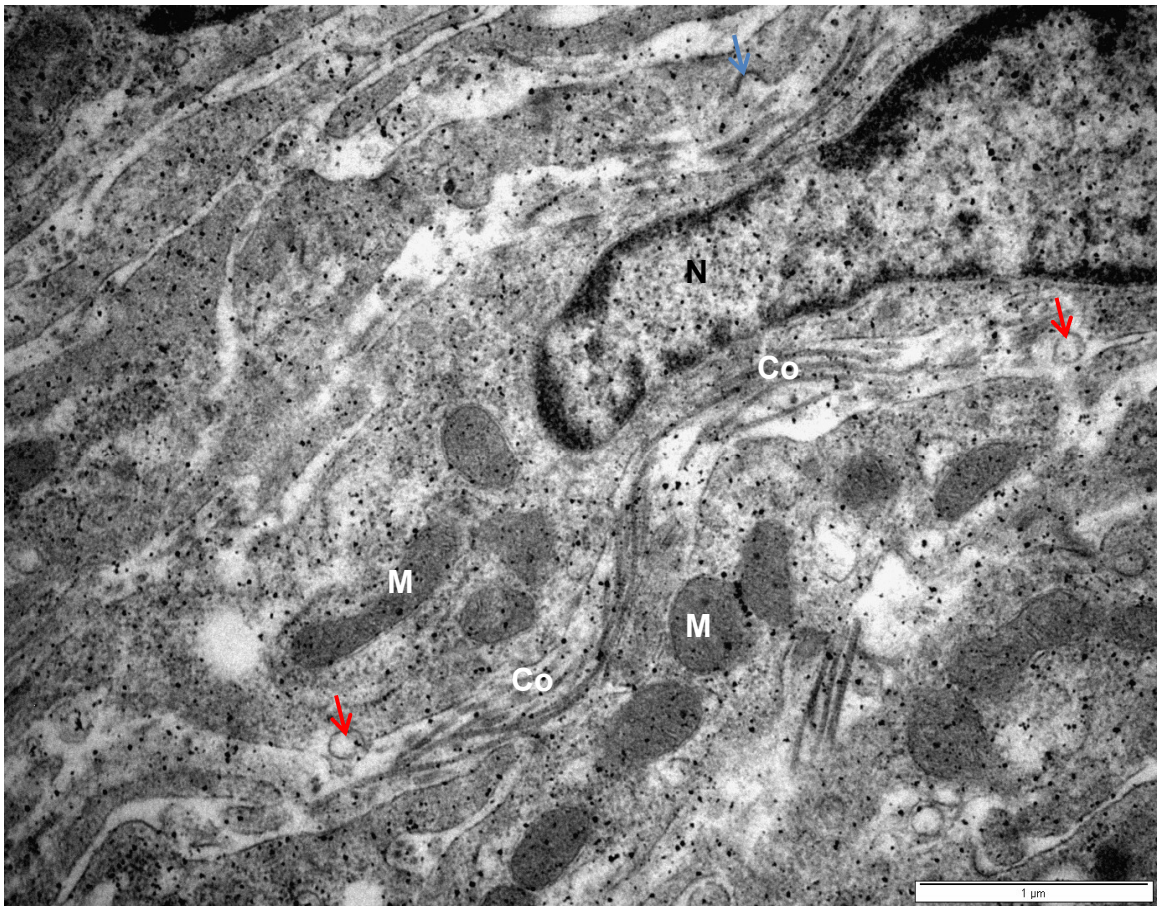

Figure 2. 38: Transmission electron micrograph showing a smooth muscle cell in the deep region of the *tunica albuginea* of a pre-pubertal bird. N: nucleus of the smooth muscle cell. Co: collagen bundles. M: mitochondria. Red arrows: pinocytotic vesicles. Blue arrow: coated pit.

Figure 2. 39: Transmission electron micrograph showing part of a smooth muscle cell located in the deep region of the *tunica albuginea* of a pre-pubertal bird. N: nucleus of the smooth muscle cell. Red arrow: pinocytotic vesicle. Blue arrow: coated pit. m: bundle of microfilaments.

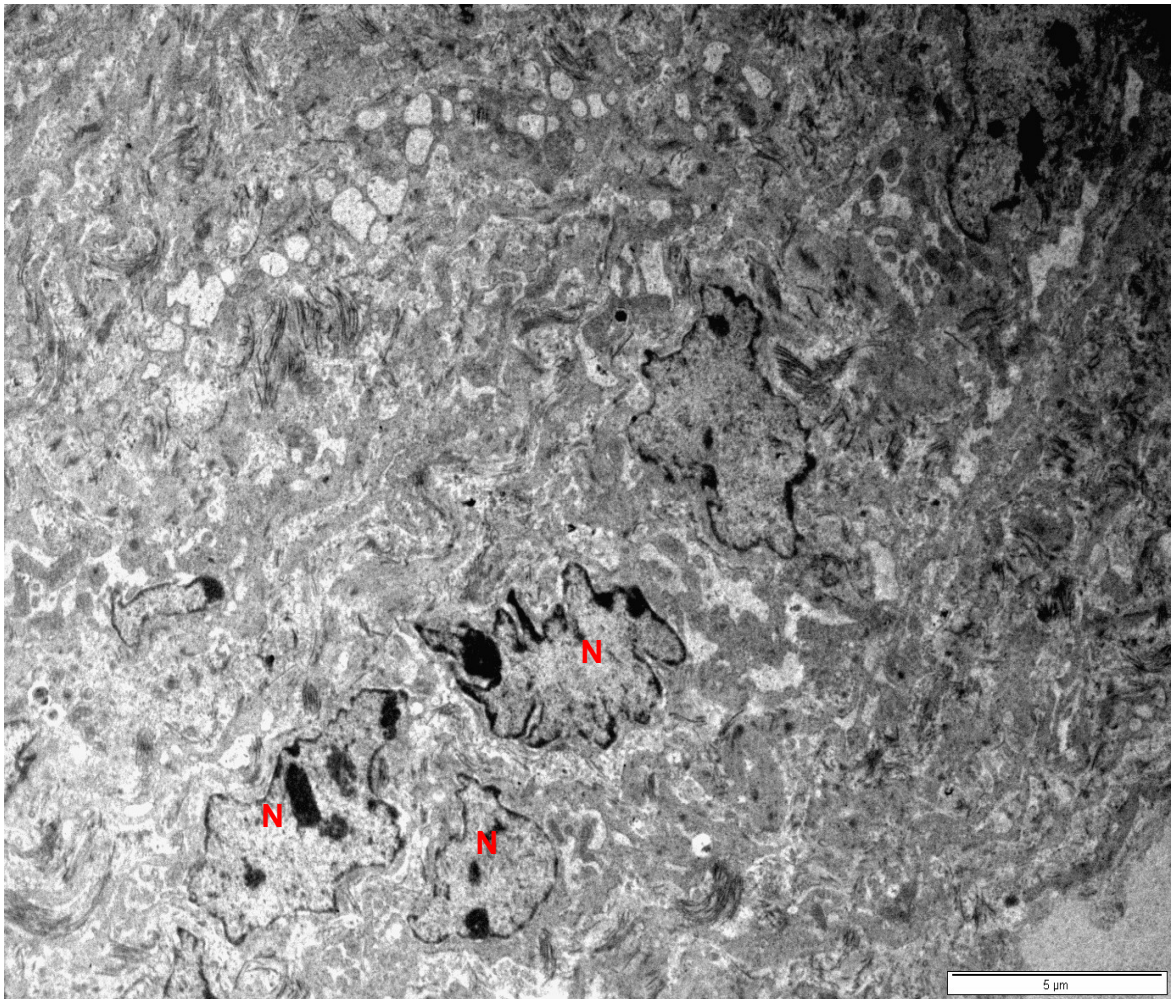

Figure 2. 40: Transmission electron micrograph showing fibroblasts in the deep region of the *tunica albuginea* of a pre-pubertal bird. N: nuclei of fibroblasts.

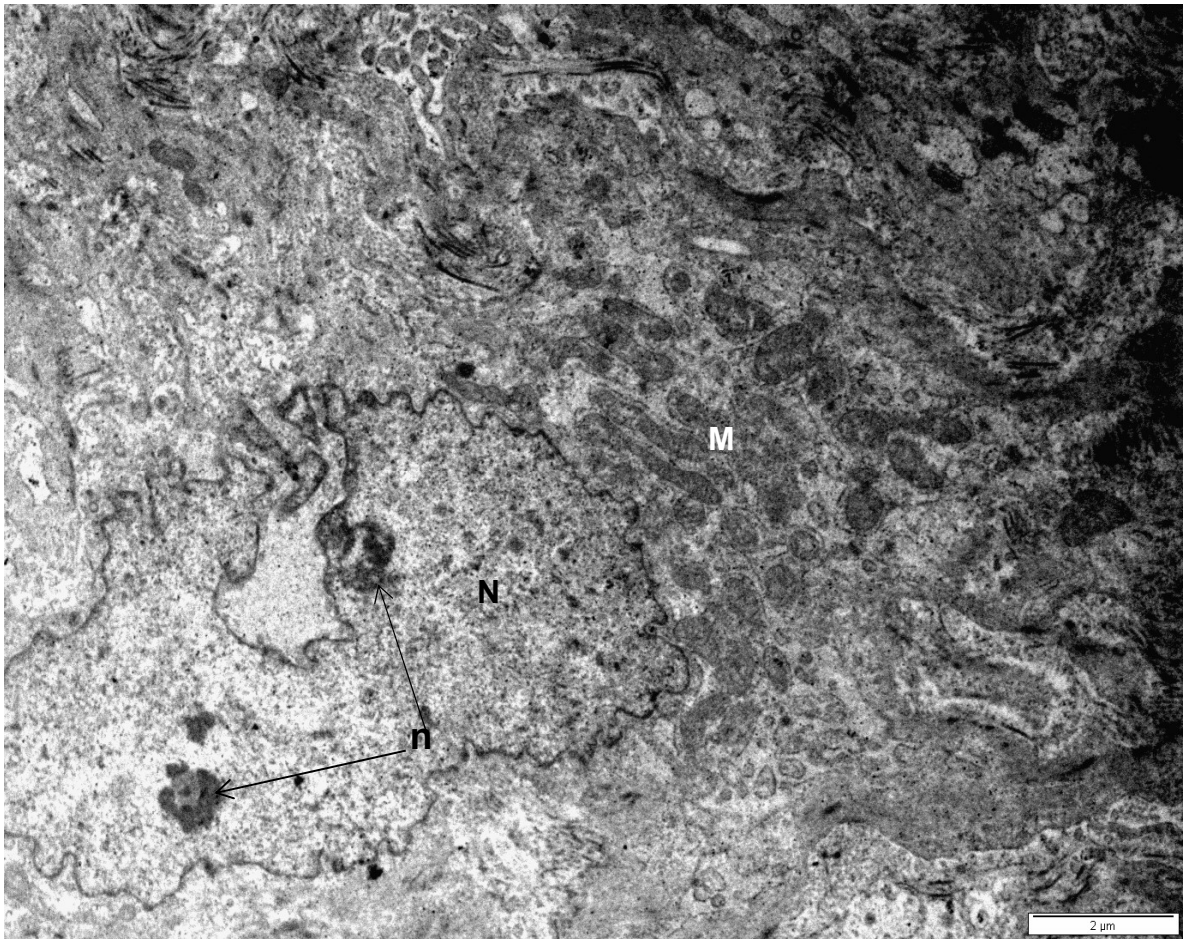

Figure 2. 41: Transmission electron micrograph of a fibroblast in the deep region of the *tunica albuginea* of a pre-pubertal bird. n: nucleoli in the nucleus (N) of a fibroblast. M: slender, elongated mitochondria.

Pubertal birds

The *tunica serosa* of pubertal birds was formed by a single-layered cuboidal to squamous mesothelium with an underlying layer of connective tissue (Figures 2.42). The mesothelial cells displayed elongated, heterochromatic nuclei (Figures 2.42). The cytoplasm of mesothelial cells contained several mitochondria, short profiles of RER, as well as a few pinocytotic vesicles (Figure 2.42). Tight junctions connected the plasma membranes of adjacent mesothelial cells (Figure 2.43).

Below the *tunica serosa* was the superficial region of the *tunica albuginea* which consisted of layers of smooth muscle cells with intervening bundles of collagen (Figure 2.44). The smooth muscle cells contained elongated heterochromatic nuclei. Golgi complexes, mitochondria, pinocytotic vesicles, cytoplasmic densities, as well as bundles of microfilaments were evident in the cytoplasm of the smooth muscle cells. Cytoplasmic densities were also observed on the inner plasma membranes of the smooth muscle cells (Figure 2.45). Gap junctions linked adjacent smooth muscle cells (Figure 2.45).

A network of veins demarcated the superficial region of the *tunica albuginea* from the deep region. The endothelial and smooth muscle cells forming the walls of the veins contained irregular-shaped euchromatic nuclei (Figure 2.46).

Smooth muscle cells in the deeper regions of the *tunica albuginea* were longitudinally orientated (Figures 2.46). The smooth muscle cells displayed attenuated cytoplasmic processes, which alternated with layers of collagen bundles (Figure 2.47). Discernable cytoplasmic organelles in the smooth muscle cells included a few mitochondria, as well as pinocytotic vesicles. In addition to smooth muscle cells a few fibroblasts were observed in the deeper regions of the tunica albuginea. The fibroblasts displayed irregular-shaped nuclei which contained one or two prominent nucleoli (Figure 2.48). Mitochondria, dilated RER cisternae and vesicles were observed in the cytoplasm of the fibroblasts.

Located between the deep layer of the *tunica albuginea* and the testicular parenchyma was the *tunica vasculosa* (Figure 2.47). The walls of the blood vessels forming the *tunica vasculosa* were formed by endothelial cells and a single layer of smooth muscle cells. Th endothelial cells exhibited oblong-shaped, heterochromatic

nuclei, while elongated nuclei were observed in the vascular smooth muscle cells (Figure 2.47).

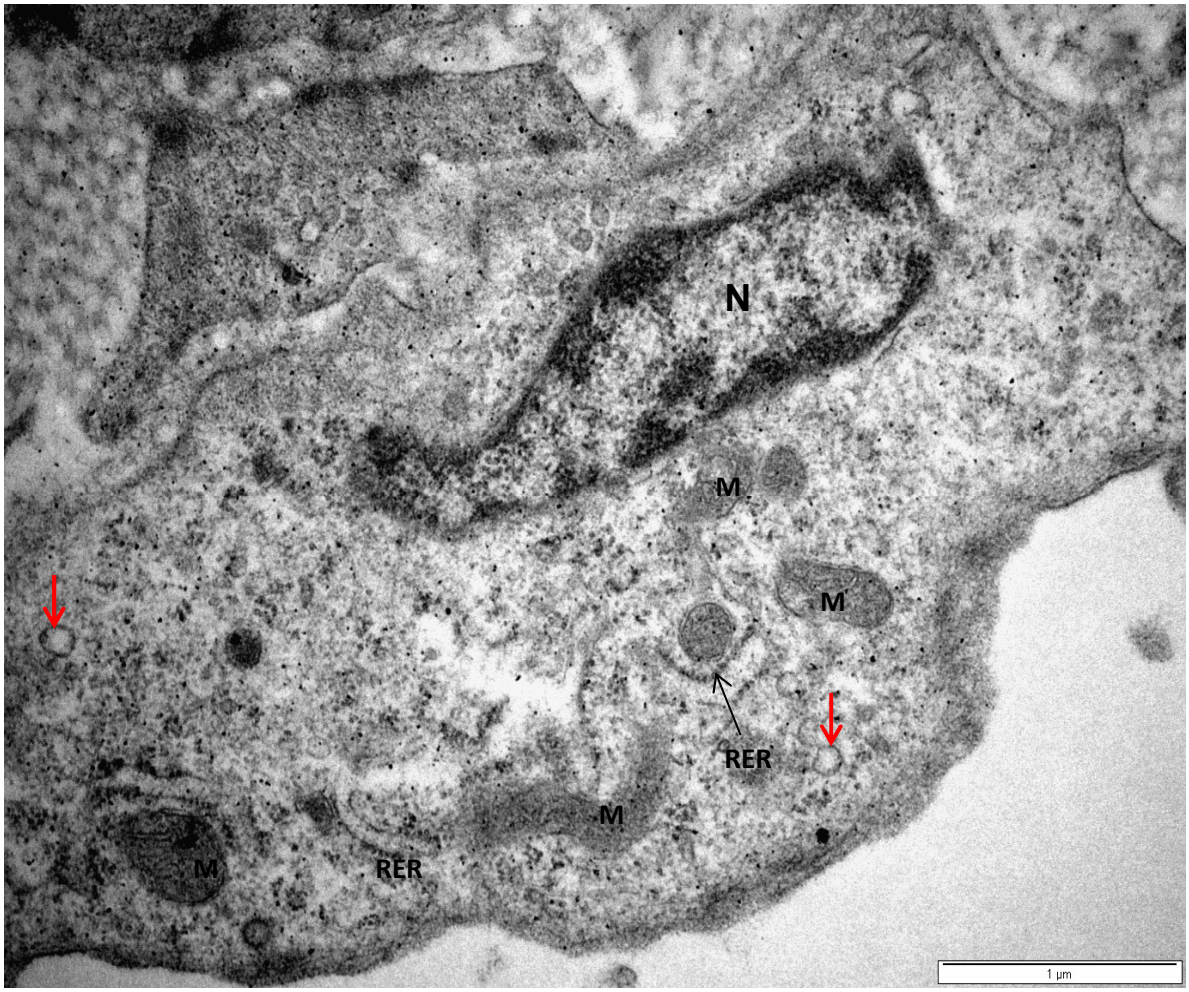

Figure 2. 42: Transmission electron micrograph of a mesothelial cell in the *tunica serosa* of a pubertal bird. N: nucleus of the mesothelial cell. Red arrows: pinocytotic vesicles. M: mitochondria. RER: rough endoplasmic reticulum.

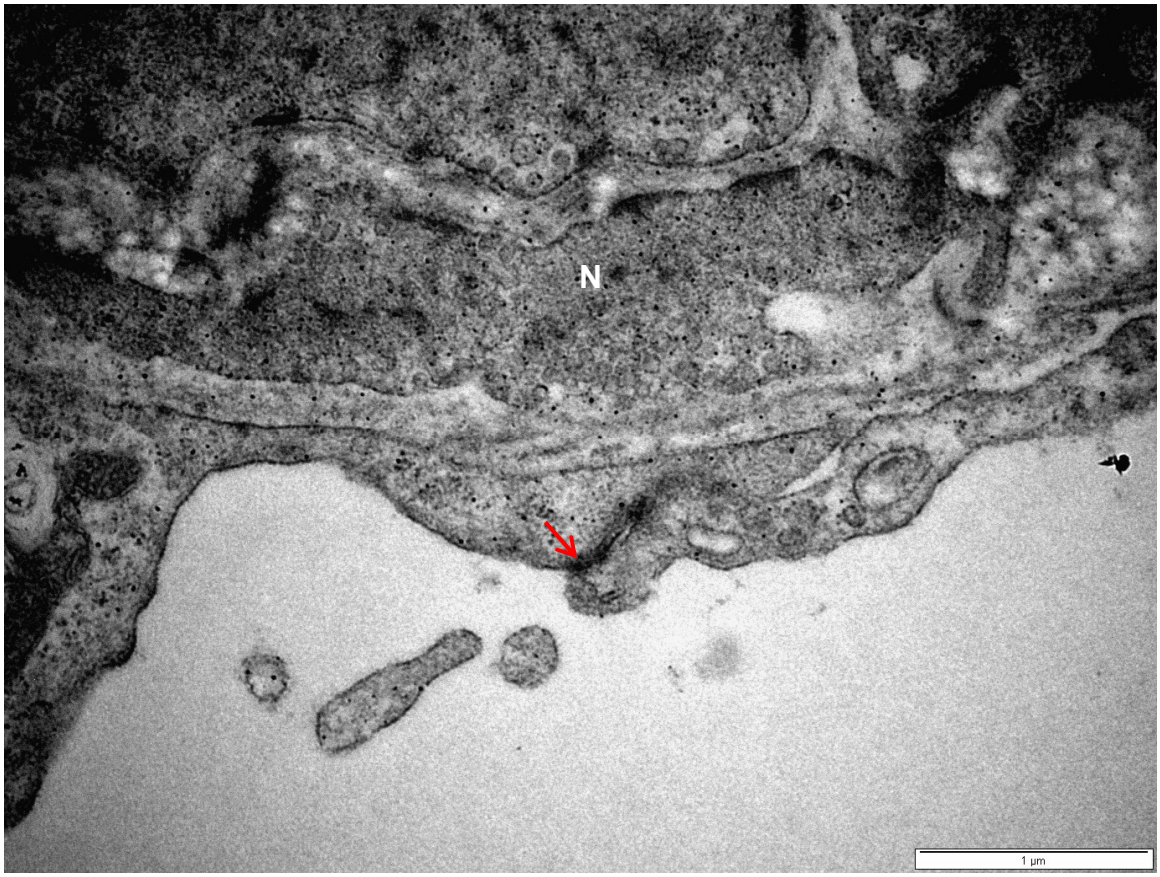

Figure 2. 43: Transmission electron micrograph of a mesothelial cell in the *tunica serosa* of a pubertal bird. N: nucleus. Red arrow: tight junction between plasma membranes of neighbouring mesothelial cells.

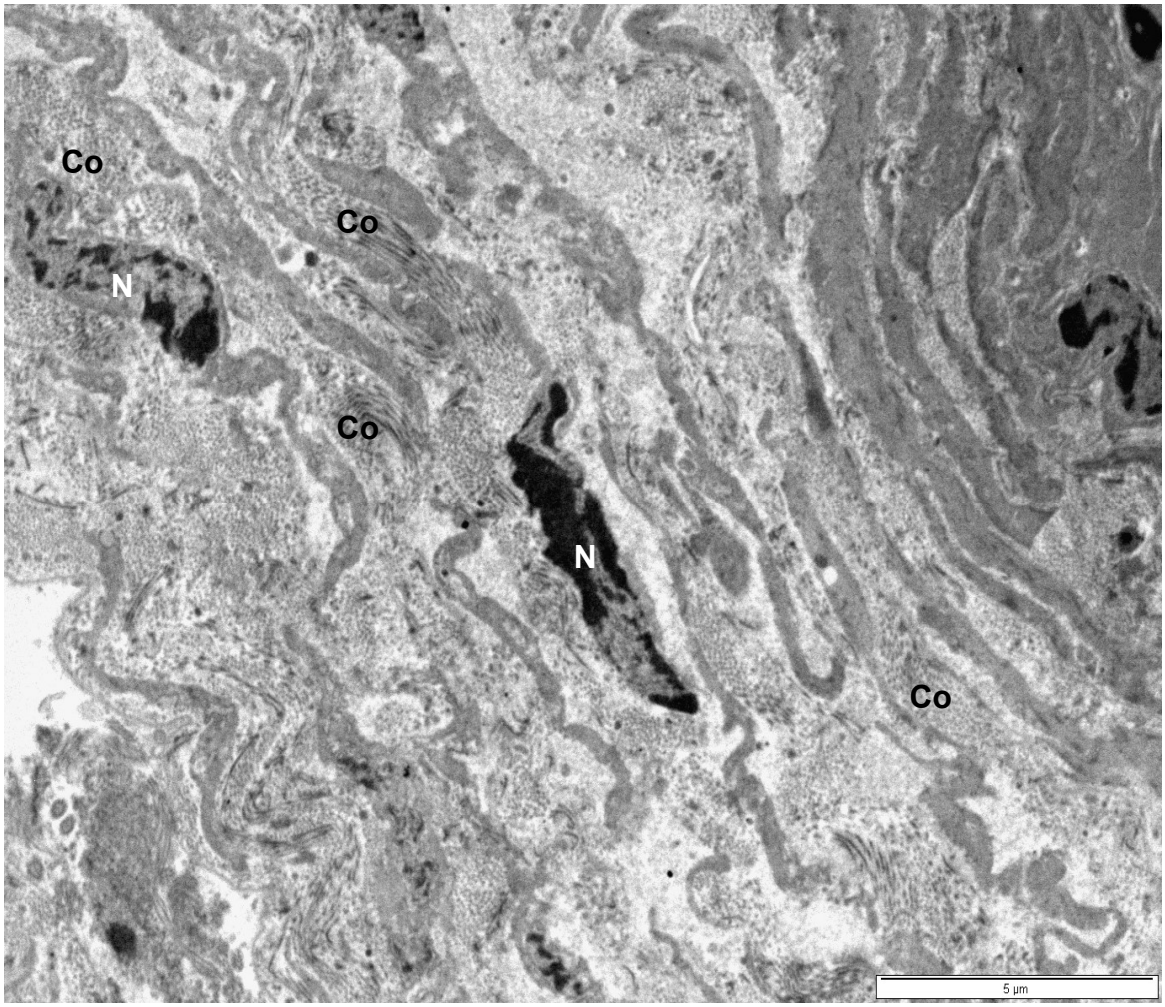

Figure 2. 44: Transmission electron micrograph of the *tunica albuginea* (superficial region) of a pubertal bird. N: nucleus of a smooth muscle cell. Co: Collagen bundles.

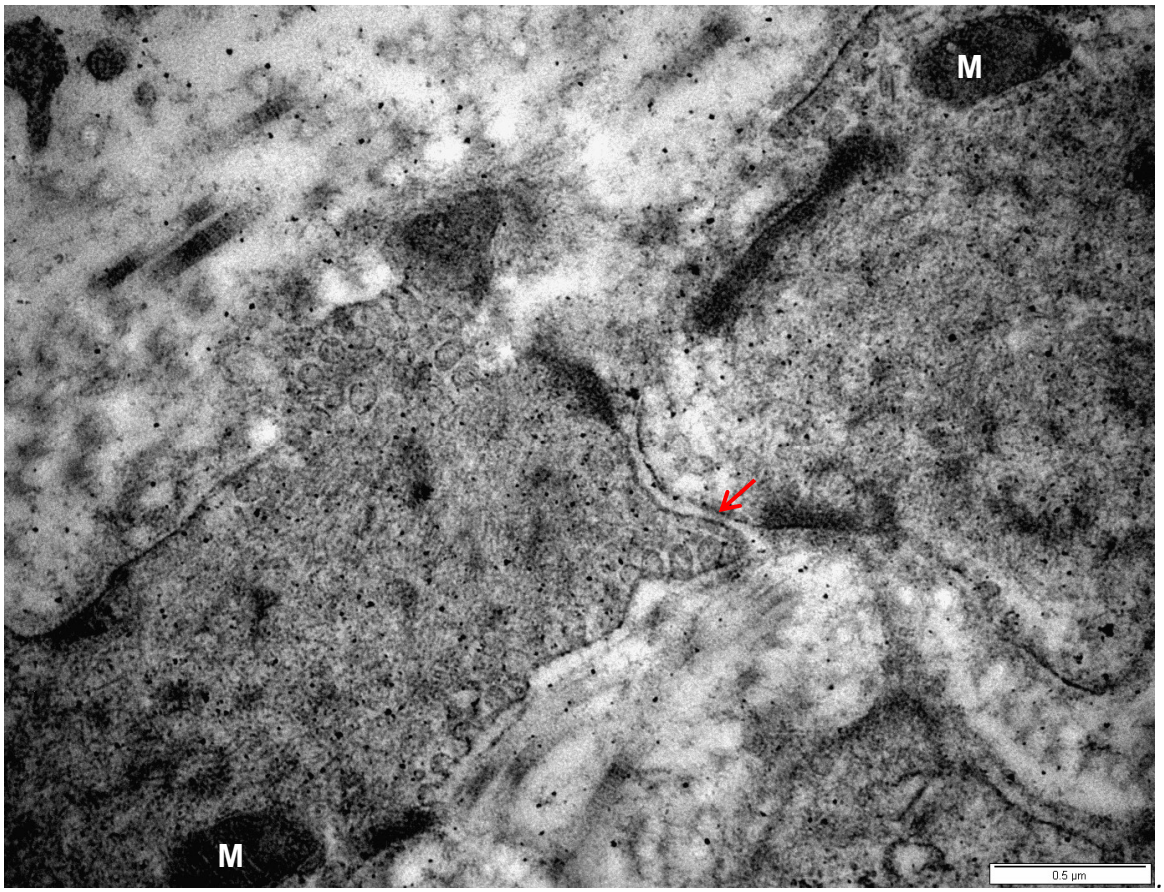

Figure 2. 45: Transmission electron micrograph of smooth muscle cells in the *tunica albuginea* of a pubertal quail. M: mitochondria. Red arrow: gap junction.

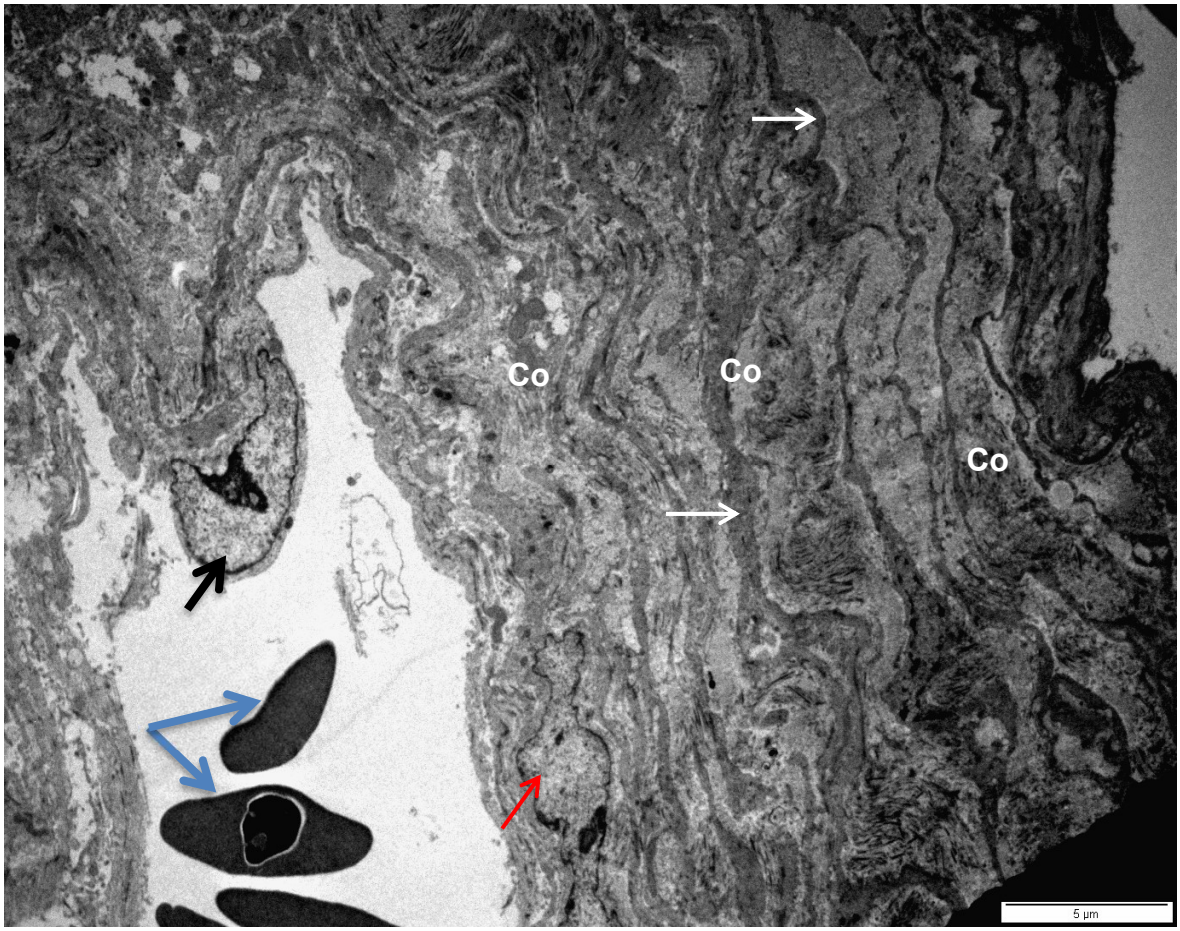

Figure 2. 46: Transmission electron micrograph of a vein dividing the *tunica albuginea* in a pubertal bird into superficial and deep regions. Black arrow: vascular endothelial cell. Red arrow: vascular smooth muscle cell. White arrows: smooth muscle cells in the deep region of the *tunica albuginea*. Blue arrows: nucleated red blood cells. Co: collagen bundles.

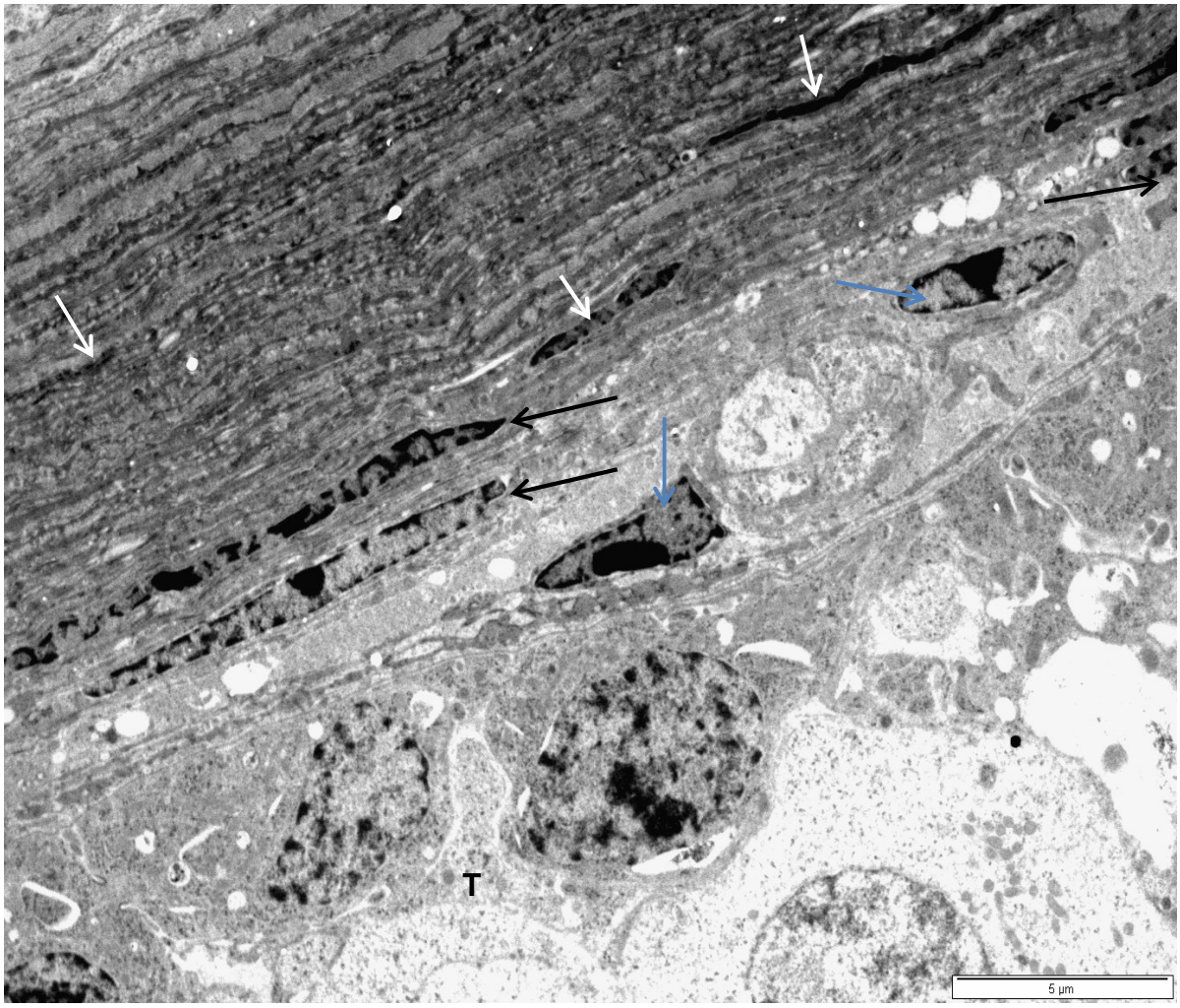

Figure 2. 47: Transmission electron micrograph of the testicular capsule and parenchyma of a pubertal bird. White arrows: nuclei of smooth muscle cells in the deeper region of the *tunica albuginea*. Black arrows: nuclei of vascular smooth muscle cells in the *tunica vasculosa*. Blue arrows: vascular endothelial cells of a blood vessel in the *tunica vasculosa*. T: testicular parenchyma.

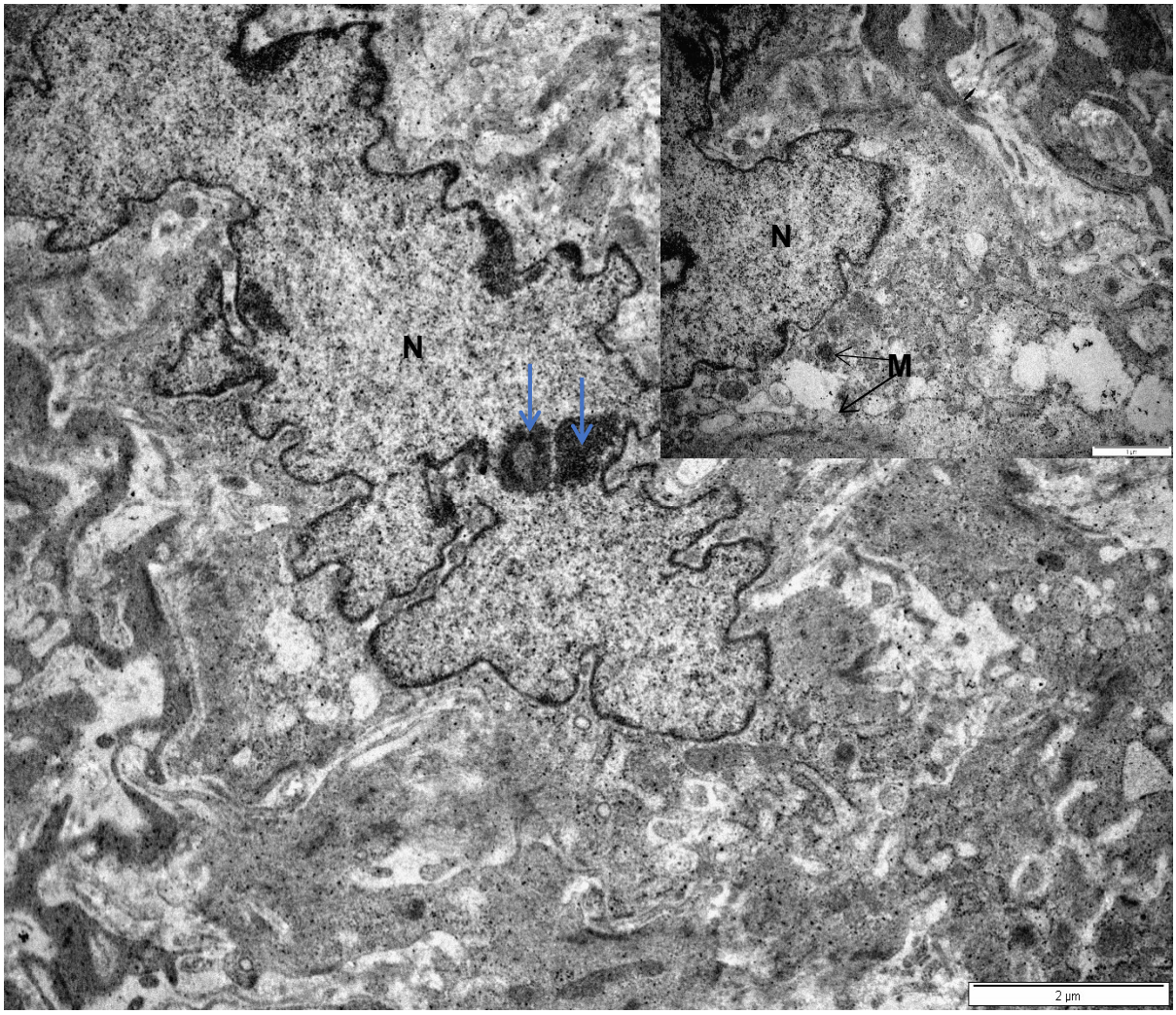

Figure 2. 48: Transmission electron micrograph of a fibroblast in the *tunica albuginea* of a pubertal bird. N: nucleus. M: mitochondria. Blue arrows: nucleoli.

Adult birds

The *tunica serosa* was formed by a single layer of mesothelial cells resting on a layer of connective tissue (Figure 2.49). The mesothelial cells exhibited oval to elongated, heterochromatic nuclei. Contained within the cytoplasm of these cells were pinocytotic vesicles, as well as several mitochondria with prominent cristae.

The superficial region of the *tunica albuginea* was formed by smooth muscle cells alternating with collagen bundles (Figure 2.50). Smooth muscle cells in this region of the *tunica albuginea* contained oblong to elongated nuclei. Both euchromatic and heterochromatic nuclei were observed in the smooth muscle cells (Figure 2.51). Prominent within the cytoplasm of the smooth muscle cells were mitochondria, RER cisternae, pinocytotic vesicles, multivesicular bodies and centrioles (Figure 2.52).

A venous network separated the superficial and deep regions of the *tunica albuginea*. Endothelial cells containing irregular-shaped heterochromatic nuclei lined the veins forming the venous network (Figure 2.53). The *tunica mediae* of the veins were formed by a single layer of smooth muscle cells.

Underlying the venous network was the deep region of the *tunica albuginea*. This deep region was characterized by the presence of longitudinally-orientated smooth muscle cells which alternated with bundles of collagen (Figure 2.54). The smooth muscle cells exhibited elongated, euchromatic nuclei. Extending from either side of the nuclei were attenuated cytoplasmic processes which contained: prominent Golgi complexes; mitochondria; profiles of RER; peripherally-located microfilaments and several vesicles (Figure 2.55).

Occasional fibroblasts were observed in the deep region of the *tunica albuginea* (Figure 2.56). The fibroblasts exhibited irregular-shaped euchromatic nuclei, which contained prominent nucleoli. Dilated RER cisternae and mitochondria were observed in the cytoplasm of the fibroblasts.

Situated between the *tunica albuginea* and testicular parenchyma was a poorly-defined *tunica vasculosa* (Figure 2.57).

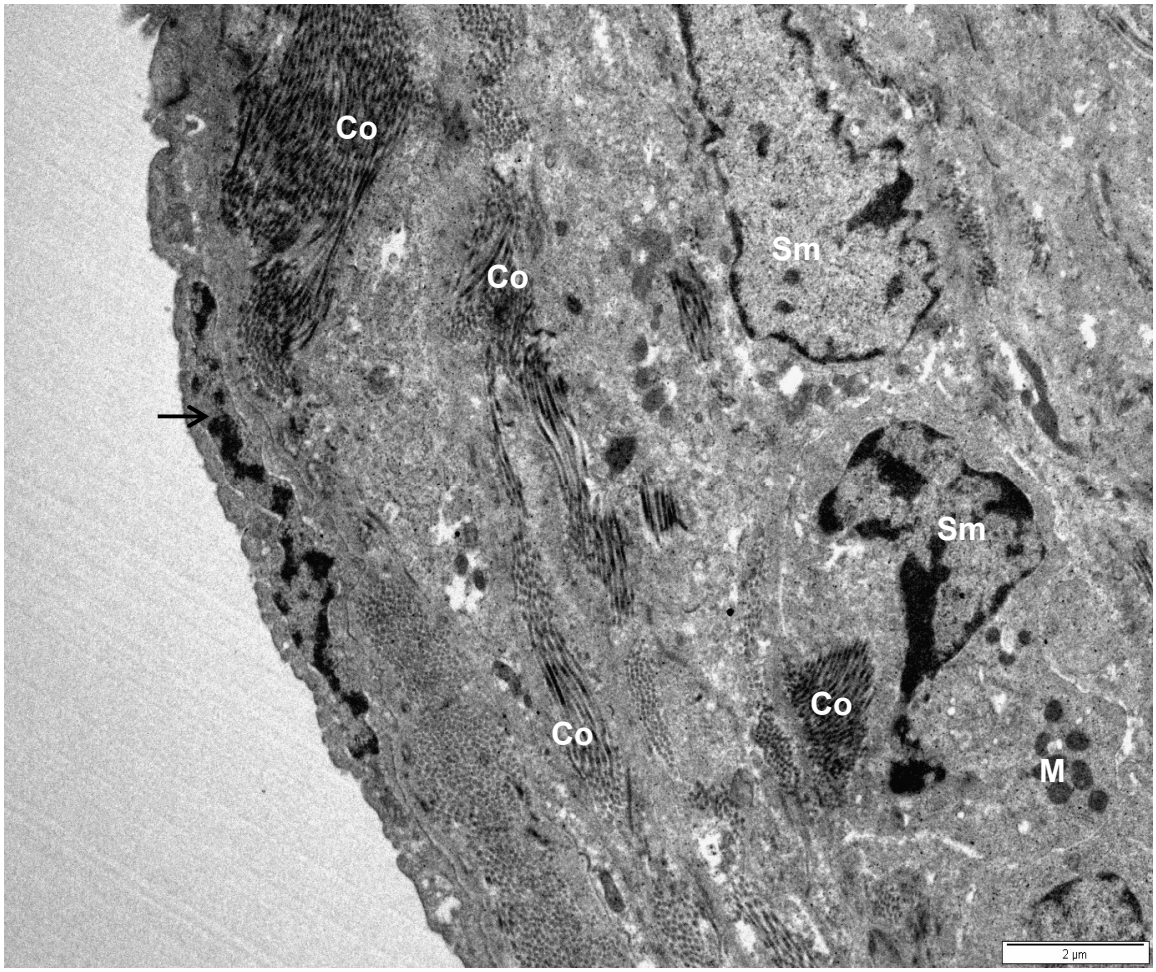

Figure 2. 49: Transmission electron micrograph of the testicular capsule of an adult bird. Black arrow: nucleus of a mesothelial cell. Sm: smooth muscle cells of the *tunica albuginea* (superficial region). M: mitochondria. Co: collagen bundles.

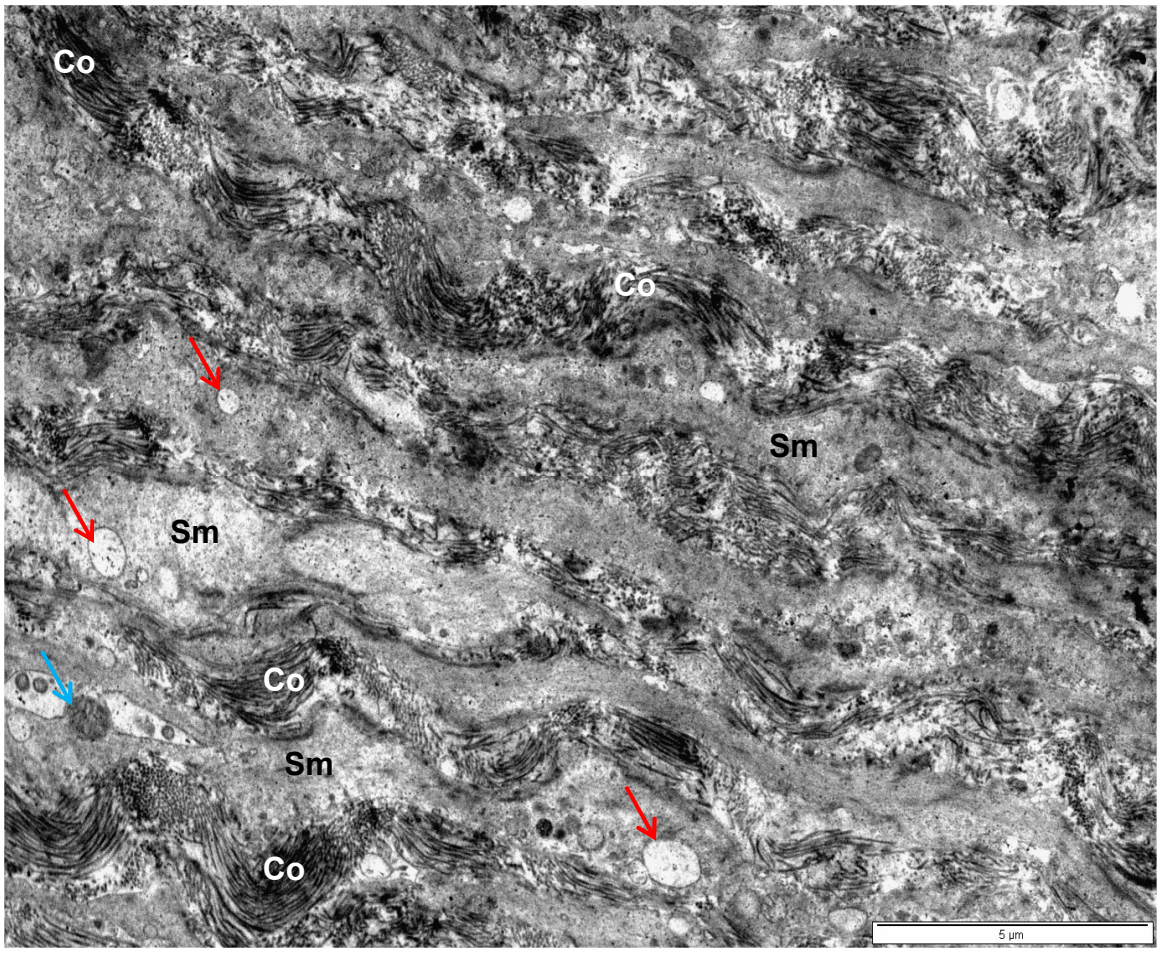

Figure 2. 50: Transmission electron micrograph showing the superficial region of the *tunica albuginea* in an adult bird. Sm: smooth muscle cells. Red arrows: dilated RER cisternae. Co: collagen bundles. Blue arrow: mitochondrion.

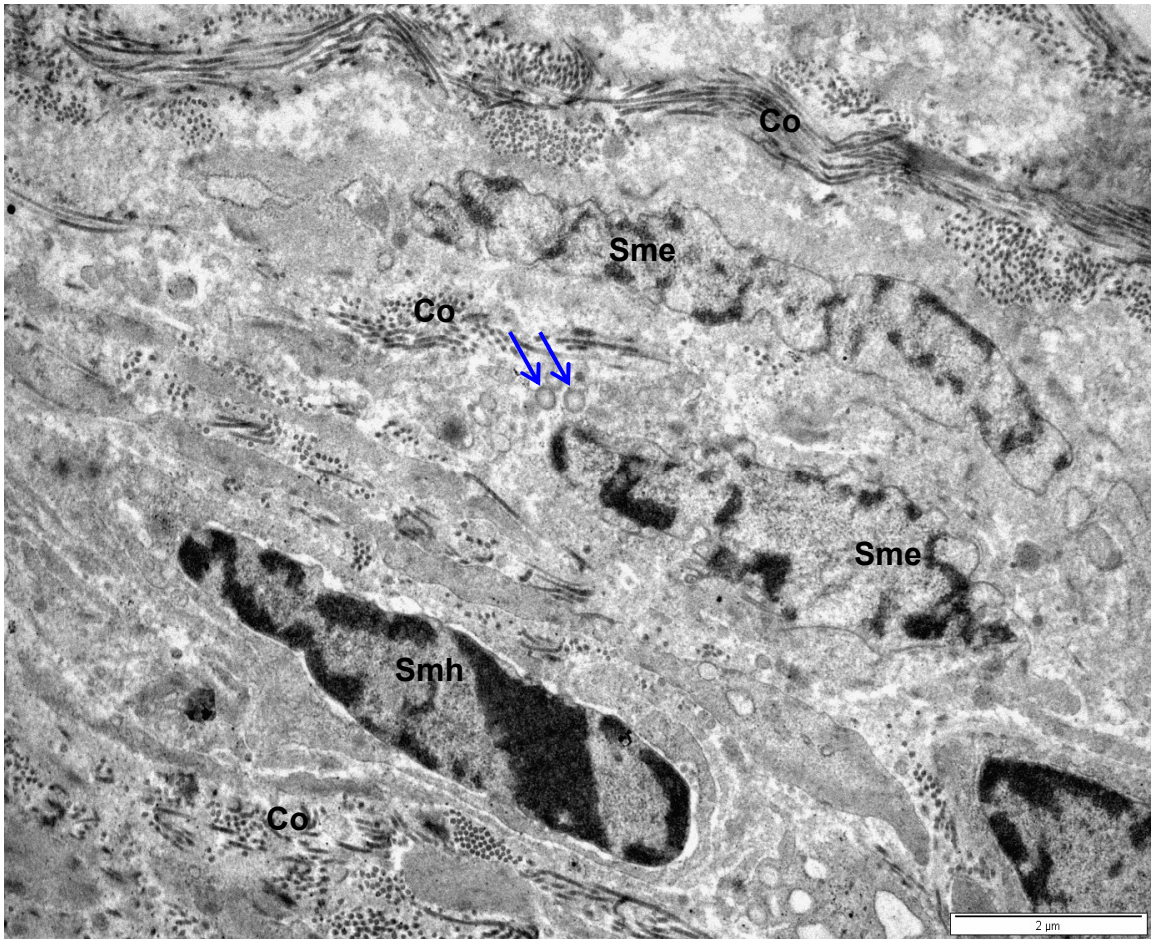

Figure 2. 51: Transmission electron micrograph showing the superficial region of the *tunica albuginea* in an adult bird. Smooth muscle cells with euchromatic (Sme) and heterochromatic (Smh) nuclei are present. Co: collagen bundles. Blue arrows: vesicles.

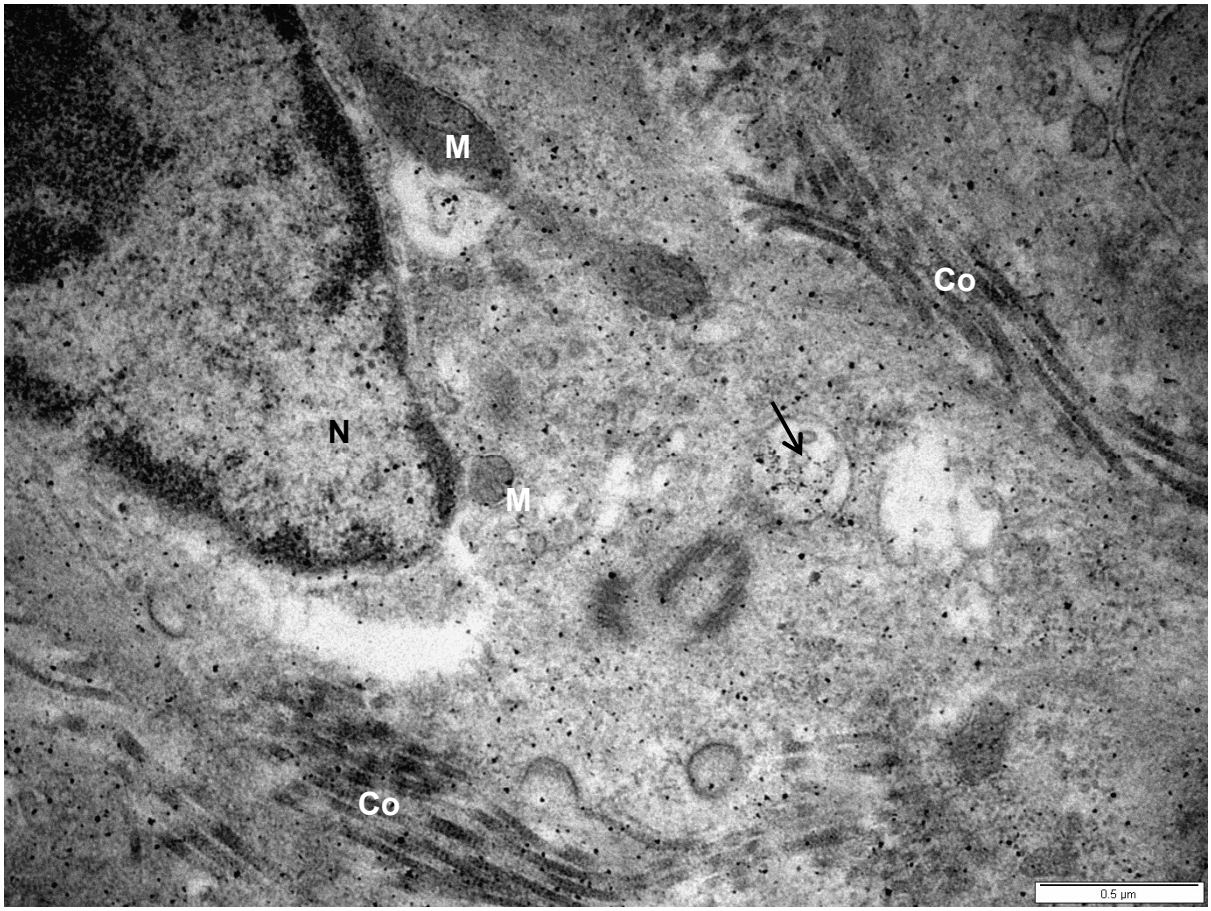

Figure 2. 52: Transmission electron micrograph showing a smooth muscle cell in the superficial region of the *tunica albuginea* in an adult bird. N: nucleus of the smooth muscle cell. M: mitochondria. Black arrow: multivesicular body. Co: collagen bundles.

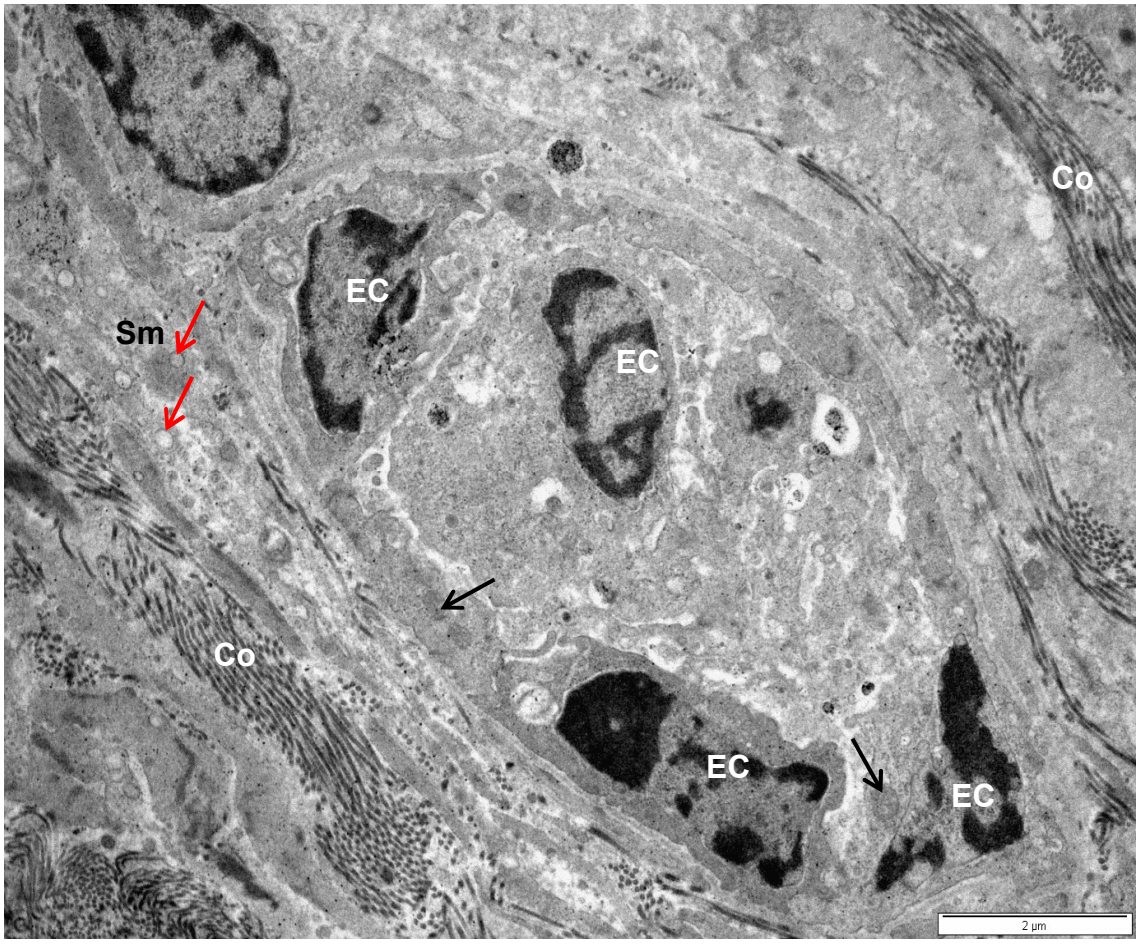

Figure 2. 53: Transmission electron micrograph of a blood vessel contributing to the venous network in the *tunica albuginea*. EC: vascular endothelial cells. Black arrows: mitochondria in the endothelial cells. Sm: vascular smooth muscle cell. Red arrows: vesicles in the vascular smooth muscle cells. Co: collagen bundles.

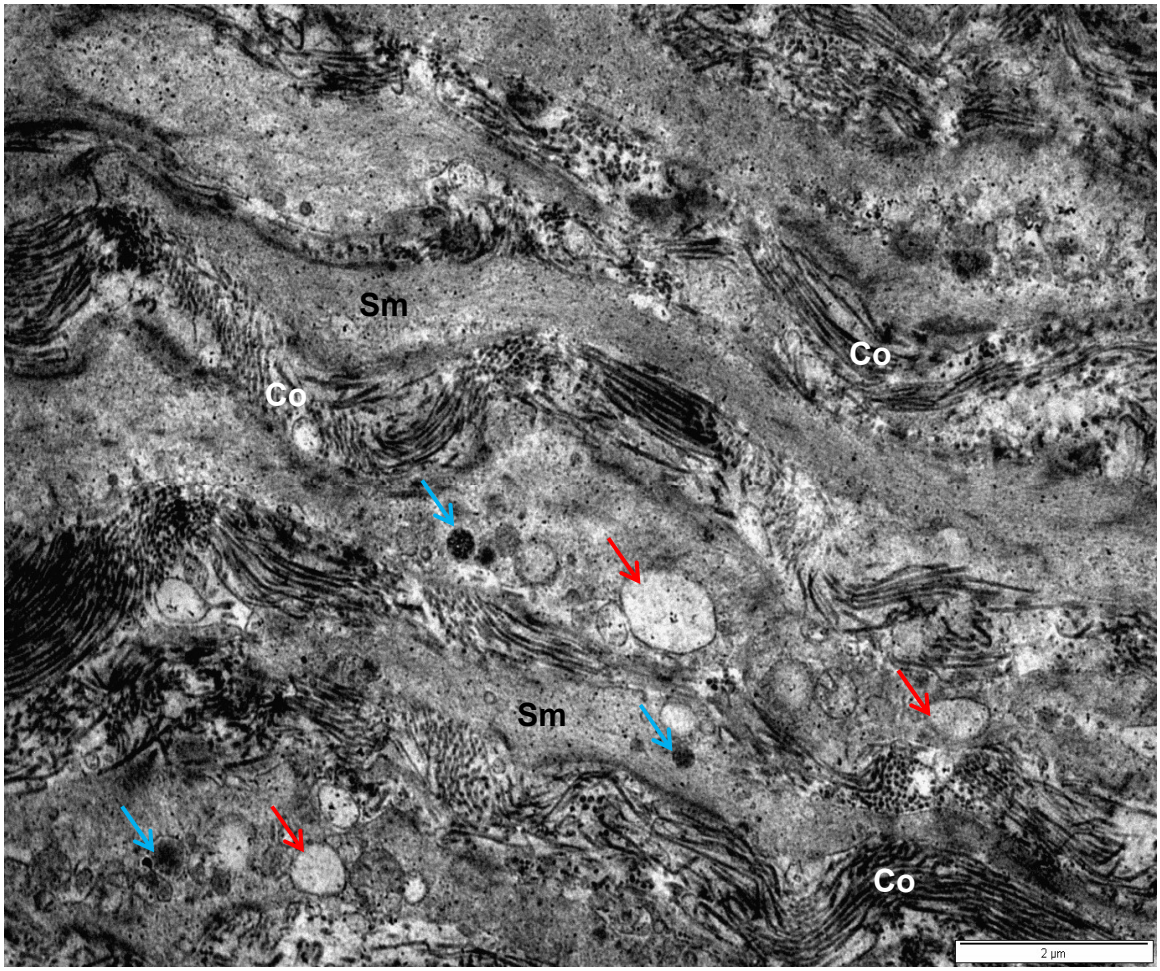

Figure 2. 54: Transmission electron micrograph of smooth muscle cells (Sm) in the *tunica albuginea* (deep region) of an adult bird. Red arrows: dilated RER cisternae. Co: collagen bundles.Blue arrows: mitochondria.

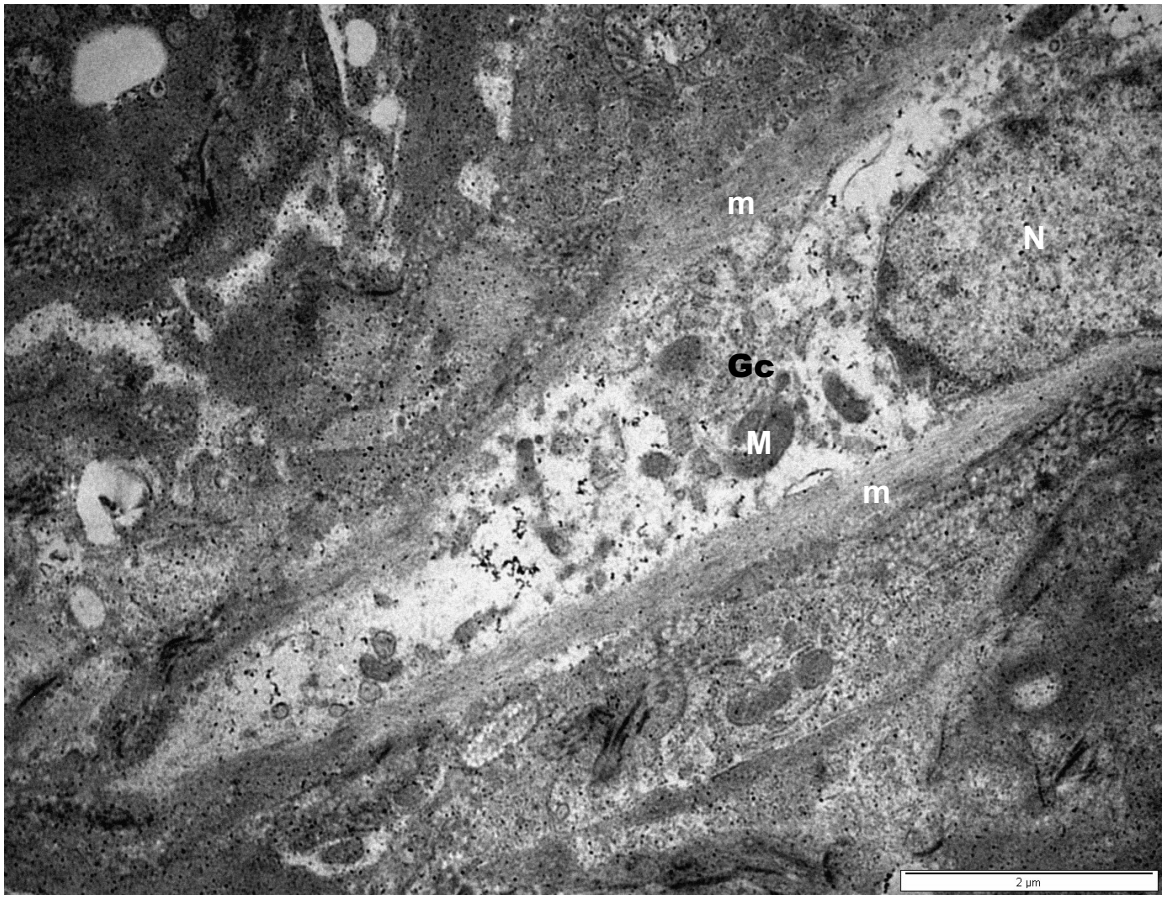

Figure 2. 55: Transmission electron micrograph of a smooth muscle cell in the *tunica albuginea* (deep region) of an adult bird. N: nucleus. m: microfilaments. M: mitochondria. Gc: Golgi complex.

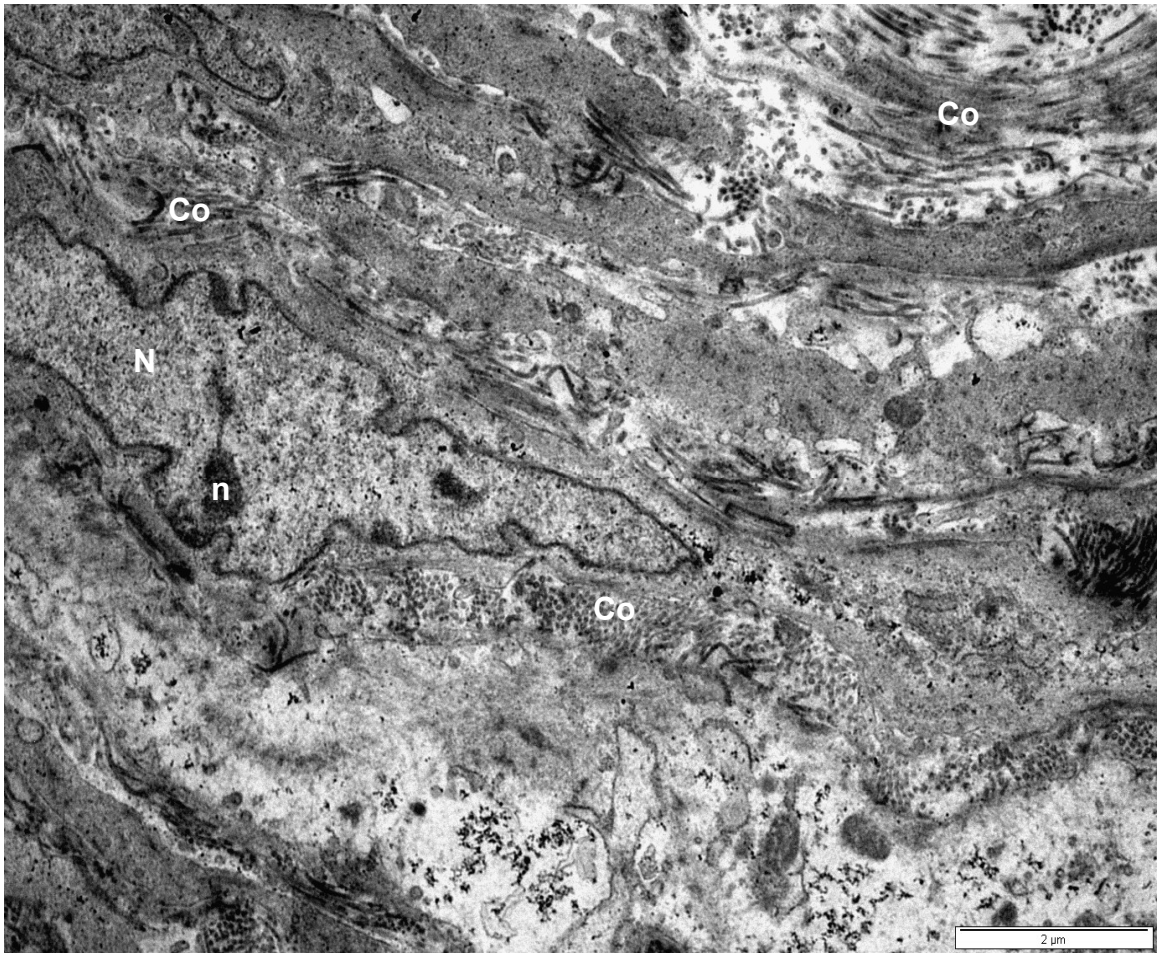

Figure 2. 56: Transmission electron micrograph of cells in the deep region of the *tunica albuginea* in an adult bird. Note the presence of a fibroblast with an irregular-shaped nucleus (N) containing a prominent nucleolus (n). Co: collagen bundles.

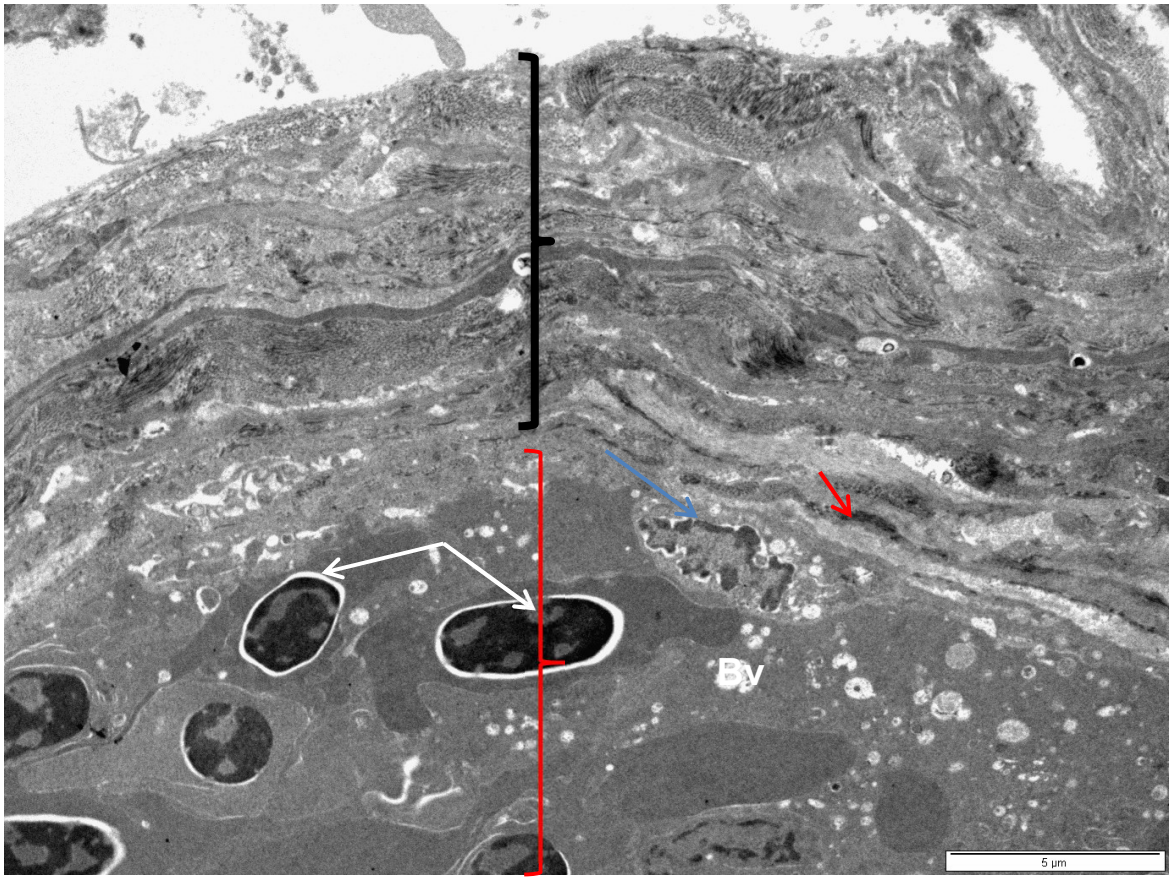

Figure 2. 57: Transmission electron micrograph of the *tunica albuginea* (black bracket) and *tunica vasculosa* (red bracket) of an adult bird. Red arrow: vascular smooth muscle cell. Blue arrow: vascular endothelial cell. White arrows: blood cells.

2.5 Discussion

2.5.1 Gross morphology

In contrast to most mammals, the testes of birds are located intra-abdominally (Artoni *et al*., 1999). The topographical relationship of the testes to other organs within the abdominal cavity has been described in adult birds (Hassanzadeh *et al.*, 2014). In the present study, the position of the testes in relation to neighbouring organs changed during sexual maturation. In pre-pubertal birds, the testes were

situated in contact with the apical extremities of the cranial divisions of the kidneys, while in pubertal and adult birds the testes covered the cranial, middle and part of the caudal divisions of the kidneys. These changes in topography were associated with developmental changes of the testes.

In the present study the shape of the testes changed with age, from elongated to ovoid in pre-pubertal birds, to round in pubertal and adult birds. These observations are consistent with those made in 8 day-to 52 day-old quails (Vatsalya and Arora, 2012). Changes in the shape of the testes have been correlated with a high production of spermatozoa and increased testosterone circulating levels (Garamnszegi *et al*., 2005). In the current study, the colour of the testes changed with maturity, as observed by Vatsalya and Arora (2012). The colour of the testes in the present study changed from cream to yellow as the birds matured. In contrast Vatsalya and Arora (2012), reported a change in colour from yellow to pinkish-red. The authors attributed the pink-red colour to the presence of numerous testicular blood vessels.

2.5.2 Biometric parameters

In the present study, the live bodyweights of the Japanese quails logically increased with age. The average bodyweight of pre-pubertal birds (88.20 ± 5.70g) in the current study was lower than that of 4-week-old quails (166.37 ± 10.29 g) studied by Rezvannejad *et al.* (2013). The average bodyweight of adult quails in the present study was higher (161.36 ± 7.52g) than that reported (115.6 5 ± 2.2 g) by Artoni *et al.* (1997). This may be attributed to breed differences, environmental conditions, diet, and genetics.

Based on the current study, the testicular weights (left and right) increased with age. These observations are in general agreement with the results of previous investigations (Mather and Wilson, 1964; Marin and Satterlee, 2004; Vatsalya and Arora, 2012; Kannan, 2015). The left testis has been shown to be more positively correlated to age and bodyweight in quails (Vatsalya and Arora, 2012). Contrary to these findings the right testes of birds in the current study were more positively correlated to the ages and bodyweights of the quails compared to the left testes.

Asymmetries in gonadal size and shape are common in nature and have been reported in birds such as the zebra finch (Birkhead *et al.*, 1998), tree swallow (Kempenaers *et al.*, 2002), Japanese quail (Clulow and Jones, 1982; Vatsalya and Arora, 2012; Kouatcho *et al.*, 2015), and turkey (Burke, 1973). The aforementioned studies indicate a dimorphism in favour of the left testis. This finding was confirmed by the results of the current study in which the left testis was generally larger than the right. However, in pubertal birds the weight of the right testis was slightly higher than that of the left testis. Similar observations were reported by Kouatcho *et al*. (2015) in 12 and 18-week-old quails.

The gonadosomatic indices of quails studied in the present investigation logically increased with testicular weight and age. Similar findings have been reported in previous studies on Japanese quails (Mather and Wilson,1964; Kouatcho *et al*., 2015). The gonadosomatic index of adult quails (3.29 ±0. 29%) in the current study was similar to that recorded by Lanna *et al.* (2013), who reported an index of 3.68%, and Kouatcho *et al*. (2015), who calculated an index of 3.20 ±0. 21%. However, the gonadosomatic index of adult quails in the present study was higher than that recorded by Clulow and Jones (1982) who reported an index of 2.26 ± 0.01%. These

differences may be due to genetic, environmental and climatic factors, as suggested by Lanna *et al*.(2013).

2.5.3 Testicular capsule thickness

The testicular capsule of avian species is relatively thin compared to that of mammals (Freneau *et al*., 2016). The thickness of the avian testicular capsule has previously been reported in the adult Japanese quail, duck, turkey, fowl (Aire and Ozegbe, 2007), emu and ostrich (Ozegbe *et al.,* 2008). However, data on age-related changes in the thickness of the testicular capsule in birds is scant. Kannan and co-authors (2015) reported a post-hatch increase in testicular capsule thickness in the Japanese quail, but did not provide any measurements. In the current study, the thickness of the testicular capsule was measured in the testes of pre-pubertal, pubertal, and adult birds. Interestingly, the results of the present investigation showed an age-related decrease in testicular capsule thickness. This is contrary to the findings of previous reports on the Japanese quail (Kannan *et al*., 2015), human (Arenas *et al*., 1997) and buffalo (Goyal and Dhingra, 1973). Kannan *et al.* (2015) reported that the testicular capsule of Japanese quails increased with advancing age due to an increase in the connective tissue component. In contrast, the increased thickness of the testicular capsule in buffaloes was due to an increase in blood vessels in the *tunica vasculosa* as the animals matured (Goyal and Dhingra, 1973). This marked discrepancy between our findings and those of previous studies was probably due to the decreased cellular density in the testicular capsule as the birds matured. Thus, the testicular capsule of pre-pubertal birds had a higher cellular density compared to the testicular capsules of pubertal and adult birds.

2.5.4 Light microscopy

The testicular capsule in all birds studied was composed of three layers: an outermost *tunica serosa*; a middle *tunica albuginea and an* innermost *tunica vasculosa*. These results are in general agreement with observations made of testicular capsules in previous studies on birds (Aire and Ozegbe, 2007; Ozegbe *et al.*, 2008; Dharani *et al*., 2017) and mammals (Leeson and Forman, 1981; Middendorff *et al*., 2002).

Tunica serosa

In all age groups, the testicular capsule was covered by a *tunica serosa* composed of mesothelial cells and a thin layer of connective tissue. A similar observation was reported in the Japanese quail, domestic fowl, turkey and duck (Aire and Ozegbe, 2007). The *tunica serosa* is derived from the peritoneum within the abdominal cavity (Aire and Ozegbe, 2007; Dharani *et al*., 2017). The *tunica serosa* in birds corresponds to the *tunica vaginalis* of mammals (Ohanian *et al*., 1979; Abd-Elhafeez *et al*., 2017). Noteworthy, the nuclei shape of mesothelial cells in the *tunica serosa* appeared to be age-specific in the present study. In pre-pubertal birds, mesothelial cells of *tunica serosa* contained oblong-to oval-shaped nuclei. This is similar to observations of previous reports in the Japanese quail (Madekurozwa, 2013) and rabbit (Leeson and Forman, 1981). In contrast, the mesothelial cells displayed a combination of both oval and elongated nuclei in pubertal birds and elongated nuclei in adult birds. The elongated nuclei of mesothelial cells have been reported in the adult quail (Aire and Ozegbe, 2007; Madekurozwa, 2013), guinea fowl (Dharani *et al.,* 2017), emu and ostrich (Ozegbe *et al*., 2008).

In the current study the mesothelial cell layer was associated with a well-defined layer of reticular fibres. This appears to be the first study to demonstrate reticular fibres in the *tunica serosa*, and indeed, testicular capsule of the Japanese quail. The presence of reticular fibres in association with epithelial cells is not a new finding as it is known that these fibres form a supportive meshwork for the epithelia in various organs (Ushiki, 2002).

Tunica albuginea

Histologically, the *tunica albuginea* formed the largest portion of the testicular capsule in all age groups. Collagen and reticular bundles were more abundant than the cellular elements in pubertal and adult Japanese quails. Furthermore, in the present study the *tunica albuginea* was divided into two regions (superficial and deeper) separated by a venous network. A similar observation was made by Dharani *et al*. (2017) in a study on the domestic fowl. In the present study, no connective tissue septa extended from the *tunica albuginea* into the testicular parenchyma. This observation is in concurrence with the findings of previous reports on the Japanese quail (Aire and Ozegbe, 2007; Kannan *et al*., 2015), guinea fowl (Dharani *et al*., 2017) and ostrich (Ye *et al*., 2018). In contrast, mammalian testes generally have well-defined septa extending from the *tunica albuginea* into the testicular parenchyma (Goyal and Dhingra, 1973; Abd-Elhafeez *et al*., 2017). Ye *et al* (2018) opined that this finding suggests that the avian testes are at a lower stage of evolution than the mammalian testes.

Tunica vasculosa

In agreement with previous reports on birds (Aire and Ozegbe, 2007; Dharani *et al*., 2017) and mammals (Leeson and Forman, 1981), the *tunica vasculosa* in the quails

studied in the present investigation was located between the *tunica albuginea* and testicular parenchyma. The *tunica vasculosa* in the present study was poorly-defined and characterized by the presence of a network of blood vessels. In agreement with observations made in the buffalo (Goyal and Dhingra, 1973) and Japanese quail (Kannan *et al.,* 2015), the vascularity of the *tunica vasculosa* became more clearly defined with testicular maturation.

2.5.5 Cytoskeletal protein immunohistochemistry

The testicular capsule has several functions including: providing protection and peripheral support to the testicular parenchymal tissue (Leeson and Forman, 1981); establishment of the appropriate intra-testicular pressure to maintain fluid homeostasis within the testis (Leeson and Forman, 1981) and transportation of semen into the excurrent duct system (Davis and Langford, 1969; Davis and Horowitz, 1978; Ellis *et al.,* 1978).

In the current study, cytoskeletal protein makers were used to identify the various cell types present in the testicular capsule. In addition, the staining intensities of these markers in relation to maturation age were also reported.

Tunica serosa

In agreement with a report on the post-hatch changes in the testes of the Japanese quail (Madekurozwa, 2013), the *tunica serosa* was desmin and smooth muscle actin-immunonegative in all age groups. In addition, the present study revealed that the *tunica serosa* was also immunonegative for tubulin. To date, there is no information on the expression and distribution of tubulin in the testicular capsule. Mesothelial cells in the *tunica serosae* of the three age groups studied were vimentin immunopositive. Interestingly, the mesothelial cells showed age-related variations in

the expression of vimentin immunostaining. Vimentin immunostaining in this serosal layer appeared to increase with testicular maturation, with moderate immunoreactivity observed in pre-pubertal birds and strong immunostaining in pubertal, as well as adult quails. These observations are in agreement with the findings of a previous study on variations in vimentin immunostaining during testicular development in the Japanese quail (Madekurozwa, 2013). Based on present and previous observations, it is probable that the *tunica serosa* consists of one type of cytoskeletal protein, which is vimentin.

Tunica albuginea

The findings of the present immunohistochemical study indicate that smooth muscle cells are the predominant cell type in the *tunicae albuginea* of the three age groups studied, with relatively few fibroblasts present in pubertal and adult quails. The predominance of smooth muscle cells in the *tunica albuginea* has previously been reported in several avian species including the domestic fowl (Aire and Ozegbe, 2007; Gonzalez-Moran and Soria-Castro, 2010), duck (Aire and Ozegbe, 2007), Japanese quail (Aire and Ozegbe, 2007; Madekurozwa, 2013) and turkey (Aire and Ozegbe, 2007). These results are contrary to a report on the *tunica albuginea* of the greater rhea, in which fibroblasts were the predominant cell type (Freneau *et al*., 2016).

In agreement with a report on the post-hatch Japanese quail (Madekurozwa, 2013), smooth muscle cells in the *tunica albuginea* were characterized by the presence desmin and smooth muscle actin. In addition, desmin and smooth muscle actin immunostaining was also observed in vascular smooth muscle cells associated with large blood vessels of the *tunica albuginea* (Madekurozwa, 2013). The presence of

cytoskeletal proteins (desmin, smooth muscle actin and vimentin) has been also reported in the *tunica albuginea* of other avian species including the domestic fowl (Maretta and Marettova, 2004; Aire and Ozegbe, 2007; Abd-Elmaksoud, 2009), turkey (Aire and Ozegbe, 2007), duck (Aire and Ozegbe, 2007), emu (Ozegbe *et al.,* 2008), ostrich (Ozegbe *et al.,* 2008) and masked weaver (Ozegbe *et al*., 2012). Interestingly, smooth muscle cells showed an age-related decrease in desmin immunostaining in the current study. This observation is contrary to the results of a similar study on the *tunica albuginea* of the Japanese quail (Madekurozwa, 2013). A noteworthy finding of the current study was the zonal immunostaining of desmin in pubertal and adult quails, in which smooth muscle cells located in the deeper regions of the *tunica albuginea* were more intensely stained than those in the superficial parts. This is in agreement with a previous report on desmin immunostaining in the *tunica albuginea* of the emu (Ozegbe *et al*., 2008).

In addition to desmin, a zonal arrangement of smooth muscle actin immunostaining has been reported in the emu (Ozegbe *et al.,* 2008), ostrich (Ozegbe *et al.,* 2008), domestic fowl (Maretta and Marettová, 2004; Abd-Elmaksoud, 2009) and Japanese quail (Madekurozwa, 2013). Previous reports on the *tunica albuginea* in the sexually mature quail (Aire and Ozegbe, 2007), domestic fowl (Aire and Ozegbe, 2007), emu (Ozegbe *et al*., 2008), domestic fowl (Maretta and Marettová, 2004; Abd-Elmaksoud, 2009) and 7- to 24-day-old quail (Madekurozwa, 2013) have shown strong smooth muscle actin immunostaining in the inner zone of the testicular capsule. In contrast, smooth muscle actin immunostaining in the present study was strong and uniformly distributed throughout the *tunica albuginea* in all age groups. This discrepancy could be due to differences in the immunostaining kits used in the various studies. The immunostaining kit (Biogenex super sensitive one-step polymer-HRP detection

system kit; Emergo Europe, The Hague, The Netherlands) used in the current study is able to detect and amplify small quantities of antigen. Thus, the system used in the current study has enhanced sensitivity and specificity.

Within avian species, vimentin expression and distribution pattern are species-specific (Devkota *et al*., 2006a, b). Previous studies have reported moderate vimentin immunostaining in the testicular capsules of the emu (Ozegbe *et al.,* 2008), and Japanese quail (Aire and Ozegbe, 2007) and weak immunostaining in that of the turkey (Aire and Ozegbe, 2007). Conversely, vimentin immunostaining was absent in the testicular capsules of the domestic fowl (Aire and Ozegbe, 2007), duck (Aire and Ozegbe, 2007), masked weaver (Ozegbe *et al.,* 2012), and ostrich (Ozegbe *et al*., 2008). In the current investigation strong vimentin immunostaining was localized in the fibroblasts of pre-pubertal and pubertal birds, while immunostaining was weak or absent in adult birds. Our findings suggest that fibroblasts in the testicular capsule of the Japanese quail develop into smooth muscle cells during testicular maturation. Thus, the *tunica albuginea* of adult birds in the current study was populated predominantly by smooth muscle cells. The results of the present study are supported by the findings of Sappino *et al*. (1990) who reported the differentiation of fibroblasts into smooth muscle cells.

Tunica vasculosa

In agreement with a previous study on the Japanese quail (Madekurozwa. 2013), vascular smooth muscle cells were desmin and smooth muscle actin-immunopositive in all birds studied in the current investigation. In addition, vascular endothelial cells were vimentin immunopositive.

2.5.6 Basement membrane immunohistochemistry

Tunica serosa

To date, no published information is available on the immunoexpression of the extracellular matrix proteins collagen type IV and fibronectin in the testicular capsules of birds. However, the extracellular matrix protein laminin has been immunolocalized in the testicular capsules of the domestic fowl, duck, pigeon and rabbit (Abd-Elmaksoud, 2009).

In the current study, basement membranes of mesothelial cells in the *tunica serosa* were collagen type IV, fibronectin and laminin-immunopositive in all age groups. Similar observations have been made in the rat lung by Rennard *et al*. (1984), as well as in cultured human peritoneal mesothelial cells (Yang *et al*., 1999). This is indicative that the presence of these extracellular matrix proteins in the basement membranes of mesothelial cells is well-conserved across species.

Tunica albuginea

The immunolocalization of extracellular matrix proteins in smooth muscle cells associated with the peritubular boundary tissue in mammals has been studied extensively (Hadley and Dym, 1987; Santamaria *et al.,* 1990; Yazama *et al*., 1997; Morales, 2004). Surprisingly, there is only a single study on laminin immunostaining in the testicular capsules of birds (Abd-Elmaksoud, 2009). Thus, the current study is the first report on the immunolocalization of the extracellular matrix proteins collagen type IV and fibronectin in birds. In addition, it also represents the first study in which the age-related changes in the intensity and distribution of extracellular matrix proteins in the testicular capsule has been studied in birds.

The immunostaining of fibronectin and laminin was consistently moderate to strong in the basement membranes of smooth muscles cells throughout the maturational stages of the testicular capsule in the quail. Interestingly, collagen type IV immunostaining in smooth muscle cells decreased with testicular maturation.

Tunica vasculosa

In the current study, extracellular matrix proteins were demonstrated immunohistochemically in basement membranes associated with endothelial and smooth muscle cells in the *tunica vasculosa* of the testicular capsule. A noteworthy finding of the current study was the decrease in collagen type IV immunostaining in the *tunica vasculosa* with testicular maturation. In contrast, fibronectin and laminin immunostaining remained moderate to strong in all stages of maturation. Strong laminin immunostaining has been reported in the testicular capsules of the fowl, duck, pigeon, and rabbit (Abd-Elmaksoud, 2009).

2.5.7 Transmission electron microscopy

Ultrastructural features of the testicular capsule have been described in the cat, rat (Leeson and Cookson, 1974), horse, sheep, pig (Chacon-Arellano and Woolley, 1980), human, rabbit (Banks *et al.,* 2006), Japanese quail, domestic fowl, turkey and duck (Aire and Ozegbe, 2007). Despite the extensive research conducted on the testicular capsule, there is still a lack of information on age-related changes in the ultrastructure of smooth muscle cells in this layer.

The ultrastructural findings in the current study corroborated the results of the histological and immunohistochemical studies reported in this chapter. In agreement with a previous study on birds (Aire and Ozegbe, 2007), transmission electron

microscopy revealed that the testicular capsule is composed of an outer *tunica serosa*, a middle *tunica albuginea* and an inner *tunica vasculosa*.

Tunica serosa

The *tunica serosa* of the testicular capsule in pre-pubertal quails contained cuboidal-shaped cells with electron-lucent cytoplasm. Similar observations have been made in the juvenile rabbit (Leeson and Forman, 1981). Mesothelial cells in the current study were cuboidal to squamous in pubertal birds, while adult quails displayed mesothelial cells which were structurally similar to those described by Aire and Ozegbe (2007). Although the reason for the change in the shape of the mesothelial cells is unclear, it is interesting to note that there is little morphological variation in the developing mesothelial cells of the Japanese quail and rabbit.

A noteworthy finding of the current study was the presence of gap and tight junctions linking cells of the mesothelial cell layer. Tight junctions between mesothelial cells play a role in the development of cell surface polarity, as well as the formation of a semi-permeable diffusion barrier, while gap junctions are aqueous intercellular channels (review by Mutsaers, 2002).

Tunica albuginea

In agreement with previous studies on the Japanese quail, domestic fowl, turkey, duck (Aire and Ozegbe, 2007), rabbit (Leeson and Forman, 1981), horse, pig and sheep (Chacon-Arellano and Woolley, 1980) smooth muscle cells were the dominant cell type in the *tunica albuginea* in all birds studied in the current investigation. In addition, smooth muscle cells in the present study varied ultrastructurally depending

on whether they were situated within the superficial or deep layers of the *tunica albuginea*. This zone-dependent variation in the shape of smooth muscle cells has been described in the testicular capsule of the rabbit (Leeson and Forman, 1980), human, rat, and mouse (Banks *et al.,* 2006).

Smooth muscle cells in the current study were characterized by the presence of microfilaments, the density which increased with testicular maturation. This increase is not surprising, as it is known that these contractile microfilaments are involved in the propulsion of sperm into the excurrent duct system (Davis *et al*., 1970; Davis and Horowitz, 1978; Ellis *et al.,* 1981).

Tunica vasculosa

Ultrastructural and immunohistochemical techniques have been used to study the *tunica vasculosa* in birds (Aire and Ozegbe, 2007; Ozegbe *et al.,* 2008) and mammals (Leeson and Cookson, 1974). It is generally accepted that the *tunica vasculosa* in birds is poorly developed. This assertion was confirmed by the results of the current study in which the venous network in the *tunica albuginea* was more prominent than blood vessels in the *tunica vasculosa*.

Chapter three:

The peritubular boundary tissue of pre-pubertal, pubertal, and adult male Japanese quails (*Coturnix coturnix japonica*): a histological, morphometric, immunohistochemical and ultrastructural study.

3.1 Introduction

The seminiferous tubules are encircled by cellular and non-cellular layers collectively known as peritubular boundary tissue (Hadley and Dym, 1987). The peritubular boundary tissue surrounds the seminiferous tubules in birds (Rothwell, 1975; Skinner and Fritz, 1985; Virtanen *et al.*, 1986; Santamaria *et al.*, 1990), reptiles (Unsicker and Burnstock, 1975; Gröschel-Stewart and Unsicker, 1977), and mammals (Virtanen *et al*., 1986; Maekawa *et al.*, 1996). The peritubular boundary tissue is also known as the *lamina propria* (Davidoff *et al*., 1990), or limiting membrane (Bressler and Ross, 1972).

Ultrastructurally, the peritubular boundary tissue is formed by four basic components, which are composed of *basal lamina*, collagen fibres, fibroblasts, and peritubular myoid cells (Moniem *et al*., 1980). Two separate *basal laminae* were observed by Hadley and Dym (1987), as well as by Lian and Enders (1994). The inner *basal lamina* was associated with the seminiferous epithelium, while the outer *basal lamina* was in contact with the innermost layer of peritubular myoid cells (Lian and Enders, 1994; Franca *et al.*, 2000). The *basal laminae* allow communication between peritubular myoid cells and Sertoli cells (Fisher *et al.*, 2003). Through this interaction the peritubular myoid cells are thought to stimulate postnatal testicular growth (Nurmio *et al.*, 2012). The *basal lamina* is composed of collagen type IV, laminin,

fibronectin and proteoglycans (Dym and Fawcett, 1970). Collagen type IV is present in both the inner and outer non-cellular layers of the peritubular boundary tissue (Hadley and Dym, 1987). Laminin plays a role in controlling cellular behaviour by providing cells with specific information through interactions with cell surface receptors (Aumailley and Krieg, 1996). Furthermore, laminin provides building blocks for tissue architecture, assembly, and stability during embryogenesis, development, and tissue remodeling (Aumailley and Krieg, 1996). The application of immunohistochemical techniques has shown that the third component of the *basal lamina*, fibronectin, is produced by peritubular myoid and Sertoli cells (Tung *et al.*, 1984). The final components of the *basal lamina* are proteoglycans which are thought to play a vital role in extracellular matrix deposition (Skinner and Fritz, 1985). Proteoglycans contain chondroitin and heparin glycosaminoglycan chains and they are identified as secretory products of both Sertoli and myoid cells in culture (Skinner and Fritz, 1985). Heparan sulfate proteoglycan is a common proteoglycan that has been immunolocalized in rat testes (Hadley and Dym, 1987). In co-culture, peritubular myoid and Sertoli cells secrete fibronectin, as well as proteoglycans consisting of chondroitin and heparin glycosaminoglycan chains (Tung *et al*., 1984; Skinner and Fritz, 1985).

The connective tissue of the peritubular boundary tissue is composed of collagen and reticular fibres (Dharani *et al*., 2017). The connective tissue forms alternating layers with fibroblasts and peritubular myoid cells (Ozegbe *et al*., 2008; Dharani *et al*., 2017). The fibroblasts located in the peritubular boundary tissue are stellate in shape with attenuated cytoplasmic processes and abundant rough endoplasmic reticulum (Rothwell, 1975). The fibroblasts lack myofilaments, as well as cellular membrane-associated densities (Davidoff *et al*., 1990). Fibroblasts are vimentin

immunopositive, but smooth muscle actin immunonegative (Davidoff *et al*., 1990; Madekurozwa, 2013).

Peritubular myoid cells in the camel are separated from the seminiferous epithelium by the inner lamella (Moniem *et al.*, 1980). These cells form circumferential layers around the seminiferous tubules (Moniem *et al.*, 1980). Peritubular myoid cells are morphologically and physiologically similar to smooth muscle cells (Losinno *et al*., 2016). The cytoplasm of peritubular myoid cells contains abundant fine filaments, micropinocytotic vesicles, Golgi complexes, mitochondria, rough endoplasmic reticulum profiles and free ribosomes (Rothwell and Tingari, 1973; Rothwell, 1975). Immunohistochemical techniques have shown that these cells are vimentin, desmin, and smooth muscle actin immunopositive (Aire and Ozegbe, 2007). Thus, peritubular myoid cells express characteristics of both fibroblasts and smooth muscle cells and are commonly refered to as “myofibroblasts” (Davidoff *et al*., 1990).

According to Dym and Fawcett (1970), the outer cellular layer of the peritubular boundary tissue is formed by a layer of endothelial cells of an extensive system of peritubular sinusoids. This endothelial cell layer is thought to regulate the movement of macromolecules from the blood system into the testes (Gunn *et al.*, 1966).

3.1.1 The peritubular boundary tissue in mammals.

The mammalian peritubular boundary tissue consists of cellular and non-cellular (fibrous) layers. The peritubular boundary tissue in the rat consists of four layers: inner non-cellular layer; inner cellular layer; outer non-cellular layer, and outer cellular layer (Leeson and Leeson, 1963). The inner non-cellular layer is comprised

of a collagen network situated between two *basal laminae*. The first *lamina* surrounds the seminiferous epithelium while the second *lamina* is located between the collagen network and peritubular myoid cells (Leeson and Leeson, 1963). The inner cellular layer consists of peritubular myoid cells displaying intra-cytoplasmic filaments and micropinocytotic vesicles (Leeson and Leeson, 1963). The outer non-cellular layer consists of scattered collagen fibrils, while the outer cellular layer is composed of fibroblasts (Leeson and Leeson, 1963). In the ovine testis, the peritubular boundary tissue consists of a *basal lamina,* non-cellular layer, and outer cellular layer (Bustos-Obregon and Courot, 1974). The non-cellular layer is formed by lamellae composed of collagen fibres (Bustos-Obregon and Courot, 1974). The outer cellular layer consists of multilayered peritubular myoid cells (Bustos-Obregon and Courot, 1974). In the camel, the peritubular boundary tissue is arranged in three lamellae, which are termed inner fibrous, inner cellular, and outer cellular (Moniem *et al*., 1980). Peritubular myoid cells in the peritubular boundary tissue of the camel testis are multi-layered and are morphologically similar to those of the human, ram, boar, and cat (Moniem *et al*., 1980). In the testes of the human, the peritubular boundary tissue consists of inner and outer cellular layers (De Kretser *et al.*, 1975). The inner cellular layer consists of three to four peritubular myoid cell layers alternating with collagen fibres (Davidoff *et al*., 1990; Santamaria *et al*., 1992). The outer cellular layer is formed by fibroblasts, which lack myofilaments and intra-cytoplasmic densities (Davidoff *et al*., 1990).

Immunohistochemical studies have shown that mammalian peritubular myoid cells express the cytoskeletal proteins smooth muscle actin, vimentin, and desmin (Virtanen *et al.*, 1986; Anthony and Skinner, 1989; Losinno *et al*., 2012; Losinno *et al.,* 2016). Smooth muscle actin and desmin impart a contractile ability on the

peritubular myoid cells, while vimentin is responsible for maintaining cell shape and cellular integrity (Losinno *et al.,* 2012).

3.1.2 The peritubular boundary tissue in birds

The peritubular boundary tissue of the domestic fowl is composed of an inner fibrous lamella and an outer cellular lamella (Rothwell and Tingari, 1973). The inner fibrous lamella lines the outer surface of the seminiferous epithelium (Rothwell, 1975; Maretta and Marettova, 2004). This lamella is composed of three components: a homogenous *basal lamina* adjacent to the seminiferous epithelium; a region of loosely arranged collagen fibres, and a dense homogeneous layer similar to a *basal lamina* (Rothwell and Tingari, 1973). The outer cellular lamella of the peritubular boundary tissue in the domestic fowl consists of multiple layers of peritubular myoid cells and fibroblast-like cells (Rothwell and Tingari, 1973). The fibroblast-like cells described by Rothwell and Tingari (1973) contained elongated nuclei with granular chromatin, as well as cytoplasm containing rough endoplasmic reticulum, Golgi complexes, elongated mitochondria, electron dense bodies, and free ribosomes. However, in contradiction to the findings of Rothwell and Tingari (1973), Aire and Ozegbe (2007) reported the presence of only peritubular myoid cells in the peritubular boundary tissue of the domestic fowl.

Immunohistochemical studies have shown that peritubular myoid cells of several birds including the masked weaver*, Ploceus velatus,* (Ozegbe *et al*., 2012), Japanese quail (Aire and Ozegbe, 2007; Madekurozwa, 2013), domestic fowl (Aire and Ozegbe, 2007), and ostrich (Ozegbe *et al*., 2008) express smooth muscle actin, vimentin and desmin.

3.1.3 Functions of the peritubular boundary tissue in mammals and birds

The testicular peritubular boundary tissue plays a physical role as a supportive tissue for the seminiferous tubules (Haider *et al*., 1993). In addition, the peritubular boundary tissue is part of the blood-testis barrier, a selective filter that regulates the passage of substances into the seminiferous epithelium (Rothwell and Tingari, 1973; Rothwell, 1975; Maekawa *et al.*, 1996). The functional features of the peritubular boundary tissue include a contractile capacity, vascular barrier maintenance, and paracrine interactions (Haider *et al*., 1993). Furthermore, the peritubular myoid cells play a critical role in the structural integrity and maintenance of the seminiferous tubules, as well as in the regulation of Sertoli cell function and development (Anthony and Skinner, 1989).

In mammals and birds, the immobile spermatozoa move from the seminiferous tubules towards the excurrent ducts in response to a pressure gradient (Chacon-Arellano and Woolley, 1980). While the origin of this hydrostatic pressure is uncertain, it is thought that the peritubular boundary tissue provides a rhythmic contraction that aids spermatozoal transport (Hargrove *et al.,* 1977). This rhythmic contraction of the peritubular boundary tissue is thought to be due to the presence of peritubular myoid cells which contain smooth muscle actin microfilaments and desmin intermediate filaments (Davis *et al.*, 1970).

In addition to a supportive function, the peritubular boundary tissue also controls the rate at which substances (for example, hormones) enter and leave the seminiferous tubules (Lacy and Rotblat, 1960). Thus, some researchers regard the peritubular boundary tissue as a component of the blood-testis barrier (Dym and Fawcett, 1970: Maekawa *et al.,* 1996). The effectiveness of the peritubular myoid cells, as a

component of the blood-testis barrier, is demonstrated by the ability of this cell layer to block the passage into the seminiferous tubules of certain substances, such as the opaque markers, lanthanum, colloidal carbon, and thorium (Dym and Fawcett, 1970; Verhoeven *et al.*, 2000).

Peritubular myoid cells are also thought to be involved in the maintenance of spermatogonial stem cells, which are the resident germline stem cell population (Potter and De Falco, 2017). Furthermore, due to the high density of androgen receptors contained in peritubular myoid cells, these cells are thought to be involved in spermatogenesis (Maekawa *et al*., 1996)

Peritubular myoid cells interact with Sertoli cells during testicular tubule morphogenesis (Verhoeven *et al*., 2000). The interaction between peritubular myoid and Sertoli cells is either environmental, which involves the production and deposition of extracellular matrix, or paracrine, involving bilateral communication mediated via diffusible factors (Skinner, 1991). In the environmental interaction, the *basal lamina*e of the peritubular myoid and Sertoli cells co-operatively form a complex extracellular matrix, which provides structural integrity to the seminiferous tubules (Dym, 1994; Maekawa *et al*., 1996). The peritubular myoid and Sertoli cells interact in a manner that guarantees the organized deposition of extracellular matrix (Verhoeven *et al.*, 2000). The components of the extracellular matrix produced include collagen (types I and IV), laminin, fibronectin, and heparan sulfate proteoglycan (Lian and Enders, 1994).

As stated above peritubular myoid and Sertoli cells interact via environmental and paracrine modes. During the paracrine interaction, peritubular myoid cells communicate with Sertoli cells via several factors, which include peritubular

modifying substance, transforming growth factor (α and β) and activin (Verhoeven *et al*., 2000). Peritubular modifying substance is one of the most important factors produced by peritubular myoid cells (Skinner and Fritz, 1985). This factor modulates the production of androgen-binding protein by Sertoli cells (Verhoeven *et al*., 2000).

3.2 Materials and methods

3.2.1 Light microscopy

Testicular tissue was fixed in 10% buffered neutral formalin for 5 days. After fixation, the samples were routinely processed for histology and embedded in paraffin wax. Tissue sections (5 µm thick) were cut, mounted on glass slides, and stained with haematoxylin and eosin. Additional sections were stained for collagen (Masson trichrome stain. Trichrome stain, ab150686, Abcam), elastic (Verhoeff-Van Gieson stain. Elastic stain kit, ab150667, Abcam), and reticular fibres (Gomori's silver impregnation stain. Reticulum stain kit, ab150684, Abcam). Stained sections were then viewed and photographed using an Olympus BX-63 microscope attached to a computer.

3.2.2 Immunohistochemistry

The immunostaining technique was performed on 5 µm thick paraffin sections using a Biogenex super sensitive one-step polymer-HRP detection system kit (Emergo Europe, The Hague, The Netherlands). Antibodies against the cytoskeletal proteins desmin, smooth muscle actin, tubulin and vimentin were utilized. Components of the basement membrane were demonstrated using primary antibodies against collagen type IV, fibronectin and laminin.

Table 3. 1: Antibodies used for immunohistochemistry in this study.

Antibody	Clone	Manufacturer	Antigen retrieval	Dilution PBS
Collagen type IV	Polyclonal rabbit ab6586	Abcam	Tris-EDTA (pH 9.0)	1:100
Anti- desmin	Monoclonal mouse ab6322	Abcam	Citrate buffer (pH 6.0)	1:300
Anti-fibronectin	Polyclonal rabbit ab2413	Abcam	Tris-EDTA (pH 9.0)	1:250
Anti-laminin	Polyclonal rabbit	DakoCytomation, Glostrup, Denmark	Proteinase K (ab64220)	1:50
Anti-smooth muscle actin	Monoclonal mouse 1A4	DakoCytomation, Glostrup, Denmark	Citrate buffer (pH 6.0	1:50
Anti-tubulin	Monoclonal mouse ab44928	Abcam	Tris-EDTA (pH 9.0)	1:500
Anti-vimentin	Monoclonal mouse Vim 3B4	DakoCytomation, Glostrup, Denmark	Citrate buffer (pH 6.0)	1:25

3.2.3 Transmission electron microscopy

Tissue samples were collected and processed as described in chapter one. Sections were examined using a Phillips CM10 transmission electron microscope (Phillips

Electron Optical Division, Eindhoven, The Netherlands), operated at 80kV. A megaview III side-mounted digital camera (Olympus Soft Imaging Solutions GmbH, Munster, Germany) was used to capture the images and iTEM software (Olympus Soft Imaging Solutions GmbH, Munster, Germany) was used to adjust the brightness and contrast.

3.2.4 Statistical analysis

Statistical analyses were performed using the statistical software package SPSS (version 25.0, SPSS Inc., Chicago, USA). One-way ANOVA was used to assess significant differences between all age groups after testing for variance homogeneity and normality. Statistical differences between different age groups were evaluated using the Tukey's Multiple Comparison Test. The level of statistical significance was set at $p < 0.05$.

3.3 Results

3.3.1. Light microscopy

Testicular interstitial tissue was composed of peritubular boundary tissue and interstitium. Haematoxylin and eosin-stained sections revealed that the testicular parenchyma in all age groups studied was composed of seminiferous tubules, which were surrounded by peritubular boundary tissue (Figures 3.1, 3.2 & 3.3). The interstitium component of the interstitial tissue contained blood vessels and Leydig cells embedded in loose connective tissue.

Pre-pubertal birds

In pre-pubertal birds, the seminiferous cords were small (approximately 33.01 μm to 51.94 μm in diameter), round in shape and lacked lumina (Figure 3.1). Closely associated with the basement membranes of the seminiferous cords were reticular fibres (Figure 3.2). The seminiferous cords were enclosed in peritubular boundary tissue, which was formed by loose connective tissue with a small amount of collagen (Figure 3.3). No elastic fibres were detected in the peritubular boundary tissue (Figure 3.4). Approximately 2 to 3 layers of peritubular myoid cells and 1 to 2 layers of fibroblasts were observed in the peritubular boundary tissue (Figure 3.1). The inner peritubular myoid cell layers encircled the seminiferous cords, while the outer fibroblastic layers ran longitudinally between the cords. Peritubular myoid cells had finely-tapered cytoplasmic ends and nuclei which exhibited darkly-stained nucleoli. In contrast, the fibroblasts were oblong-shaped cells with elongated nuclei, which exhibited prominent dark nucleoli.

The interstitium was composed of Leydig cells, fibroblasts and blood vessels, which were surrounded by loose connective tissue (Figure 3.1).

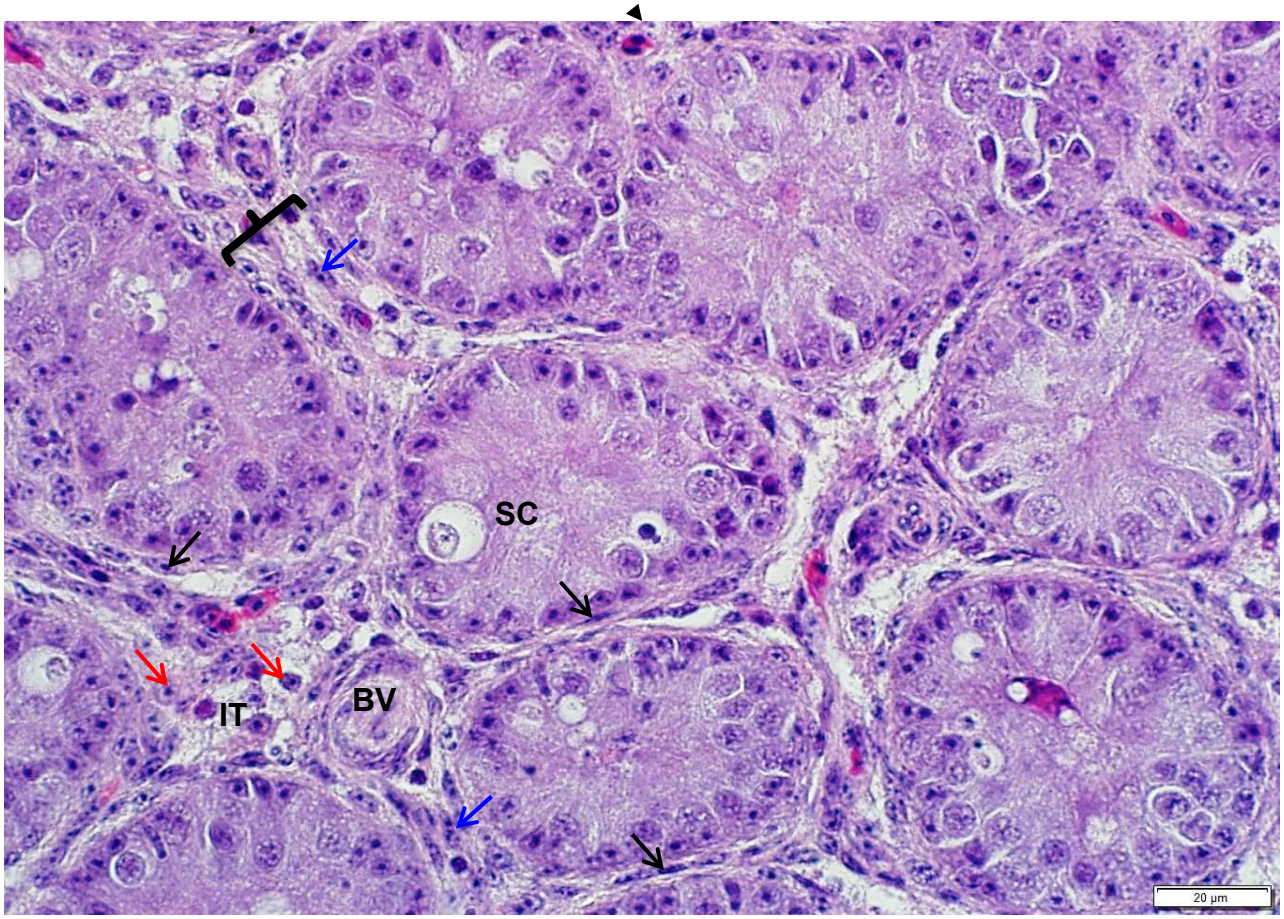

Figure 3. 1. Light photomicrograph of the testicular parenchyma in a pre-pubertal bird. SC: seminiferous cord. Bracket: peritubular boundary tissue composed of multiple cell layers. Peritubular myoid cells with dark nuclei (black arrows) and fibroblasts with prominent nucleoli (blue arrow) are observed. IT: interstitium containing Leydig cells (red arrows) and a blood vessel (BV). Haematoxylin and eosin.

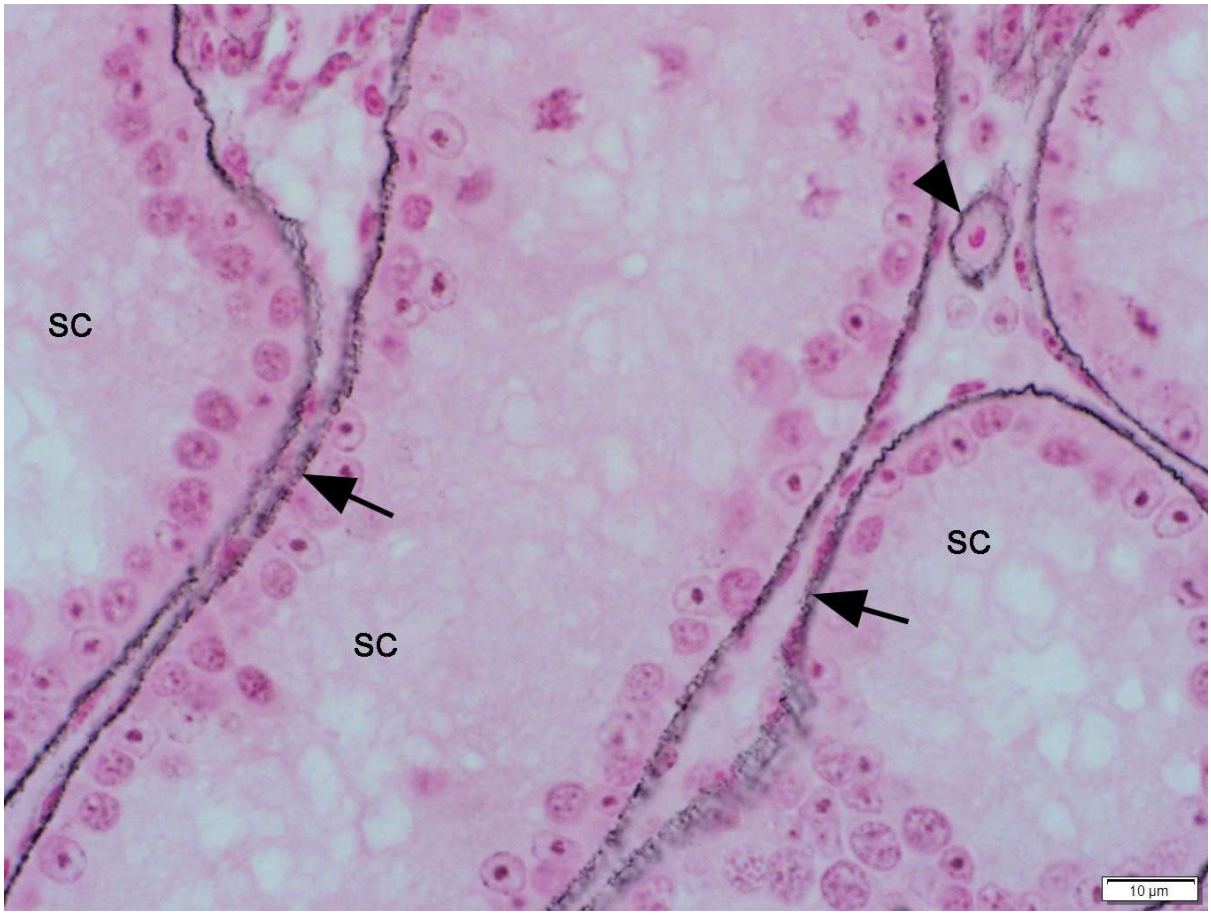

Figure 3. 2. Light photomicrograph of the testicular parenchyma in a pre-pubertal bird. SC: seminiferous cords. Arrows: reticular fibres associated with basement membranes of the seminiferous cords. Arrowhead: reticular fibres associated with a blood vessel. Gomori's silver impregnation stain.

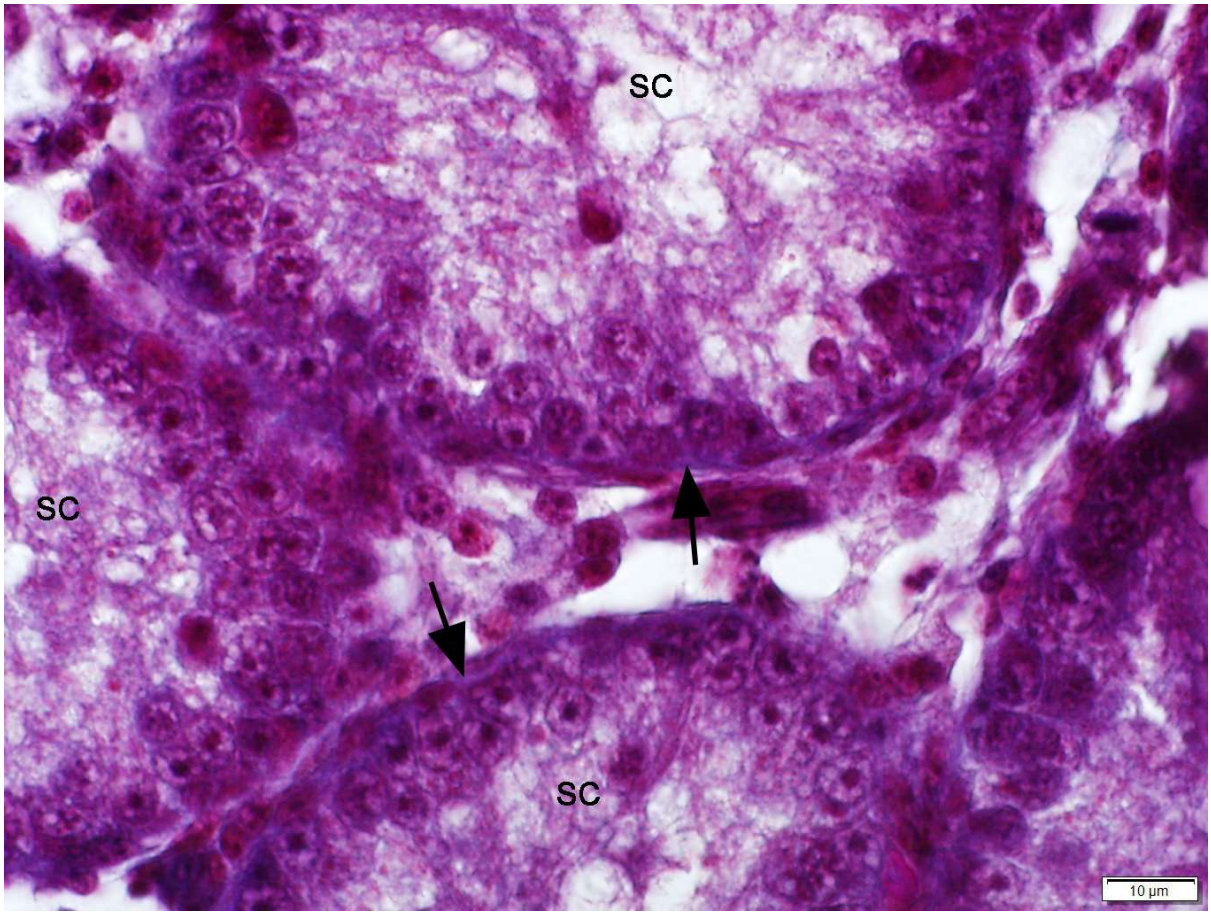

Figure 3. 3. Light photomicrograph of the testicular parenchyma in a pre-pubertal bird. SC: seminiferous cords. Arrows: collagen fibres. Masson trichrome stain.

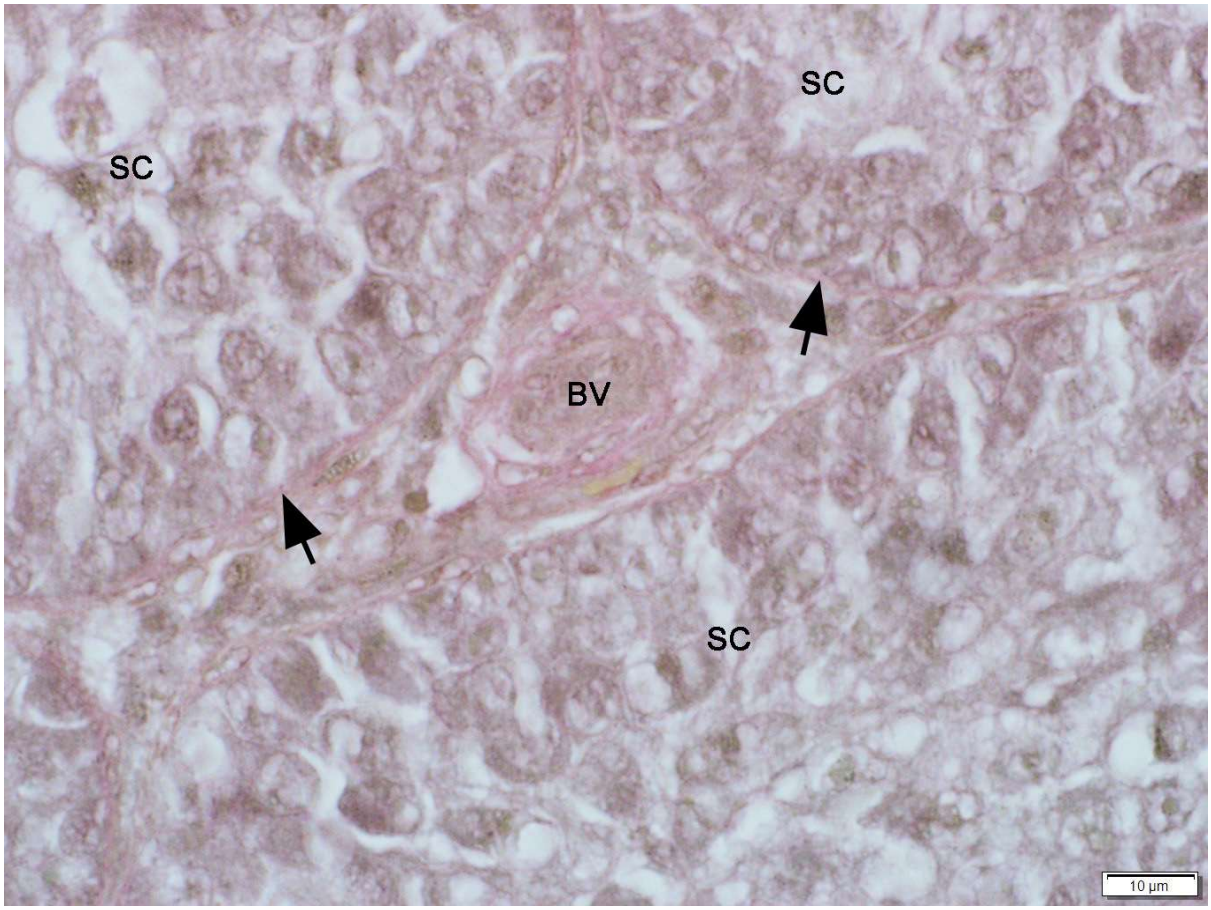

Figure 3. 4. Light photomicrograph of the testicular parenchyma in a pre-pubertal bird. SC: seminiferous cords. BV: blood vessel. Arrows: collagen fibres. Verhoeff-Van Gieson stain.

Pubertal birds

In pubertal birds, seminiferous tubules with diameters ranging from approximately 77.22µm to 141.67 µm, formed elongated structures which contained distinct lumina (Figure 3.5). Associated with the basement membranes of the seminiferous tubules was a layer of reticular fibres (Figure 3.6). The peritubular boundary tissue surrounding the seminiferous tubules contained collagen fibres (Figure 3.7), but lacked elastic fibres (Figure 3.8). The cellular component of the peritubular boundary

tissue was formed by 1 to 2 layers of elongated peritubular myoid cells (Figure 3.5), as well as fibroblasts.

The interstitium contained loose connective tissue, Leydig cells and blood vessels.

Figure 3. 5: A light photomicrograph of the testicular parenchyma in a pubertal bird. ST: seminiferous tubule. Bracket: peritubular boundary tissue. Arrows: peritubular myoid cells. Red arrows: Leydig cells in the interstitium (IT). Arrowhead: red blood cells in intertubular blood vessels. BV: blood vessels. Haematoxylin and eosin stain.

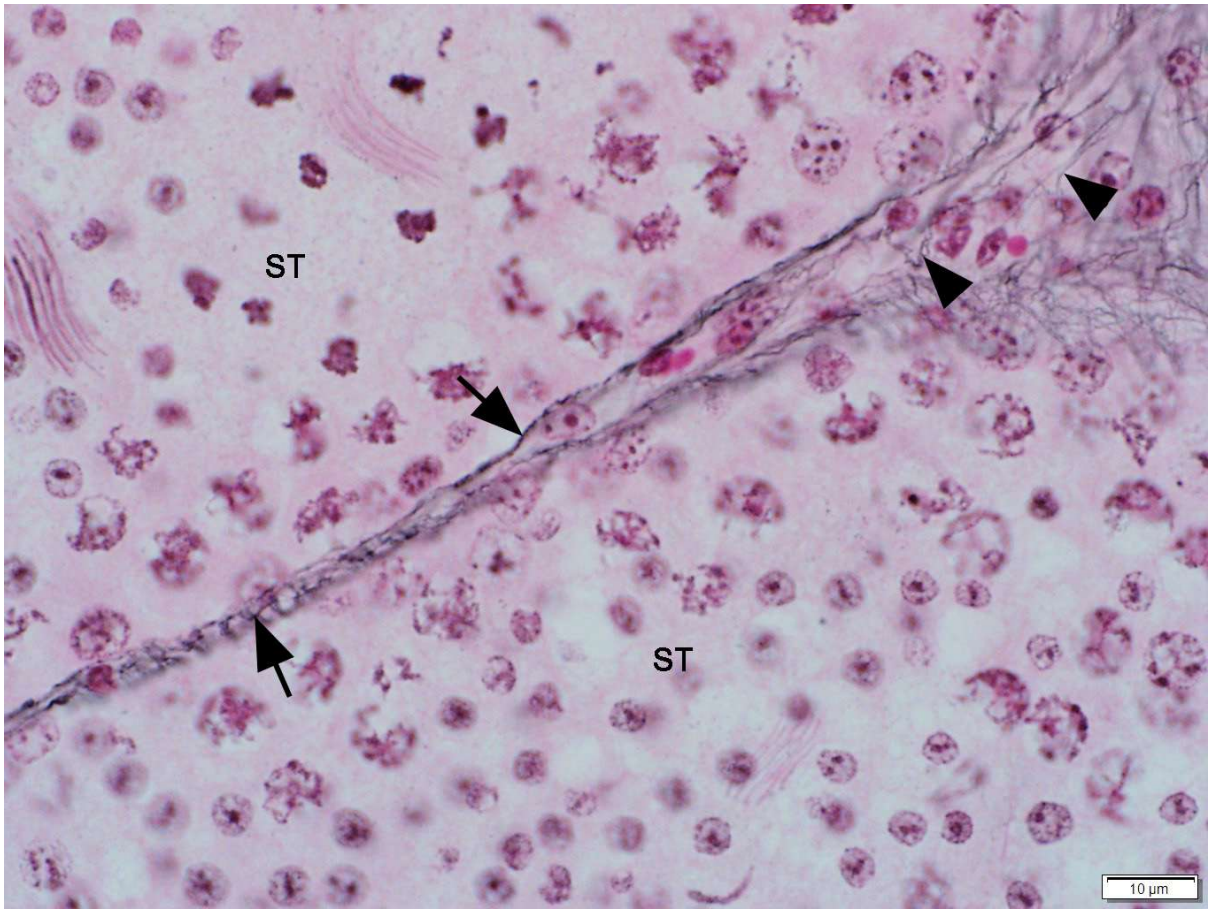

Figure 3. 6: A light photomicrograph of the testicular parenchyma in a pubertal bird. ST: seminiferous tubules. Arrows: reticular fibres associated with the basement membranes of seminiferous tubules. Arrowheads: reticular fibres in the interstitium. Gomori's silver impregnation stain.

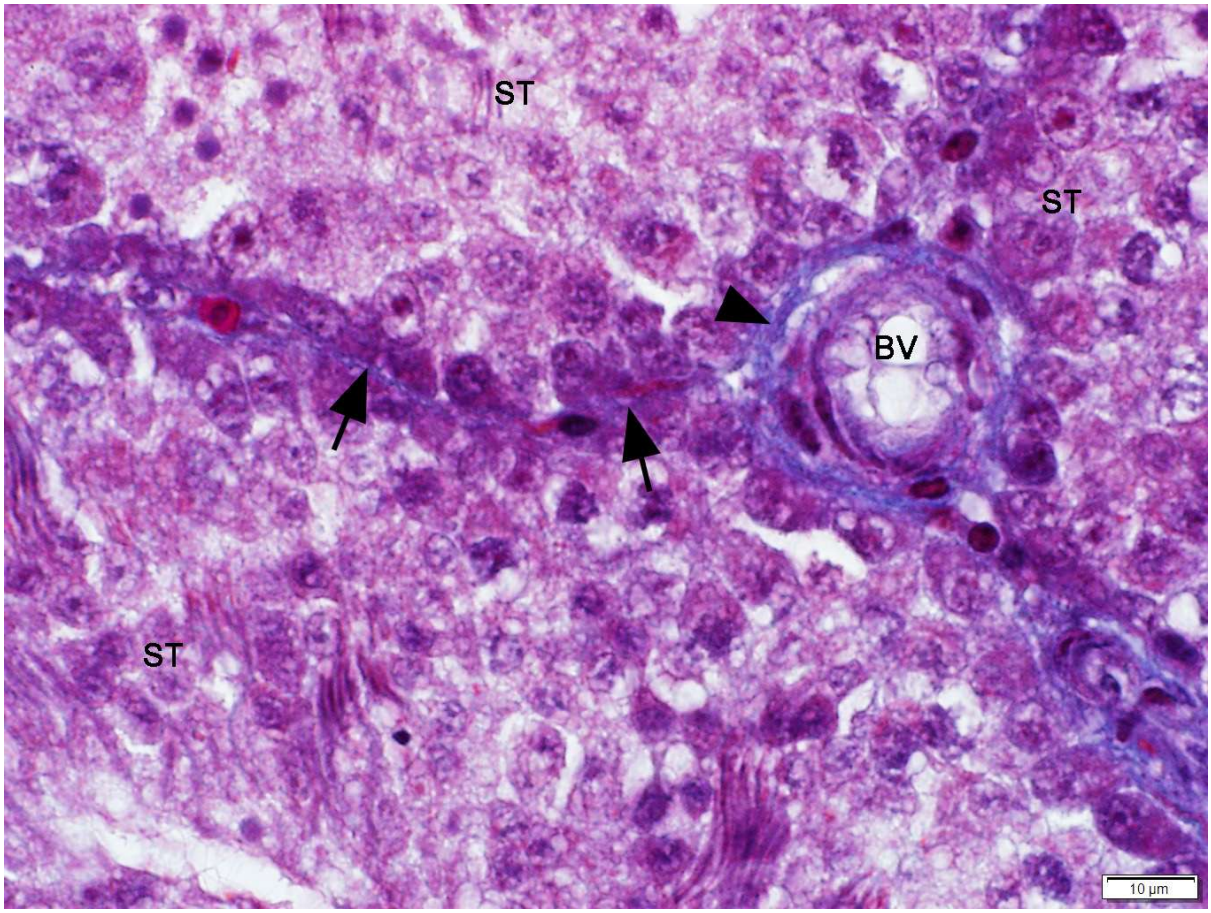

Figure 3. 7: A light photomicrograph of the testicular parenchyma in a pubertal bird. ST: seminiferous tubules. Arrows: collagen fibres in the peritubular boundary tissue. Arrowhead: collagen fibres in the *tunica adventitia* of a blood vessel (BV). Masson trichrome stain.

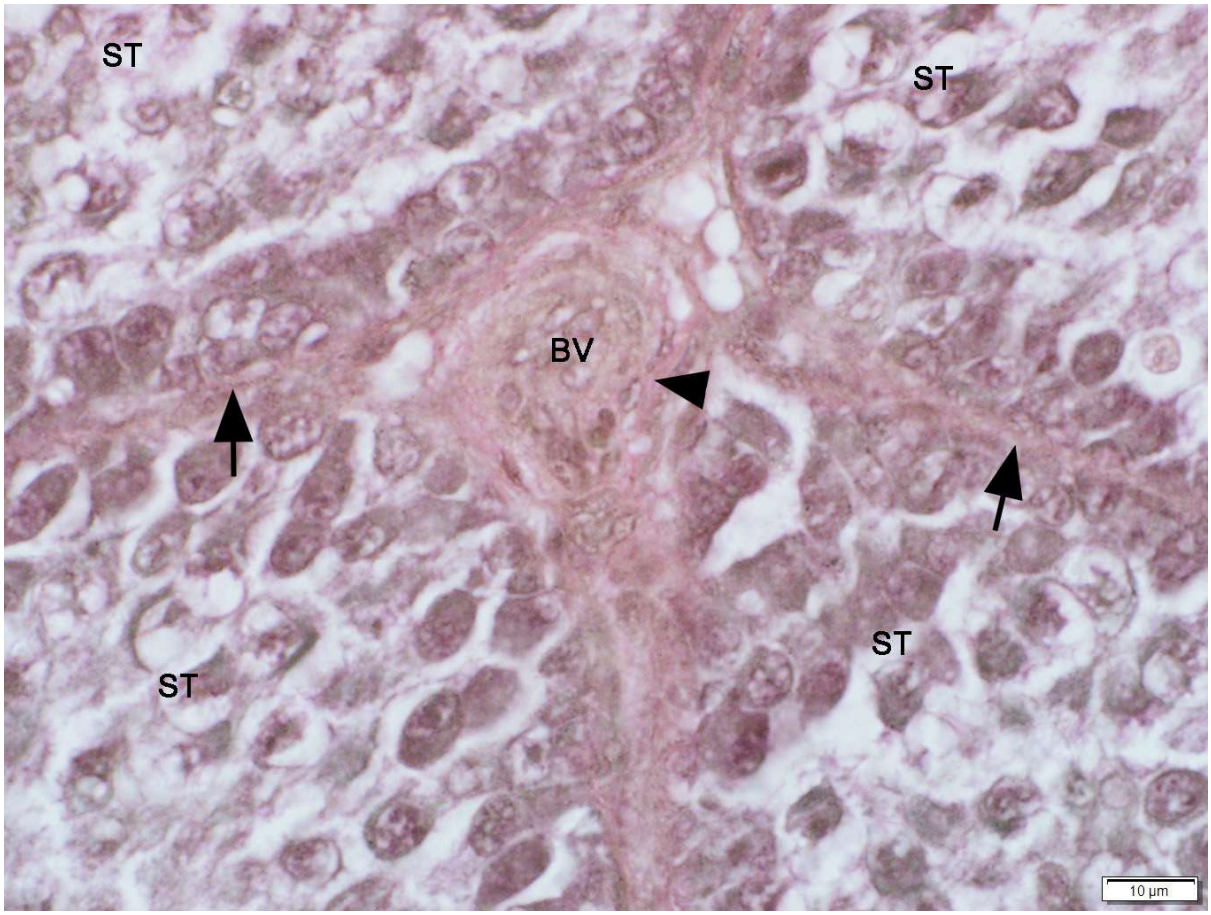

Figure 3. 8: A light photomicrograph of the testicular parenchyma in a pubertal bird. ST: seminiferous tubules. Arrows: collagen fibres in the peritubular boundary tissue. Arrowhead: collagen fibres in the *tunica adventitia* of a blood vessel (BV). Verhoeff-Van Gieson stain.

Adult birds

The seminiferous tubules were large (approximately 83.38 µm to 147.11µm in diameter) and elongated in form, with well-developed lumina (Figure 3.9). A layer of reticular fibres was associated with the basement membranes of the seminiferous tubules (Figure 3.10). Peritubular myoid cells, which contained elongated nuclei surrounded the seminiferous tubules. The connective tissue enclosing the peritubular

myoid cells contained collagen fibres (Figure 3.11). Elastic fibres were not demonstrated in the connective tissue (3.12).

Leydig cells and blood vessels, with a small amount of connective tissue, were observed in the interstitium.

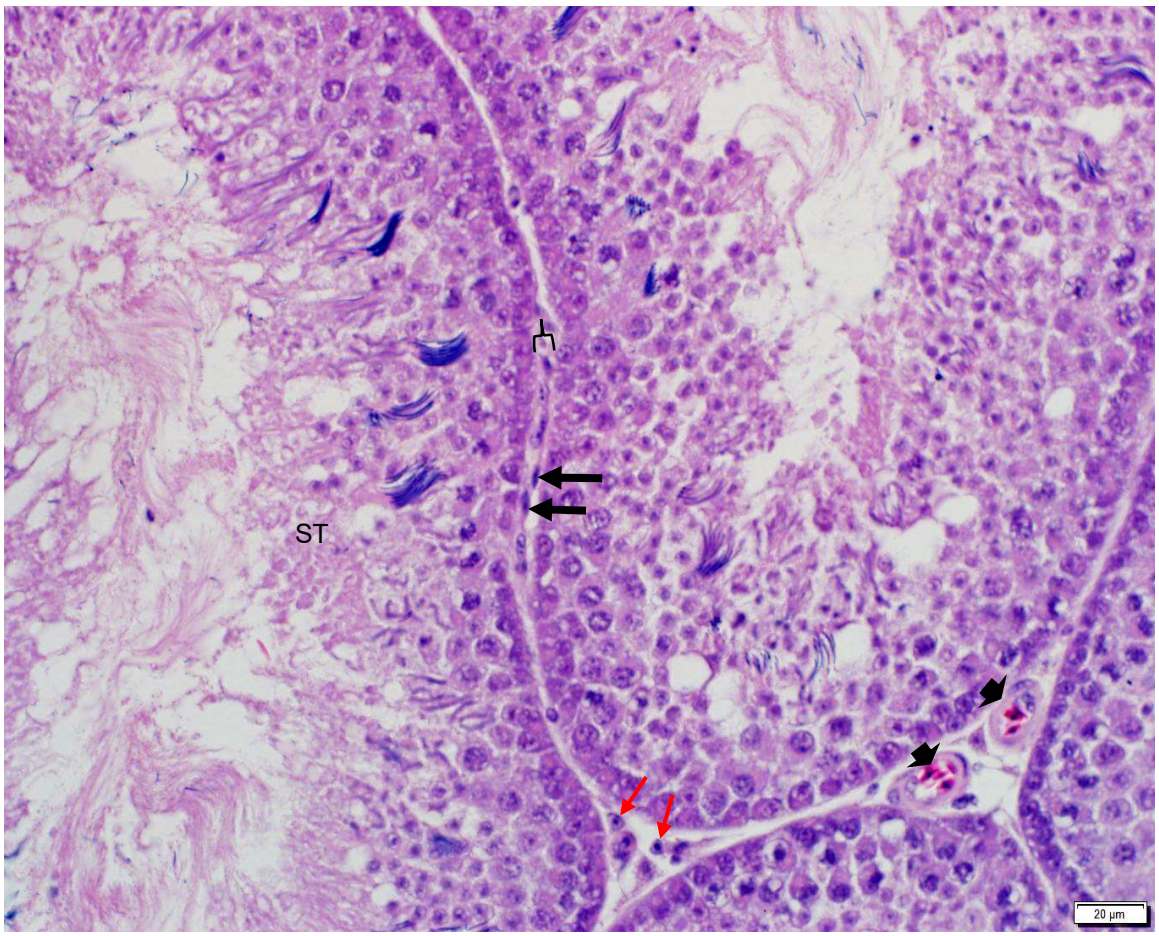

Figure 3. 9: A light photomicrograph of the testicular parenchyma in an adult bird. ST: seminiferous tubule. Bracket: peritubular boundary tissue. Thick arrows: peritubular myoid cells with elongated nuclei. Note the presence of blood vessels (arrowheads) and Leydig cells (red arrows) in the interstitium. Haematoxylin and eosin stain.

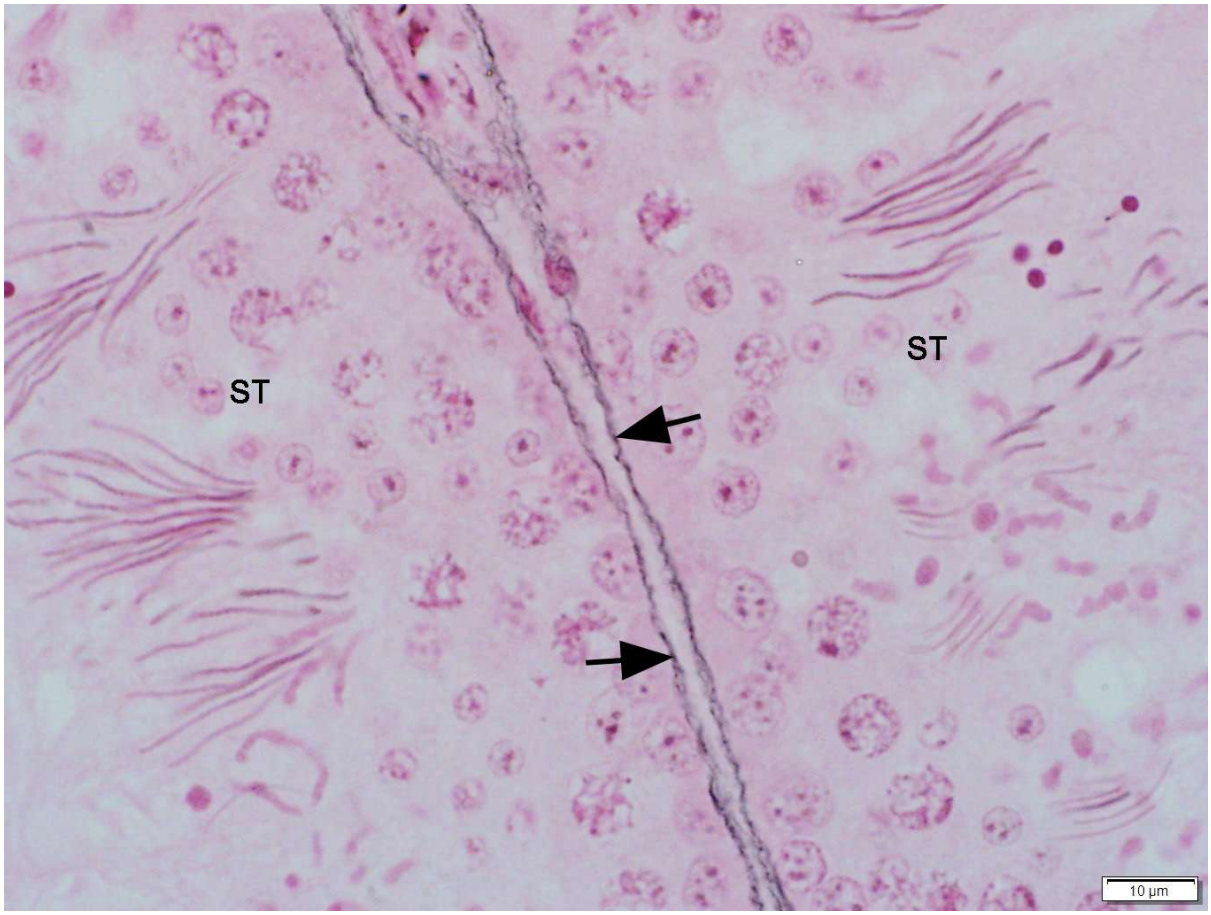

Figure 3. 10: A light photomicrograph of the testicular parenchyma in an adult bird.

ST: seminiferous tubules. Arrows: reticular fibres. Gomori's silver impregnation stain.

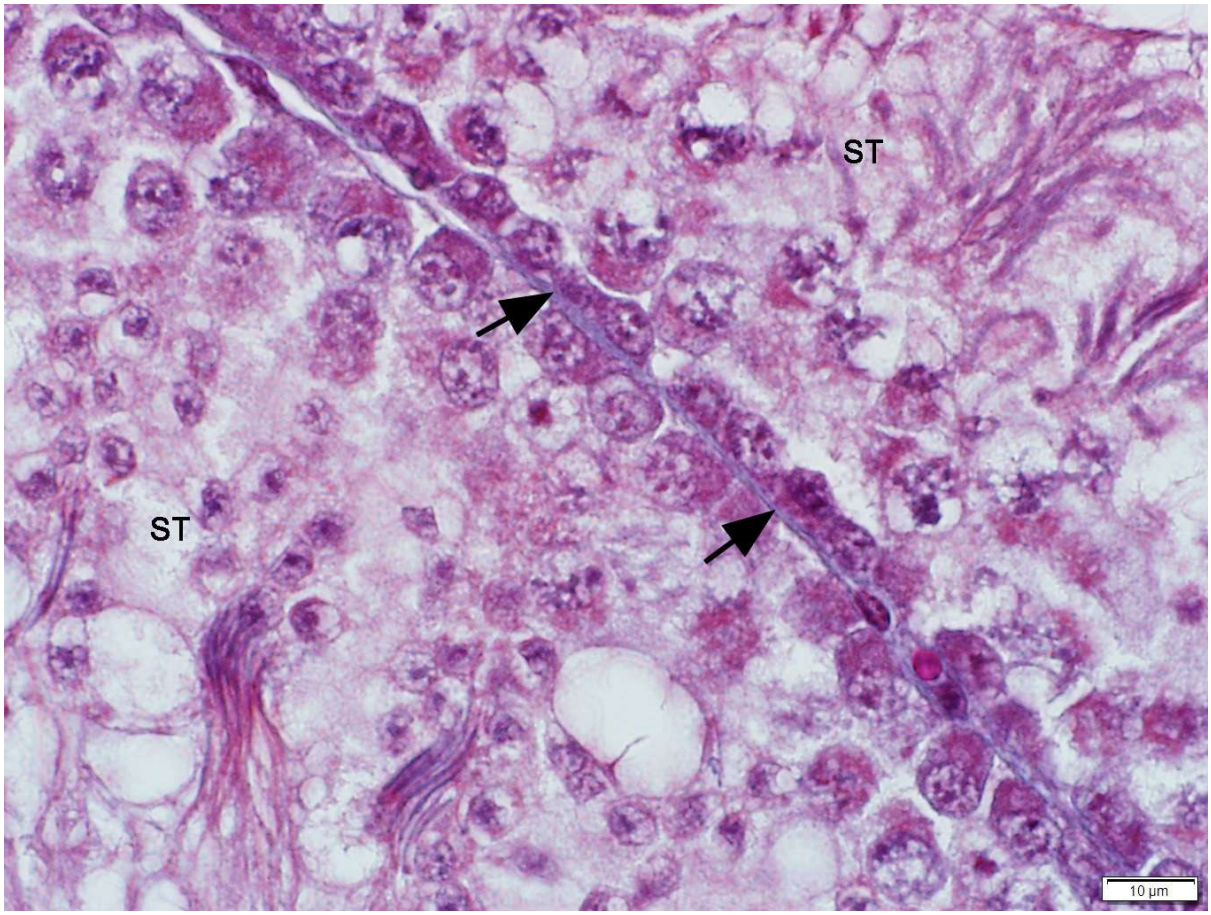

Figure 3. 11: A light photomicrograph of the testicular parenchyma in an adult bird.

ST: seminiferous tubules. Arrows: collagen fibres. Masson trichrome stain.

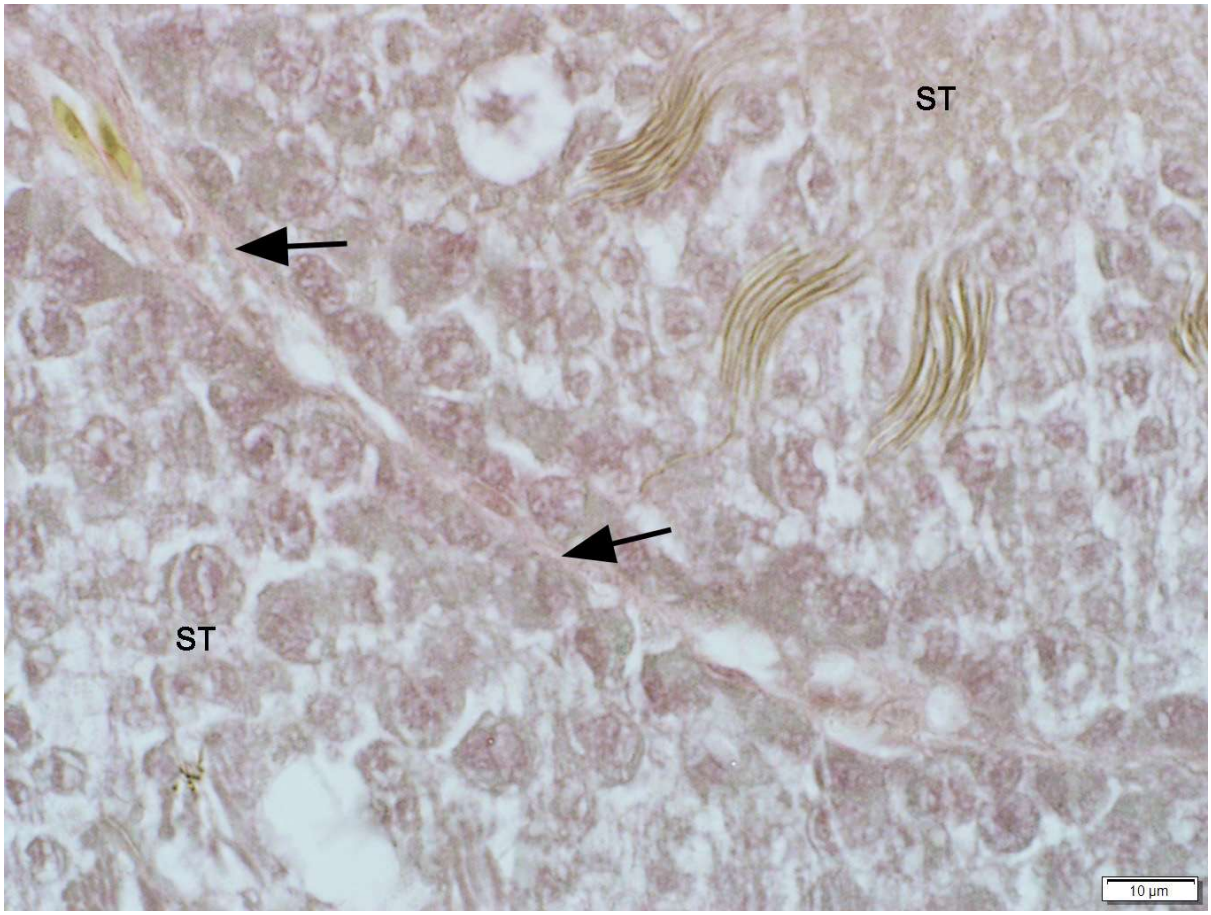

Figure 3. 12: A light photomicrograph of the testicular parenchyma in an adult bird. ST: seminiferous tubules. Arrows: collagen fibres. Verhoeff-Van Gieson stain.

3.3.2. Cytoskeletal protein immunohistochemistry

Cytoskeletal proteins (desmin, smooth muscle actin, tubulin and vimentin) and extracellular matrix components (collagen type IV, fibronectin and laminin) were immunolocalized in the peritubular boundary tissue of pre-pubertal, pubertal and adult Japanese quails. Variations in the staining intensities of cytoskeletal proteins and extracellular matrix components are shown in Tables 3.2 and 3.3 respectively.

3.3.2.1 Desmin

Pre-pubertal birds

The peritubular myoid cell layer displayed weak desmin immunostaining (Figure 3.13 A). No desmin immunostaining was detected in the endothelial cells lining intertubular blood vessels. However, weak to moderate desmin immunostaining was localized in smooth muscle cells forming the *tunica media* of the intertubular blood vessels. Fibroblasts and Leydig cells were desmin immunonegative (Figure 3.13A).

Pubertal birds

Desmin immunostaining in peritubular myoid cells varied from weak to strong. Vascular smooth muscle cells displayed strong desmin immunostaining (Figure 3.13 B, C). No immunostaining was detected in fibroblasts, vascular endothelial cells and Leydig cells (Figure 3.13 B, C).

Adult birds

Weak to strong desmin immunostaining was demonstrated in the peritubular myoid cell layer (Figure 3.13 D, E). Vascular smooth muscle cells displayed strong desmin immunostaining (Figure 3.13 D, E). Fibroblasts, endothelial and Leydig cells did not display desmin immunostaining.

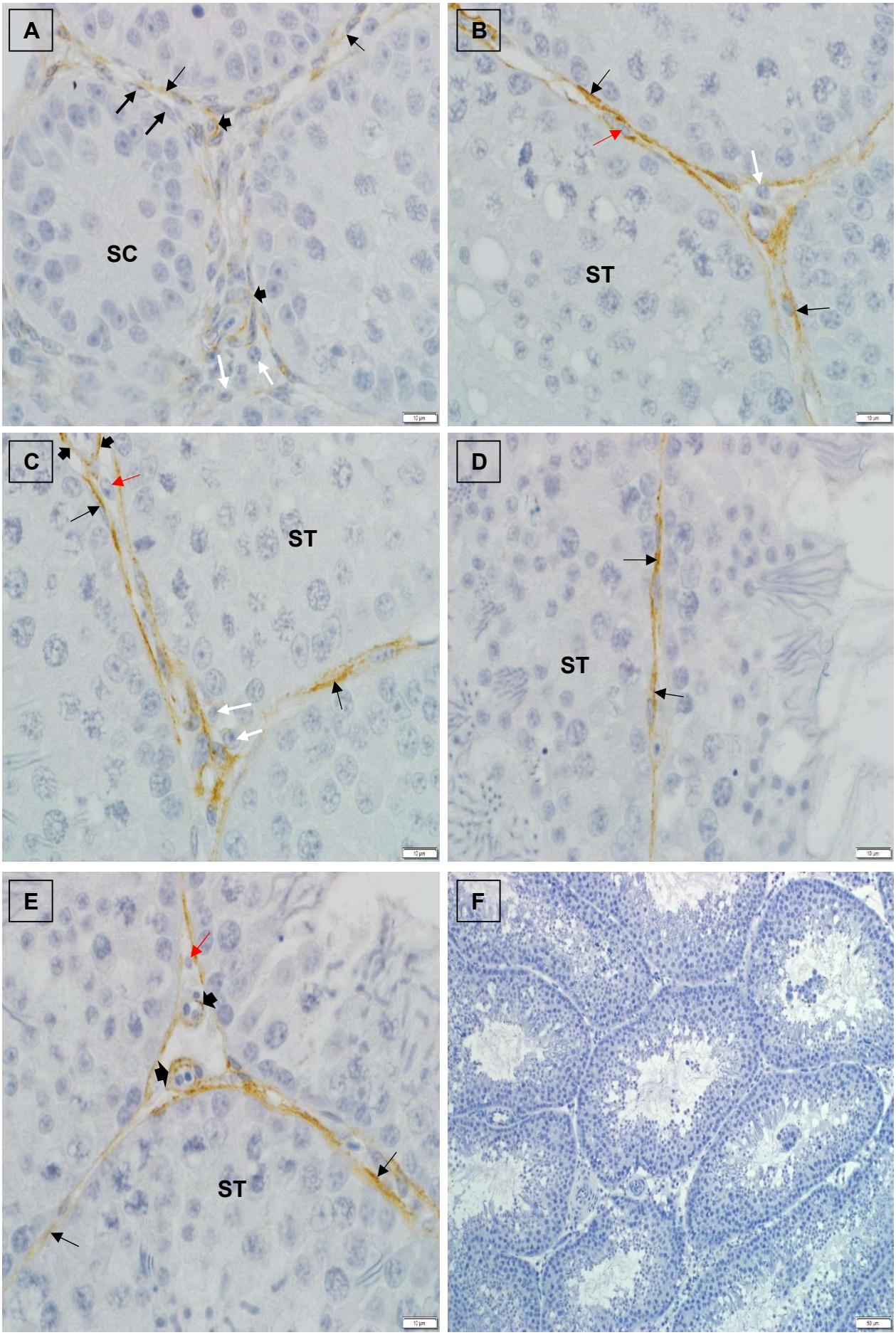
A
SC
B
ST
C
ST
D
ST
E
ST
F

Figure 3. 13: Light photomicrographs showing desmin immunoexpression in the peritubular boundary tissue of pre-pubertal (A), pubertal (B, C), and adult (D, E) quails. A light photomicrograph (F) of the negative control section is included.

A. Testicular parenchyma of a pre-pubertal quail. Thin black arrows: weak desmin immunostaining in peritubular myoid cells. Thick black arrows: desmin immunonegative fibroblasts. White arrows: desmin immunonegative Leydig cells. Arrowheads: desmin immunopositive vascular smooth muscle cells. SC: seminiferous cords. Scale bar = 10μm.

B, C. Testicular parenchyma of pubertal quails. Peritubular myoid cells (black arrows) and vascular smooth muscle cells (arrowheads) display positive desmin immunostaining. Red arrows: desmin immunonegative fibroblasts. White arrows: desmin immunonegative Leydig cells. ST: seminiferous tubules. Scale bars = 10μm.

D, E. Testicular parenchyma of adult quails. Positive desmin immunostaining is demonstrated in peritubular myoid cells (black arrows) and vascular smooth muscle cells (arrowheads). Red arrow: desmin immunonegative fibroblast. ST: seminiferous tubules. Scale bars = 10μm.

F. Negative control section. Scale bar = 50μm.

3.3.2.2 Smooth muscle actin

Variations in the staining intensities of smooth muscle actin in pre-pubertal, pubertal and adult quails are summarized in Table 3.2.

Pre-pubertal birds

Peritubular myoid cells encircling the seminiferous cords, displayed weak to moderate smooth muscle actin immunostaining (Figure 3.14 A, B). Weak smooth muscle actin immunostaining was observed in the smooth muscle cells forming the *tunica media* of intertubular blood vessels. The endothelial cells of the intertubular blood vessels was immunonegative for smooth muscle actin. Similarly, fibroblasts, as well as Leydig cells were smooth muscle actin immunonegative (Figure 3.14 A, B).

Pubertal birds

Strong smooth muscle actin immunostaining was localized in the peritubular myoid cells of pubertal birds (Figures 3.14 C, D). Likewise, the smooth muscle cells forming the walls of intertubular blood vessels exhibited strong smooth muscle actin immunostaining. Fibroblasts, vascular endothelial cells and Leydig cells were smooth muscle immunonegative (Figures 3.14 C, D).

Adult birds

The peritubular myoid cell layer displayed strong smooth muscle actin immunostaining (Figures 3.14 E, F). Strong smooth muscle actin immunoreactivity was also observed in the *tunica media* of intertubular blood vessels. Fibroblasts, vascular endothelial cells and Leydig cells did not display smooth muscle actin immunostaining (Figures 3.14 E, F).

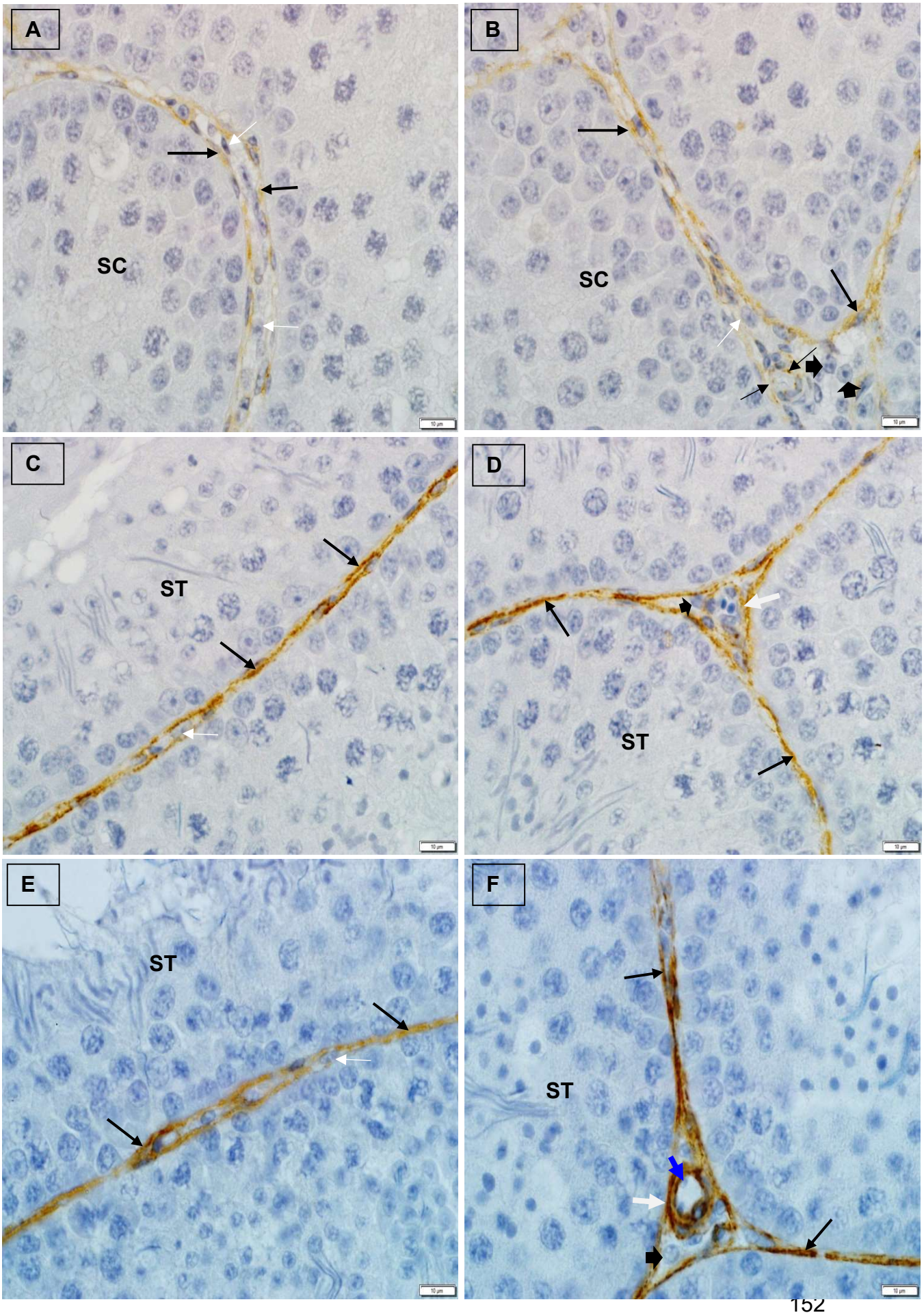
A
SC
B
SC
C
ST
D
ST
E
ST
F
ST

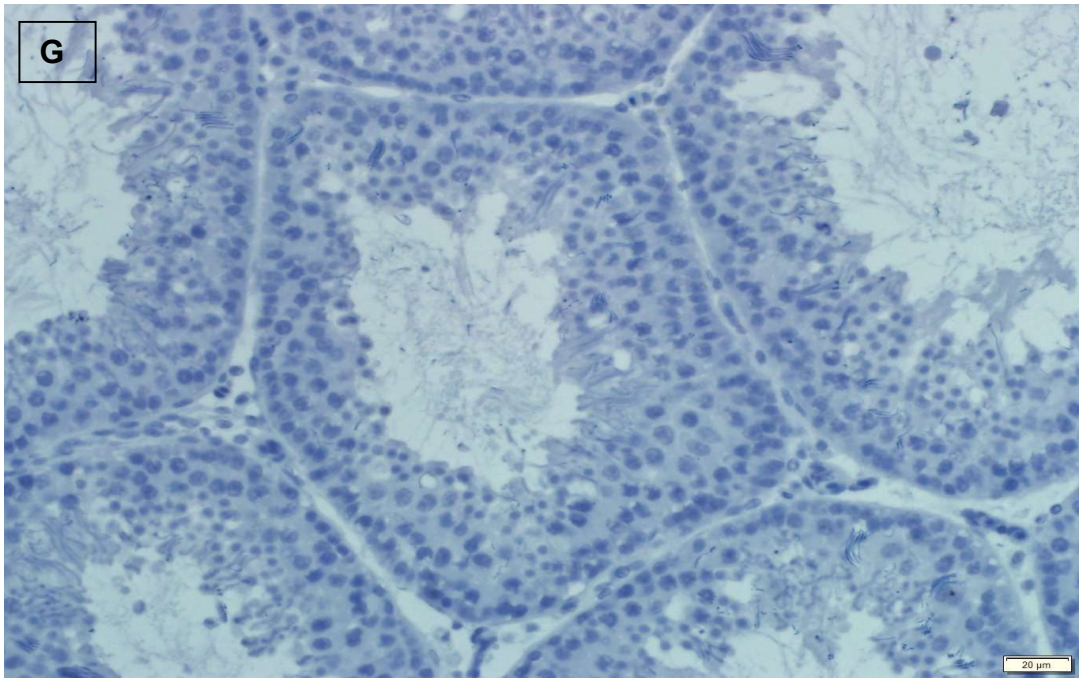

Figure 3. 14: Light photomicrographs showing the immunolocalization of smooth muscle actin in the peritubular boundary tissue and interstitium of pre-pubertal (A, B), pubertal (C, D), and adult (E, F) quails. A light photomicrograph (G) of the negative control section is included.

A, B. Testicular parenchyma of pre-pubertal quails. Thick black arrows: weak to moderate smooth muscle actin immunostaining in peritubular myoid cells. White arrows: smooth muscle actin immunonegative fibroblasts. Thin black arrows: smooth muscle actin immunopositive vascular smooth muscle cells. Arrowheads: smooth muscle actin immunonegative Leydig cells. SC: seminiferous cords. Scale bars = 10μm.

C- F. Testicular parenchyma of pubertal (C & D) and adult (E & F) quails. Black arrows: strong smooth muscle actin immunostaining in peritubular myoid cells. Thick white arrows: immunopositive smooth muscle cells of intertubular blood vessels. Blue arrow: immunonegative endothelial cell. Thin white arrows: immunonegative

fibroblasts. Arrowheads: immunonegative Leydig cells. ST: seminiferous tubules. Scale bars = 10μm.

G. Negative control section. Scale bar = 20μm.

3.3.2.3 Tubulin

Variations in the staining intensities of tubulin in pre-pubertal, pubertal and adult quails are summarized in Table 3.2.

Pre-pubertal birds

Tubulin immunostaining was weak or absent in the peritubular myoid cells of pre-pubertal birds. Sertoli cells displayed strong tubulin immunostaining. The endothelial cells of intertubular blood vessels exhibited moderate tubulin immunostaining, while the *tunica media* of the blood vessels was tubulin immunonegative (Figure 3.15 A). Fibroblasts and Leydig cells were tubulin immunonegative (Figure 3.15 A).

Pubertal birds

Weak to moderate tubulin immunostaining was observed in the peritubular myoid cells of pubertal quails. Sertoli cells lining the seminiferous tubules displayed moderate tubulin immunostaining. Strong tubulin immunostaining was observed in the developing spermatids associated with the Sertoli cells. Endothelial cells of intertubular blood vessels exhibited moderate tubulin immunostaining, while the smooth muscle cells forming the walls of the blood vessels were tubulin immunonegative. Fibroblasts and Leydig cells in the peritubular boundary tissue and interstitium were tubulin immunonegative. (Figure 3.15 B, C).

Adult birds

Peritubular myoid cells in adult quails exhibited weak to moderate tubulin immunoreactivity (Figure 3.15 D, E). Weak to moderate tubulin immunostaining was also demonstrated in Sertoli cells, while strong immunostaining was observed in spermatids. The endothelial cells and smooth muscle cells of intertubular blood vessels were tubulin positive and negative respectively. Fibroblasts and Leydig cells did not display tubulin immunostaining (Figure 3.15 D, E).

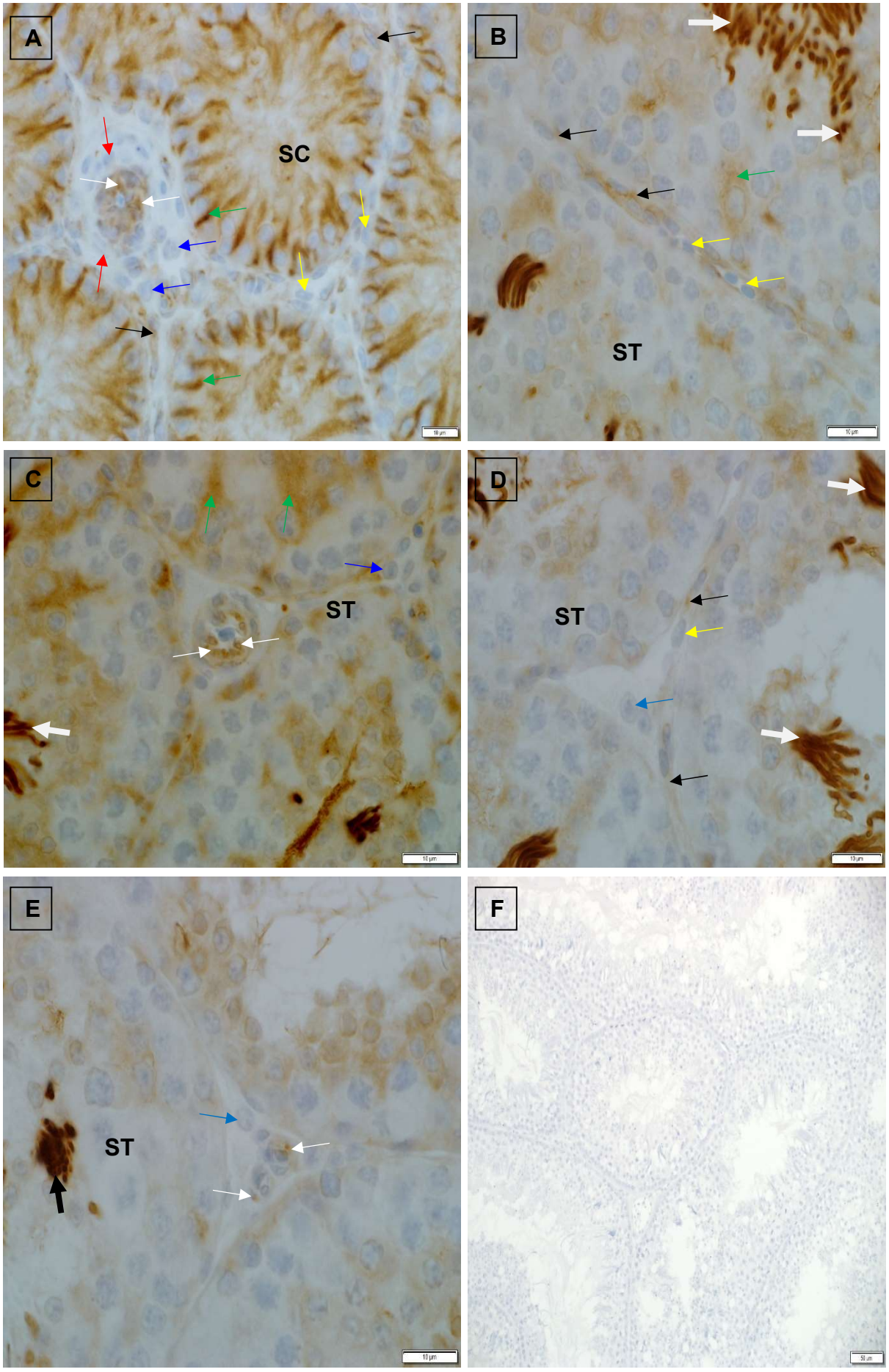
A
SC
B
ST
C
ST
D
ST
E
ST
F

Figure 3. 15: Light photomicrographs showing tubulin immunostaining in the peritubular boundary tissue of pre-pubertal (A), pubertal (B, C), and adult (D, E) quails. No immunostaining was observed in the negative control section (F).

A. Testicular parenchyma of a pre-pubertal quail. Black arrows: weak tubulin immunostaining in peritubular myoid cells. Yellow arrows: tubulin immunonegative fibroblasts. Red arrows: tubulin immunonegative vascular smooth muscle cells. Green arrows: strong tubulin immunostaining in Sertoli cells. White arrows: moderate tubulin immunostaining in vascular endothelial cells. Blue arrows: tubulin immunonegative Leydig cells. Scale bars: 10μm

B, C. Testicular parenchyma of pubertal quails. Black arrows: weak to moderate tubulin immunostaining in peritubular myoid cells. Yellow arrows: tubulin immunonegative fibroblasts. Green arrows: moderate tubulin immunostaining in Sertoli cells. Thick white arrows: strong tubulin immunostaining in spermatids. Thin white arrows: moderate tubulin immunostaining in vascular endothelial cells. Blue arrow: tubulin immunonegative Leydig cell. Scale bars: 10μm

D, E. Testicular parenchyma of adult quails. Thin black arrows: weak to moderate tubulin immunostaining in peritubular myoid cells. Yellow arrow: tubulin immunonegative fibroblast. Thick white arrows: strong tubulin immunostaining in spermatids. White arrows: weak to moderate tubulin immunostaining in vascular endothelial cells. Blue arrows: tubulin immunonegative Leydig cells. Scale bars: 10μm

F. Negative control. Scale bar = 50μm.

3.3.2.4 Vimentin

Variations in the staining intensities of vimentin in pre-pubertal, pubertal and adult quails are summarized in Table 3.2.

Pre-pubertal birds

Vimentin immunostaining in peritubular myoid cells was weak or absent (Figure 3.16 A). Moderate to strong vimentin immunostaining was observed in fibroblasts, which were located in the peritubular boundary tissue and interstitium. Leydig cells located in the interstitium exhibited moderate vimentin immunoreactivity (Figure 3.16 A). Strong vimentin immunostaining was demonstrated in the endothelial cells of intertubular blood vessels. Vascular smooth muscle cells were vimentin immunonegative (Figure 3.16 A).

Pubertal birds

Moderate to strong vimentin immunostaining was demonstrated in the peritubular myoid and Leydig cells of pubertal birds (Figure 3.16 B, C). Fibroblasts displayed strong vimentin immunostaining (Figure 3.16 B, C). The endothelial cells of intertubular blood vessels were strongly vimentin immunopositive, while the smooth muscle cells forming the tunica media were immunonegative.

Adult birds

Peritubular myoid and Leydig cells in adult quails exhibited moderate to strong vimentin immunostaining (Figure 3.16 D, E). Strong vimentin immunostaining was observed in fibroblasts, as well as in the endothelial cells of intertubular blood vessels. The smooth muscle cells forming the *tunica media* of the blood vessels were vimentin immunonegative (Figure 3.16 D, E).

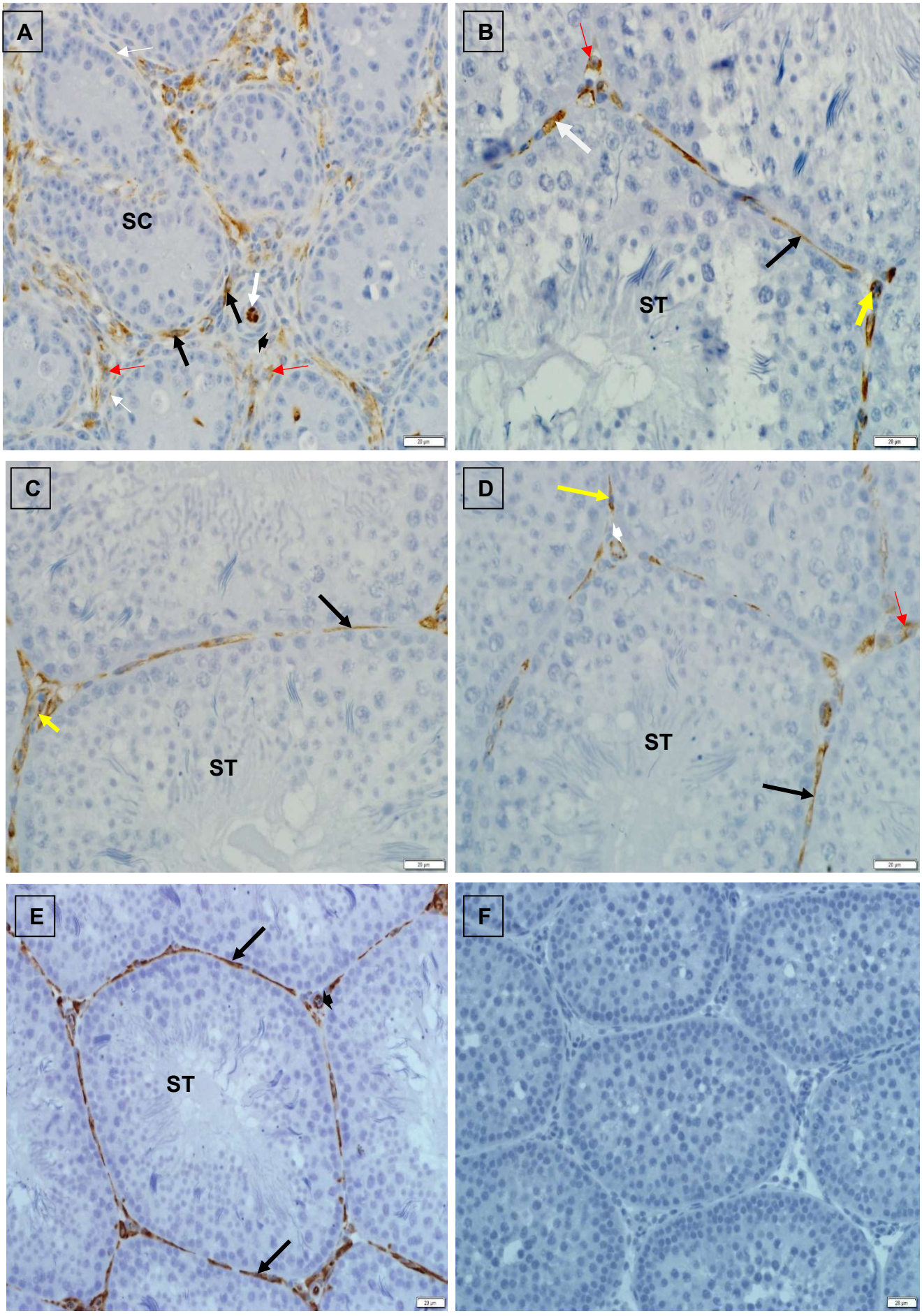
A
SC
B
ST
C
ST
D
ST
E
ST
F

Figure 3. 16: Light photomicrographs showing vimentin immunoexpression in the peritubular boundary tissue and interstitium of pre-pubertal (A), pubertal (B, C), and adult (D, E) quails. No immunostaining was observed in the negative control section (F).

A. Testicular parenchyma of a pre-pubertal quail. Thin white arrows: weak vimentin immunostaining in peritubular myoid cells. Thick black arrows: moderate to strong vimentin immunostaining in fibroblasts. Red arrows: moderate vimentin immunostaining in Leydig cells. Arrowhead: vimentin immunonegative vascular smooth muscle cells. Thick white arrow: endothelial cell displaying strong vimentin immunostaining. SC: seminiferous cord. Scale bar = 20μm

B, C. Testicular parenchyma of pubertal quails. Black arrows: vimentin immunopositive peritubular myoid cells. White arrow: strong vimentin immunostaining in a fibroblast. Red arrow: immunopositive Leydig cell. Yellow arrows: strong vimentin immunostaining in endothelial cells. ST: seminiferous tubules. Scale bars = 20μm.

D, E. Testicular parenchyma of adult quails. Black arrows: vimentin immunostaining in peritubular myoid cells. Yellow arrow: vimentin immunopositive fibroblast. Red arrow: immunopositive Leydig cells. Black arrowhead: immunopositive endothelial cells. White arrowhead: vimentin immunonegative *tunica media* of an intertubular blood vessel. ST: seminiferous tubule. Scale bars = 20μm.

F. Negative control. Scale bar = 20μm.

Table 3. 2**:** Summary of intensities of cytoskeletal proteins (desmin, smooth muscle actin, tubulin and vimentin) in the cells of the peritubular boundary tissue in pre-pubertal, pubertal, and adult Japanese quails (*Coturnix coturnix japonica*).

Age group	Cytoskeletal protein	Peritubular myoid cells	Fibroblasts	Leydig cells	Blood vessels
Pre-pubertal	Desmin	+	-	-	+/++[b]
	Smooth muscle actin	+/++	-	-	+[b]
	Tubulin	-/+	-	-	++[a]
	Vimentin	-/+	++/+++	++	+++[a]
Pubertal	Desmin	+/++/+++	-	-	+++[b]
	Smooth muscle actin	+++	-	-	++[b]
	Tubulin	+/++	-	-	+++[a]
	Vimentin	++/+++	+++	++/+++	++/+++[a]
Adult	Desmin	+/++/+++	-	-	+++[b]
	Smooth muscle actin	+++	-	-	+++[b]
	Tubulin	+/++	-	-	+/++[a]
	Vimentin	++/+++	+++	++/+++	+++[a]

Intensities of immunostaining: - absent, + weak, ++ moderate, +++ strong. Blood vessel ([a] endothelium, [b] *tunica media*).

3.3.3. Basement membrane immunohistochemistry

3.3.3.1 Collagen type IV

Pre-pubertal birds

Moderate collagen type IV immunostaining was observed in the basement membranes associated with the seminiferous cords. Basement membranes of the peritubular myoid cells displayed weak collagen type IV immunostaining (Figure 3.17 A, B). No immunostaining for collagen type IV was demonstrated in Leydig cells, fibroblasts or vascular endothelial cells (Figure 3.17 A, B).

Pubertal birds

Moderate collagen type IV immunostaining was observed in the basement membranes of the seminiferous tubules, while weak immunostaining was demonstrated in those associated with peritubular myoid cells (Figure 3.17 C, D). Immunostaining in the smooth muscle cells forming the *tunica media* of intertubular blood vessels varied from weak to moderate. Fibroblasts, Leydig cells and vascular endothelial cells were collagen type IV immunonegative.

Adult birds

Strong collagen type IV immunostaining was demonstrated in the basement membranes associated with the seminiferous tubules (Figure 3.17 E, F). The basement membranes of peritubular myoid cells exhibited moderate collagen type IV immunostaining. Collagen type IV immunostaining in vascular smooth muscle cells was weak to moderate. Fibroblasts, vascular endothelial cells and Leydig cells were collagen type IV immunonegative.

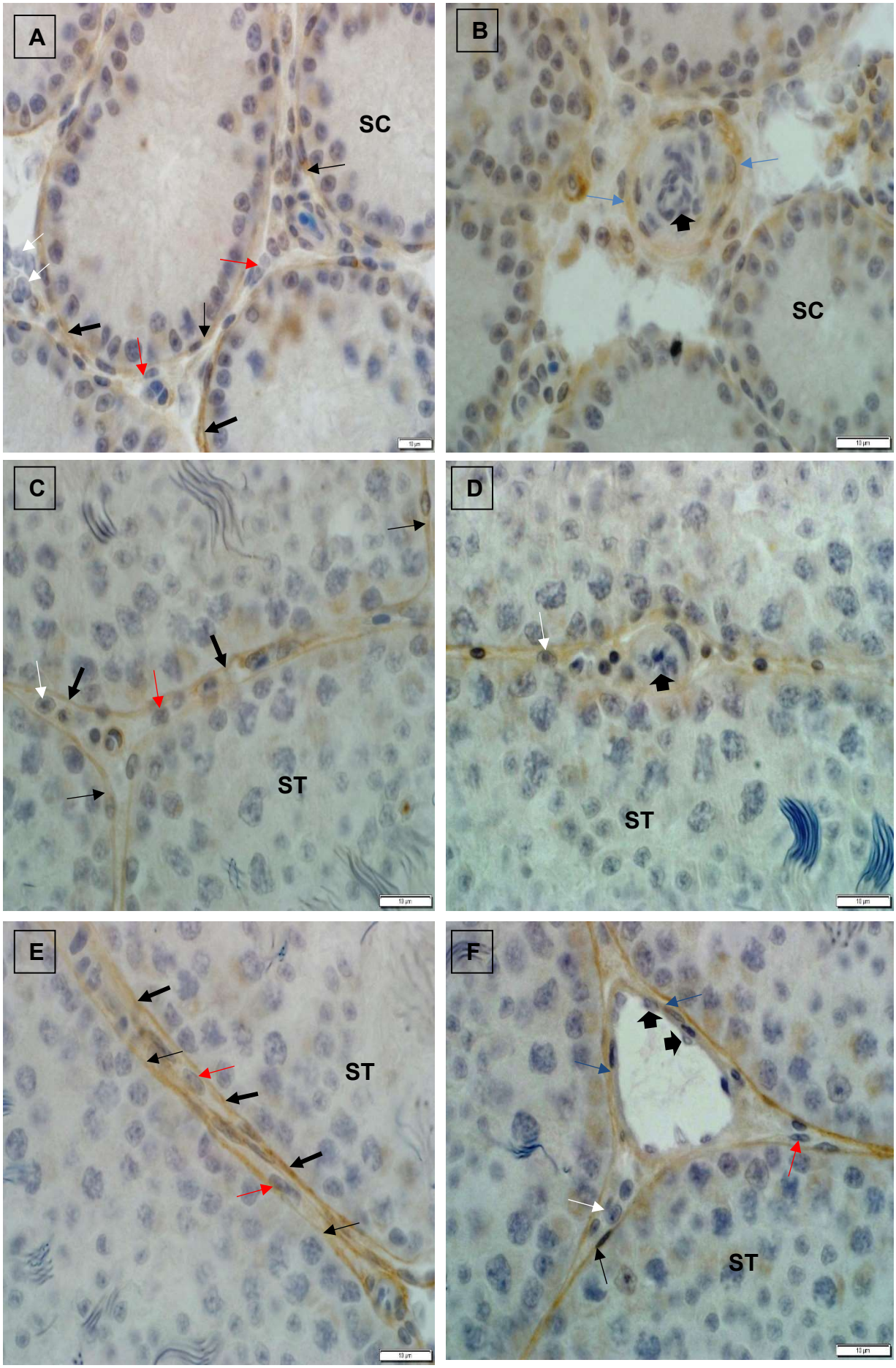
A
SC
B
SC
C
ST
D
ST
E
ST
F
ST

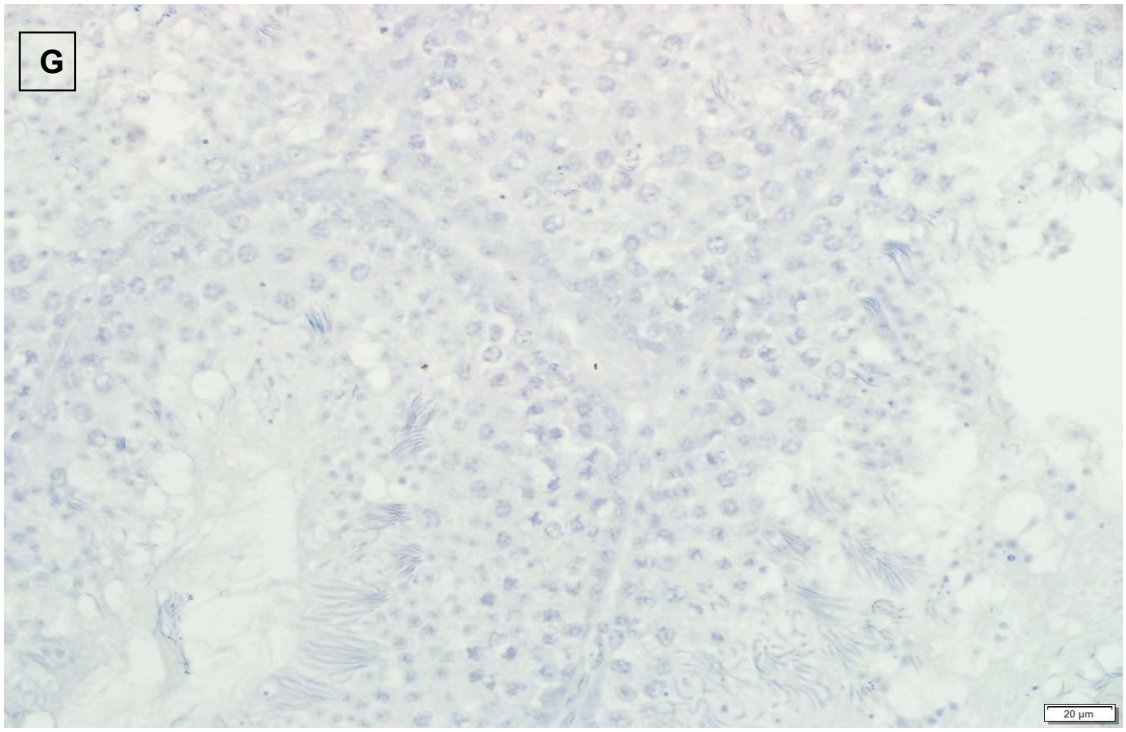

Figure 3. 17: Light photomicrographs showing collagen type IV immunostaining in the peritubular boundary tissue of pre-pubertal (A, B), pubertal (C, D), and adult (E, F) birds. G. Negative control. Scale bar = 20μm.

Thick black arrows: Basement membranes of seminiferous cords or tubules.

Thin black arrows: Basement membranes of peritubular myoid cells.

Blue arrows: Basement membranes of vascular smooth muscle cells.

Red arrows: collagen type IV immunonegative fibroblasts.

White arrows: collagen type IV immunonegative Leydig cells.

Arrowhead: collagen type IV immunonegative vascular endothelial cells.

SC: seminiferous cord. ST: Seminiferous tubule. Scale bars = 10μm.

3.3.3.2 Fibronectin

Pre-pubertal birds

Moderate to strong fibronectin immunostaining was observed in the basement membranes of peritubular myoid (Figure 3.18 A), vascular smooth muscle and endothelial cells. Basement membranes enclosing the seminiferous cords were fibronectin immunonegative. Similarly, Leydig cells and fibroblasts were fibronectin immunonegative.

Pubertal birds

The basement membranes of peritubular myoid, vascular smooth muscle and endothelial cells exhibited moderate to strong fibronectin immunostaining (Figure 3.18 B, C). The basement membranes associated with the seminiferous tubules were fibronectin immunonegative. Leydig cells and fibroblasts did not display fibronectin immunostaining.

Adult birds

The basement membranes associated with peritubular myoid cells exhibited strong fibronectin immunostaining (Figure 3.18 D, E). Similarly, strong fibronectin immunostaining was also observed in the basement membranes of vascular smooth muscle and endothelial cells. No fibronectin immunostaining was demonstrated in the basement membranes of the seminiferous tubules. Likewise, Leydig cells and fibroblasts were fibronectin immunonegative.

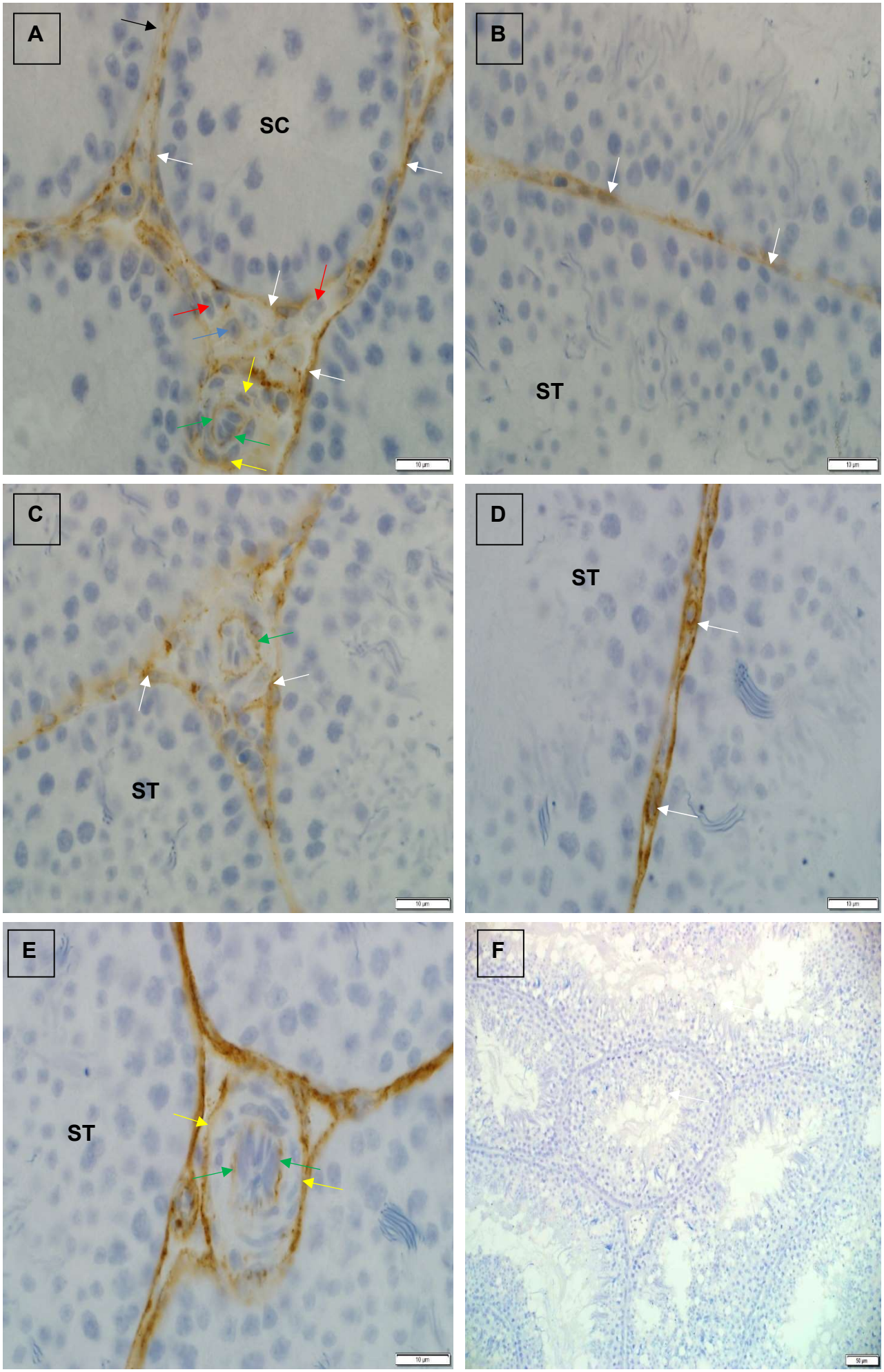
A
SC
B
ST
C
ST
D
ST
E
ST
F

Figure 3. 18: Light photomicrographs showing fibronectin immunostaining in the peritubular boundary tissue of pre-pubertal (A), pubertal (B, C) and adult (D, E) birds. No fibronectin immunostaining was demonstrated in the negative control section (D).

A-C. Testicular parenchyma of pre-pubertal and pubertal quails. Moderate to strong fibronectin immunostaining in the basement membranes of peritubular myoid cells (white arrows) and vascular smooth muscle (yellow arrows) and endothelial (green arrows) cells. Red arrows: fibronectin immunonegative fibroblasts. Blue arrow: fibronectin immunonegative Leydig cell. SC: seminiferous cords. ST: seminiferous tubules. Scale bars = 10μm.

D, E. Testicular parenchyma of adult quails. Strong fibronectin immunostaining in the basement membranes of peritubular myoid cells (white arrows), vascular smooth muscle (yellow arrows) and endothelial cells (green arrows) Red arrow: immunonegative fibroblast. ST: seminiferous tubules. Scale bars = 10μm.

F. Negative control section. Scale bar = 50μm.

3.3.3.3 Laminin

Pre-pubertal birds

Laminin immunostaining was weak or absent in the basement membranes of the seminiferous cords (Figures 3.19 A, B). Weak laminin immunostaining was demonstrated in the basement membranes of the peritubular myoid cells. The basement membranes of vascular smooth muscle cells displayed moderate immunostaining, while the endothelial cells of these blood vessels were laminin immunonegative (Figure 3.19 B). Strong laminin immunostaining was demonstrated

in the endothelial cells lining intertubular lymphatic vessels (Figure 3.19 B). Fibroblasts and Leydig cells were laminin immunonegative.

Pubertal birds

The basement membranes of the seminiferous tubules, peritubular myoid cells, as well as vascular smooth muscle and endothelial cells exhibited weak to moderate laminin immunostaining (Figures 3.19 C, D). Laminin immunostaining was absent in fibroblasts and Leydig cells.

Adult birds

Moderate to strong laminin immunostaining was observed in the basement membranes of the seminiferous tubules and peritubular myoid cells (Figures 3.19 E, F). Laminin immunostaining in the basement membranes of vascular smooth muscle cells was weak to moderate, while immunostaining in the associated basement membranes of endothelial cells was weak (Figures 3.19 E, F). Leydig cells and fibroblasts were laminin immunonegative.

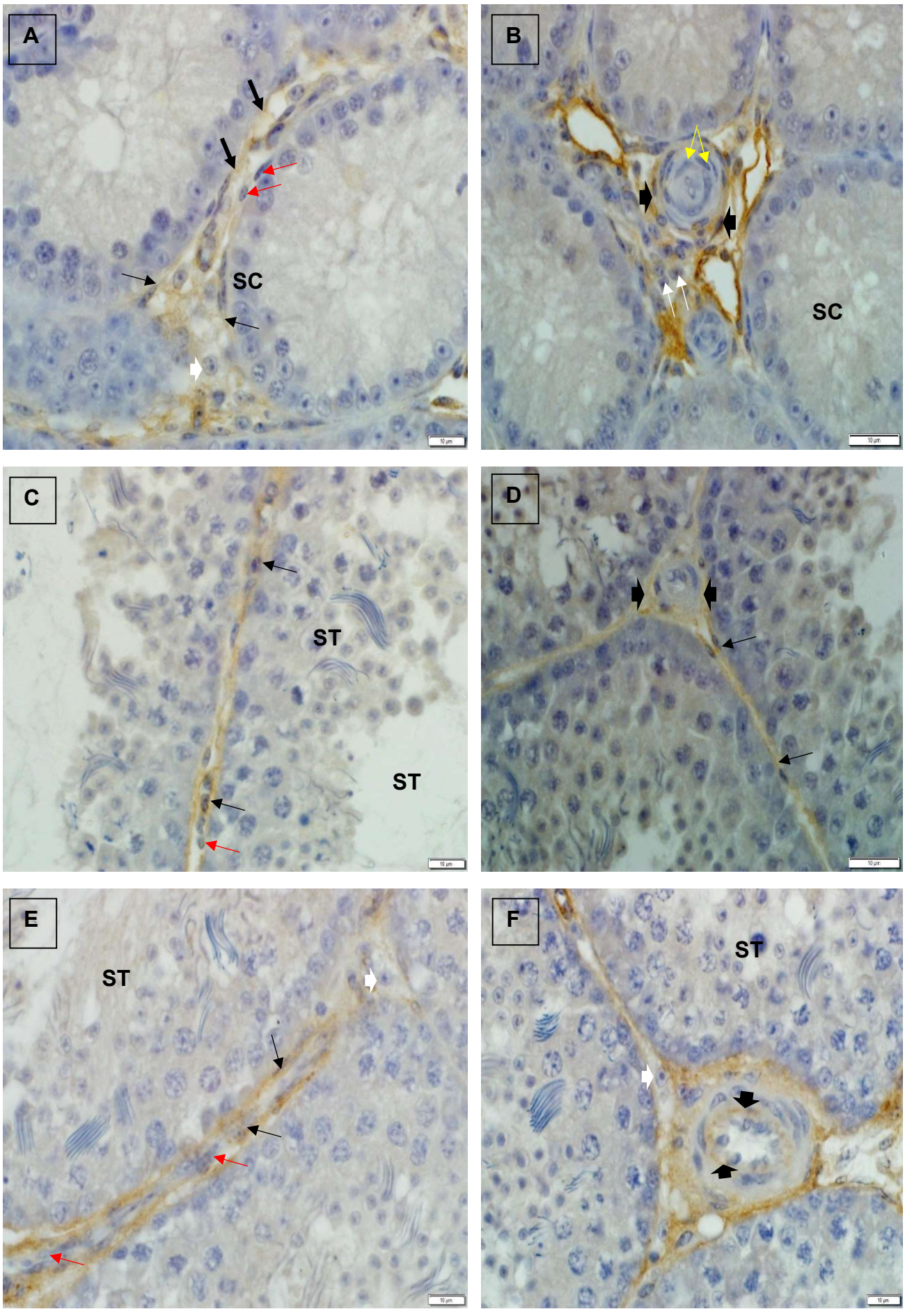
A
SC
B
SC
C
ST
ST
D
E
ST
F
ST

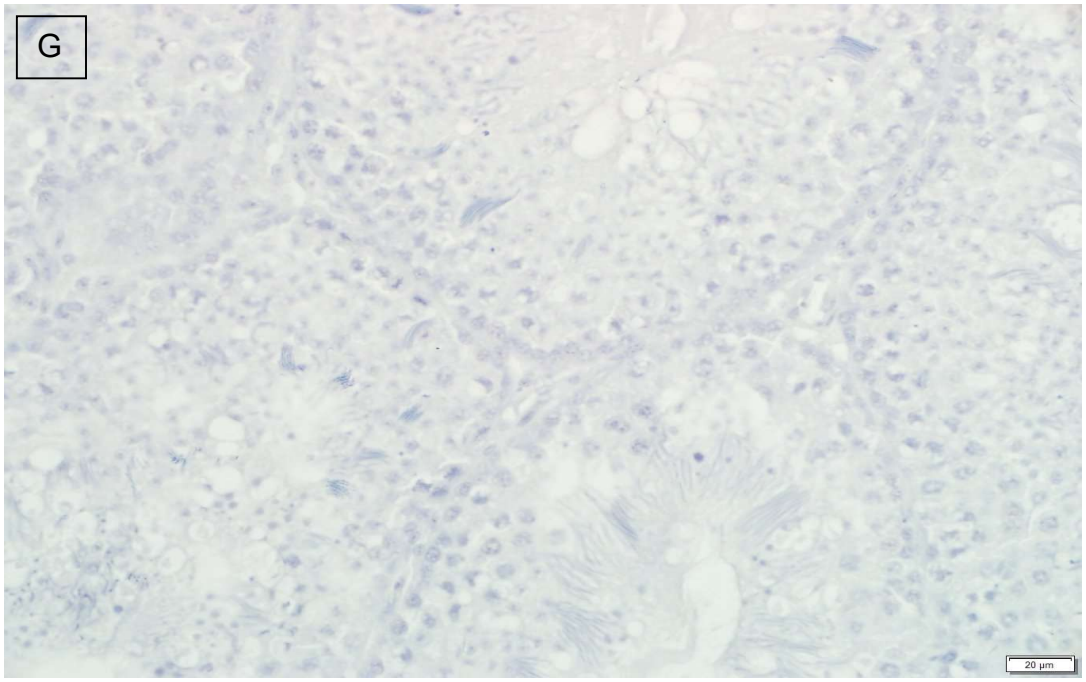

Figure 3. 19: Light photomicrographs showing laminin immunostaining in the peritubular boundary tissue of pre-pubertal (A, B), pubertal (C, D) and adult (E, F) birds.

A, B. Testicular parenchyma of pre-pubertal quails. Weak laminin immunostaining is exhibited by basement membranes of the seminiferous tubules (thick black arrows) and peritubular myoid cells (thin black arrows). Black arrowheads: moderate laminin immunostaining in the basement membranes of vascular smooth muscle cells. Yellow arrows: laminin immunonegative endothelial cells. Red arrows: laminin immunonegative fibroblasts. White arrowhead: laminin immunonegative Leydig cells. SC: seminiferous cords. Scale bars = 10μm.

C, D. Testicular parenchyma of pubertal quails. Weak to moderate laminin immunostaining is demonstrated in the basement membranes of peritubular myoid cells (black arrows) and vascular smooth muscle cells (arrowheads). Red arrow: Laminin immunonegative fibroblast. ST: seminiferous tubules. Scale bars = 10μm.

E, F. Testicular parenchyma of adult quails. Moderate to strong laminin immunostaining is exhibited in the basement membranes of peritubular myoid cells (black arrows). Vascular endothelial cells (arrowheads) display weak laminin immunoreactivity. Laminin immunonegative Leydig cells (white arrowheads) and fibroblasts (red arrows) are present. ST: seminiferous tubules. Scale bars = 10μm.

G. Negative control section. Scale bar = 20μm.

Table 3. 3**:** Summary of intensities of extracellular matrix proteins (collagen type IV, fibronectin and laminin) in the basement membranes of components of the testicular parenchyma in pre-pubertal, pubertal, and adult Japanese quails (*Coturnix coturnix japonica*).

		Basement membranes			
Age group	Matrix proteins	Seminiferous tubules	Peritubular myoid cells	Vascular smooth muscle cells	Vascular endothelial cells
Pre-pubertal	Collagen type IV	++	+	+/++	-
	Fibronectin	_	++/+++	++/+++	++/+++
	Laminin	-/+	+	++	-
Pubertal	Collagen type IV	++	+	+/++	-
	Fibronectin	-	++/+++	++/+++	++/+++
	Laminin	+/++	+/++	+/++	+
Adult	Collagen type IV	+++	++	+/++	+
	Fibronectin	-	+++	+++	+++
	Laminin	++/+++	++/+++	++/++	+

Intensities of immunostaining: - absent, + weak, ++ moderate, +++ strong. Blood vessel ([a] endothelium, [b] *tunica media*).

3.3.4. Transmission electron microscopy

The seminiferous cords in pre-pubertal birds were surrounded by inner fibrous and outer cellular lamellae (Figure 3.20). The inner fibrous lamella comprised of the homogenously electron dense *basal laminae* of the seminiferous cords, as well as adjacently-positioned collagen fibres (Figure 3.21). The cellular lamella was formed by peritubular myoid cells (Figures 3.20, 3.21 & 3.22) and fibroblasts (Figure 3.20), the former of which encircled the seminiferous cords. Peritubular myoid cells exhibited elongated, euchromatic nuclei (Figures 3.20 & 3.21). The cytoplasmic organelles contained within these cells included: mitochondria, Golgi complexes and dilated RER (Figure 3.21 & 3.22). The inner surfaces of the plasma membranes of peritubular myoid cells displayed dense plaques (Figure 3.23) and coated pits (Figure 3.24). In addition, gap junctions were observed between the plasma membranes of adjacent peritubular myoid cells (Figure 3.25).

Fibroblasts were the second cell type forming the cellular lamella (Figure 3.20). The fibroblasts contained oval- to spindle-shaped euchromatic nuclei, with single, eccentrically-located nucleoli (Figure 3.20). Scant cytoplasm with round mitochondria and dilated RER profiles surrounded the nuclei.

Intertubular blood vessels were observed in the interstitial tissue between seminiferous cords (Figures 3.26). The walls of the intertubular blood vessels were formed by one or two endothelial cells and a single layer of smooth muscle cells.

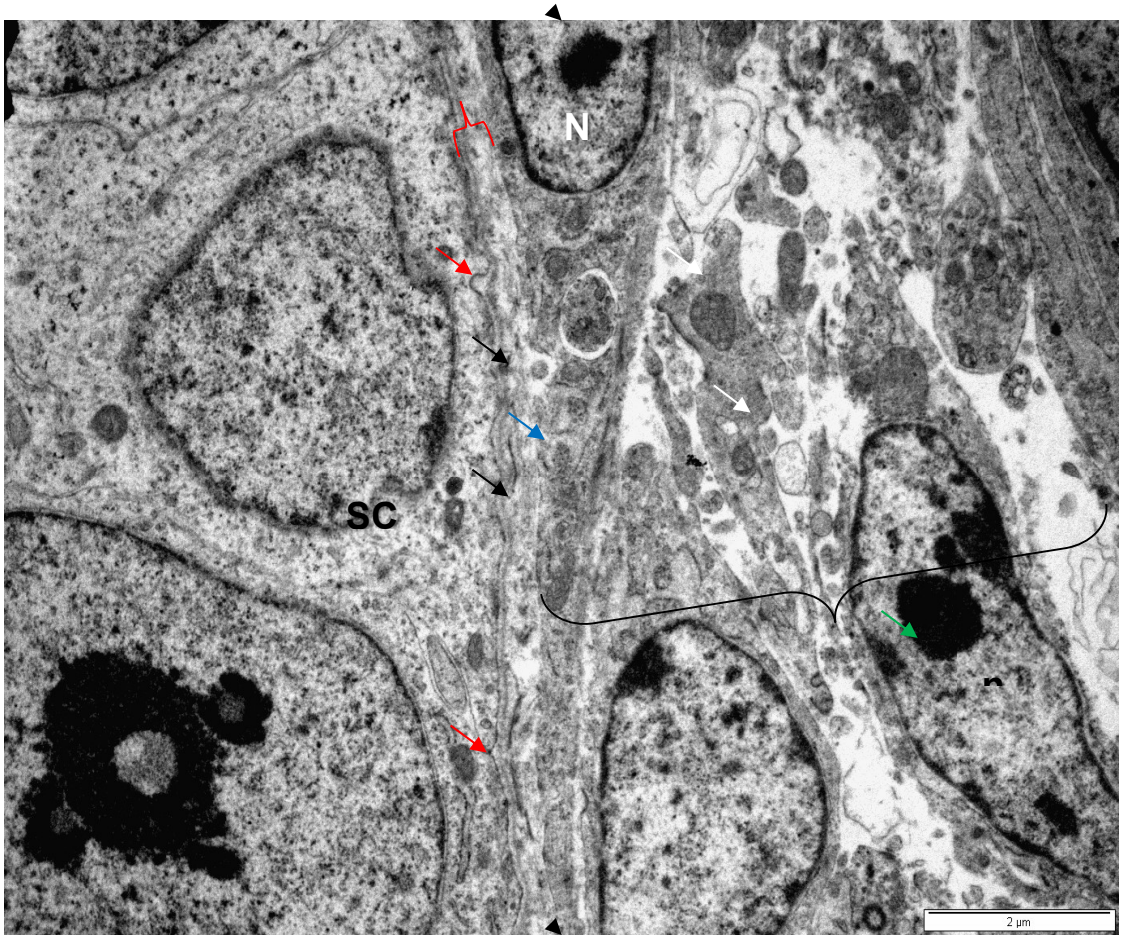

Figure 3. 20: Transmission electron photomicrograph of the peritubular boundary tissue of a pre-pubertal bird. Red bracket: inner fibrous lamella. Black bracket: outer cellular lamella. Red arrows: invaginations of the basal plasma membrane of a seminiferous cord (SC). Black arrows: *basal lamina* of the seminiferous cord. Blue arrow: cytoplasmic process of a peritubular myoid cell. N: nucleus of a peritubular myoid cell. n: nucleus of a fibroblast with a prominent nucleolus (green arrow).

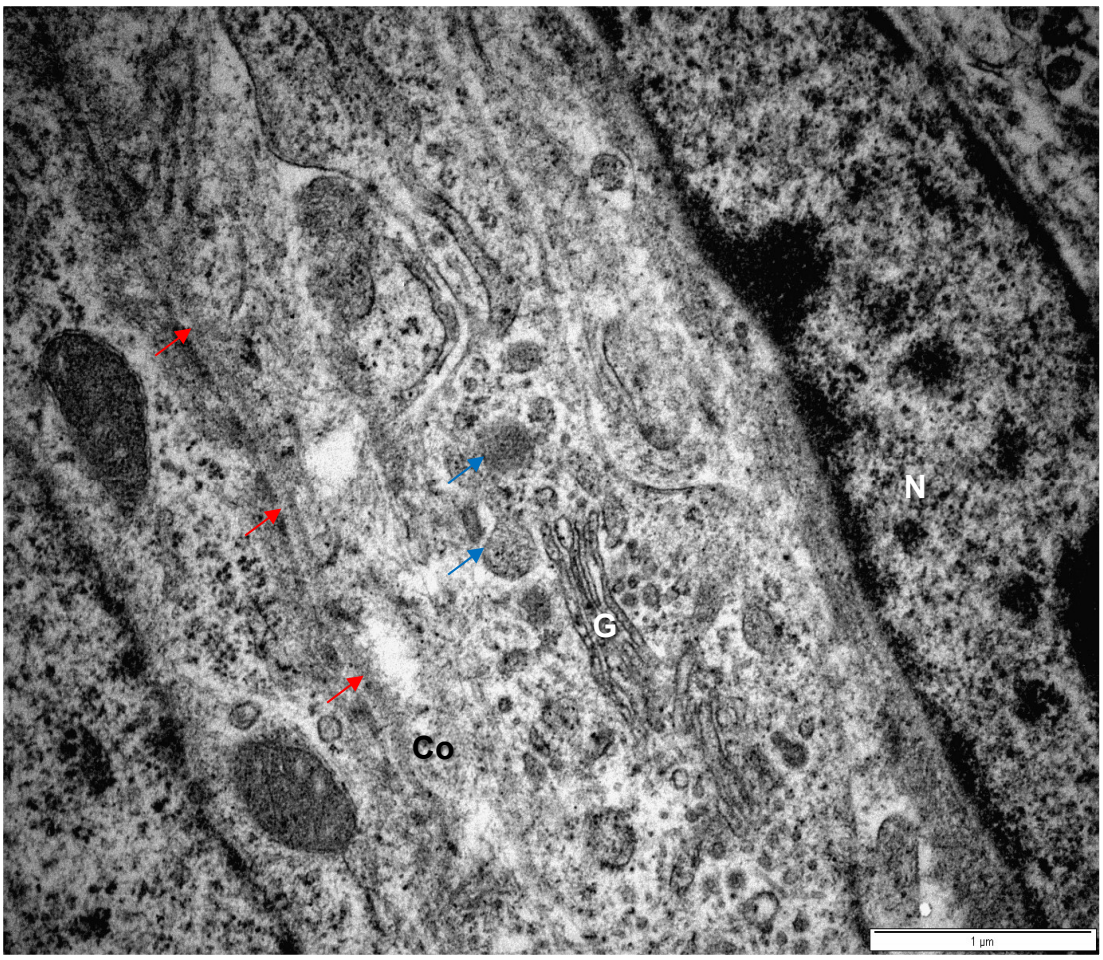

Figure 3. 21: Transmission electron photomicrograph of the peritubular boundary tissue of a pre-pubertal bird. Red arrows: *basal lamina* of a seminiferous cord. Co: collagen fibres. Mitochondria (blue arrows) and a prominent Golgi complex (G) are observed in a peritubular myoid cell. N: nucleus of a peritubular myoid cell.

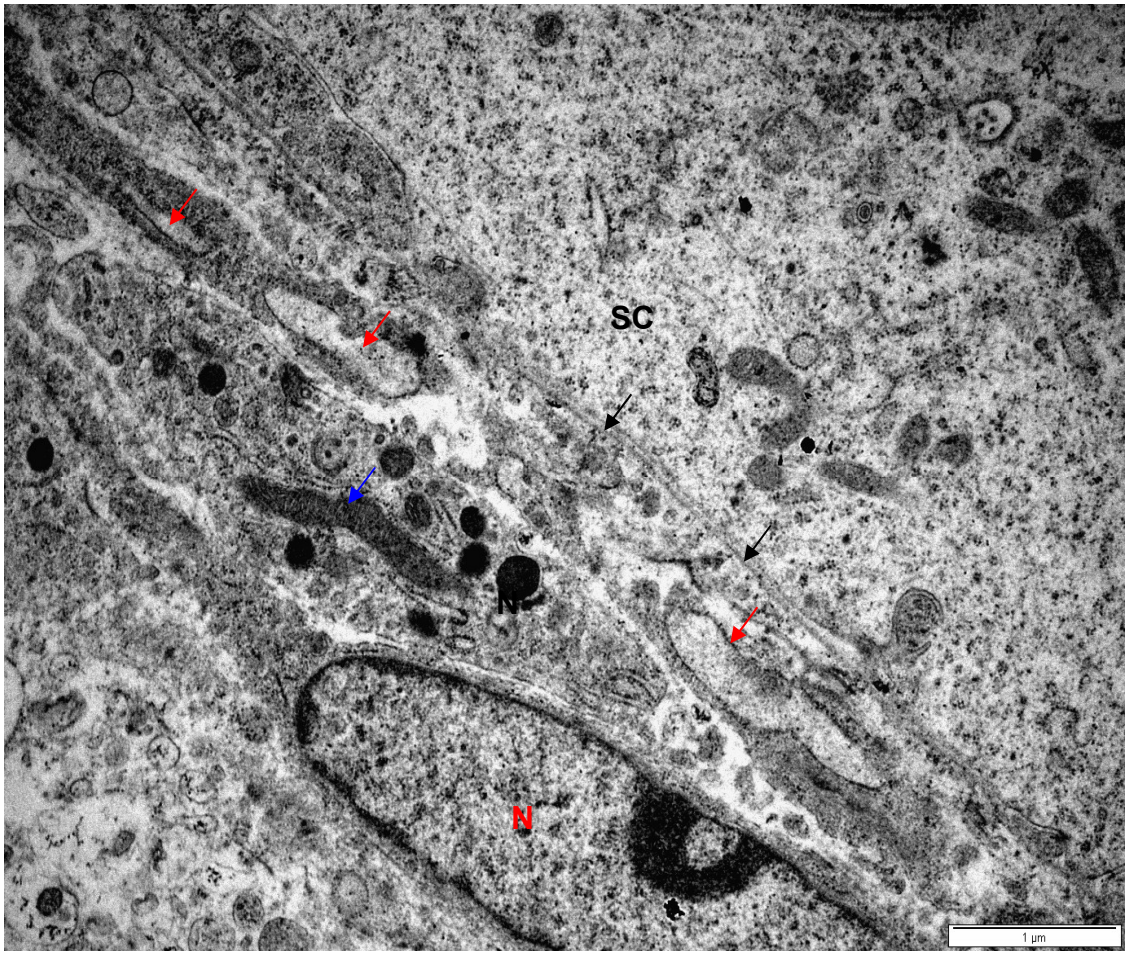

Figure 3. 22: Transmission electron photomicrograph of the peritubular boundary tissue of a pre-pubertal bird. Black arrows: *basal lamina* of a seminiferous cord (SC). A mitochondrion (blue arrow) and dilated RER cisternae (red arrows) are observed in peritubular myoid cells. N: elongated euchromatic nucleus of a peritubular myoid cell.

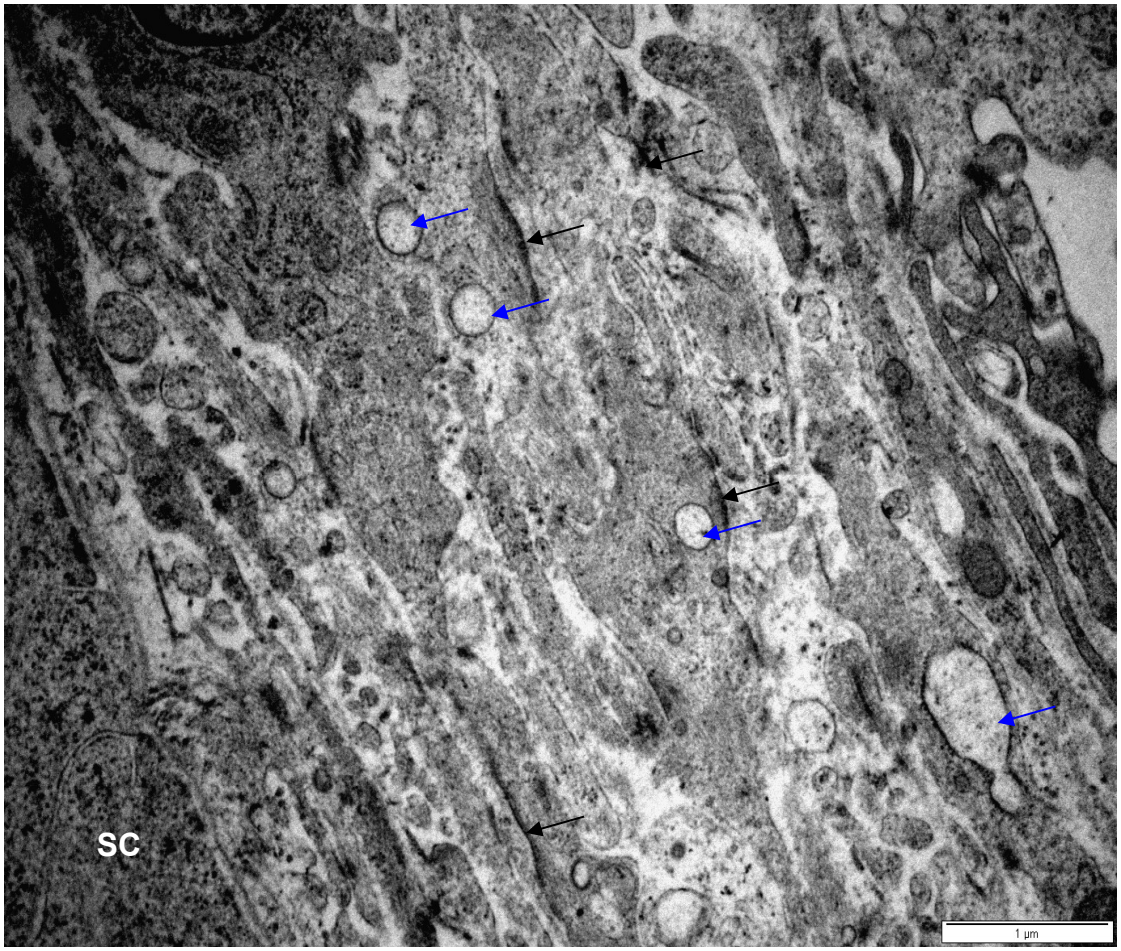

Figure 3. 23: Transmission electron photomicrograph of the peritubular boundary tissue of a pre-pubertal bird. Black arrows: dense plaques of peritubular myoid cells. Blue arrows: dilated profiles of rough endoplasmic reticulum. SC: seminiferous cord.

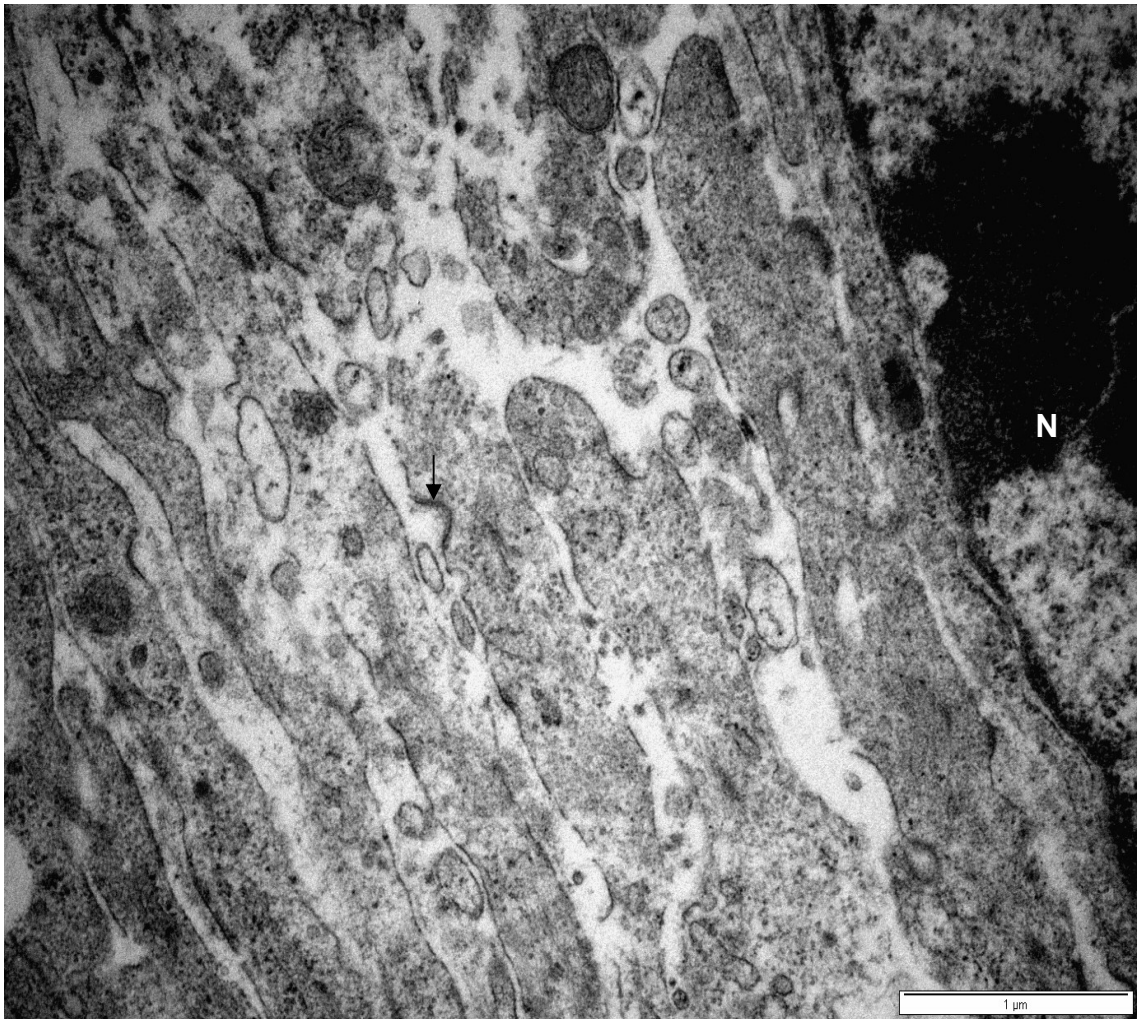

Figure 3. 24: Transmission electron photomicrograph of the peritubular boundary tissue of a pre-pubertal bird. Black arrow: coated pit on the plasma membrane of a peritubular myoid cell. N: nucleus of a peritubular myoid cell.

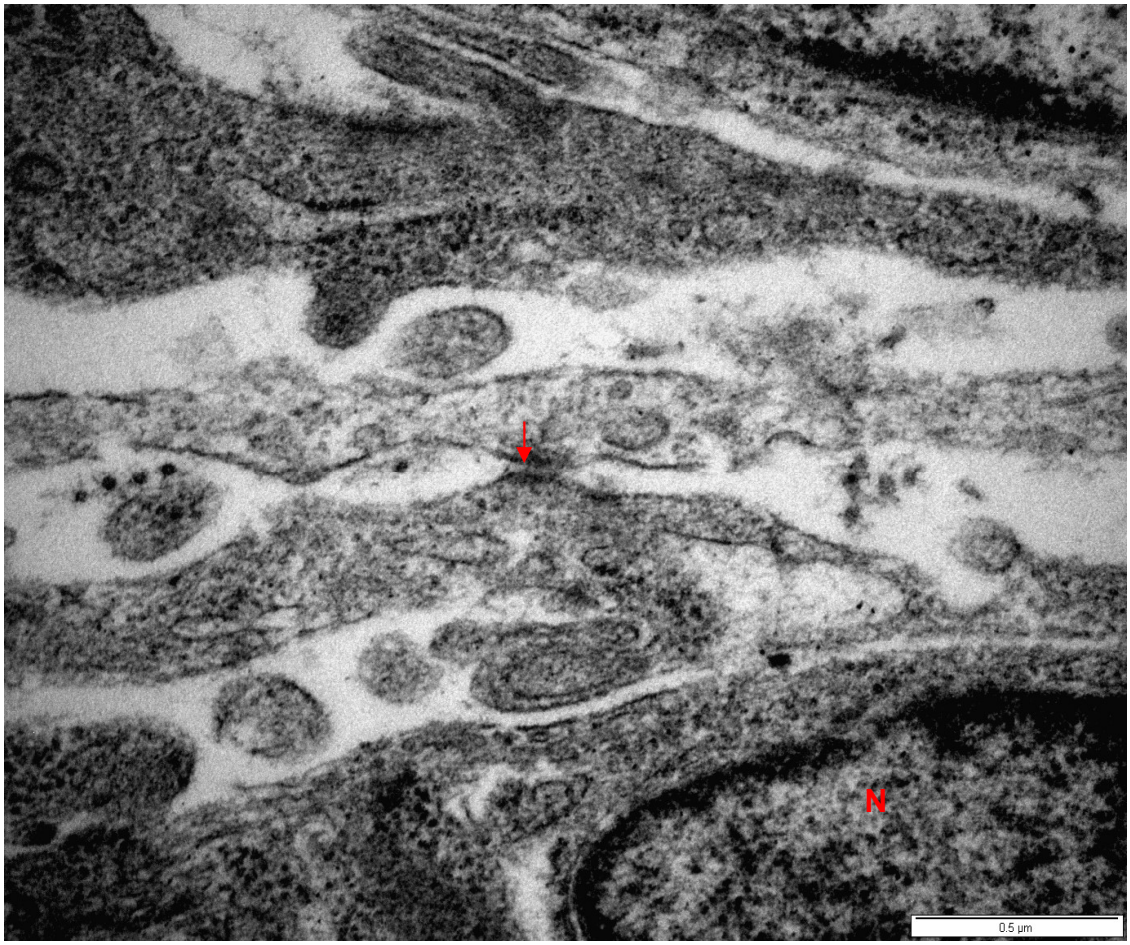

Figure 3. 25: Transmission electron photomicrograph of the peritubular boundary tissue of a pre-pubertal bird. Red arrow: gap junction between plasma membranes of adjacent peritubular myoid cells. N: nucleus of a peritubular myoid cell.

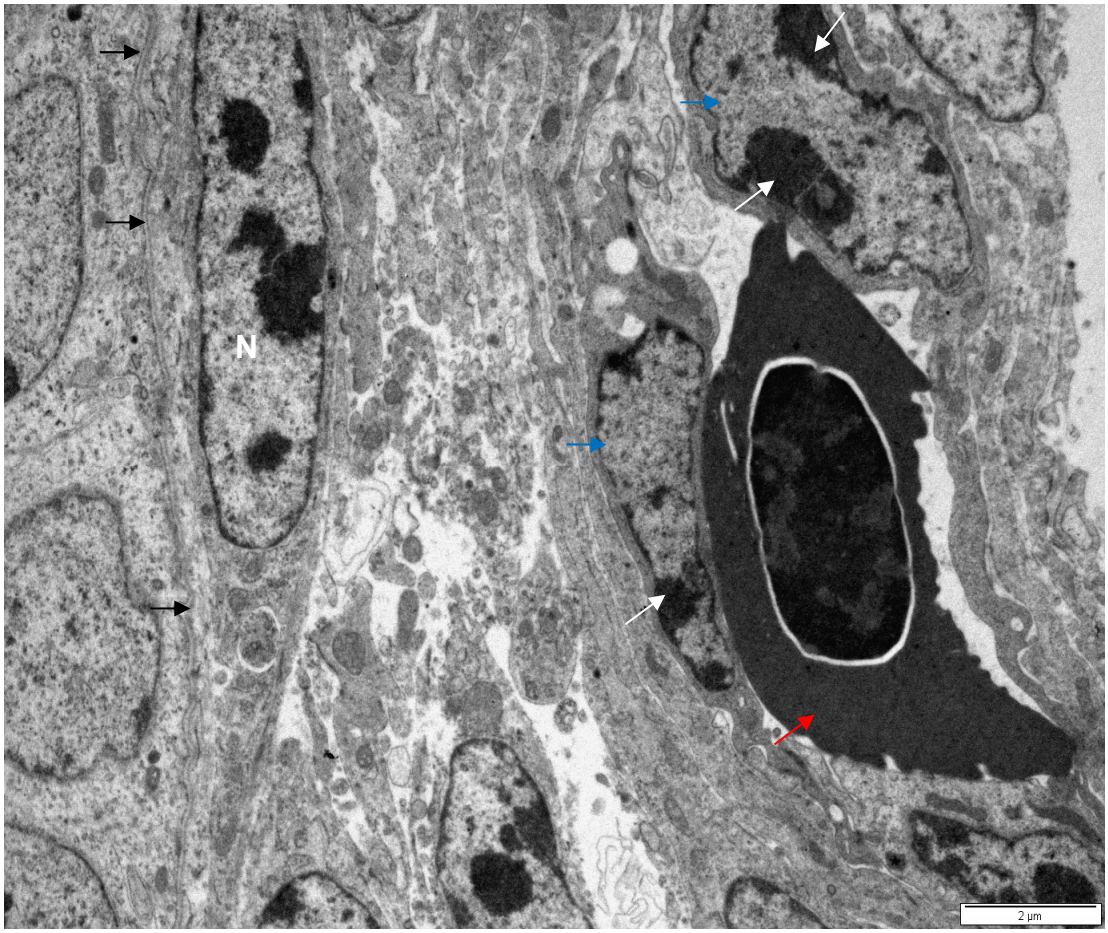

Figure 3. 26: Transmission electron photomicrograph of the interstitial tissue of a pre-pubertal bird. Black arrows: *basal lamina* of a seminiferous cord. N: nucleus of a peritubular myoid cell. Blue arrows: endothelial cells of an intertubular blood vessel. White arrows: clumps of chromatin in the nuclei of the endothelial cells. Red arrow: a nucleated red blood cell.

Pubertal birds

Peritubular boundary tissue, composed of inner fibrous and outer cellular lamellae, surrounded the seminiferous tubules in pubertal birds (Figures 3.27 & 3.28). The inner fibrous lamella was formed by the *basal laminae* of the seminiferous tubules

and underlying collagen fibres (Figure 3.27). The *basal laminae* of the seminiferous tubules were composed of a homogenous electron dense material (Figure 3.27).

The outer cellular lamella was formed by peritubular myoid cells and fibroblasts (Figures 3.27 & 3.28). Peritubular myoid cells exhibited elongated, euchromatic nuclei. Contained within the cytoplasm of these cells were dilated profiles of rough endoplasmic reticulum (Figure 3.28), mitochondria and myofilaments (Figure 3.29). The plasma membranes of the peritubular myoid cells exhibited dense plaques (Figure 3.28), as well as coated pits (Figure 3.29). In addition, gap junctions linked the plasma membranes of adjacent peritubular myoid cells (Figure 3.27).

Fibroblasts were situated adjacent to the peritubular myoid cells (Figure 3.28). The fibroblasts were typically spindle-shaped cells with euchromatic nuclei containing peripheral clumps of chromatin.

In addition to fibroblasts, Leydig cells (Figure 3.30) were observed between the seminiferous tubules. The Leydig cells exhibited oblong-shaped euchromatic nuclei with prominent nucleoli (Figure 3.30). The Leydig cells were characterized by the presence of round mitochondria and numerous lipid droplets (Figure 3.30).

Intertubular blood vessels were observed in the peritubular boundary tissue between the seminiferous tubules (Figures 3.31 & 3.32). Contained within the endothelial cells lining the blood vessels were euchromatic nuclei (Figures 3.31) and numerous mitochondria (Figure 3.32).

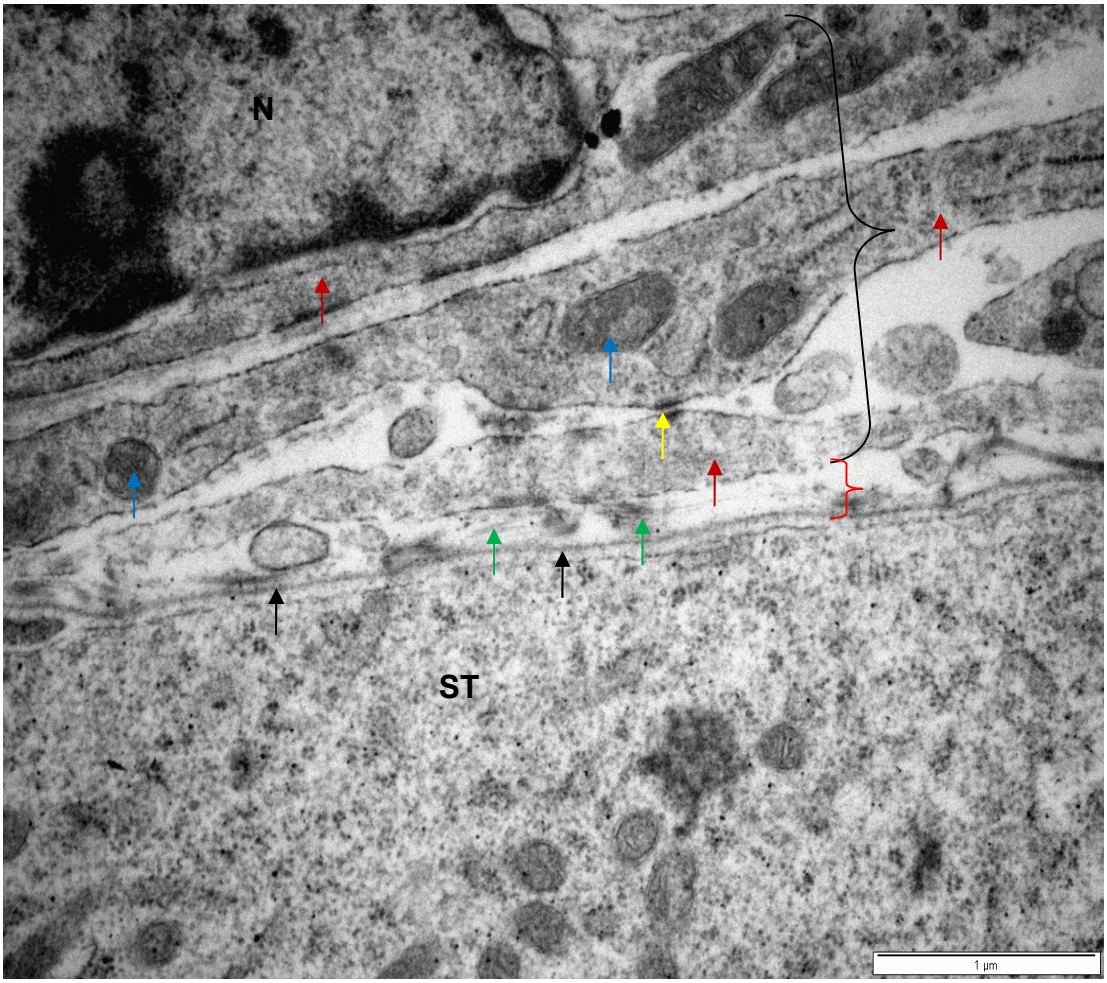

Figure 3. 27: Transmission electron photomicrograph of the peritubular boundary tissue of a pubertal bird. Red bracket: fibrous lamella. Black bracket: cellular lamella. Black arrows: *basal lamina* of a seminiferous tubule (ST). Green arrows: collagen fibres. Red arrows: peritubular myoid cells. Blue arrows: mitochondria in a peritubular myoid cell. Yellow Arrow: gap junction between adjacent peritubular myoid cells. N: nucleus of a peritubular myoid cell.

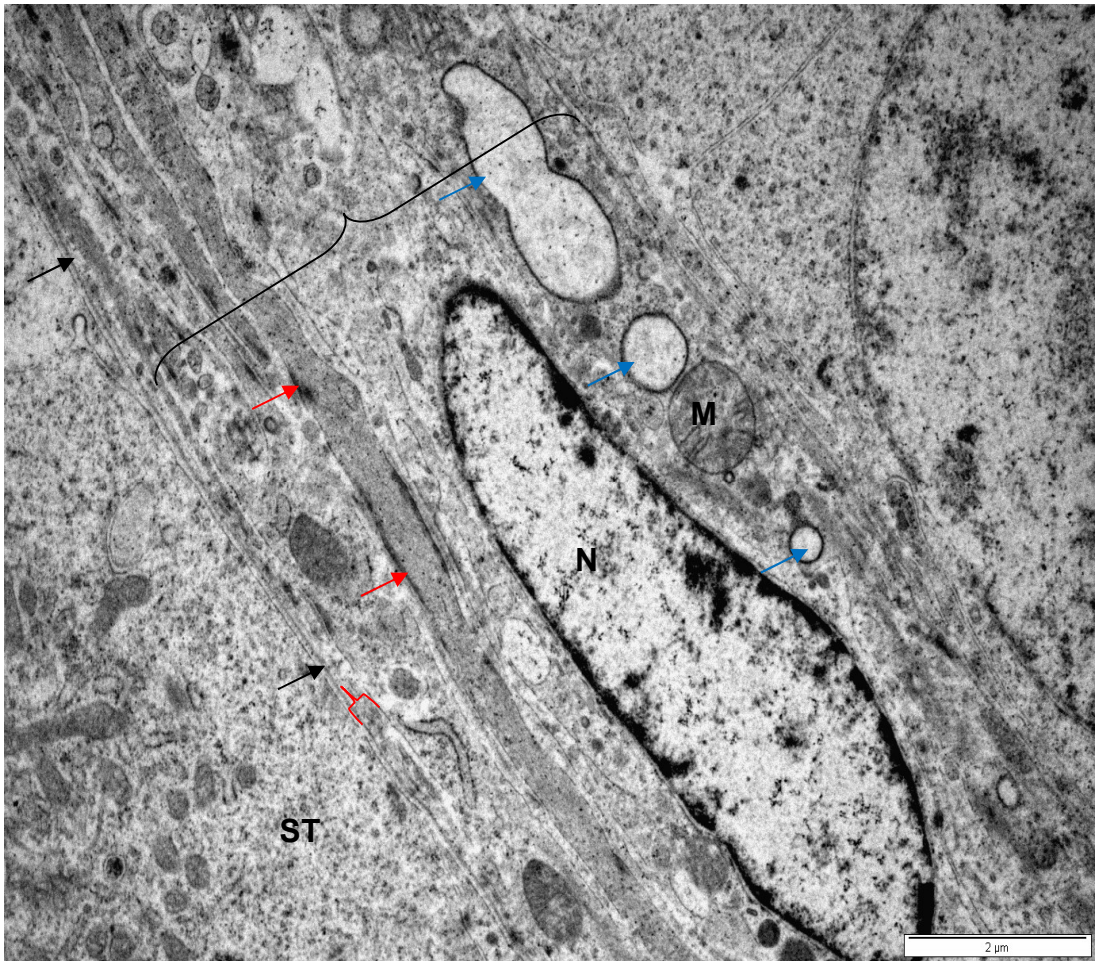

Figure 3. 28: Transmission electron photomicrograph of the peritubular boundary tissue of a pubertal bird. Red bracket: fibrous lamella. Black bracket: cellular lamella. Black arrows: *basal lamina* of a seminiferous tubule (ST). Red arrows: dense plaques on the plasma membranes of peritubular myoid cells. Blue arrows: dilated RER cisternae in a peritubular myoid cell. N: elongated nucleus of a fibroblast. M: mitochondrion.

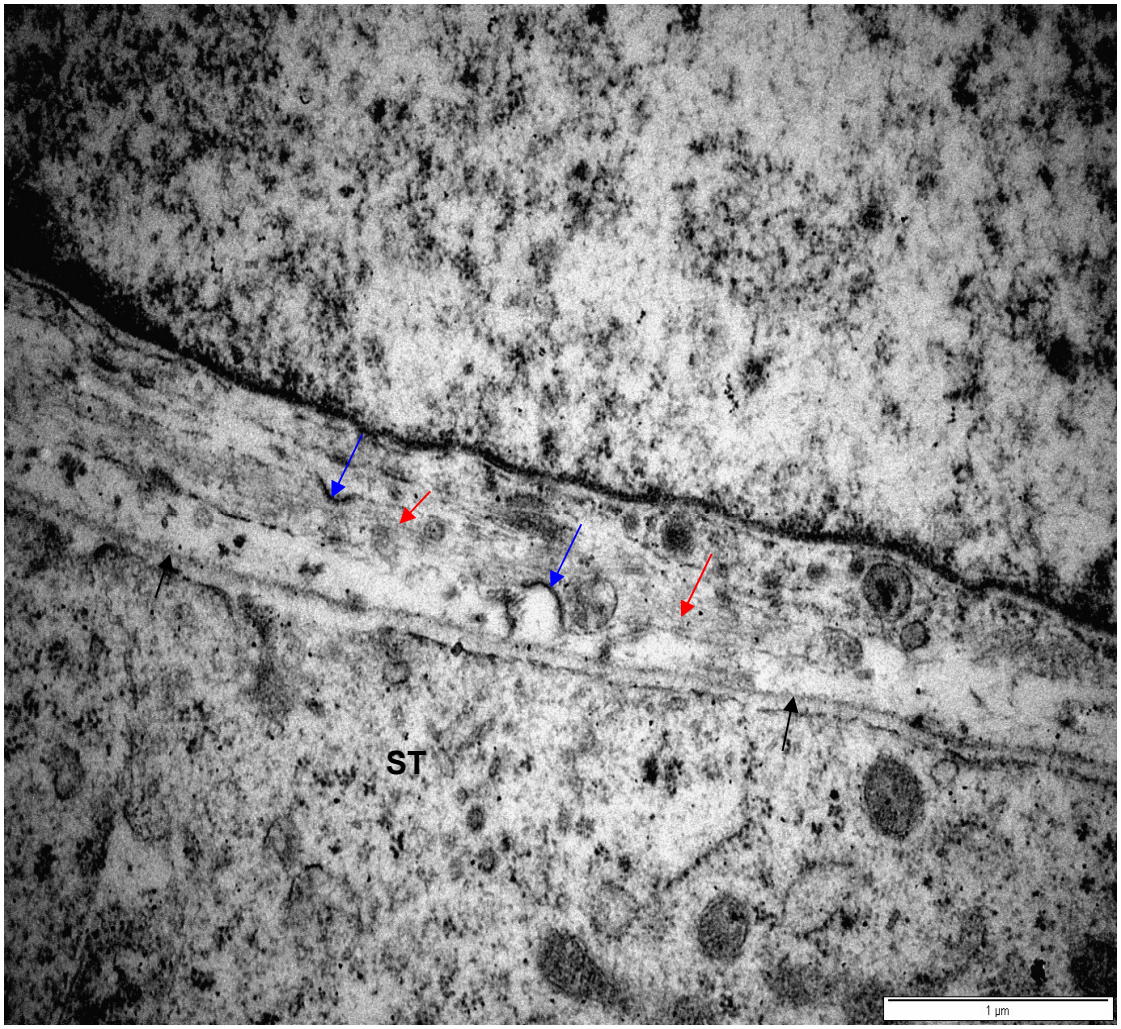

Figure 3. 29: Transmission electron photomicrograph of the peritubular boundary tissue of a pubertal bird. Red arrows: myofilaments in a peritubular myoid cell. Black arrows: *basal lamina* of a seminiferous tubule (ST). Blue arrows: coated pits.

Figure 3. 30: Transmission electron photomicrograph of the peritubular boundary tissue of a pubertal bird. N: oblong-shaped nucleus of a Leydig cell. n: nucleolus. Red arrows: mitochondria. Black arrows: Lipid droplets.

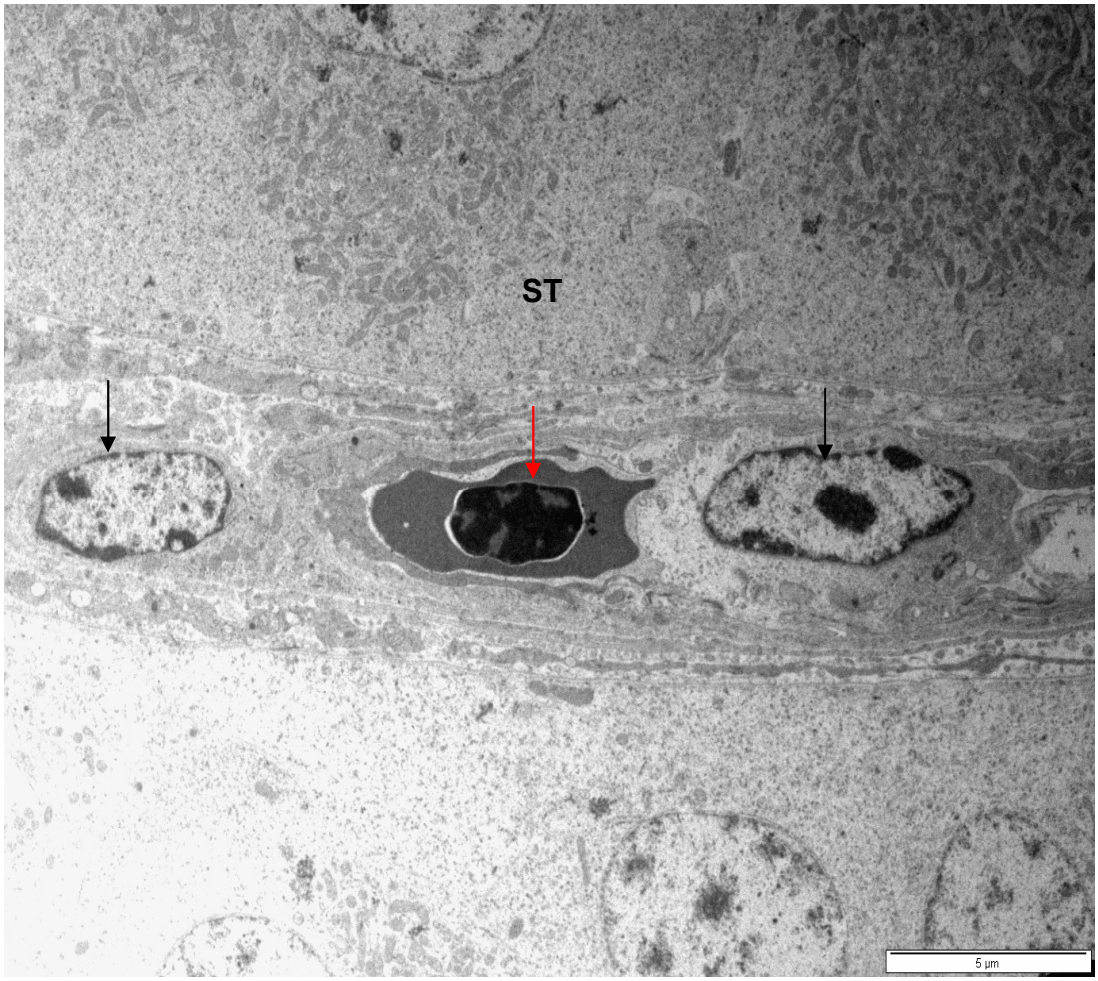

Figure 3. 31: Transmission electron photomicrograph of an intertubular blood vessel in the interstitial tissue of a pubertal bird. Black arrows: endothelial cells. Red arrow: a nucleated red blood cell. ST: seminiferous tubule.

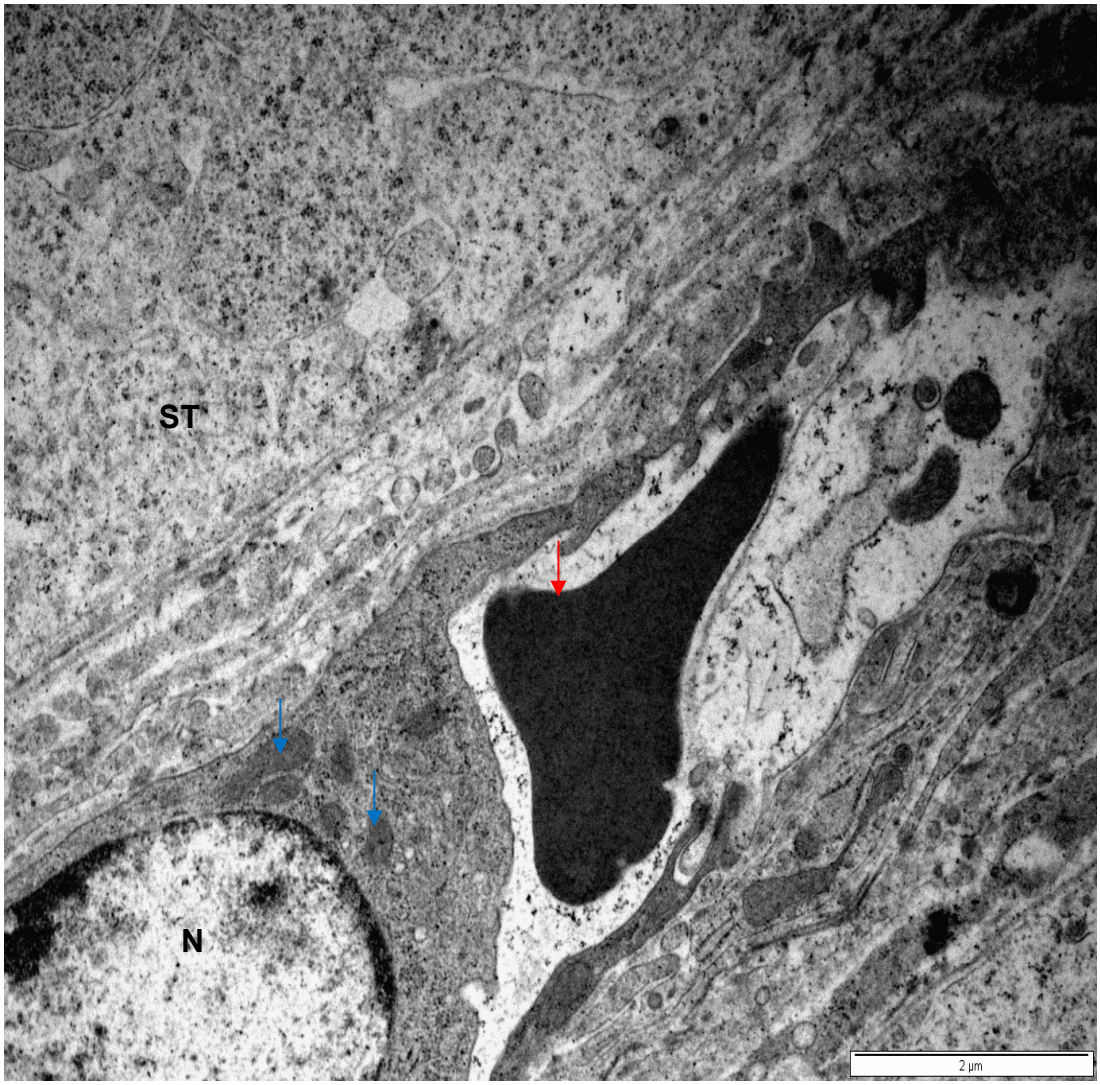

Figure 3. 32: Transmission electron photomicrograph of an intertubular blood vessel in the interstitial tissue of a pubertal bird. Blue arrows: mitochondria in an endothelial cell. N: nucleus of an endothelial cell. Red arrow: red blood cell.

Adult birds

Seminiferous tubules in adult birds were surrounded by peritubular boundary tissue composed of fibrous and cellular lamellae (Figures 3.33). Homogenously electron dense *basal laminae* of the seminiferous tubules and peritubular myoid cells, as well as collagen fibres formed the fibrous lamella (Figures 3.34 & 3.35). The cellular lamella of the peritubular boundary tissue was formed by peritubular myoid cells

(Figure 3.36) and fibroblasts (Figure 3.37). The peritubular myoid cells formed overlapping layers, which were connected by gap junctions (Figure 3.36). Peritubular myoid cells contained elongated, euchromatic nuclei with finely distributed chromatin. The cytoplasmic organelles of peritubular myoid cells included: round and elongated mitochondria; Golgi complexes; dilated RER; vesicles and bundles of myofilaments (Figures 3.36 & 3.38). Associated with the plasma membranes of the peritubular myoid cells were electron dense plaques, coated pits (Figures 3.33 & 3.38), and pinocytotic vesicles in various stages of development (Figures 3.36, 3.38 & 3.39). A homogeneous *basal lamina* enclosed the peritubular myoid cells (Figure 3.34).

Fibroblasts displayed elongated or irregular-shaped, euchromatic nuclei (Figure 3.37). Prominent nucleoli were evident in some nuclei (Figure 3.37). Contained within the cytoplasm of the fibroblasts were a few dilated cisternae of RER and round mitochondria (Figure 3.37).

Peripheral to the peritubular myoid cells were the endothelial cells of intertubular blood vessels (Figure 3.37). Contained within a typical endothelial cell was an irregular-shaped euchromatic nucleus, a Golgi complex, mitochondria and a few cisternae of RER (Figure 3.40). The endothelial cells had attenuated cytoplasmic processes which were linked by tight junctions (Figure 3.40). *Basal laminae* coated the periphery of the endothelial cells (Figure 3.40). Closely associated with the intertubular blood vessels were Leydig cells which contained numerous cytoplasmic lipid droplets (Figure 3.41).

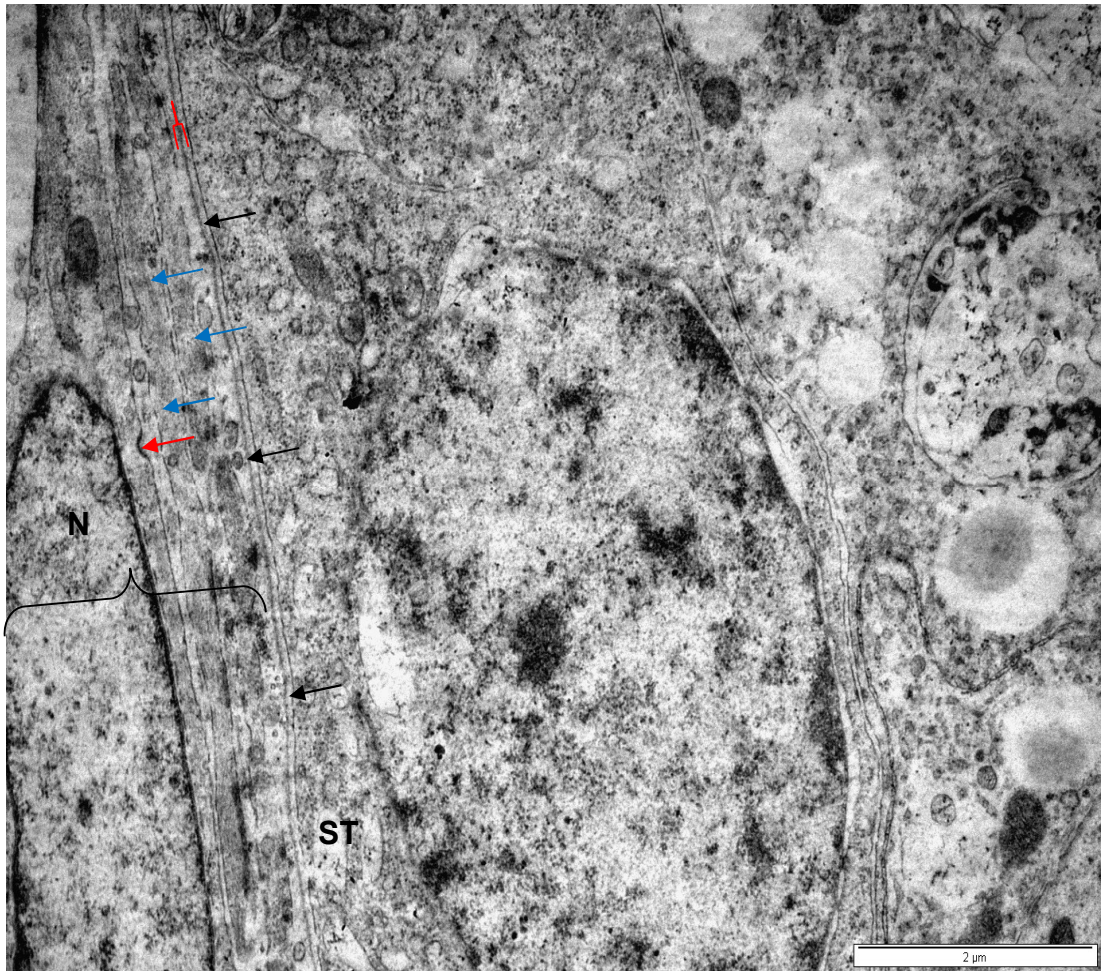

Figure 3. 33: Transmission electron photomicrograph of the peritubular boundary tissue of an adult bird. Red bracket: fibrous lamella. Black bracket: cellular lamella. Black arrows: *basal lamina* of a seminiferous tubule (ST). Blue arrows: peritubular myoid cells. N: nucleus of a peritubular myoid cell. Red arrow: coated pit.

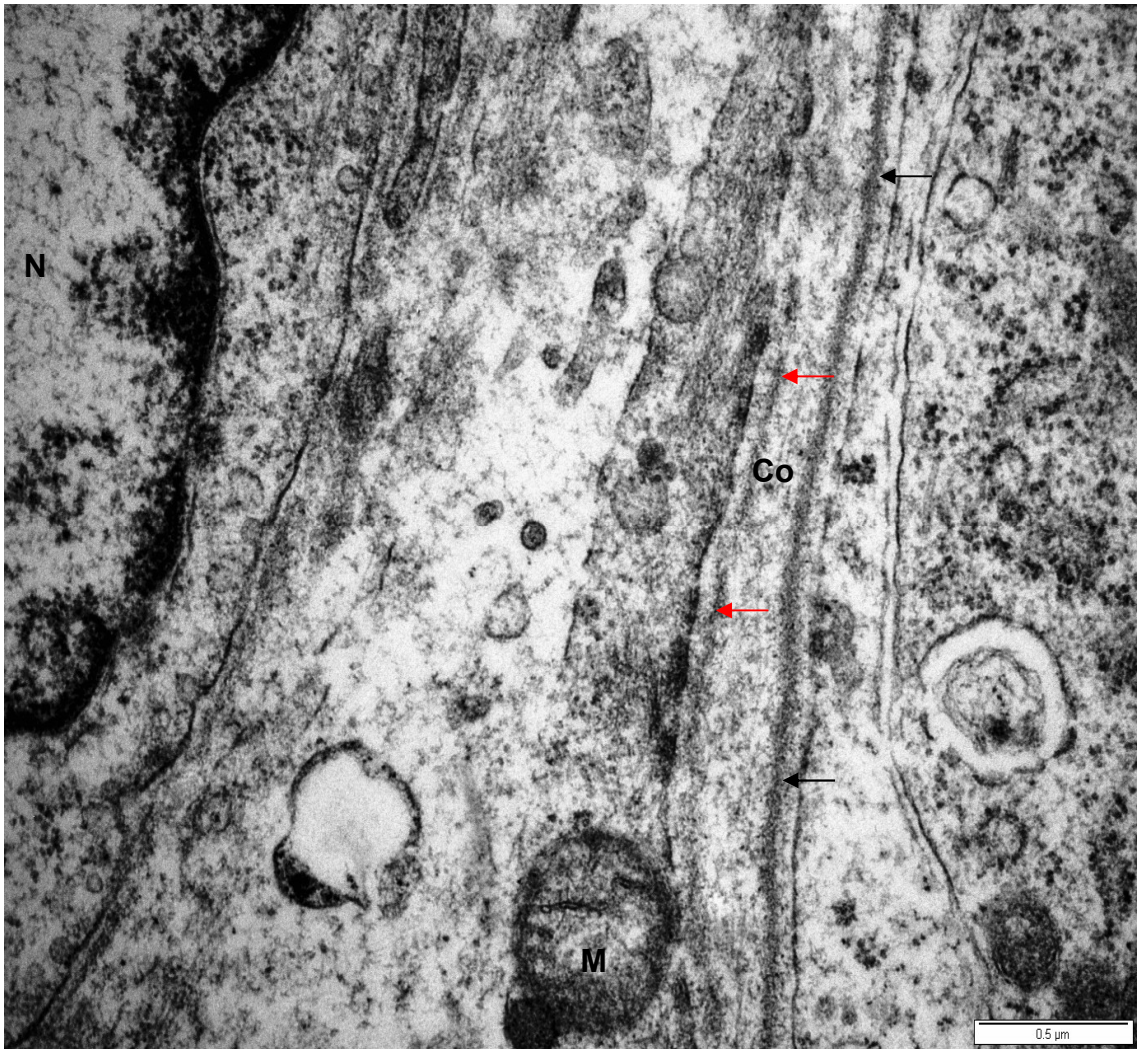

Figure 3. 34: Transmission electron photomicrograph of the peritubular boundary tissue of an adult bird. Black arrows: *basal lamina* of a seminiferous tubule. Co: collagen fibres. M: mitochondrion of a peritubular myoid cell. Red arrows: *basal lamina* of a peritubular myoid cell. N: nucleus of a fibroblast.

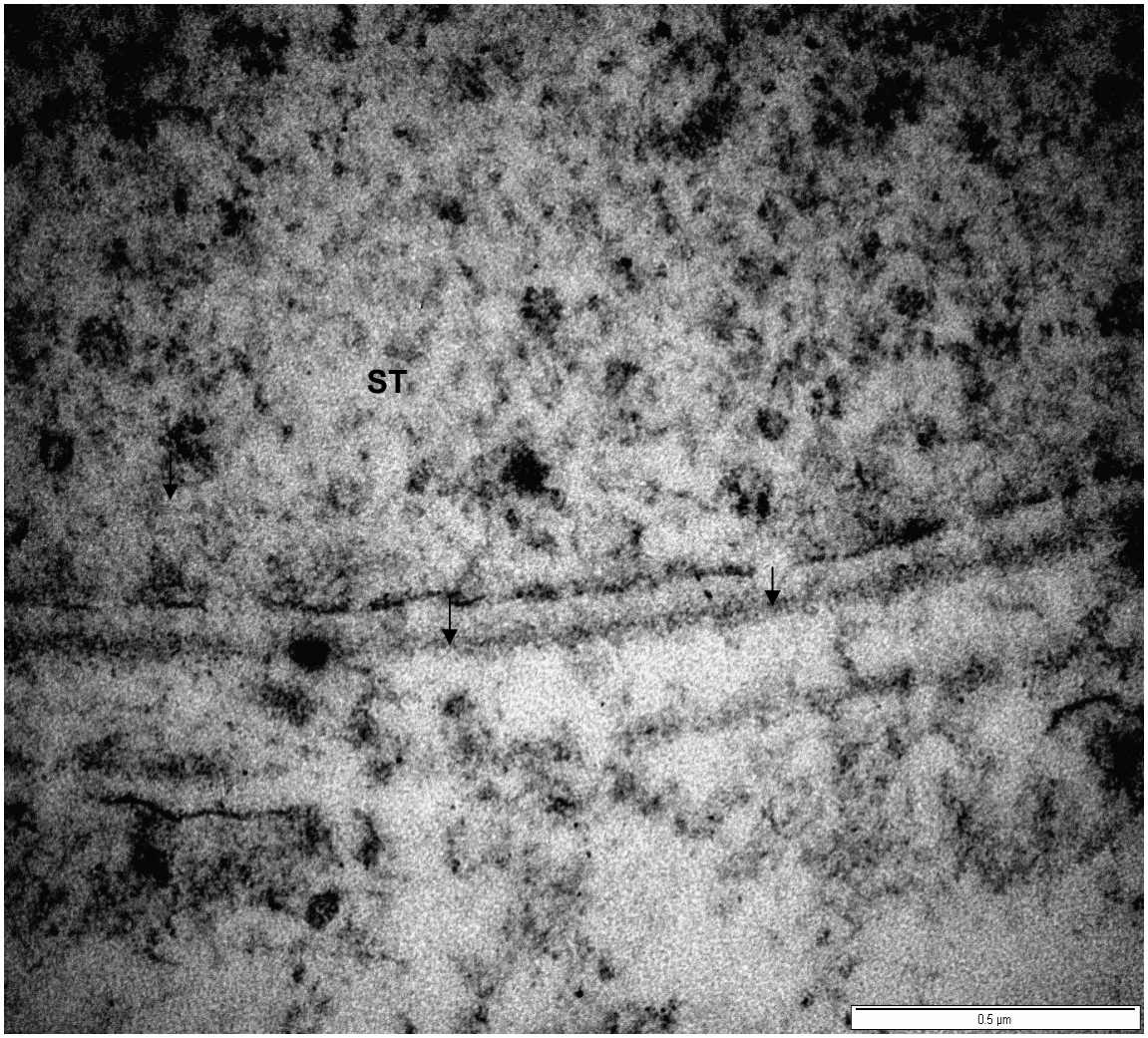

Figure 3. 35: Transmission electron photomicrograph of the peritubular boundary tissue in an adult bird. Black arrows: *basal lamina* of a seminiferous tubule (ST).

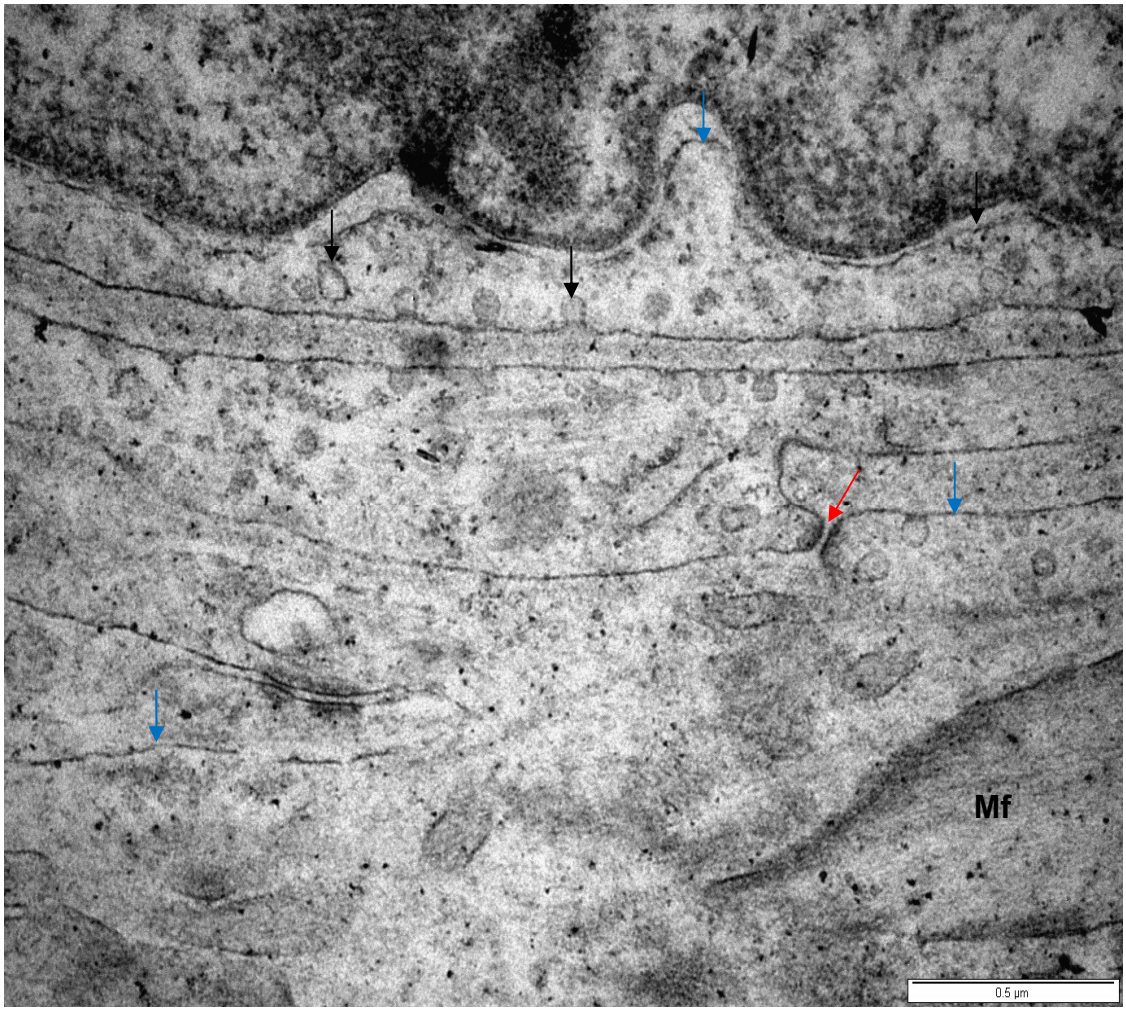

Figure 3. 36: Transmission electron photomicrograph of the peritubular boundary tissue in an adult bird. Blue arrows: attenuated cytoplasmic processes of peritubular myoid cells. Red arrow: gap junction. Black arrows: formed or forming pinocytotic vesicles. Mf: myofilaments.

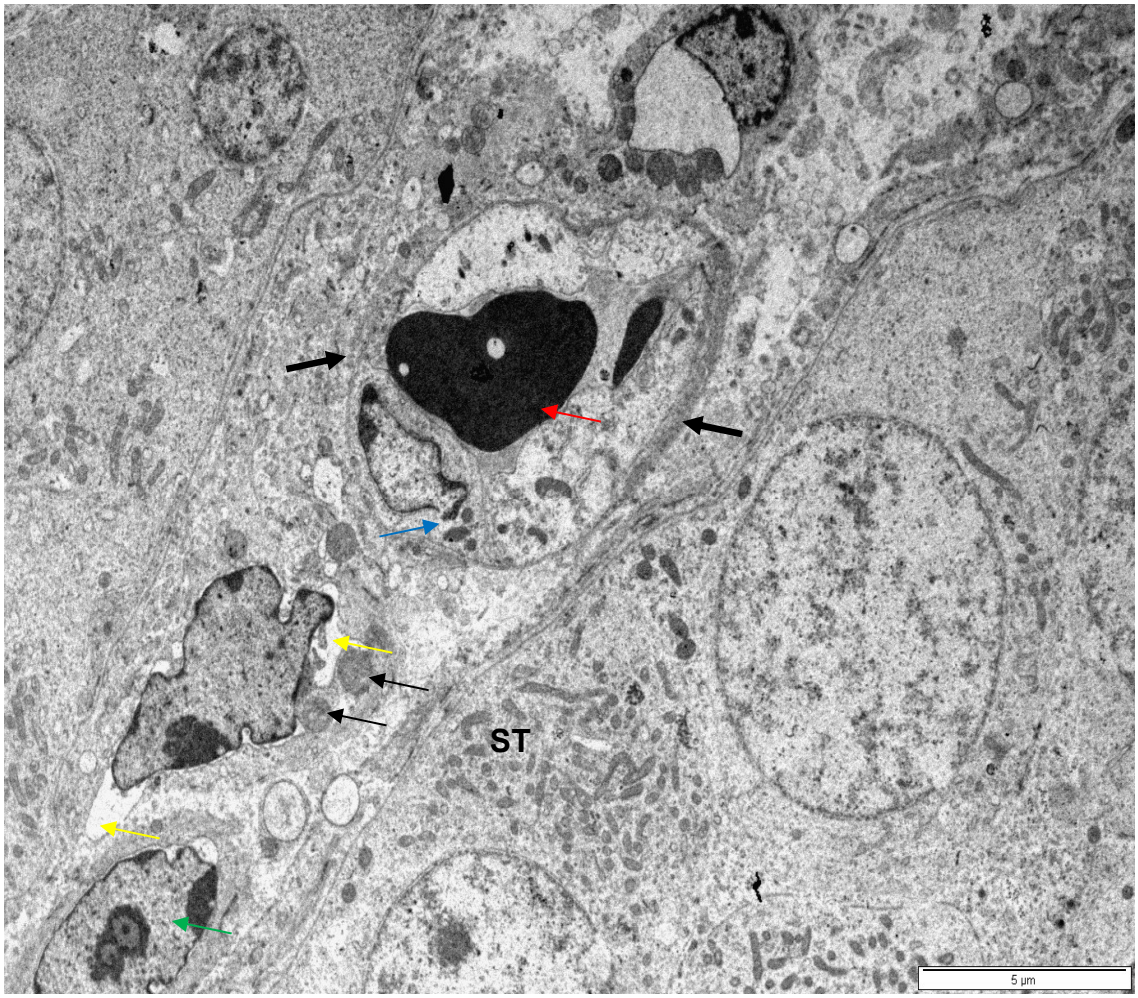

Figure 3. 37: Transmission electron photomicrograph of an intertubular blood vessel in an adult bird. Green arrow: nucleus of a fibroblast. Thick black arrows: *basal lamina* surrounding endothelial cells. Blue arrow: endothelial cell. Red arrow: red blood cell. Thin black arrows: mitochondria in a fibroblast. Yellow arrows: dilated profile of RER in a fibroblast.

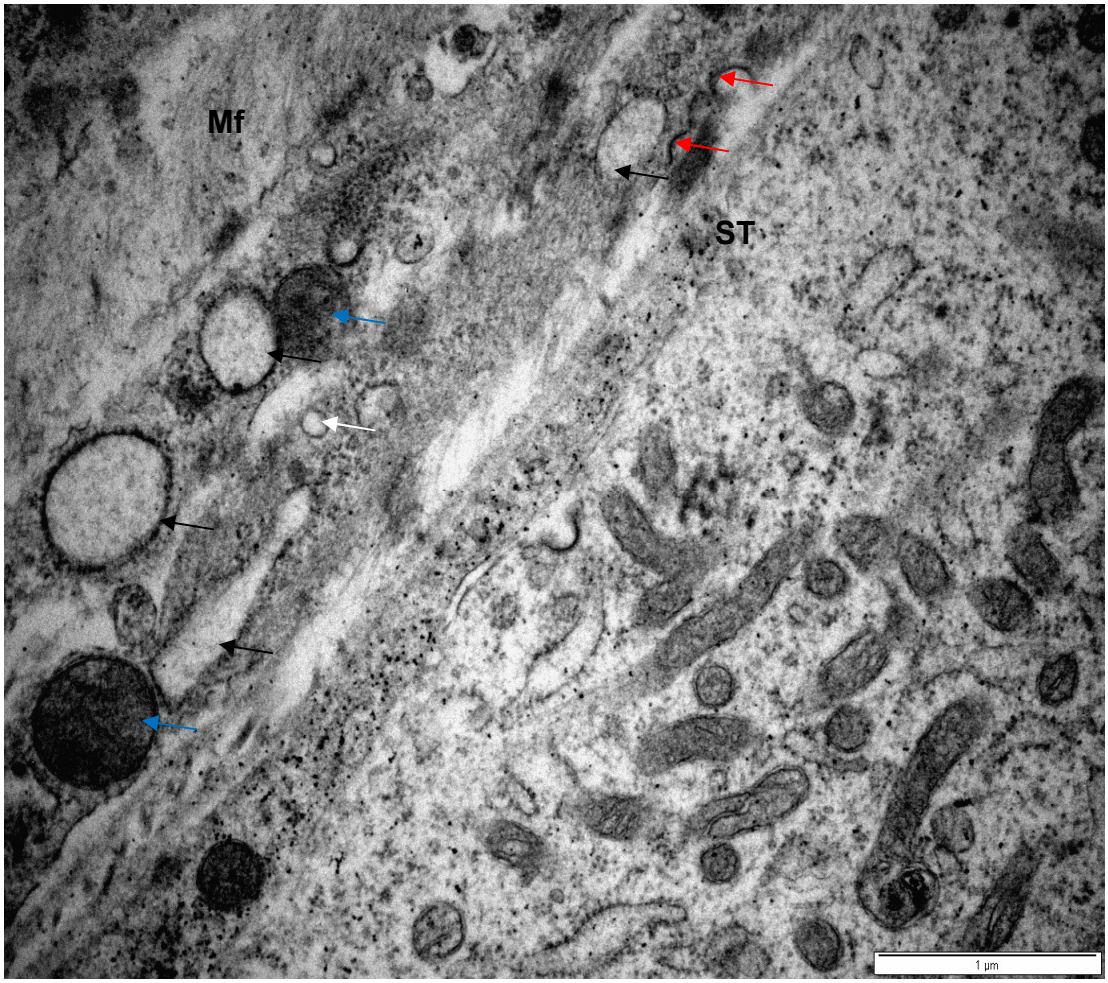

Figure 3. 38: Transmission electron photomicrograph of the peritubular boundary tissue in an adult bird. Mf: myofilaments in a peritubular myoid cell. Black arrows: dilated RER cisternae. White arrow: vesicle. Blue arrows: mitochondria. Red arrows: coated pits. ST: seminiferous tubule.

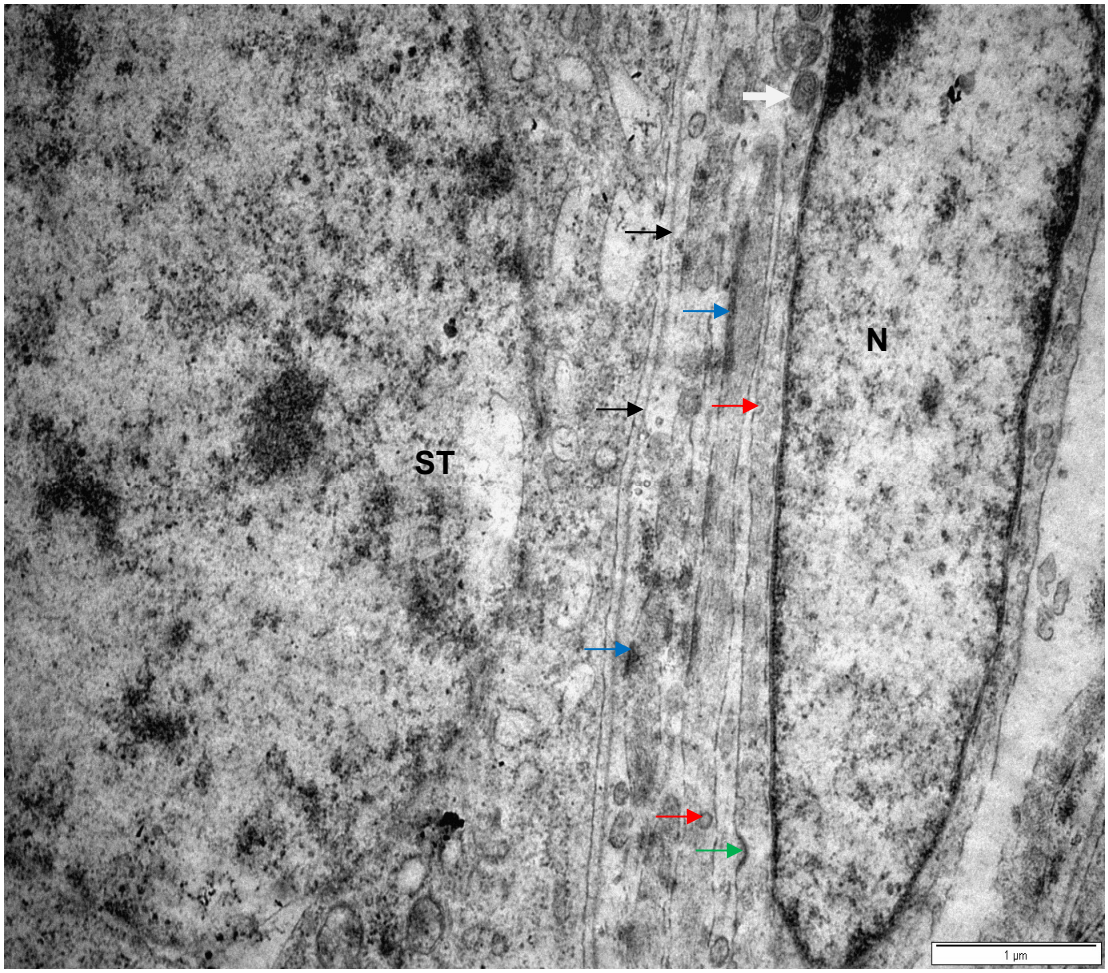

Figure 3. 39: Transmission electron photomicrograph of the peritubular boundary tissue in an adult bird. Black arrows: *basal lamina* of a seminiferous tubule (ST). Blue arrows: electron dense plaques of peritubular myoid cells. Red arrows: forming or formed pinocytotic vesicles. N: elongated euchromatic nucleus of a peritubular myoid cell. Green arrow: coated pit. White arrow: mitochondrion.

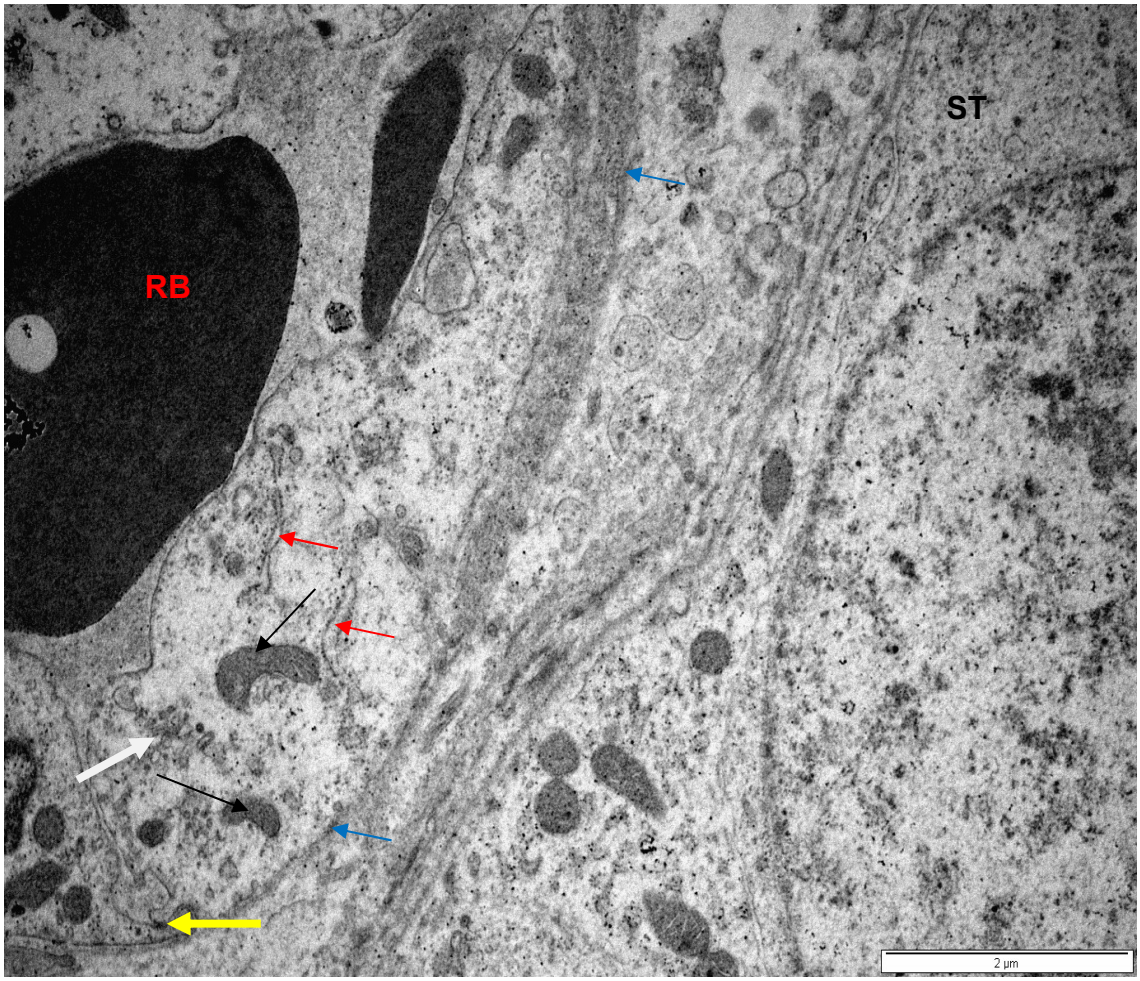

Figure 3. 40: Transmission electron photomicrograph of peritubular boundary tissue in an adult bird. ST: seminiferous tubule. Mitochondria (black arrows), RER profiles (red arrows) and a Golgi complex (white arrow) are present in the cytoplasm of an endothelial cell. Blue arrows: *basal lamina* surrounding the blood vessel. Yellow arrow: tight junction between endothelial cells. RB: red blood cell.

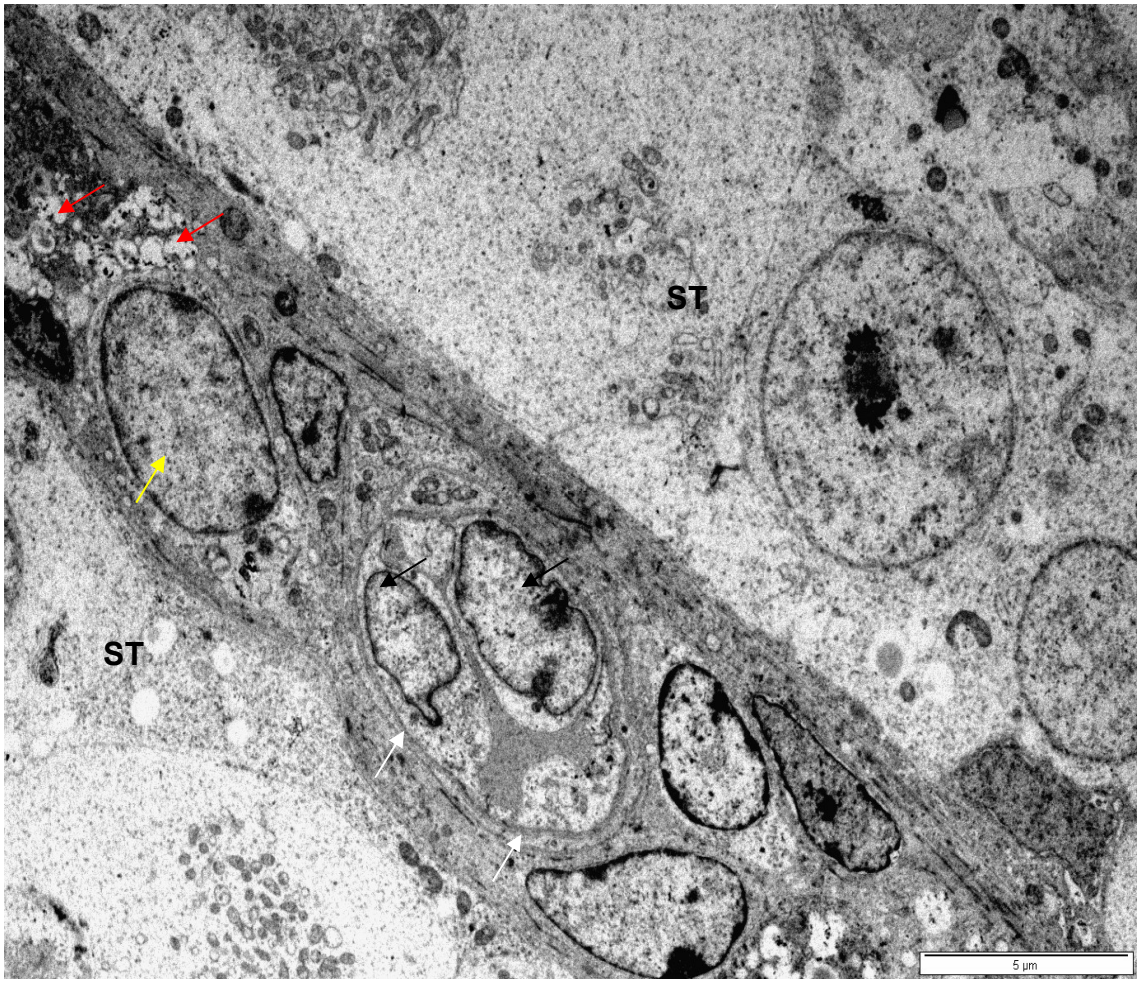

Figure 3. 41: Transmission electron photomicrograph of an intertubular blood vessel in the peritubular boundary tissue of an adult bird. Black arrows: endothelial cells. White arrows: *basal lamina* of the endothelial cells. Red arrows: lipid droplets of a Leydig cell with an oblong-shaped nucleus (yellow arrow). ST: seminiferous tubules.

3.4 Discussion

The seminiferous tubules of mammalian and avian species are surrounded by peritubular boundary tissue (*lamina propria*). The morphology of this tissue is age- and species-specific (Maekawa *et al*., 1996). The information on the age-related changes in the peritubular boundary tissue of birds, particularly the Japanese quail is very scanty. In particular, existing information does not highlight any age-related variations in the cellular and connective tissue components of the peritubular boundary tissue. The current study utilized histological, immunohistochemical and ultrastructural techniques to elucidate age-related changes in the peritubular boundary tissue of the Japanese quail.

3.4.1 Light microscopy

The number of peritubular myoid cells surrounding the seminiferous tubules is species-specific (Maekawa *et al.,* 1996). In the mouse and rat, peritubular myoid cells form a single layer (Maekawa *et al.,* 1996). In contrast, peritubular myoid cells are arranged in several overlapping layers in the testes of the dog (Egger and Witter, 2008), man (Davidoff *et al.,* 1990; Santamaria *et al*., 1992; Haider *et al.,* 1993; Holstein *et al.,* 1996), camel (Moniem *et al.,* 1980) and avian (Rothwell and Tingari, 1973; Aire and Ozegbe, 2007). In agreement with a previous report on the testis of the Japanense quail (Madekurozwa, 2013), the number of peritubular myoid cell layers surrounding the seminiferous cords or tubules was age-dependent. Histologically, the peritubular boundary tissue of pre-pubertal birds was formed by multiple layers of peritubular myoid cells and fibroblasts. In contrast, peritubular boundary tissues in pubertal and adult birds were formed by fewer layers of peritubular myoid cells and fibroblasts. This age-related decrease in cellular layers

was associated with an increase in seminiferous tubule diameter. In agreement with a study on the peritubular boundary tissue in the domestic fowl (Rothwell and Tingari, 1973), the peritubular myoid cells in the current investigation formed the inner layers, while fibroblasts formed the outer layers.

3.4.2 Cytoskeletal protein immunohistochemistry

Cytoskeletal proteins play a vital role in the maintenance of cell polarity and shape, arrangement of intracellular organelles, formation of cytoplasmic extensions and adhesion of organelles to the plasma membrane (Hess and França, 2005; Devkota *et al.*, 2006,a). The distribution and immuno-intensity of the cytoskeletal proteins desmin and smooth muscle actin are species, as well as age-dependent. Desmin and smooth muscle actin are muscle cell specific-markers (Hasegawa *et al*., 2003), which have been shown to be involved in peritubular myoid cell differentiation (Virtanen *et al*., 1986). In the ovine testes, desmin is present in peritubular myoid cells during the early prepubertal period, but disappears completely with the onset of puberty (Steger and Wrobel, 1994). This is contrary to the findings of the present study in which the intensity of desmin immunostaining increased marginally with testicular maturation.

Smooth muscle actin has been used as a marker for testicular development and maturity (Holt *et al.,* 2004). In the current investigation, smooth muscle actin was immunolocalized in peritubular myoid cells and vascular smooth muscle cells in the testes of all the age groups studied. The intensity of smooth muscle actin immunostaining increased with testicular maturation. An age-related increase in the intensity of smooth muscle actin immunostaining has been reported in the sheep (Steger and Wrobel, 1994), porpoise (Holt *et al*., 2004), bovine (Devkota *et al*., 2006a, b) and Japanese quail (Madekurozwa, 2013). This marked increase in

smooth muscle actin immunostaining has been correlated with testicular development and blood testis-barrier formation (Holt *et al*., 2004).

The immunoexpression of tubulin has only been reported in Sertoli cells (Steger and Wrobel, 1994; Holt *et al.,* 2004; Sasaki *et al.,* 2010) and spermatids (Holt *et al*., 2004). Prior to the current study no information was available on the immunoexpression of tubulin in cells of the peritubular boundary tissue. In the current study, weak tubulin immunostaining was observed in peritubular myoid cells in all age groups. These results are contrary to findings in the ovine and bovine in which the peritubular boundary tissue was reported as being tubulin immunonegative. Thus, the results of the current study, as well as previous investigations conducted by other researchers suggest that tubulin immunoexpression in the peritubular boundary tissue is species-specific.

Vimentin is extensively used as a marker of cells of mesenchymal origin. Similar to smooth muscle actin and desmin, vimentin immunostaining in peritubular myoid cells increased with testicular maturation in the present study. Interestingly, studies by Aire and Ozegbe (2007), as well as Ozegbe *et al*. (2012) reported a lack of vimentin immunostaining in the peritubular tissue of various bird species including the domestic fowl, Japanese quail, duck and masked weaver. However, weak vimentin immunostaining was demonstrated in the peritubular tissue of the turkey (Aire and Ozegbe, 2007). The lack of vimentin immunostaining reported by Aire and Ozegbe (2007), as well as Ozegbe *et al*. (2012) was probably due to the immunostaining kit (LSAB) used by authors. The immunostaining kit (Biogenex super sensitive one-step polymer-HRP detection system kit, Emergo Europe, The Hague, The Netherlands) used in the present study has a very high sensitivity.

3.4.3 Basement membrane immunohistochemistry

Extracellular matrix proteins play a key role in the formation, architecture, and the stability of basement membranes (Aumailley and Smyth, 1998). The presence of the extracellular matrix proteins collagen type IV, fibronectin and laminin has been described in the testes of the rat (Davis *et al*., 1990) and human (Gulkusen *et al*., 2002). However, only the presence of the extracellular matrix component laminin has been reported in the avian testis (Abd-Elmaksoud, 2009). The current study is the first report of age-related changes in the immunolocalization of collagen type IV, fibronectin and laminin in the testis of the Japanese quail.

In concurrence with previous reports in the rat (Davis *et al*., 1990) and human (Gulkusen *et al*., 2002), the basement membranes of the seminiferous tubules in all the quails studied in the present investigation displayed collagen type IV and laminin immunostaining. The increase in the staining intensity of these extracellular matrix proteins with age was a note-worthy finding of the current study. In the present study the basement membranes of the seminiferous tubules were fibronectin-immunonegative in all age groups. Interestingly, fibronectin has been localized in the basement membranes of the seminiferous tubules in the rat (Yazama *et al*., 1997) and hamster (Morales *et al*., 2004) using immunoelectron microscopy. Thus, further research on the immunolocalization of fibronectin in the Japanese quail using electron microscopy is required.

In the current study, the basement membranes of peritubular myoid cells displayed collagen type IV, fibronectin and laminin immunostaining. Furthermore, the staining intensity of these proteins increased with testicular maturation. Only laminin has previously been immunolocalized in peritubular myoid cells of the sexually mature chicken and duck (Abd-Elmaksoud, 2009). Thus, the present study is the first report

of collagen type IV and fibronectin in the basement membranes of peritubular myoid cells in the birds. In addition, this is the first study in which the distribution and staining intensity of collagen type IV, fibronectin and laminin in peritubular myoid cells, of quails from different age groups, has been compared.

3.4.4 Transmission electron microscopy

In agreement with previous studies on the testes of birds (Rothwell and Tingari, 1973; Aire, 1997), the peritubular boundary tissue in the present study was formed by fibrous and cellular lamellae. As noted by Rothwell and Tingari (1973) the inner fibrous lamella was composed of the *basal lamina* of seminiferous tubules, a layer of collagen fibres and lastly a second *basal lamina* which was associated with peritubular myoid cells. In the current study the *basal lamina* associated with the peritubular myoid cells was only distinct in adult birds.

The ultrastructural results of the present study revealed the presence of contractile (peritubular myoid cells) and non-contractile (fibroblasts) cells in the cellular lamella of the peritubular boundary tissue. Thus, these results confirm the findings of the immunohistochemical study (3.3.2). In all age groups, peritubular myoid cells were characterized by elongated, euchromatic nuclei and cytoplasmic organelles which included round mitochondria, Golgi complexes and rough endoplasmic reticulum. Noteworthy was the abundance of myofilaments in pubertal to adult birds, but not in the prepubertal birds. This finding is not surprising as the immunohistochemical study (3.3.2.2) revealed weak to moderate smooth muscle actin immunostaining in prepubertal birds, and strong immunostaining in pubertal and adult birds. The presence of abundant myofilaments in peritubular myoid cells has been reported in the domestic fowl (Rothwell and Tingari, 1973; Rothwell, 1975; Aire and Ozegbe,

2007), Japanese quail (Van Naussauw *et al.,* 1993; Aire and Ozegbe, 2007), and duck (Aire and Ozegbe, 2007).

Peritubular myoid cells in the current study displayed several plasma membrane modifications which included electron dense plaques, coated pits, as well as pinocytotic vesicles. These modifications are characteristics of smooth muscle cells. In addition, the plasma membranes of peritubular myoid cells in the present investigation came into apposition with one another at their lateral margins, forming gap junctions. This confirms the findings of Van Naussauw *et al.* (1993). Similarly, junctional complexes have been reported between overlapping peritubular myoid cells in the drake (Aire, 1997). It is probable that these junctional complexes allow cell-to-cell communication between the peritubular myoid cells.

Fibroblasts, and in some instances intertubular blood vessels, were located adjacent to the peritubular myoid cells in all the age groups studied in the present investigation. The presence of fibroblasts in the cellular lamella of the peritubular boundary tissue has been reported in several avian species (Rothwell and Tingari, 1973; Rothwell, 1975; Aire, 1997). It is well documented that fibroblasts are collagen-producing cells (Smith, 1993; Martin, 1997; Ebihara *et al.*, 2006) and would have been responsible for the small amounts of collagen present in the peritubular boundary tissue. The presence of blood vessels adjacent to peritubular myoid cells is an interesting finding as it lends credence to the concept of a blood-testis barrier in which peritubular myoid cells play a significant role. Most studies on the blood-testis barrier have merely focused on Sertoli cells (Cooksey and Rothwell, 1973; Osman *et al*., 1980; Bergmann *et al*., 1984; Bergmann and Schindelmeiser, 1987). However, the possible role of peritubular myoid cells as components of the blood-testis barrier has been investigated in the rat (Dym and Fawcett, 1970; Fawcett *et al.,* 1969). In

the current study, the morphology and composition of the intertubular blood vessels were studied in depth. The structure of intertubular blood vessels has also been studied in the testes of the camel (Moniem *et al.,* 1980) and rat (Dym and Fawcett, 1970). It is plausible that the peritubular boundary tissue acts as a filter that regulates the passage of substances into and out of the seminiferous tubules.

Chapter four:

Conclusion

In conclusion, the findings of this study have established that the morphology of the testicular capsule and peritubular boundary tissue of the Japanese quail changes as the birds mature. Based on the observation of cells with contractile characteristics, in both the testicular capsule and peritubular boundary tissue, the present study has provided morphological evidence that these components of the testis may be involved in the spermatozoal transport mechanism. In addition, the results of the current study provide credence to suggestions that the peritubular boundary tissue is a component of the blood-testis barrier. Thus, the peritubular boundary tissue may be involved in the regulation of substances that enter and leave the seminiferous tubules.

References

Abd-Elhafeez, H., Moustafa, M., Zayed, A. and Sayed, R., 2017. The development of the intratesticular excurrent duct system of donkey (Equus asinus) from birth to maturity. Histology, Cytology and Embryology (HCE), 1(2): 1-8.

Abd-Elmaksoud, A., 2009. Comparative expression of laminin and smooth muscle actin in the testis and epididymis of poultry and rabbit. Journal of Molecular Histology, 40(5-6): 407-416.

Aire, T.A., 1997. The structure of the interstitial tissue of the active and resting avian testis. Onderstepoort Journal of Veterinary Research, 64: 291-299.

Aire, T.A. and Ozegbe, P. C, 2007. The testicular capsule and peritubular tissue of birds: morphometry, histology, ultrastructure and immunohistochemistry. Journal of Anatomy, 210(6): 731-740.

Anthony, C.T. and Skinner, M.K., 1989. Cytochemical and biochemical characterization of testicular peritubular myoid cells. Biology of Reproduction, 40(4): 811-823.

Arenas, M. I., Bethencourt, F. R., De Miguel, M. P., Fraile, B., Romo, E., Paniagua, R., 1997. Immunocytochemical and quantitative study of actin, desmin and vimentin in the peritubular cells of the testes from elderly men. Journal of Reproduction and Fertility, 110:183-193.

Artoni, S., Orsi, A.M., Carvalho, T.L, Vicentini, C. and Stefanini, M., 1999. Seasonal morphology of the domestic quail (*Coturnix coturnix japonica*) testis. Anatomia, Histologia, Embryologia, 28(4): 217-220.

Artoni, S.M., Orsi, A.M., Carvalho, T.L. and Lopes, R.A., 1997. The annual testicular cycle of the domestic quail (*Coturnix coturnix japonica*). Anatomia, Histologia, Embryologia, 26(4): 337-9.

Aumailley, M. and Krieg, T., 1996. Laminins: a family of diverse multifunctional molecules of basement membranes. Journal of Investigative Dermatology, 106(2): 209-214.

Aumailley, M. and Smyth, N., 1998. The role of laminins in basement membrane function. Journal of Anatomy, 193(1): 1-21.

Ball, G.F. and Balthazart, J., 2010. Japanese quail as a model system for studying the neuroendocrine control of reproductive and social behaviors. ILAR journal, 51(4): 310-325.

Banks, F.C., Knight, G.E., Calvert, R.C., Turmaine, M., Thompson, C.S., Mikhailidis, D.P., Morgan, R.J. and Burnstock, G., 2006. Smooth muscle and purinergic contraction of the human, rabbit, rat, and mouse testicular capsule. Biology of Reproduction, 74(3): 473-480.

Bergmann, M. and Schindelmeiser, J., 1987. Development of the blood-testis barrier in the domestic fowl (*Gallus domesticus*). International Journal of Andrology, 10:481-488.

Bergmann, M., Schindelmeiser, J., Greven, H., 1984, The blood-testis barrier in vertebrates having different testieular organization. Cell and Tissue Research, 238:145-150

Birkhead, T.R., Fletcher, F. and Pellatt, E.J., 1998. Testes asymmetry, condition and sexual selection in birds: an experimental test. Proceedings of the Royal Society B: Biological Sciences, 265(1402): 1185-1189.

Bressler, R.S. and Ross, M.H., 1972. Differentiation of peritubular myoid cells of the testis: effects of intratesticular implantation of newborn mouse testes into normal and hypophysectomized adults. Biology of Reproduction, 6(1): 148-159.

Bucala, R., Spiegel, L., Chesney, J., Hogan, M. and Cerami, A., 1994. Circulating fibrocytes define a new leukocyte subpopulation that mediates tissue repair. Molecular Medicine, 1(1): 71.

Burke, W.H., 1973. Testicular asymmetry in the Turkey. Poultry Science, 52(4): 1652-1654.

Bustos-Obregon, E. and Courot, M., 1974. Ultrastructure of the lamina propria in the ovine seminiferous tubule. Cell and Tissue Research, 150(4): 481-492.

Calhim, S. and Montgomerie, R., 2015. Testis asymmetry in birds: The influences of sexual and natural selection. Journal of Avian Biology, 46(2): 175-185.

Campion, S., Catlin, N., Heger, N., McDonnell, E.V., Pacheco, S.E., Saffarini, C., Sandrof, M.A. and Boekelheide, K., 2012. Male reprotoxicity and endocrine disruption, Molecular, Clinical and Environmental Toxicology. Springer, pp. 315-360.

Chacon-Arellano, J. and Woolley, D., 1980. Smooth muscle cells in the testicular capsule of the horse, pig and sheep. Journal of Anatomy, 131(Pt 2): 263.

Charles, D. 1996. Differential expression of tubulin isotypes during the cell cycle. Cell Motility, 35(1): 49-58.

Clulow, J. and Jones, R., 1982. Production, transport, maturation, storage and survival of spermatozoa in the male Japanese quail, *Coturnix coturnix*. Journal of Reproduction and Fertility, 64(2): 259-266.

Coban, O., Lacin, E., Sabuncuoglu, N. and Ozudogru, Z., 2009. Effect of self-photoperiod on live weight, carcass and growth traits in quails (*Coturnix Coturnix japonica*). Asian-Australasian Journal of Animal Sciences, 22(3): 410.

Cooksey, J.,E., Rothwell, B., 1973. The ultrastructure of the Sertoli cell and its differentiation in the domestic fowl (*Gallus domesticus*). Joarnal of Anatomy, 114(3): 329-345

Davidoff, M., Breucker, H., Holstein, A. and Seidl, K., 1990. Cellular architecture of the lamina propria of human seminiferous tubules. Cell and Tissue Research, 262(2): 253-261.

Davis, J. and Horowitz, A., 1978. Effects of hyperthermia and hypothermia on spontaneous contractions of the adult rabbit testicular capsule. International Journal of Biometeorology, 22(4): 303-311.

Davis, J.R., Langford, G.A. and Kirby, P.J., 1970. The testicular capsule. The testis, 1: 281-337.

Davis, C.M., Papadopoijlos, V., Sommers, C.L., Kleinman, H.K. and Dym, M., 1990. Differential expression of extracellular matrix components in rat Sertoli cells. Biology of Reproduction, 43(5): 860-869.

De Kretser, D., Kerr, J. and Paulsen, C., 1975. The peritubular tissue in the normal and pathological human testis. An ultrastructural study. Biology of Reproduction, 12(3): 317-324.

Derégnaucourt, S., Saar, S. and Gahr, M., 2009. Dynamics of crowing development in the domestic Japanese quail (*Coturnix coturnix japonica*). Proceedings of the Royal Society of London B: Biological Sciences: rspb. 2009.0016.

Deviche, P., Hurley, L.L. and Fokidis, H.B., 2011. Avian testicular structure, function, and regulation, Hormones and Reproduction of Vertebrates: Birds. Elsevier, pp. 27-70.

Devkota, B., Sasaki, M., Takahashi, K.-I., Matsukazi, S., Matsui, M., Haneda, S., Takahashi, M., Osawa, T. and Miyake, Y.-I., 2006a. Postnatal developmental changes in immunohistochemical localization of α-smooth muscle actin (SMA) and vimentin in bovine testes. Journal of Reproduction and Development, 52(1): 43-49.

Devkota, B., Sasaki, M., Matsui, M., Montoya, C.A. and Miyake, Y.-I., 2006b. Alterations in the immunohistochemical localization patterns of α-smooth muscle actin (SMA) and vimentin in the postnatally developing bovine cryptorchid testis. Journal of Reproduction and Development, 52(3): 329-334.

Dharani, P., Kumary, S.U., Venkatesan, S., Joseph, C., Ramesh, G., Dharani, P., Kumary, S., Venkatesan, S., Joseph, C. and Ramesh, G., 2017. Morphology of the interstitial tissue of active and resting testis of the guinea fowl. International Journal of Morphology, 35(4): 1359-1362.

Dym, M., 1994. Basement membrane regulation of Sertoli cells. Endocrine Reviews, 15: 102-102.

Dym, M. and Fawcett, D.W., 1970. The blood-testis barrier in the rat and the physiological compartmentation of the seminiferous epithelium. Biology of Reproduction, 3(3): 308-326.

Ebihara, Y., Masuya, M., La Rue, A.C., Fleming, P.A., Visconti, R.P., Minamiguchi, H., Drake, C.J. and Ogawa, M., 2006. Hematopoietic origins of fibroblasts: II. In vitro studies of fibroblasts, CFU-F, and fibrocytes. Experimental Hematology, 34(2): 219-229.

Egger, G.F. and Witter, K., 2008. Peritubular contractile cells in testis and epididymis of the dog, *canis lupus familiaris*. Acta Veterinaria Brno, 78(1): 3-11.

Ellis, L.C., Buhrley, L.E. and Hargrove, J.L., 1978. Species differences in contractility of seminiferous tubules and tunica albuginea as related to sperm transport through the testis. Archives of Andrology, 1(2): 139-146.

Ellis, L.C., Farr, G.C. and Tesi, R., 1981. Contractility of seminiferous tubules as related to sperm transport in the male. Archives of Andrology, 6(4): 283-294.

Fawcett, D.W., Heidger, P.M. and Leak, L.V., 1969. Lymph vascular system of the interstitial tissue of the testis revealed by electron microscopy. Journal of Reproduction and Fertility, 19: 109-119.

Fakoya, F.A., 2002. Reticulin fibres in the tunica albuginea and peritubular tissue of seminiferous tubules of adult male Wistar rats. Acta Histochemica, 104(3): 279-283.

Fisher, J.S., Macpherson, S., Marchetti, N. and Sharpe, R.M., 2003. Human 'testicular dysgenesis syndrome': a possible model using in-utero exposure of the rat to dibutyl phthalate. Human Reproduction, 18(7): 1383-1394.

Flavell, S., Hou, T., Lax, S., Filer, A., Salmon, M. and Buckley, C., 2008. Fibroblasts as novel therapeutic targets in chronic inflammation. British Journal of Pharmacology, 153(S1).

Franca, L.R., Leal, M.C., Sasso-Cerri, E., Vasconcelos, A., Debeljuk, L. and Russell, L.D., 2000. Cimetidine (Tagamet) is a reproductive toxicant in male rats affecting peritubular cells. Biology of Reproduction, 63(5): 1403-1412.

Freneau, G.E., Carvalho, S.F., Saboia-Morais, S.M. and Freneau, B.N., 2016. Aspects of spermatogenesis and microscopic testicular morphology in Greater

Rhea, *Rhea americana* (Linnaeus, 1758). Pesquisa Veterinária Brasileira, 36(10): 1045-1052.

Garamszegi, L.Z., Eens, M., Hurtrez-Boussès, S. and Møller, A.P., 2005. Testosterone, testes size, and mating success in birds: a comparative study. Hormones and Behavior, 47(4): 389-409.

Gerzilov, V., Bochukov, A., Penchev, G. and Petrov, P., 2016. Testicular development in the Muscovy duck (*Cairina moschata*). Bulgarian Journal of Veterinary Medicine, 19(1).

Ghazanfari, S., Khademhosseini, A. and Smit, T.H., 2016. Mechanisms of lamellar collagen formation in connective tissues. Biomaterials, 97: 74-84.

González-Morán, M. and Soria-Castro, E., 2010. Changes in the tubular compartment of the testis of *Gallus domesticus* during development. British Poultry Science, 51(2): 296-307.

Gorgas, K. and Böck, P., 1974. Myofibroblasts in the rat testicular capsule. Cell and Tissue Research, 154(4): 533-541.

Goyal, H.O. and Dhingra, L., 1973. A study on the postnatal histology of the testis in buffalo (*Bubalus bubalis*). Cells Tissues Organs, 84(2): 237-250.

Gröschel-Stewart, U. and Unsicker, K., 1977. Direct visualization of contractile proteins in peritubular cells of the guinea-pig testis using antibodies against highly purified actin and myosin. Histochemistry, 51(4): 315-319.

Gulkesen, K., Erdogru, T., Sargin, C.F. and Karpuzoglu, G., 2002. Expression of extracellular matrix proteins and vimentin in testes of azoospermic man: an immunohistochemical and morphometric study. Asian Journal of Andrology, 4(1): 55-60.

Gunn, S.A., Gould, T.C. and Anderson, W., 1966. Protective effect of thiol compounds against cadmium-induced vascular damage to testis. Proceedings of the Society for Experimental Biology and Medicine, 122(4): 1036-1039.

Hadley, M.A. and Dym, M., 1987. Immunocytochemistry of extracellular matrix in the lamina propria of the rat testis: electron microscopic localization. Biology of Reproduction, 37(5): 1283-1289.

Haider, S., Talati, J. and Servos, G., 1993. Ultrastructure of peritubular tissue in association with tubular hyalinization in human testis. Tissue and Cell, 31(1): 90-98.

Halldin, K., 2005. Impact of endocrine disrupting chemicals on reproduction in Japanese quail. Domestic Animal Endocrinology, 29(2): 420-429.

Hargrove, J.L., MacIndoe, J.H. and Ellis, L.C., 1977. Testicular contractile cells and sperm transport. Fertility and sterility, 28(11): 1146-1157.

Hasegawa, T., Hasegawa, F., Hirose, T., Sano, T., Matsuno, Y., 2003. Expression of smooth muscle markers in so called malignant fibrous histiocytomas. Journal of Clinical Pathology, 56:666–671

Hassanzadeh, B., Nabipour, A., Behnam Rassouli, M. and Dehghani, H., 2014. Morphological development of testes in ostrich (*Struthio camelus*) embryo. Anatomical Science International, 89(3): 129-139.

Hernández-Morera, P., Travieso-González, C.M., Castaño-González, I., Mompeó-Corredera, B. and Ortega-Santana, F., 2017. Segmentation of elastic fibres in images of vessel wall sections stained with Weigert's resorcin–fuchsin. Computer methods and programs in biomedicine, 142: 43-54.

Hess, R. and França, L.R., 2005. Structure of the Sertoli cell. Sertoli cell biology, 19: 40.

Holstein, A.F., Maekawa, M., Nagano, T. and Davidoff, M.S., 1996. Myofibroblasts in the lamina propria of human seminiferous tubules are dynamic structures of heterogeneous phenotype. Archives of Histology and Cytology, 59(2): 109-125.

Holt, W.V., Waller, J., Moore, A., Jepson, P.D., Deaville, R. and Bennett, P.M., 2004. Smooth muscle actin and vimentin as markers of testis development in the harbour porpoise (*Phocoena phocoena*). Journal of Anatomy, 205(3): 201-211.

Huss, D., Poynter, G. and Lansford, R., 2008. Japanese quail (*Coturnix japonica*) as a laboratory animal model. Journal of Lab animal, 37(11): 513.

Jones, R.E. and Lopez, K.H., 2014. Chapter 4 - The Male Reproductive System, Human Reproductive Biology (Fourth Edition). Academic Press, San Diego, pp. 67-83.

Kannan, T., Ramesh, G. and Sivakumar, M., 2015. Age related changes in the gross and histoarchitecture of testis in Japanese Quails (*Coturnix coturnix japonica*). International Journal of Livestock Research, 5(6): 26-33.

Kempenaers, B., Peer, K., Vermeirssen, E.L. and Robertson, R.J., 2002. Testis size and asymmetry in the tree swallow: a test of the compensation hypothesis. Avian Science, 2: 115-122.

Kendall, R.J., Lacker, T.E., Bunck, C., Daniel, B., Driver, C., Grue, C.E., Leighton, F., Stansley, W., Watanabe, P.G. and Whitworth, M., 1996. An ecological risk assessment of lead shot exposure in non-waterfowl avian species: Upland game birds and raptors. Environmental Toxicology and Chemistry, 15(1): 4-20.

Kew, S., Gwynne, J., Enea, D., Abu-Rub, M., Pandit, A., Zeugolis, D., Brooks, R., Rushton, N., Best, S. and Cameron, R., 2011. Regeneration and repair of tendon and ligament tissue using collagen fibre biomaterials. Acta Biomaterialia, 7(9): 3237-3247.

Kielty, C.M., Sherratt, M.J. and Shuttleworth, C.A., 2002. Elastic fibres. Journal of Cell Science, 115(14): 2817-2828.

Kouatcho, F.D., Kenfack, A., Ngoula, F. and Teguia, A., 2015. Sexual maturity prediction based on hormonal profiles, testes and semen characteristics in male Coturnix quail (Garsault, 1764) in the Western Highlands of Cameroon. International Journal of Agronomy and Agriculture Research, 7(4): 143-154.

Kühnel, W., 2003. Color Atlas of Cytology, Histology and Microscopic Anatomy. Georg Thieme Verlag.

Lacy, D. and Rotblat, J., 1960. Study of normal and irradiated boundary tissue of the seminiferous tubules of the rat. Experimental Cell Research, 21(1): 49-70.

Lanna, L.L., Soares, F.A., Santos, T.M., Oliveira, J.N. and Marques-Júnior, A.P., 2013. Índice gonadossomático e correlações entre dimensões e peso testiculares na codorna japonesa (*Coturnix coturnix japonica*) aos 60 dias de idade. Arquivo Brasileiro de Medicina Veterinária e Zootecnia, 65: 955-960.

Lannoy, M., Slove, S. and Jacob, M.-P., 2014. The function of elastic fibers in the arteries: beyond elasticity. Pathologie Biologie, 62(2): 79-83.

Leeson, C.R. and Forman, D.E., 1981. Postnatal development and differentiation of contractile cells within the rabbit testis. Journal of Anatomy, 132(Pt 4): 491-511.

Leeson, C.R. and Leeson, T.S., 1963. The postnatal development and differentiation of the boundary tissue of the seminiferous tubule of the rat. The Anatomical Record, 147(2): 243-259.

Leeson, T.S. and Cookson, F.B., 1974. The mammalian testicular capsule and its muscle elements. Journal of Morphology, 144(2): 237-253.

Lian, G. and Enders, G.C., 1994. Entactin ultrastructural immunolocalization in the *basal lamina*e of mouse seminiferous tubules and with only subtle changes following hypophysectomy. Journal of Andrology, 15(1): 52-60.

Losinno, A.D., Morales, A., Fernández, D. and Lopez, L.A., 2012. Peritubular myoid cells from rat seminiferous tubules contain actin and myosin filaments distributed in two independent layers. Biology of Reproduction, 86(5): 150, 1-8.

Losinno, A.D., Sorrivas, V., Ezquer, M., Ezquer, F., López, L.A. and Morales, A., 2016. Changes of myoid and endothelial cells in the peritubular wall during contraction of the seminiferous tubule. Cell and Tissue Research, 365(2): 425-435.

Lydka, M., Kotula-Balak, M., Kopera-Sobota, I., Tischner, M. and Bilińska, B., 2011. Vimentin expression in testes of Arabian stallions. Equine Veterinary Journal, 43(2): 184-189.

Madekurozwa, M.C., 2013. Post-hatch changes in the immunoexpression of desmin, smooth muscle actin and vimentin in the testicular capsule and interstitial tissue of the Japanese quail (*Coturnix coturnix japonica*). Anatomia, Histologia, Embryologia, 42(5): 369-378.

Madekurozwa, M.C. and Kimaro, W., 2006. A morphological and immunohistochemical study of healthy and atretic follicles in the ovary of the

sexually immature ostrich (*Struthio camelus)*. Anatomia, Histologia, Embryologia, 35(4): 253-258.

Maekawa, M., Kamimura, K. and Nagano, T., 1996. Peritubular myoid cells in the testis: their structure and function. Archives of Histology and Cytology, 59(1): 1-13.

Maretta, M. and Marettova, E., 2004. Immunohistochemical demonstration of myoid cells in the testis and its excurrent ducts in the domestic fowl. British Poultry Science, 45(5): 585-589.

Marin, R. and Satterlee, D., 2004. Cloacal gland and testes development in male Japanese quail selected for divergent adrenocortical responsiveness. Poultry Science, 83(6): 1028-1034.

Martin, P., 1997. Wound healing-aiming for perfect skin regeneration. Science, 276(5309): 75-81.

Mather, F. and Wilson, W., 1964. Post-natal testicular development in Japanese quail (*Coturnix coturnix japonica*). Poultry Science, 43(4): 860-864.

McLendon, P.M. and Robbins, J., 2011. Desmin-related cardiomyopathy: an unfolding story. American Journal of Physiology-Heart and Circulatory Physiology, 301(4): H1220-H1228.

Michael, H., Romrell, L.J. and Gordon, I., 1995. Histology: a text and atlas. Williams & Wilkins.

Middendorff, R., Müller, D., Mewe, M., Mukhopadhyay, A.K., Holstein, A.F. and Davidoff, M.S., 2002. The tunica albuginea of the human testis is characterized by complex contraction and relaxation activities regulated by cyclic GMP. The Journal of Clinical Endocrinology and Metabolism, 87(7): 3486-3499.

Mills, A.D., Crawford, L.L., Domjan, M. and Faure, J.M., 1997. The behavior of the Japanese or domestic quail *Coturnix japonica*. Neuroscience and Biobehavioral Reviews, 21(3): 261-281.

Minvielle, F., 2004. The future of Japanese quail for research and production. World's Poultry Science Journal, 60(4): 500-507.

Moniem, K., Tingari, M. and Künzel, E., 1980. The fine structure of the boundary tissue of the seminiferous tubule of the camel (*Camelus dromedarius*). Cells Tissues Organs, 107(2): 169-176.

Morales, E., Horn, R., Pastor, L., Santamaria, L., Pallarés, J., Zuasti, A., Ferrer, C. and Canteras, M., 2004. Involution of seminiferous tubules in aged hamsters: an ultrastructural, immunohistochemical and quantitative morphological study. Histology and Histopathology, 19(2): 445-456.

Morrione, T.G., 1952. The formation of collagen fibers by the action of heparin on soluble collagen: an electron microscope study. The Journal of Experimental Medicine, 96(2): 107.

Mutsaers, S.E., 2002. Mesothelial cells: Their structure, function and role in serosal repair. Respirology, 7:171–191

Nixon, B., Ewen, K.A., Krivanek, K.M., Clulow, J., Kidd, G., Ecroyd, H. and Jones, R.C., 2014. Post-testicular sperm maturation and identification of an epididymal protein in the Japanese quail (*Coturnix coturnix japonica*). Reproduction, 147(3): 265-77.

Nunome, M., Nakano, M., Tadano, R., Kawahara-Miki, R., Kono, T., Takahashi, S., Kawashima, T., Fujiwara, A., Nirasawa, K. and Mizutani, M., 2017. Genetic divergence in domestic Japanese quail inferred from mitochondrial DNA D-loop and microsatellite markers. PloS one, 12(1): e0169978.

Nurmio, M., Kallio, J., Adam, M., Mayerhofer, A., Toppari, J. and Jahnukainen, K., 2012. Peritubular myoid cells have a role in postnatal testicular growth. Spermatogenesis, 2(2): 79-87.

Ohanian, C., Rodriguez, H., Piriz, H., Martino, I., Rieppi, G., Garófalo, E.G. and Roca, R., 1979. Studies on the contractile activity and ultrastructure of the boar testicular capsule. Journal of Reproduction and Fertility, 57(1): 79-85.

Ortega, H., Lorente, J. and Salvetti, N., 2004. Immunohistochemical study of intermediate filaments and neuroendocrine marker expression in Leydig cells of laboratory rodents. Anatomia, Histologia, Embryologia, 33(5): 309-315.

Osman, D., I., Ekwall, H., Ploen, L.,1980. Specialized cell contacts and the blood-testis barrier in the seminiferous tubules of the domestic fowl (*Gallus domesticus*). International Journal of Andrology 3:553-562

Ozegbe, P., Aire, T. and Deokar, M., 2012. The cytoskeletal proteins in the contractile tissues of the testis and its excurrent ducts of the passerine bird, Masked Weaver (*Ploceus velatus*). Tissue and Cell, 44(1): 22-31.

Ozegbe, P., Aire, T.A., Madekurozwa, M.-C. and Soley, J.T., 2008. Morphological and immunohistochemical study of testicular capsule and peritubular tissue of emu (*Dromaius novaehollandiae*) and ostrich (*Struthio camelus*). Cell and Tissue Research, 332(1): 151-158.

Paulin, D. and Li, Z., 2004. Desmin: a major intermediate filament protein essential for the structural integrity and function of muscle. Experimental Cell Research, 301(1): 1-7.

Polyák, E., Boopathi, E., Mohanan, S., Deng, M., Zderic, S.A., Wein, A.J. and Chacko, S., 2009. Alterations in caveolin expression and ultrastructure after

bladder smooth muscle hypertrophy. The Journal of Urology, 182(5): 2497-2503.

Potter, S.J., and DeFalco, T, 2017. Role of the testis interstitial component in spermatogonial stem cell function. Reproduction, 153(4): R151-R162.

Rennard, S.I., Jaurand, M.C., Bignon, J., 1984. Role of pleural mesothelial cells in the production of the submesothelial connective tissue matrix of lung. American Reviews of Respiratory Diseases, 130: 267–74.

Rezvannejad, E., Pakdel, A., Ashtianee, S.R.M., Yeganeh, H.M. and Yaghoobi, M.M., 2013. Analysis of growth characteristics in short-term divergently selected Japanese quail lines and their cross. The Journal of Applied Poultry Research, 22(4): 663-670.

Rothwell, B., 1975. Designation of the cellular component of the peritubular boundary tissue of the seminiferous tubule in the testis of the fowl (*Gallus domesticus*). British Poultry Science, 16:527-529.

Rothwell, B. and Tingari, M., 1973. The ultrastructure of the boundary tissue of the seminiferous tubule in the testis of the domestic fowl (*Gallus domesticus*). Journal of Anatomy, 114(Pt 3): 321.

Santamaria, L., Martin, R., Nistal, M. and Paniagua, R., 1992. The peritubular myoid cells in the testes from men with varicocele: an ultrastructural, immunohistochemical and quantitative study. Histopathology, 21(5): 423-433.

Santamaria, L., Reoyo, A., Regadera, J. and Paniagua, R., 1990. Histochemistry and infrastructure of nerve fibres and contractile cells in the tunica albuginea of the rat testis. Cells Tissues Organs, 139(2): 126-133.

Sappino, A.P.,Schurach, W. and Gabbiani, G., 1990. Differentiation repertoire of fibroblastic cells: Expression of cytoskeletal proteins as marker of phenotypic modulations. Laboratory investigation, 63:144-161.

Sasaki, M., Endo, H., Kimura, J., Rerkamnuaychoke, W., Hayakawa, D., Bhuminand, D., Kitamura, N. and Fukuta, K., 2010. Immunohistochemical localization of the cytoskeletal proteins in the testes of the lesser mouse deer (*Tragulus javanicus*). Mammal Study, 35(1): 57-64.

Satterlee, D., Marin, R. and Jonest, R., 2002. Selection of Japanese quail for reduced adrenocortical responsiveness accelerates puberty in males. Poultry Science, 81(7): 1071-1076.

Sezer, M., Berberoglu, E. and Ulutas, Z., 2006. Genetic association between sexual maturity and weekly live-weights in laying-type Japanese quail. South African Journal of Animal Science, 36(2): 142-148.

Skalli, O., Pelte, M., Peclet, M., Gabbiani, G., Gugliotta, P., Bussolati, G., Ravazzola, M. and Orci, L., 1989. Alpha-smooth muscle actin, a differentiation marker of smooth muscle cells, is present in microfilamentous bundles of pericytes. Journal of Histochemistry and Cytochemistry, 37(3): 315-321.

Skalli, O., Ropraz, P., Trzeciak, A., Benzonana, G., Gillessen, D. and Gabbiani, G., 1986. A monoclonal antibody against alpha-smooth muscle actin: a new probe for smooth muscle differentiation. The Journal of Cell Biology, 103(6): 2787-2796.

Skinner, M.K., 1991. Cell-cell interactions in the testis. Endocrine Reviews, 12(1): 45-77.

Skinner, M.K. and Fritz, I.B., 1985. Testicular peritubular cells secrete a protein under androgen control that modulates Sertoli cell functions. Proceedings of the National Academy of Sciences, 82(1): 114-118.

Smith, K., 1993. Textbook of Veterinary Histology, 4th edn., HD. Dellman (Ed.). Lea & Febiger, Rome (1993). WB Saunders.

Steger, K., Schimmel, M. and Wrobel, K.-H., 1994. Immunocytochemical demonstration of cytoskeletal proteins in seminiferous tubules of adult rams and bulls. Archives of Histology and Cytology, 57(1): 17-28.

Steger, K. and Wrobel, K.-H., 1994. Immunohistochemical demonstration of cytoskeletal proteins in the ovine testis during postnatal development. Anatomy and Embryology, 189(6): 521-530.

Steinert, P.M., Jones, J. and Goldman, R.D., 1984. Intermediate filaments. The Journal of Cell Biology, 99(1 Pt 2): 22s.

Sweeney, M., Jones, C., Greenwood, S., Baker, P. and Taggart, M., 2006. Ultrastructural features of smooth muscle and endothelial cells of isolated isobaric human placental and maternal arteries. Placenta, 27(6): 635-647.

Tung, P.S., Skinner, M.K. and Fritz, I.B., 1984. Fibronectin synthesis is a marker for peritubular cell contaminants in Sertoli cell-enriched cultures. Biology of Reproduction, 30(1): 199-211.

Unsicker, K. and Burnstock, G., 1975. Myoid cells in the peritubular tissue (Lamina propria) of the reptilian testis. Cell and Tissue Research, 163(4): 545-560.

Ushiki, T., 2002. Collagen fibers, reticular fibers and elastic fibers. A comprehensive understanding from a morphological viewpoint. Archives of Histology and Cytology, 65(2): 109-126.

Van Nassauw, L., Harrisson, F. and Callebaut, M., 1993. Smooth muscle cells in the peritubular tissue of the quail testis. European Journal of Morphology, 31: 60-64.

Vatsalya, V. and Arora, K.L., 2012. Allometric growth of testes in relation to age, body weight and selected blood parameters in male Japanese quail (*Coturnix japonica*). International Journal of Poultry Science, 11(4): 251.

Verhoeven, G., Hoeben, E. and De Gendt, K., 2000. Peritubular cell-Sertoli cell interactions: factors involved in PmodS activity. Andrologia, 32(1): 42-45.

Virtanen, I., Kallajoki, M., Näurväunen, O., Paranko, J., Thornell, L.E., Miettinen, M. and Lehto, V.P., 1986. Peritubular myoid cells of human and rat testis are smooth muscle cells that contain desmin-type intermediate filaments. The Anatomical Record, 215(1): 10-20.

Wang, J., Peng, K., Liu, H.Z., Song, H., Chen, X. and Liu, M., 2009. Distribution and developmental changes in ghrelin-immunopositive cells in the gastrointestinal tract of African ostrich chicks. Regulatory Peptides, 154(1-3): 97-101.

Wang, K., 1985. Sarcomere-associated cytoskeletal lattices in striated muscle, Cell and muscle motility. Springer, pp. 315-369.

Wrobel, K.-H., Dostal, S. and Schimmel, M., 1988. Postnatal development of the tubular lamina propria and the intertubular tissue in the bovine testis. Cell and Tissue Research, 252(3): 639-653.

Yang, W.S., Kim, B.S., Lee, S.K., Park, J.S., Kim, S.B.,1999. Interleukin-1beta stimulates the production of extracellular matrix in cultured human peritoneal mesothelial cells. Peritoneal Dialysis International, 19: 211–20.

Yazama, F., Esaki, M. and Sawada, H., 1997. Immunocytochemistry of extracellular matrix components in the rat seminiferous tubule: electron microscopic

localization with improved methodology. The Anatomical Record. 248(1): 51-62.

Ye, L.X., Wang, J.X., Li, P. and Zang, X.T., 2018. Distribution and Morphology of Ghrelin-Immunopositive Cells in the Testes of the African Ostrich. Parkistan Journal of Zoology, 50(1): 29-34.

Zhou, Q., Nie, R., Prins, G.S., Saunders, P.T., Katzenellenbogen, B.S. and Hess, R.A., 2002. Localization of androgen and estrogen receptors in adult male mouse reproductive tract. Journal of Andrology, 23(6): 870-881.